# Pumps as Turbines used with Induction Generators for stand-alone Micro-hydroelectric Power Plants

A A Williams

PhD

1992

PhD

9/2/ MIL

SUG

Ref.

# PUMPS AS TURBINES USED WITH INDUCTION GENERATORS FOR STAND-ALONE MICRO-HYDROELECTRIC POWER PLANTS

**Arthur A Williams**

A thesis submitted for the degree of
Doctor of Philosophy

Faculty of Engineering,
**The Nottingham Trent University**
(Formerly Nottingham Polytechnic)
in collaboration with
The Intermediate Technology Development Group

**October 1992**

This thesis is dedicated to
**the villagers of Hamàran, Pakistan**
for whom the operation of a pump-as-turbine
is of more than academic interest!

# CONTENTS

# ACKNOWLEDGEMENTS

**This research was supported financially by Nottingham Polytechnic, the Intermediate Technology Development Group and the UK Overseas Development Administration.**

I acknowledge the contribution of the following individuals:

My project supervisors, Dr Keith Pratt and Mr Max Keysell, for their support and encouragement throughout the project.

Prof Peter Holmes and Prof Bryan Button for their interest in the project from start to finish.

My colleague Nigel Smith, who acted as a sounding board for many crazy ideas, providing constructive criticism and solidarity during the difficult stages of the project.

The staff of Intermediate Technology Development Group, especially Andy Brown and Adam Harvey for their technical assistance and encouragement.

During the construction of the test rig and laboratory testing I received invaluable support from the following technicians: Bob Oreszczyn, Jeff Baines, Rob Potter, Vincent Bartley, Dave Carmicheal, Tony Maides and Alan Crisp, former principal technician in the Department of Mechanical Engineering.

Bill and Ann Cowperthwaite for hospitality, hard work and patience during the setting up of the demonstration scheme at Tennant Gill Farm.

Dr John Burton of the University of Reading, who acted as mentor and put forward several important ideas during the formulation of the turbine prediction method.

Claudio Alatorre-Frenk of Warwick University for regular meetings which led to a fruitful exchange of ideas and information.

Dr Brian O'Neill, for support during the preparation of the thesis, not only in providing tuition in desk-top publishing, but also in joining in training for a half-marathon.

Mrs Lynda Aucott for the preparation of the diagrams.

Ms Rosemary Olver, who gave encouragement during the project, and carried out final proof reading of the thesis.

The support of the following organizations is also acknowledged:-

**ITT Flygt Ltd** - for use of test facilities at Colwick, Nottingham; advice and assistance in carrying out tests; permission for publication of pump data; donation of a 5 kW pump unit for testing and field trials.

**Sterling Fluids (Hayward-Tyler)** - for donation of a 5 kW pump unit for testing, and for assistance with travel costs to Nepal.

**Dresser Pumps (Worthington-Simpson)** - for donation of a 1.1 kW pump unit for testing and field trials; for advice and assistance in the selection of pumps.

**Development and Consulting Services** - for arranging site visits; providing information on micro-hydro; for hospitality in Butwal, Nepal.

**Pakistan Council for Appropriate Technology** - for providing information and for donation of a 3 kW pump unit for field trials.

**Aga Khan Rural Support Programme** - for arranging site visits and providing information; for use of test facilities; for setting up and monitoring a demonstration scheme; for hospitality in Gilgit, Pakistan.

**MECO Pumps (Pvt)** - for use of test facilities; for hospitality in Lahore, Pakistan.

**The National Trust** - for providing a successful site for field trials, and for playing a crucial role in setting up the demonstration scheme.

# NOMENCLATURE

**Subscripts**

1 - refers to pump impeller eye; induction machine stator

2 - refers to pump impeller tip; induction machine rotor

gen - refers to generator operation

m - refers to motor operation; magnetization branch (in induction machine model)

p - refers to pump operation

t - refers to turbine operation

(imp) - refers to impeller

**Superscript**

' - refers to 'stator-referred' rotor parameters (in induction machine model)

* - refers to 'model' pump for Kittredge's turbine prediction method

Note: where no units are given, the quatities are dimensionless.

**Upper case letters**

B - effective throat width: $B^2$ - Area of the volute throat ($m^2$)

C - capacitance (F)

D - impeller diameter (m)

H - head (m)

$K_r$ - dimensionless loss coefficient for locked rotor.

N - shaft rotational speed (rpm)

P - power (W)

R - resistance (Ω)

Q - volumetric flow rate ($m^3/s$ or l/s)

T - torque (Nm)

U - impeller tangential velocity (m/s)

V - voltage (V)

V - absolute flow velocity (m/s)

$V_m$ - absolute meridional velocity (m/s)

$V_u$ - absolute tangential flow velocity (m/s)

$V_{th}$ - throat velocity $= \frac{Q}{B^2}$ (m/s)

X - reactance (Ω): $X_L$ - inductive reactance; $X_C$ - capacitative reactance

Y - Area ratio i.e. $\frac{\text{area between impeller blades at exit}}{\text{throat area of volute}}$

Z - number of impeller blades

**Lower case letters**

a - circumferential area between impeller blades ($m^2$)

$\frac{a_2}{a_1}$ - Ratio of areas: $\frac{\text{Circumferential area between impeller blades at tip}}{\text{Circumferential area between impeller blades at eye}} = \frac{V_{m1}}{V_{m2}}$

b - width of impeller flow channel in axial direction (m)

d - distance between consecutive vanes (m)

g - gravitational constant ($m/s^2$)

h - normalized head (Kittredge's method)

$h_0$ - impeller slip factor - pump operation

$h_f$ - fractional head loss (in penstock)

l - length of penstock (m)

m - normalized pump or turbine torque (Kittredge's method)

$m_p$ - slope of pump rotor characteristic

$m_v$ - slope of volute characteristic

$m_t$ - slope of the turbine characteristic

$n_q$ - specific speed (rpm) $= \frac{N\sqrt{Q}}{H^{0.75}}$ (where N is in rpm, Q in $m^3/s$ and H in m)

p - normalized power (Kittredge's method)

q - normalized flow (Kittredge's method)

$q_p$, $q_t$ - leakage flow through wearing rings (l/s)

s - electrical slip

s - thickness of impeller vane normal to vane (m)

t - circumferential thickness of impeller blade $= \frac{s}{\sin \beta}$ (m)

w - velocity of flow relative to impeller blades (m/s)

**Greek letters**

$\alpha_v$ - angle of log spiral volute

$\beta$ - impeller blade angle

$\delta$ - diametrical leakage clearance at wear ring (m)

$\varepsilon$ - factor of utilization= $\frac{\text{Energy per unit mass utilised by the turbine}}{\text{Energy per unit mass available to the turbine}}$

$\eta$ - efficiency

$\eta_v$ - hydraulic efficiency of volute

$\nu$ - normalized rotational speed (Kittredge's method)

$\nu$ - ratio of diameters: $\frac{D_1}{D_2} = \frac{U_1}{U_2}$

$\rho$ - density (kg/m$^3$)

$\phi$ - electrical phase angle

$\phi$ - flow coefficient

$\psi$ - head coefficient

$\omega$ - shaft angular velocity (rad/s); $\omega_s$ - shaft angular velocity at synchronous speed

# ABSTRACT

Centrifugal pumps have been used as turbines for various applications, particularly over the last 20 years. The aim of the current research is to investigate the use of induction motor-driven pump units for micro-hydroelectric generators, particularly for isolated generating schemes.

The research covers an assessment of the potential for the application of direct-drive pump-induction motor units to micro-hydro schemes. An investigation of the requirements of typical micro-hydro schemes has been carried out, including an economic evaluation, with particular reference to installations in developing countries. The advantages and disadvantages of a pump-as-turbine relative to other types of turbine have been assessed. Induction motors used as generators have several advantages over synchronous generators for micro-hydro schemes and have been found to be compatible with the use of pumps-as-turbines.

The main problem with the implementation of pumps-as-turbines, until now, has been the difficulty of obtaining the turbine performance of a particular pump. A review was made of the methods published so far for predicting the turbine performance of pumps, and these predicted characteristics compared with published test data for a wide range of pumps. A criterion was formulated for assessing the accuracy of these prediction methods, taking into account the hydrology and layout of a typical micro-hydro scheme. The most accurate of the existing methods was found to be the method of Sharma.

A new method for the prediction of the turbine performance of centrifugal pumps was derived from the 'area-ratio' pump design method. Tests were carried out on five different pumps and the results compared with the performance predicted by Sharma's method and by the 'area-ratio' method. This new method was found to give, on average, a more accurate turbine performance prediction than the method of Sharma. The method also has other advantages because it is based purely on geometrical data. It can therefore be used even when accurate pump performance data is not available, and can predict the effects on the turbine mode performance of certain modifications to the pump design.

CHAPTER 1

# INTRODUCTION

## 1.1 Outline of the Research Project.

### 1.1.1 Historical context of the project.

The use of water to drive rotating machinery has been a crucial factor in economic and social development for over 2,000 years. It is not certain when or where this technology was first used, but the development of different types of water wheel can be traced back to Egypt, Persia (Iran) and China (USNAS[1] and Bingli[2]). Water Power was also a crucial catalyst in the first stage of the Industrial Revolution, being the main source of mechanical power before the development of steam engines. Water power continued to be important with the invention of the reaction turbine by Fourneyron in the 1830's.

Nowadays, the main use of water power is for large hydroelectric power plants. However, these schemes require massive capital investment and technological back-up, which often makes them inappropriate for installation in developing countries. In contrast to these large projects, 'micro-hydro' schemes are designed to provide a local supply of electricity using local resources, producing outputs of up to 100 kW. They are rarely connected to an electricity generation network and are 'run-of-river' schemes, with no significant water storage. It is at this 'micro' end of the hydroelectric power spectrum that the use of standard centrifugal pumps as turbines, in conjunction with induction generators, can be applied to greatest advantage.

The design of an effective centrifugal pump was first exhibited by Appold in 1851, and further developed by James Thomson. Its complete performance characteristic, including operation as a turbine, was first described by Thoma[3], who was investigating the transient operation of a pump under conditions of sudden power supply failure.

As early as the 1930's a reversible pump-turbine was installed in a pumped storage scheme, as described by Spetzler[4]. However, this idea was not widely implemented until the 1960's. Many pumped storage schemes were built with separate pumps and turbines, partly because the technology of reversible machines would not allow them to change rapidly from pump operation to turbine operation (see Strub[5]). A Francis turbine will not operate well as a pump, but a pump will run well as a turbine. Therefore the design of a radial-flow pump-turbine is essentially

the same as that of a centrifugal pump (Meier[6]). In a turbine impeller, the blades are too short, and the channels too divergent, to operate efficiently as a pump.

The idea of using a pump-as-turbine (PAT) for a scheme without pumped storage appears to have come out of U.S. Department of Energy investigations into low-cost renewable energy supplies, following the Oil Crisis of the 1970's. Investigations were carried out by Acres American[7] and Cooper and Worthen[8] into grid-connected schemes in the 100-5,000 kW range. Later, reports by McKinney et al[9] and Marquis[10] looked at the application of various types of turbine, including reverse-running pumps, in the 5-100 kW range. Some practical information from various types of installation was gathered together by Chappell et al[11]. Other engineers, including Laux[12], McClaskey and Lundquist[13] and Apfelbacher[14], realized the application of PATs to industrial processes and in water supply systems (Steel[15], Mikus[16]) at points where a pressure reduction is required in the fluid flow. Instead of dissipating the energy in a valve, a PAT could be installed with the recovered energy used in other parts of the plant. Some limitations must be taken into account in this type of application, as noted by Taylor[17], which are due to the fixed geometry of the pump and the fact that, at low flow rates, a reverse running pump will actually absorb mechanical power, as illustrated in Fig. 1.1.

One of the main problems associated with the application of standard pumps as turbines has been the need for accurate turbine performance data. Very few manufacturers have readily available data on the turbine performance of their pumps. Other manufacturers will supply a pump for operation as a turbine only after carrying out a full performance test, for which the customer would have to pay a significant amount above the usual pump price. Much of the research into the application of pumps-as-turbines has therefore concentrated on prediction of the turbine performance from manufacturers' pump performance data, which in industrial countries, is readily available to the customer. Engels[18], de Kovats[19], Stepanoff[20] and Kittredge[21] were among the first people to propose various prediction methods. These ideas were developed by others and have been presented in the reports mentioned earlier[8-10]. A comparison of these prediction methods is included in Chapter 3 of this thesis.

Research work at Nottingham Polytechnic (formerly Trent Polytechnic) began in 1980 with the investigation of a pump provided by a local manufacturer, Worthington-Simpson. This research has become more focussed because of the development of a successful Induction Generator Controller by Nigel Smith, another researcher at the Polytechnic, and through working closely with the Intermediate Technology Development Group (ITDG), a charity which aims to transfer appropriate technologies to developing countries.

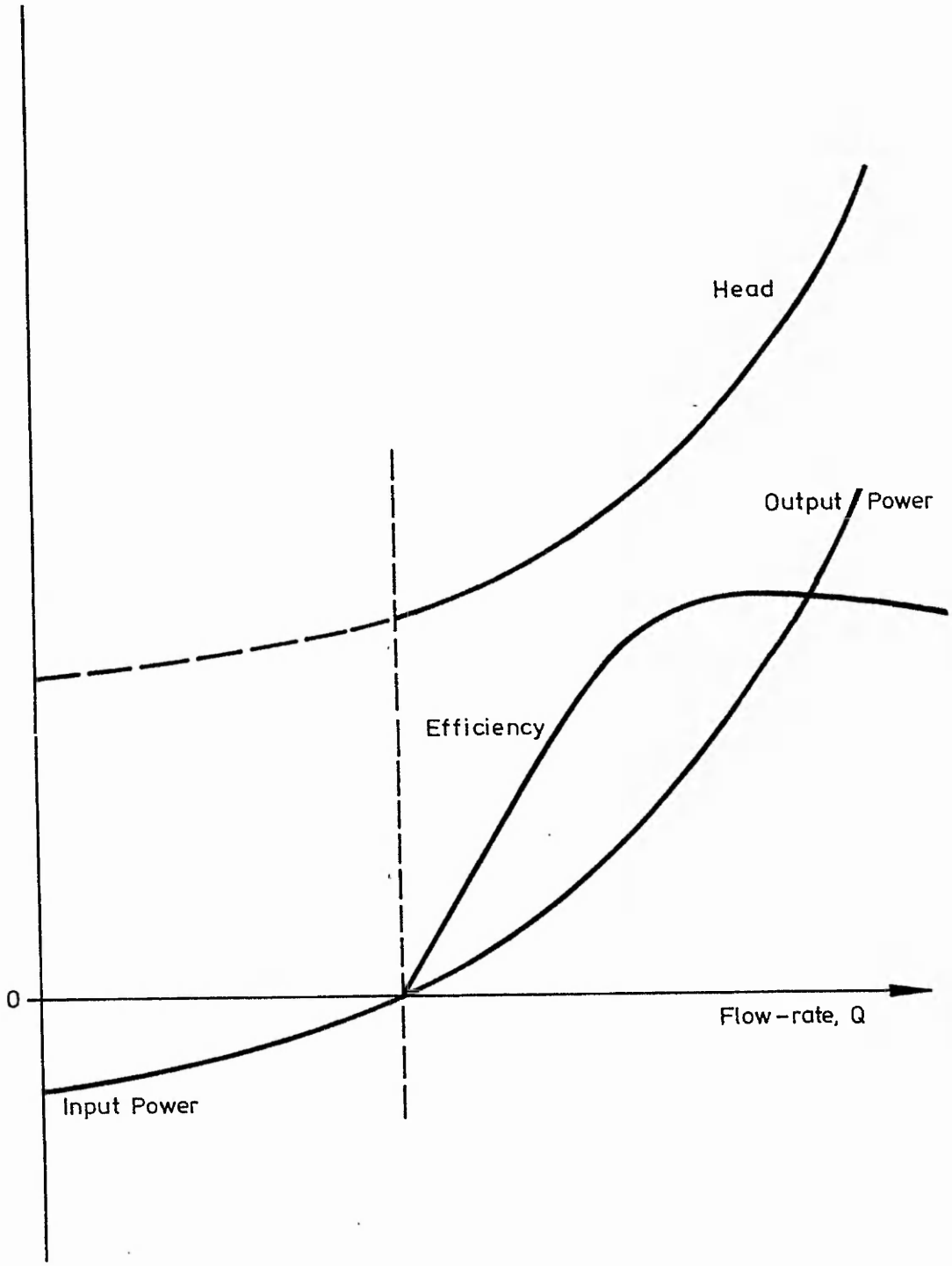


Fig. 1.1 Typical Pump-as-Turbine Curves

### 1.1.2 Aims and objectives of the research project.

The aim of the current research project is to investigate direct-drive pump-induction motor units for use as micro-hydro generators. From its outset in 1987, the project has concentrated on the use of pumps-as-turbines for isolated electricity generating systems in developing countries. The initial funding from the Polytechnic was given because of the potential benefit to development in the 'Third World'. Collaboration was set up with Sterling Fluids, through their subsidiary, Hayward-Tyler Pumps, based in Luton, UK.

After September, 1990, the research continued alongside a technology transfer project funded from the UK government's Overseas Development Administration (ODA), through ITDG. This project aims to demonstrate the technology and begin its transfer to developing countries. The investigation of pumps-as-turbines is one of three parts to the project, which aims to increase the use of induction generators for micro-hydro. The other parts are the dissemination of the technology for the Induction Generator Controller, and an investigation into Dedicated Induction Generators, ie, induction machines which are rewound for use as stand-alone generators. During this time, collaboration has been extended to two locally-based pump manufacturers, Dresser Pumps (Worthington-Simpson) and ITT Flygt Ltd. Overseas collaboration has also been set up with MECO Pumps of Lahore, Pakistan.

The objectives of this research project were as follows:-

- to determine what research has already been carried out into the use of pumps-as-turbines through a thorough literature search;
- to carry out tests on a number of complete pump-induction motor units running as turbine and generator;
- to develop a method for the prediction of turbine performance;
- to check the prediction method against test data;
- to show the feasibility of using a combined motor-pump unit together with an IGC as an isolated micro-hydro system.

## 1.2 Benefits of using Pumps as Turbines.

### 1.2.1 Advantages and limitations of using pumps-as-turbines

Standard pump units, when operated in reverse, have a number of advantages over conventional turbines for micro-hydroelectric power generation. Unlike conventional turbines, which even for small sizes are designed and made for a particular site, pumps are mass-produced. As a result, they are available for a wide range of heads and flows at considerably lower cost and with shorter delivery times

than the equivalent turbines. Spare parts such as seals, which may need replacing from time to time are easily available, especially if centrifugal pumps are in common use for irrigation or water supply. Installation of a pump-as-turbine is also simplified because the inlet and outlet connections are sized to fit standard pipe fittings.

A purpose-built water turbine is fitted with a variable guide vane (or vanes) or a spear valve, which allow the machine to run efficiently with a range of flow rates, whereas no such adjustment is possible when a standard centrifugal pump is used as a turbine. A PAT is therefore a fixed-geometry turbine, with optimum running at one set of steady-state conditions. A typical head-flow curve for a pump-as-turbine is shown in Fig. 1.1.

The range of flow rate over which a pump-as-turbine can operate is much less than that required by a conventional turbine. In most cases power is generated when the flow rate falls a little below the normal operating point (see Appendix A), but any additional flow cannot be used unless more than one pump unit is installed. The additional cost of installing more than one unit may outweigh the advantage of buying a pump instead of a conventional turbine, as shown by Nicholas[22].

### 1.2.2 Advantages of using pumps-as-turbines direct-coupled to induction generators.

When running as a turbine, the output power for maximum efficiency is similar to the rated input power for the pump. It is therefore possible to use the induction motor supplied with the pump as an induction generator when running the unit in the turbine mode. Thus the complete unit can be bought and installed as supplied from the factory, with the pump and motor already aligned. The turbine and generator come together as a unit, complete with a suitable baseplate and coupling. A PAT may be fitted with a belt drive, if required, and there are a few advantages to this configuration. The advantages and disadvantages of using a direct coupled drive are outlined in Table 1.1.

When a direct-drive electric pump is used, the rotational speed of the turbine is constrained by the speed of the generator, which is proportional to the generated frequency. In a stand-alone system, the frequency may be allowed to vary between 50 and 55 Hz for a nominal 50 Hz generator, and the speed of the turbine may therefore vary by of ±5%, as explained by Smith[23]. The power output of the turbine must also be limited to prevent overloading of the generator, either mechanically or electrically.

**Table 1.1 Advantages of a direct drive for a pump-as-turbine.**

| ADVANTAGES | DISADVANTAGES |
|---|---|
| Very *low friction loss* in drive (saving approx 5% of output power). | Fixes turbine speed to speed of generator - thus *reducing flexibility* when matching the PAT performance to the site conditions. |
| *Easier installation* - PAT and generator come as one unit. | *Limited choice of generators* available for a particular PAT. |
| *Lower cost* - no pulleys, smaller baseplate. | |
| - (for 'mono-bloc' design) simpler construction, fewer bearings, etc. | |
| *Longer bearing life* - no sideways force on PAT or generator bearings. | |
| *Less maintenance* - no need to adjust belt tension or replace belts. | |

### 1.2.3 Economic comparison of pumps-as-turbines with conventional turbine systems

One of the benefits of using a pump-as-turbine, as stated earlier, is its low cost. A comparison of costs for pumps-as-turbines against standard Pelton and crossflow turbines manufactured in Europe is shown in Table 1.2. The cost of small Francis or Kaplan turbines is much greater than for Pelton or crossflow turbines of the same power output, and they have therefore not been considered for this comparison. The table shows that using a pump has cost advantages over a crossflow turbine, but not over a Pelton turbine. The comparison of costs should be interpreted with caution, because the pump-as-turbine is not directly comparable to a crossflow or Pelton unit. One difference which can be seen from the table is that the efficiency of a turbine may be greater than, or less than, the equivalent PAT. The Pelton turbine used in the comparison has a bronze runner mounted directly on the shaft of an induction generator, with a casing which is fabricated to suit. Therefore, unlike the equivalent pump-as-turbine, this type of Pelton turbine is not a unit which is available 'off the shelf'. However, it is likely to be more efficient than a PAT, and therefore will require a smaller flow-rate for the same generated power, which may result in further cost savings by using a smaller diameter penstock.

Another difference between a standard turbine and a pump-as-turbine, which has implications for the economics of the plant, is the range of flows over which a high efficiency may be maintained. This is important when the available flow rate falls

below that required for the pump-as-turbine. A standard turbine may still be able to generate some power even when the flow-rate falls to below one-third of that required for full output, whereas if a PAT is installed, there may be periods when no electricity is available.

**Table 1.2 Cost comparison for European PATs and turbines**

| | Head (m) | Flow (l/s) | Power(elec) kW | Poles | Cost of turbine & generator (£) |
|---|---|---|---|---|---|
| PAT | 70 | 8 | 2.2 | 2 | 500 |
| 1-jet Pelton | 70 | 6 | 2.2 | 2 | 500 |
| PAT | 55 | 22 | 6.0 | 4 | 1 350 |
| 2-jet Pelton | 55 | 18 | 6.0 | 4 | 900 |
| PAT | 18 | 13 | 1.1 | 4 | 570 |
| 3-jet Pelton | 18 | 13 | 1.1 | 4 | 470 |
| PAT | 55 | 20 | 5.7 | 2 | 750 |
| 3-jet Pelton | 55 | 19 | 5.7 | 2 | 650 |
| Submers. PAT | 25 | 42 | 5.5 | 2 | 1 200 |
| Crossflow | 25 | 38 | 5.5 | 4 | 3 000 |
| PAT | 20 | 130 | 18.5 | 4 | 1 750 |
| Crossflow | 20 | 140 | 18.5 | 4 | 4 000 |

## 1.3 Application of pumps-as-turbines to micro-hydropower.

### 1.3.1 Types of pump suitable for micro-hydro application.

Investigations on various types of pump as turbine suggest that there are several which are suitable for micro-hydro, running in reverse with an induction generator. Of the main types, end-suction centrifugal pumps are nearly always suitable for this application. Axial-flow pumps are suitable for low-head applications, but small sizes (below 30kW) are not commonly available. A summary of the other types of pump is shown in the attached chart (Fig. 1.2).

End-suction centrifugal pumps are the most commonly available, used extensively for water supply and irrigation. They are of relatively simple design, and are easily maintained. In-line and double-suction pumps may be suitable but sometimes they have considerably lower efficiencies in turbine mode. Some small centrifugal pumps do not have a spiral volute, but a simple round casing with an angled outlet pipe (see section 1.3 of chapter 5). Although this type of unit may have a high pump efficiency, it has been found to run inefficiently as a turbine.

STANDARD CENTRIFUGAL PUMPS

END-SUCTION PUMPS – SUITABLE

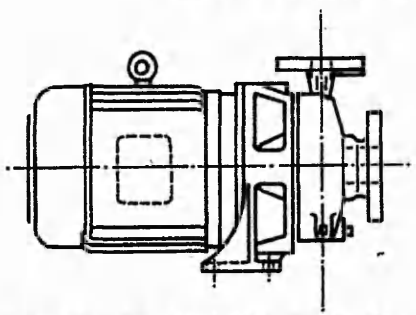

Close-coupled ('Monobloc')

or

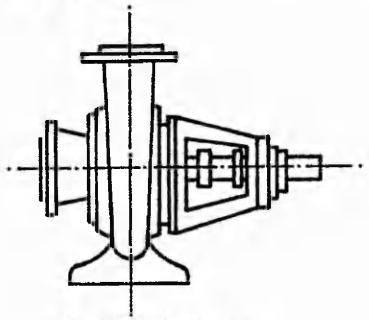

Pedestal Type

DOUBLE-SUCTION PUMPS - MAY BE SUITABLE

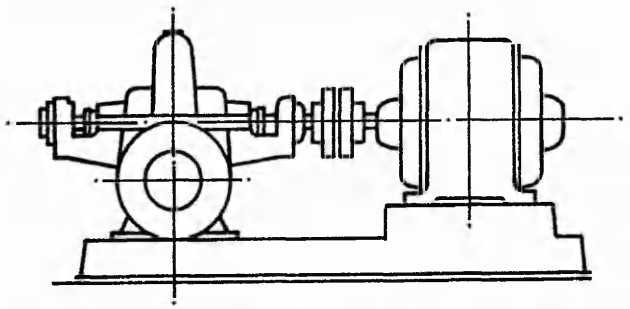

May have low efficiency in Turbine mode

SUBMERSIBLE PUMPS

Dry-motor (pump below motor)

Remove strainer for turbine operation

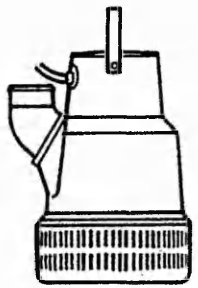

JACKET-COOLED
-MAY BE SUITABLE

Wet-motor (pump above motor) NOT USUALLY SUITABLE for various reasons

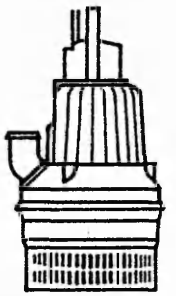

FIN-COOLED
-NOT SUITABLE
Can only run fully submerged

Fig. 1·2 Pumps suitable for use as Turbines

A centrifugal pump may have its own bearings, or may be close-coupled to an induction motor which contains the necessary bearings. Close-coupled units are sometimes referred to as 'monobloc' pumps. On smaller sizes of end-suction pump, the impeller is screwed on to the shaft. However, the impeller will not unscrew in turbine mode, unless a solid object causes the impeller to stick, because the torque is applied in the same direction as in pump mode. Care must be taken with certain types of seal which incorporate a spring, to ensure that the spring will operate effectively with reverse rotation. Self-priming pumps are not suitable for PATs since they contain a non-return valve which prevents reverse flow.

Dry-motor submersible pumps are widely used for construction site drainage and for pumping from open wells. The motor is integral with the pump, and is cooled by the pumped water flowing either through a jacket or across fins on the motor housing. Those with fin-cooling are not suitable for use as turbines, as they will overheat unless submerged below water level. Also, some pumps of this type have rubber linings on the diffuser parts, which may prevent the impeller from running in reverse. Wet-motor submersible borehole pumps are of a more specialised design and may not be suitable for use as turbines. They usually contain a non-return valve, and may also incorporate a thrust bearing designed only for pump operation.

Many small centrifugal pumps have the impeller made from carbon-impregnated nylon. This material is satisfactory for use in a PAT, as long as there are not many hard particles in the water. The material for the pump volute is usually cast iron. If the inside of the casting is very rough, there will be increased volute losses in turbine operation, when the flow velocities are higher than in pump mode.

Although tests by Yang[24] show that for the particular type of pump tested the axial thrust in turbine mode is lower than in pump mode, additional bearing wear may be a problem when running a pump-as-turbine. Bearing wear was found to be a problem on belt-drive pumps-as-turbines installed in Northern India, and also in Pakistan (see Appendices B and C). On direct-drive units there is less likely to be a problem, since there is no radial load on the bearings.

Both mechanical seals and stuffing glands have been found to operate satisfactorily in turbine mode. Stuffing glands are used in many developing countries because of their low cost, and the availability of replacement material. Mechanical seals are preferred where they can be obtained easily from the pump manufacturer, since they require less maintenance, as long as they are correctly fitted, and cause less resistance to the rotation of the pump shaft.

### 1.3.2 Head and flow range for pumps-as-turbines

Standard centrifugal pumps are manufactured in a large number of sizes, to cover a wide range of heads and flows. Given the right conditions, pumps-as-turbines can be used over the range normally covered by multi-jet Pelton turbines, crossflow turbines and small Francis turbines. However, as shown in section 1.2.3, for high head, low flow applications, a Pelton turbine is likely to be more efficient than a pump, and no more expensive. The greatest cost advantage is obtained for the part of the PAT range where a crossflow turbine would be required. A small Francis turbine could also be used in part of this range, but would be even more expensive than a crossflow turbine.

The chart in Fig. 1.3 shows the range of heads and flows over which various turbine options may be used. The range of pumps-as-turbines is based on the pumps produced by a major manufacturer in Pakistan, driven directly by a 4-pole induction motor. The turbine performance is based on the prediction method of Sharma, as described in chapter 3. The range of Pelton and crossflow turbines shown is based on information supplied by Waltham[25] about the range of turbines manufactured in Nepal. A larger range of heads and flows is possible by using PATs with 2-pole and 6-pole generators. The range for a UK manufacturer of monoblock pumps is shown in Fig. 1.4. This diagram also shows the range of submersible dewatering pumps when operating as turbines.

### 1.3.3 Typical applications of pumps-as-turbines

The simplest micro-hydroelectric systems are those which have a fixed electrical load. This type of system is commonly used in developing countries, where the generator is often used to supply lighting for a few hours each evening. All the lights come on at the same time and are switched off at the same time, so that the power produced by the turbine is constant, and the speed and voltage remain stable. In order to allow loads to be switched on and off, a load controller has been designed which diverts spare power to a set of 'ballast' loads - usually electric heaters. Electronic Load Controllers were first used in conjunction with synchronous generators, as described by Holland[26]. With the development of the Induction Generator Controller (IGC), it is now possible to use a combined pump and induction motor unit for micro-hydroelectric generation with a variable load. Details of the IGC, and its effect on the operation of a PAT, are given in Chapter 2.

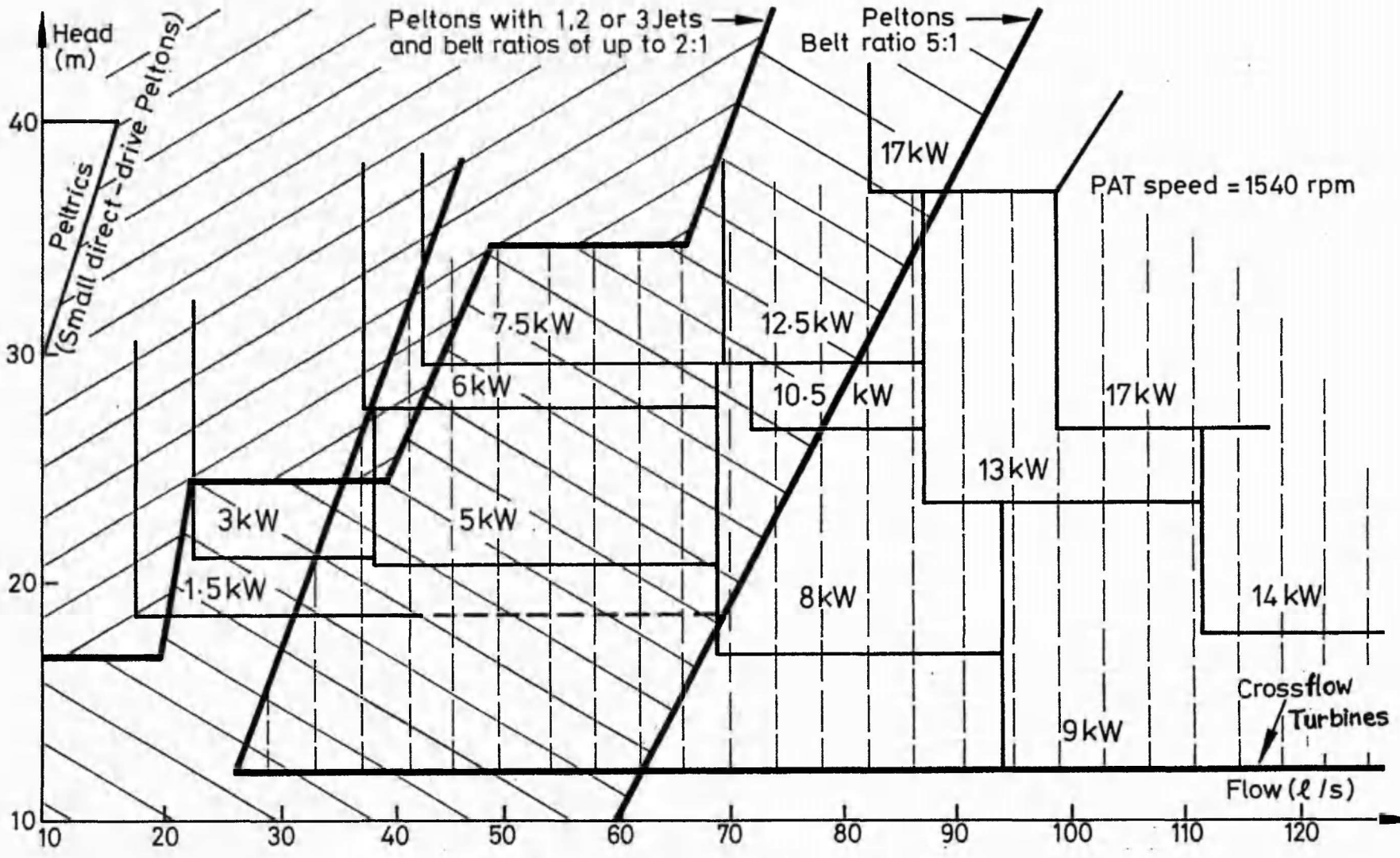


Fig. 1·3 Estimated head-flow range for Peco Pumps-as-Turbines compared with crossflows & Pelton Turbines

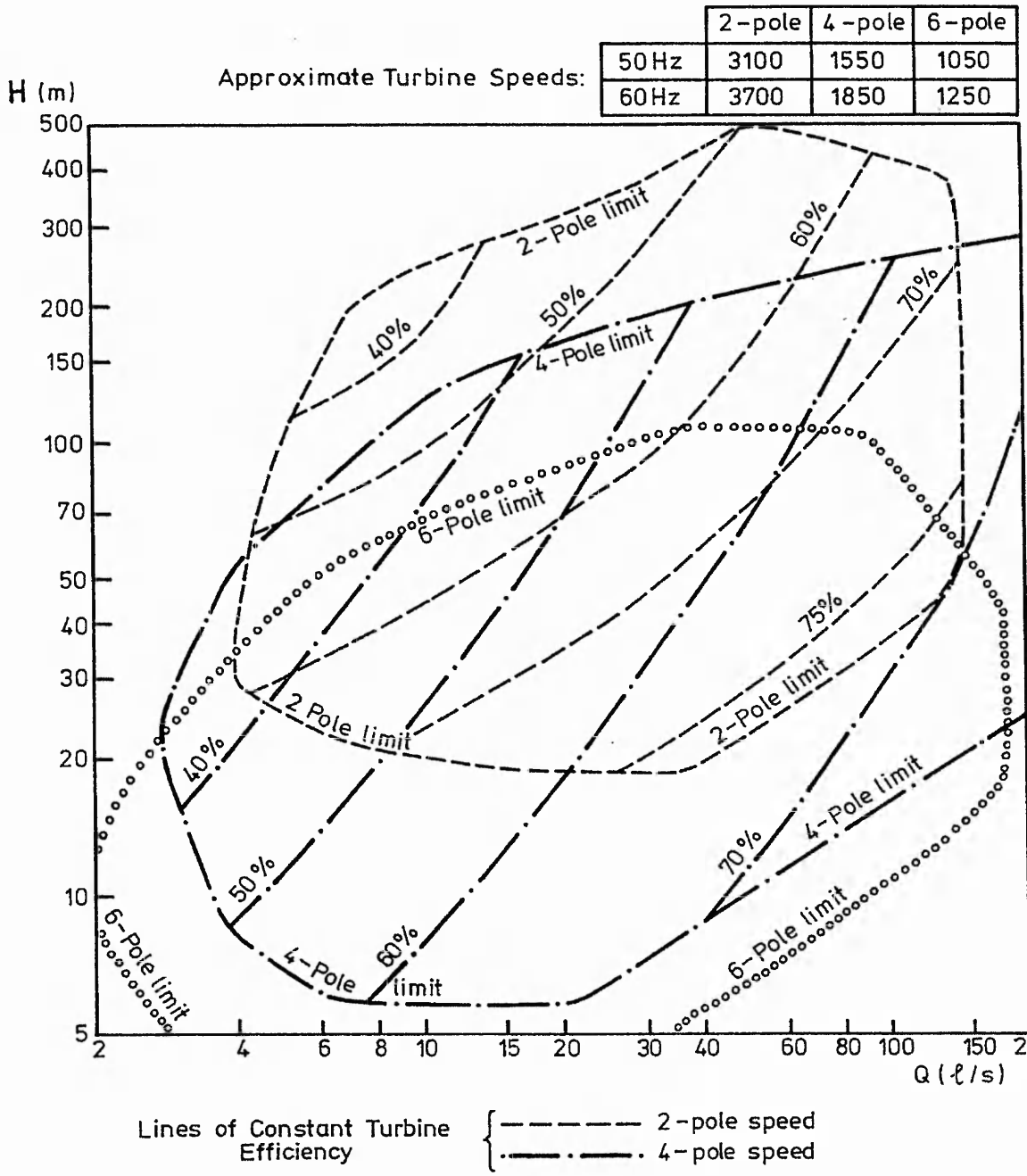


Fig.1-4 Application range of standard centrifugal pumps as turbines

Taking into consideration the limitation of having a fixed flow rate when using a pump-as-turbine, the most appropriate application is where a sufficient supply of water is available throughout the year. For a micro-hydro scheme it is very rare to have any long-term water storage capability, because of the high cost of constructing a reservoir. In many village schemes in developing countries, where the main electric load is lighting in the evening, a pump-as-turbine is suitable. During the daytime, the generator can also be used to power equipment which will benefit the economy of the village, eg. a circular saw, crop dryer or sewing machines. In this type of scheme, the PAT will be designed to run using the flow available at the driest time of the year. Sometimes, where only lighting loads are important, the water supplying the micro-hydro scheme is used during the daytime for irrigation or for running a water mill for grinding corn.

In more temperate climates, a PAT can be used to provide electric power for background heating. In this case, it is not essential that the power is available continuously, and by using a special intake and a small storage tank, it is possible to allow the PAT to run intermittently. The system is described in more detail by Noyce[27]. This arrangement could also be used for charging batteries, which has become a popular means of supplying rural electricity in some countries, for example Sri Lanka (see Hettiaratchi and Brown[28]).

Pumps-as-turbines can also be used for pumping water for domestic use, where a farm or village is situated above the main stream level. In this case the PAT is connected directly to a centrifugal or positive displacement pump, which pumps a small quantity of water to a high head, an example of which is given by Ndeuwo[29].

## 1.4 Appropriate Technology aspects of the Research Project

### 1.4.1 Micro-hydro power in developing countries

Given the lack of infrastructure in many of the non-industrial countries of the world, the choice of technology for water power and the manner in which the technology is implemented, may have beneficial effects or may be detrimental to overall development. The concept of 'appropriate technology' has been developed from the ideas of Fritz Schumacher[30], who brought human and environmental factors into the economic assessment of development projects. Appropriate Technology has been defined more rigorously in a recent ITDG report[31] as any productive process or any piece of equipment which meets all of the following criteria:

- it meets the needs of the majority, not a small minority, of a community;
- it employs natural resources, capital and labour in proportion to their long-

term sustainable availability;

- it is ownable, controllable, operable and maintainable within the community it serves;
- it enhances the skills and dignity of those people employed by it;
- it is non-violent both to the environment and to people;
- it is socially, economically and environmentally sustainable.

Many developing countries have considerable untapped hydroelectric resources which could be harnessed by installing large modern schemes, each producing several thousand megawatts of electrical power with an enormous reservoir and dam. Such schemes at present contribute more than 20% of the world total of generated electricity but they often have disastrous effects on the people and the environment in the locality of the reservoir, as highlighted by Monosowski[32] and also in a recent study by Raphals[33]. Problems associated with large hydro-electric schemes include loss of productive land, leading to poverty and disruption of the local economy; silting up of the reservoir and loss of fertility in the area of the downstream floodplain; creation of adverse micro-climates and endemic conditions for water-borne diseases (see Jobin[33]). National economic and political problems may also result from the accumulation of large debts, and the need to make agreements with neighbouring countries, for example between Hungary and Czechoslovakia, as described by Borsos[35]. This type of technology is therefore far from the level which is appropriate for a poor country with little technical resources.

In developing these large schemes, governments, aid agencies and international organizations have accepted certain assumptions concerning the relationship between electrification and rural development. An analysis of the experience of rural electrification in Bolivia, Costa Rica and the Philippines, led Jackson[36] to the conclusion that electrification has no significant impact on rural development unless the following conditions are fulfilled:-

- there is sufficient demand for electricity to enable it to be affordable by a large proportion of the local people;
- there is potential for productive use of electricity in the long term;
- electrification is co-ordinated with other aspects of an integrated development programme.

It is also important to recognize that economies of scale do not necessarily hold for hydro-electric schemes in developing countries. In terms of capital, a micro-hydro scheme employing local skills and materials costs around $1,000 per kW(Hislop[37]), which is nearly half the figure of $1,900 which the World Bank has calculated to be

the average cost of electricity supply in developing countries (Munasinghe[38]). It also compares favourably with the cost of between $1,250 and $3,000 per kW for schemes in the 30-250 kW range, published by the Water Energy Commision of Nepal[39].

Figures for Tanzania given by Brown and Howe[40] show that where there is a possibility of installing a micro-hydro scheme, the electricity produced is likely to be cheaper than that produced by a wind or diesel generator, or supplied by a grid extension to a rural area. The comparitive costs, which are given in more detail in a previous paper[41], are shown in Table 1.4.

**Table 1.4 Comparison of generation costs for rural supply in Tanzania**

| | Micro-Hydro (15 kW) | Wind Power (10 kW) | Diesel Gen. (6 kW) | Grid Extension (300 houses) |
|---|---|---|---|---|
| Installation cost (000's shillings) | 136 | 484 | 320 | 2,180 |
| Life length (years) | 20 | 15 | 10 | 20 |
| Cost/kWh (incl. fuel & maintenance)(s.) | 0.74 | 1.66 | 2.34 | 1.58 |

**(1978 prices: 1s. = US$ 0.12)**

In Nepal, the only practical alternative to micro hydro is generation using diesel. Table 1.5 shows the cost of a scheme using a crossflow turbine compared with the cost of generation using diesel and the cost of kerosene lighting. Although in this case the turbine is used during the daytime to drive agro-processing machinery, the full cost of the installation has been used to calculate the cost of electric lighting.

**Table 1.5 Comparison of costs for household lighting in rural Nepal.**

| | | Micro-hydro | | Diesel Generator |
|---|---|---|---|---|
| Crossflow turbine: | | 18,000 | | |
| Generator & control panel: | | 30,000 | | 50,000 |
| Penstock & trashrack: | | 12,100 | | |
| Total Equipment Cost: | | 60,100 | | 50,000 |
| Civil Works: | | 96,000 | | |
| Generator House: | | 15,000 | | 15,000 |
| Installation: | | 5,000 | | 1,000 |
| Transmission: | (400m) | 16,500 | (100m) | 6,500 |
| Land: | | 5,000 | | 2,000 |
| Transport: | | 2,500 | | 2,500 |
| **Total Capital Cost (Rs):** | | 200,100 | | 77,000 |
| Annual Interest on above: (17%) | | 34,017 | | 13,090 |
| *Depreciation:-* | | | | |
| Equipment: (5%) | | 3,005 | | 2,500 |
| Civil Works: (5%) | | 5,550 | | |
| Transmission Line: (3%) | | 495 | | 195 |
| *Repair & Maintenance:-* | | | | |
| Equipment: (3%) | | 1,803 | (20%) | 10,000 |
| Civil Works: (5%) | | 5,550 | (3%) | 450 |
| Lubrication: | | 200 | | 3,600 |
| + Fuel Cost @ Rs 7.5/l x 5 hrs x 365 days x 3.5 l: | | | | 47,905 |
| **Total Annual Cost:** | | 50,420 | | 77,740 |
| **Cost/kWh:** (5 hr/day, 10 kW) | | Rs 2.76 | | Rs 4.26 |

**Kerosene Lamps:** 100 W electric lamps replace 3 lamps each burning 0.05 l/hour

At Rs 6/litre = 10 x 6 x 3 x .05 = Rs 9.00/kWh

**Note:** The price of diesel oil and kerosene increase with distance from the nearest road, due to portering costs of Rs 50 per 30 kg per day. At four days' walk from a road (not unusual in Nepal), costs become Rs 6.54/kWh for diesel generation, and Rs 18.6/kWh equivalent for kerosene lighting.

Above costs are for 1988: **£1 Sterling = 45 Nepali Rupees.**

### 1.4.2 Development of micro-hydro in Nepal

The development of micro-hydropower in many countries has been a process of improvement and modernization of a technology which has been in use in agricultural communities for many centuries. From Peru to China, water mills are used for grinding corn in order to save human muscle power. In Nepal, for example, there are an estimated 20,000 small mills, which are driven by traditional vertical-axis *'ghattas'*, the layout of which is shown in Fig. 1.5. The history of the development of micro-hydropower in Nepal has been well documented by Hislop[42]. The specific aspects of this development which have resulted in the application of appropriate technology will be presented in this section.Much of the impetus for the development of micro-hydropower in Nepal has come from within the country. Where overseas organizations have been involved, they have had a long-term committment to developing a locally-based industry. Through training people in appropriate skills, new ideas have come from within Nepal. The traditional *'ghatta'* technology was developed by a Nepalese entrepreneur and became the basis for low-cost micro-hydro, as described by Shrestha and Singh[43].

The availability of credit has been important, since micro hydro schemes require a relatively long-term investment. In Nepal, the Agricultural Development Bank has not only provided credit, but has also helped with training, which is crucial to the successful dissemination of appropriate technology (Wishart[44]). Limited government subsidies have also helped to generate an initial market for equipment, but Waltham[45] points out the negative impact which indescriminate government subsidies could have on the development of the technology. The trend towards using micro-hydro technology has occurred over a period of more than ten years, beginning with schemes with a small add-on generator, and growing to include 10 schemes supplying continuous electricity by 1991. Artificially stimulating demand at this stage may result in the market being flooded by imported equipment, which would undermine the development of the local industry.

The development organizations involved in micro-hydro in Nepal have attempted to monitor the effects of its implementation to ensure that it is of benefit to people other than just the mill owners and turbine manufacturers. The use of local monitoring has been beneficial in this respect, because it has enabled an evaluation based not only on technical and financial success, but on a range of issues,. Pandey and Cromwell[46] found that non-technical factors, such as social organization, have a significant effect on the success of micro-hydro schemes.

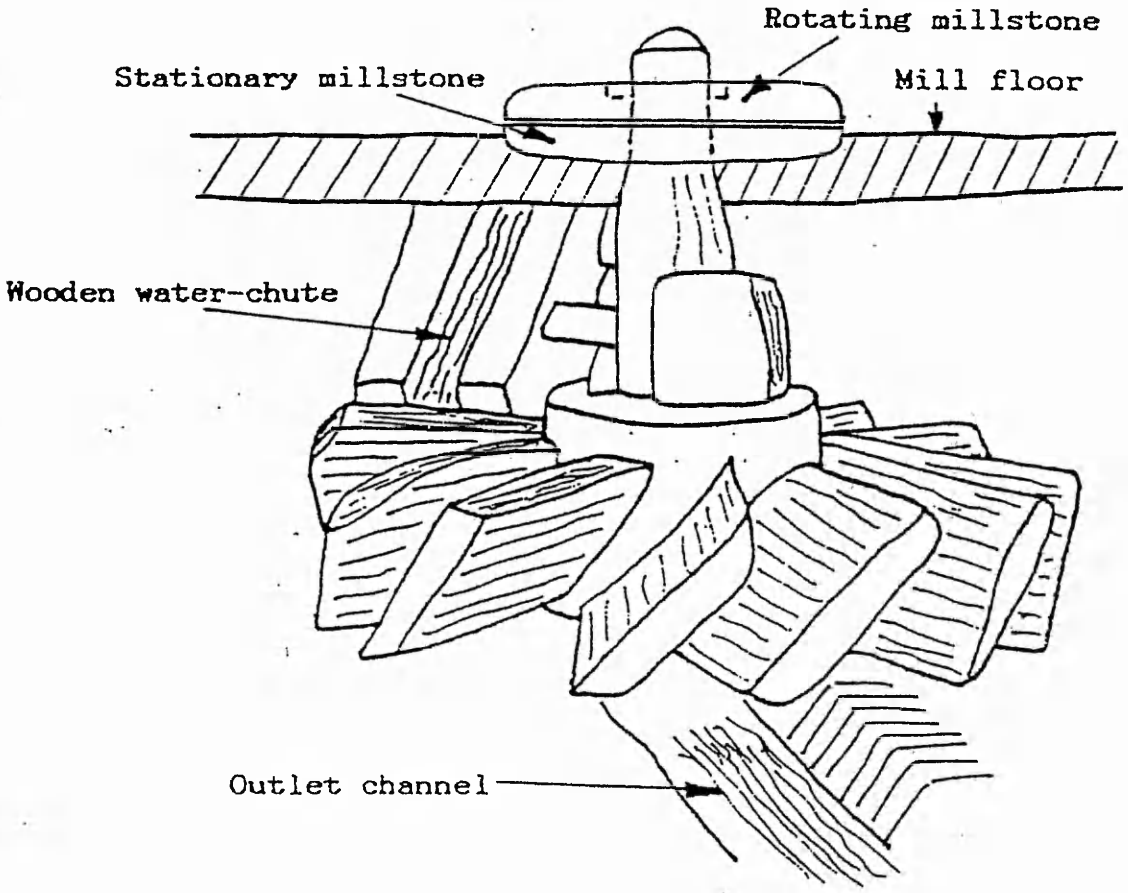


Fig. 1.5. Layout of traditional Nepalese Water Mill

The introduction of pumps-as-turbines would not be appropriate in Nepal, because there are no pump manufacturers in the country. However, the popularity of a newly-developed direct-drive Pelton turbine and induction generator unit (Smith et al[47]) shows that there is a market for a standard micro-hydroelectric set for generating 5 kW or less.

### 1.4.3 Development of micro-hydro in Pakistan

In Northern Pakistan, as in Nepal, water power has been used traditionally for grinding corn. The development of micro-hydroelectric power began with the initiative of the government's Appropriate Technology Development Organization (ATDO)[48], which set up a workshop for manufacturing crossflow turbines, the first of which was installed in 1976. Initially, the ATDO covered the cost of the equipment and gave technical assistance, while the villagers built the civil works, assisted with the installation, and were responsible for managing the scheme once it was installed. As the technology became accepted on a wider scale, the amount of government subsidy was reduced.

By 1988, 85 plants had been installed, but only 37 of these were in operation. Junejo[49] gives the reasons for the number of inoperative schemes as one-quarter technical and three-quarters institutional. ATDO, now known as the Pakistan Council for Appropriate Technology (PCAT), has recently completed a new workshop for turbine manufacture, with the help of a grant from USAID. The local management problems associated with the schemes do not appear to have been given much attention, and according to Meier[50], there are more enquiries than the field staff can investigate.

In contrast, the work of the Aga Khan Rural Support Programme (AKRSP) in the far north of the country has concentrated more on organizational than on technical matters. The approach of the AKRSP, described in a paper by Conroy[51], is to encourage the villagers to work co-operatively through forming Village Organizations (VOs). AKRSP then provides a grant and technical assistance for the VO to build a productive physical infrastructure project. Often this is a link road or irrigation canal, but since 1983 assistance has also been given for the installation of 18 micro-hydro schemes.

Most of the schemes use simple axial-flow turbines, locally manufactured; crossflow turbines and four pumps-as-turbines have also been installed. The PAT schemes, one of which is described in Appendix C, use Pakistani-made radial or axial-flow pumps and belt driven synchronous generators rated between 3 and 10 kW. A test site has also been set up, where a Pelton turbine and crossflow turbine have been installed.

A pump-as-turbine scheme has also been installed in collaboration with ITDG (see Appendix D). It was hoped to make this a demonstration site for an induction generator, but the AKRSP engineers are cautious about installing a new type of generator before they are fully familiar with the technology themselves. Engineers from AKRSP are visiting Nepal during 1992 in order to learn about induction generator technology.

AKRSP are keen to install more and larger schemes with the aim of using electricity for more than just lighting. In particular, for remote villages, the installation of electric cookers would take pressure off limited fuelwood resources. In 1991, a crossflow turbine capable of producing over 30 kW was installed at the village of Ahmedabad. In this case, finance was raised by the Village Organization, and only technical assistance was necessary from AKRSP.

### 1.4.4 Appropriate technology for micro-hydropower: Conclusions.

The installations in Nepal and Pakistan show that the introduction of micro hydroelectric power is most successful when co-ordinated with other aspects of development. Electric lights will only improve the quality of life in a remote village if there are other resources available. Given the right conditions, even a small quantity of electricity may bring many benefits - for example, enabling people to study in the evenings, or carry out craft work which can generate additional income. During the daytime, electricity may be used for small industries, for refrigeration of vaccines at a village health centre, and also for cooking. Through the development of low-wattage storage cookers, it is hoped to be able to use micro-hydropower to replace the use of firewood, which is becoming a scarce resource. Brown[52] has shown that the widespread use of electric cookers could make a significant change to the rate of deforestation in a country such as Nepal.

Implementing technology in a manner which will bring long-term benefits to the poorest people requires step by step progress and careful monitoring. Demonstrating the technology and providing appropriate training are two of the most important requirements for disseminating an appropriate technology. Equipment supplied from Europe will not be affordable by a large number of people in a developing country unless it can be manufactured, or at least assembled, in that country. It is therefore necessary to train engineers from developing countries in the design and manufacture of equipment. These engineers can then train technicians to install the equipment and also train local people in maintenance, so that the technology is sustainable at remote sites.

It is also important that the equipment is proven, and that all major design faults have been eliminated before it is taken to a village site. News of the failure of one scheme soon spreads to other villages, and the technology is then likely to be rejected. Setting up a demonstration scheme which can be closely monitored can prevent later difficulties in disseminating a new technology. In the case of pumps-as-turbines used with induction generators, a demonstration scheme has been installed in North Yorkshire. This scheme, which is described in Appendix E, used different types of pump unit, including one which was imported from Pakistan, in order to provide experience of running this type of equipment at an isolated site.

In the context of appropriate technology, the installation of pump-as-turbine schemes has sometimes been seen as a bridging phase, as it was in Tanzania[29]. This is because crossflow and Pelton turbines offer more opportunity for manufacture in regional workshops. One of the main difficulties in using pumps-as-turbines has been the matching of turbine performance to site conditions and generator characteristics, as was observed in Pakistan (see Appendix C) and in Nepal (see Appendix F). The investigation of pump-as-turbine performance prediction is therefore of more than practical interest, particularly considering the cost advantage that a PAT has over a crossflow turbine.

CHAPTER 2

# INDUCTION GENERATORS AND THE INDUCTION GENERATOR CONTROLLER

## 2.1 Induction Generator Performance

The advantages of using induction generators for micro-hydro have already been outlined in section 1.1. Before considering the use of this type of generator with pumps-as-turbines, an explanation of the performance characteristics will be presented.

### 2.1.1 Theory of Induction Generator Operation

The performance characteristic of an induction machine is illustrated most simply by considering the torque-slip curve. The machine slip is defined as:

$$s = \frac{\omega_s - \omega}{\omega_s} \tag{2.1}$$

The equivalent circuit of an induction machine is the same for both motoring and generating operation. The usual equivalent circuit is shown in Fig. 2.1. From this, the electromagnetic torque produced by the machine, as shown by Hindmarsh[53], is given by:

$$T_e = \frac{k_t R_2'}{s} \cdot \frac{1}{\left(\frac{R_1 + R_2'}{s}\right)^2 + (X_1 + X_2')^2} \tag{2.2}$$

where $k_t = \frac{3V_1^2}{\omega_s}$

The torque-slip characteristic for $s<0$ is thus a mirror image of the characteristic for $s>0$. Therefore, in order to run as a generator, the machine must be driven above synchronous speed. A typical induction machine torque-slip characteristic is shown in Fig. 2.2.

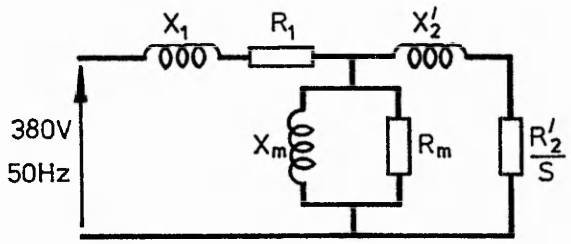


Fig. 2·1. Equivalent circuit of Induction Machine

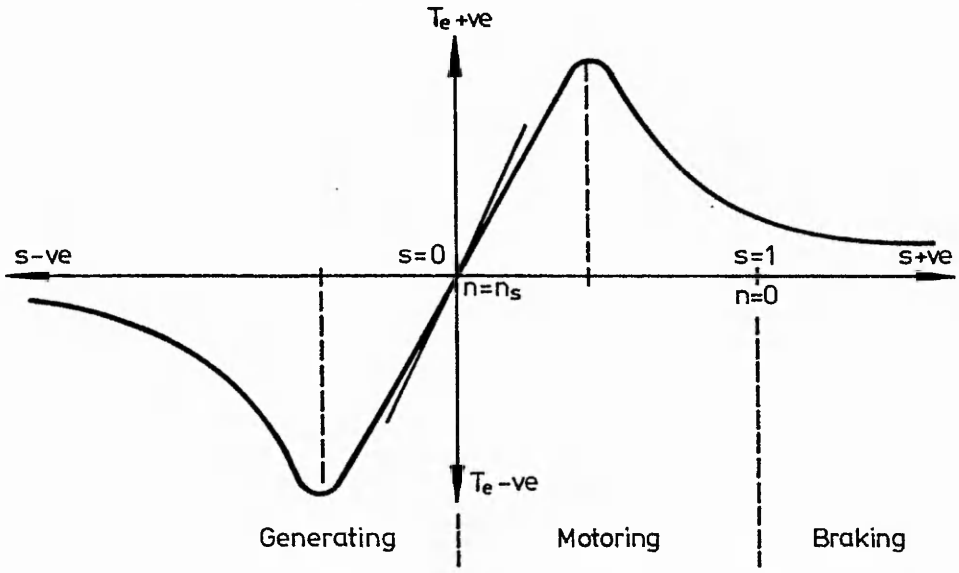


Fig. 2·2 Torque-slip characteristic of Induction Machine

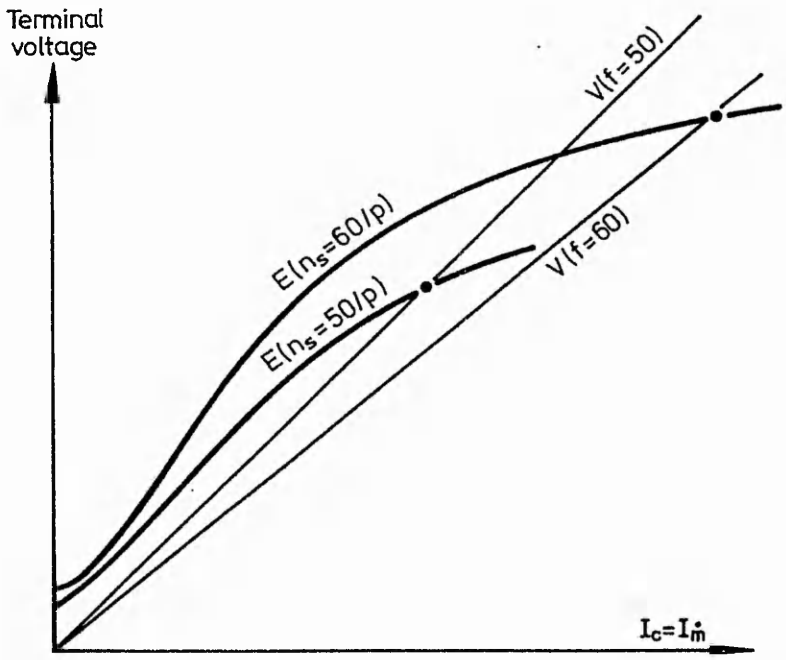


Fig. 2·3 Voltage-current characteristic showing the operating point of a self-excited induction generator

For an induction generator which is being run stand-alone, the magnetising current, $I_m$, must be provided by an excitation capacitor placed across the output terminals of the machine. If the generator load is purely resistive, then the current flowing through the excitation capacitance must equal the reactive current flowing in the generator.

### 2.1.2 Determination of the Excitation Capacitance

As an example to illustrate the determination of excitation capacitance for an induction generator, let us consider a standard 4-pole motor which was tested in the Polytechnic. The simplest method for determination of the excitation capacitance, $X_C$, is to use the manufacturer's quoted power factor for rated output. The motor is rated as a star-connected, 3-phase, 415 V, 2.2 kW unit. The rated load current is 4.7 A at 0.82 power factor.

With the motor used as a generator, the stator windings were connected in delta to produce a 240 V, 3-phase output. The overall reactance of the motor at full load is given by:

$$X_L = \frac{V}{\sqrt{3}\, I_{line} \sin\phi} \qquad (2.3)$$

$$= \frac{240}{4.7 \sin\left(\cos^{-1} 0.82\right)} = 89.3\ \Omega/\text{phase}$$

For generation into a purely resistive load, the value of $X_C$ must equal the value of $X_L$. For generation at 240 V, 50 Hz, the value of excitation capacitance is therefore:

$$C = \frac{1}{2\pi \times 50 \times 89.3} = 36\ \mu\text{F/phase}$$

In order to produce rated voltage at the output of the generator, the voltage across the magnetising branch, $V_m$, must be greater than $V_{rated}$ (see Fig 2.1). As a motor, $V_m < V_{rated}$ due to the voltage drop across $R_1$. Hence, the magnetising current is greater when the machine is generating, than when it is used as a motor, and the value of C required is greater than that calculated from the motor power factor. In this case, it was found that C needed to be 55 μF, rather than 36 μF as calculated previously. It appears that the manufacturer's quoted figure for power factor is optimistic, and that the machine is highly saturated when operating in generator mode, hence the high value of excitation capacitance required. A comparison between rated motor data, and generating conditions for a Δ-connected 2.2 kW, 4-pole machine is shown in table 2.1.

### 2.1.3 The process of self-excitation

When an induction machine is rotated initially , there is a very low voltage across the output terminals. This is caused by the remanent magnetism of the rotor cutting the coils of the stator circuit. The generator is thus acting as a synchronous machine with a very weak permanent magnet rotor. The voltage in the stator circuit will increase with the speed of rotation of the machine, resulting in a magnetising current through the capacitor. This current increases more rapidly if the remanent magnetism is stronger. At a certain speed, depending on the value of the capacitance, the current will be great enough to cause self-excitation to occur. The actual operating point as an induction generator is determined by the intersection of the machine magnetization characteristic with the voltage-current line determined by the excitation capacitance, as shown in Fig. 2.3. A more detailed analysis of the self-excitation process is given in a paper by Elder, Boys and Woodward[54].

If the remanent magnetism is weak, self-excitation may be induced by increasing the value of the excitation capacitance, and by running the machine above its normal running speed. Whether or not the machine has enough remanent magnetism for the build-up of self-excitation to commence under normal conditions depends on several factors, in particular the permeability of the iron at low flux levels. In general, the remanent magnetism will be lost if the machine has been allowed to come to a standstill as a generator with the load connected, because the generator will run at a high value of slip, causing the flux in the rotor to cycle. The remanent magnetism may also be lost due to knocks during transport. However, with certain induction machines, eg. those made in China, it has been found to be almost impossible to lose the remanent magnetism of the machine. In all cases, remanent magnetism may be reintroduced by connecting a 12-volt vehicle battery to the machine terminals; often, with small generators, a 1.5-volt dry cell battery will give enough current to achieve this.

### 2.1.4. Stand-alone generator connections.

For very small sizes, usually below 3 kW, induction motors are available for single-phase or three-phase operation. There are several types of single-phase motors which can be used as induction generators. Three common types with their generator connections are shown in Fig 2.4. Apart from very small motors, all single-phase induction motors have an auxiliary winding which is needed in order to produce a rotating field, but in some cases this winding is not rated for permanent use and must be disconnected when used as a generator. In other cases a centrifugal switch is used to disconnect a start capacitor once the motor has run up to speed.

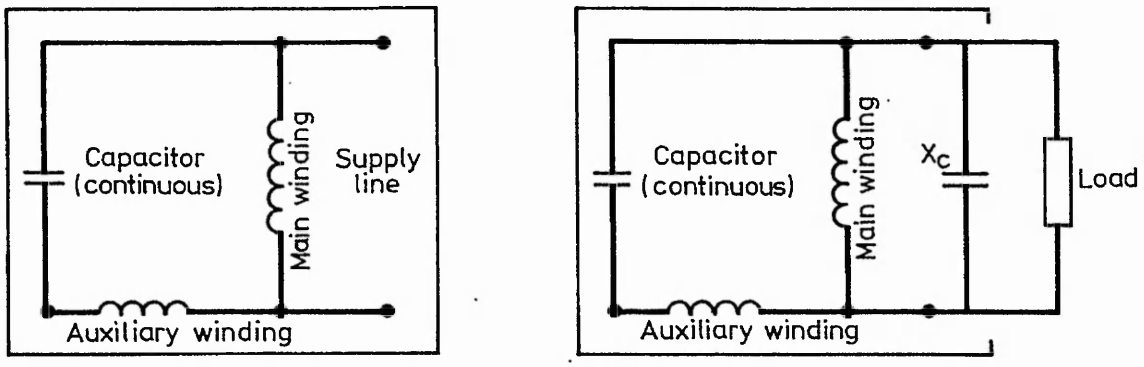


Type 1 Permanent capacitor motor

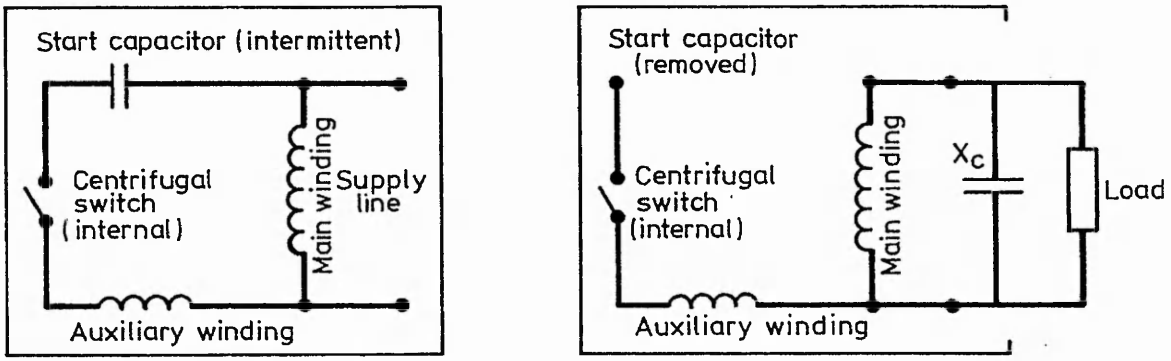


Type 2 Capacitor-start induction-run motor

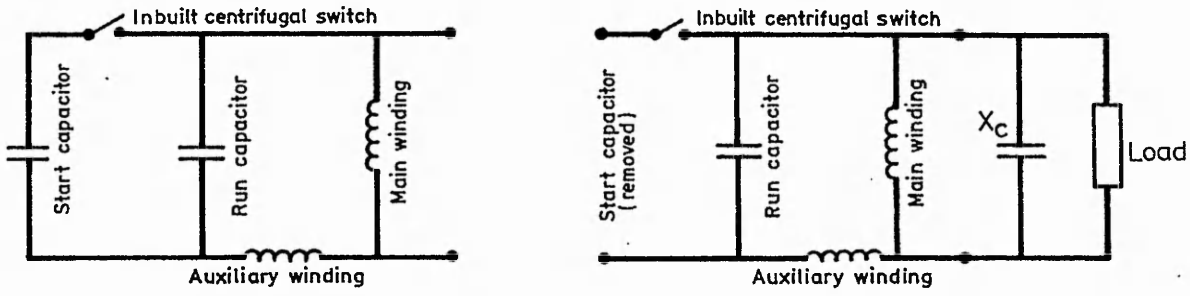


Type 3 Capacitor-start capacitor-run motor

Fig. 2.4 Generator connections for Single-phase induction machines

This is to improve the starting torque of the motor, but must be disconnected when the machine is used as a generator. The types of machine with a permanently connected auxiliary winding (types 1 and 3 in Fig. 2.4) are likely to be more efficient than type 2 when used as a generator.

For larger sizes of motor, only three-phase units are available. However, for stand-alone generation, it is often useful to be able to produce a single-phase output. This simplifies the distribution system, and eliminates the need for balancing the load between three different phases. A three-phase induction generator can be connected to produce a single-phase output using the 'C-2C' method described by Bhattacharya and Woodward[55]. This requires a motor which has been wound for star connection to a three-phase supply. The machine is then connected in delta as a generator, with two capacitors connected across two of the phases as shown in Fig. 2.5. The capacitor across R-B phase has twice the value of the capacitor across Y-R phase. The load is connected to the Y-R phase, and for full-load, the phase currents will be balanced. In order to cope with a load power factor of 0.8, it has been found to be necessary to derate the generator by at least 20% when using the 'C-2C' connection. This connection is also useful for motors below 3 kW, because a three-phase machine is more efficient than a single-phase machine and is often more readily available. At a demonstration site in the UK, a pump as turbine driving a 1.1 kW three-phase induction machine is connected in this way to produce a single-phase output of 800 W.

**Table 2.1 2.2 kW Induction Machine Data**

| | motor: data | generator | tests |
|---|---|---|---|
| Voltage (V) | 240 | 220 | 240 |
| Frequency (Hz) | 50.0 | 50.5 | 52.6 |
| Speed (rpm) | 1420 | 1575 | 1630 |
| Slip (%) | 5.3 | 3.9 | 3.7 |
| Capacitance (μF) | | 55 | 55 |
| Output Power (W) | 2200 | 2200 | 2200 |
| Input Power (W) | 2750 | 2760 | 2895 |
| Efficiency (%) | 80 | 80 | 76 |
| Power factor | 0.82 | 0.66 | 0.57 |

As the figures in Table 2.1 show, the efficiency of the induction machine when running as a generator is similar to its rated motor efficiency. Therefore, if the generator electrical output is fixed at the motor mechanical output power, then the losses will be approximately the same as the motor losses. This has been confirmed

by readings of stator winding temperature, which showed that the temperature is similar in motor and generator mode as long as the generator output is restricted to the rated power of the motor, in this case, 2.2 kW. Since the speed is greater in generator mode, the cooling effect of the fan is greater. However, there may be additional harmonics produced when running as a generator, and it is therefore advisable to derate the generator by 10%.

### 2.1.5 Use of generator performance to calculate PAT efficiency

For some of the pump tests carried out, it was not possible to measure the mechanical power input directly. In these cases, the pump was connected to an induction motor for which the efficiency could be measured. The pump efficiency was then calculated from the following equation:-

$$\eta_p = \frac{\rho Q_p g H_p}{\eta_m V I \cos\phi} \qquad (2.4)$$

For the tests in turbine mode the generator electrical output was measured, and the PAT efficiency calculated from the equation:-

$$\eta_t = \frac{V I \cos\phi}{\eta_{gen} \rho Q_t g H_t} \qquad (2.5)$$

Tests were carried out on a 2-pole, 1.1 kW induction motor, running both as a motor and as a generator. For some of the turbine tests, the generator was connected to a single-phase resistive load using the C-2C connection. For other tests, the generator was connected to the three-phase mains, and the per phase power output measured. The measured efficiency curves from the tests on this induction machine, as a motor and as a generator, are given in Fig. 2.7.

## 2.2 Electronic Control of Induction Generators

### 2.2.1 Control approaches for micro-hydro systems

The output from a micro-hydro generator needs to be regulated in some way in order to safeguard the equipment which is being supplied wit power. This requires the output voltage and frequency, and therefore the turbine speed, to be controlled within certain limits. The acceptable limits for voltage and frequency depend on the type of equipment being supplied. In industrialised countries the standards for public supply are very stringent, but in developing countries both voltage and frequency may vary outside these acceptable limits. The type of equipment used in villages is unlikely to be affected as long as voltage varies between +10% and -25%

and frequency between -0% and +5% of rated values. An explanation of these limits is given in Smith[56]. There are four approaches that have been taken for the control of micro-hydro systems, as described below.

1. In the past it was common to use a mechanical load governing system, which detected turbine speed changes and adjusted the flow of water into the turbine to keep the turbine speed constant. These systems are very costly, require considerable maintenance, and have been found to be impractical in remote parts of the world. This method of regulation is not suitable for a fixed geometry machine, such as a pump-as-turbine, for which the only method of regulating the flow rate is to close a control valve, which reduces the input head available to the turbine.

2. Induction generators can be used for stand-alone generation without a controller, and this has been done with some success on micro-hydro schemes in Nepal. However, the load on the generator must be kept constant, otherwise the speed of the turbine will increase and hence the voltage will increase beyond the range suitable for the appliances connected. In a typical village scheme without a controller, all the lights in the houses are turned on and off at the same time by a switch in the power house. This operates satisfactorily until some of the villagers decide that they no longer need the light, and remove the bulbs from their sockets. The generated voltage will then increase, possibly leading to other light bulbs blowing, which will result in further overspeeding of the turbine and possible runaway conditions.

3. Another possibility for regulating the system is to have an operator in the power house whenever the generator is running. This method of control is quite expensive, but is being used in many sites in Nepal and the north of Pakistan. However, for systems supplying large motor loads, the response-time of manual control cannot be fast enough to avoid large voltage fluctuations on the system which may result in damage to the equipment being supplied. As with method 1, this method is not really suitable for a fixed geometry machine such as a pump-as-turbine.

4. The most reliable method of regulation is to control the generator output electronically, by diverting a variable amount of the power to a ballast or 'dump' load. A controller for use with stand-alone induction generators has been designed at Nottingham Polytechnic by N Smith[56]. It has a fast response time, and keeps the generator speed within +5% or -0% for the range of loads which can normally be expected on such a system. It can be produced relatively cheaply, and can easily be maintained by a suitably trained engineer. A brief description of the operation of this controller is given below.

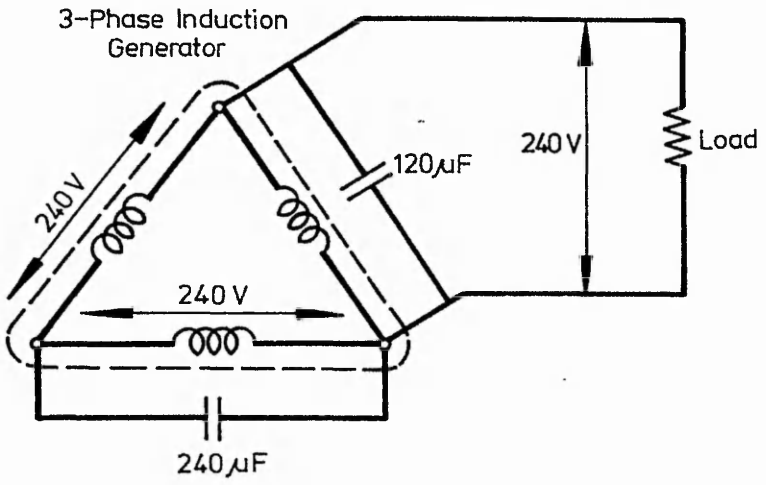


Fig. 2.5 Three-phase Induction Generator connected for single-phase output

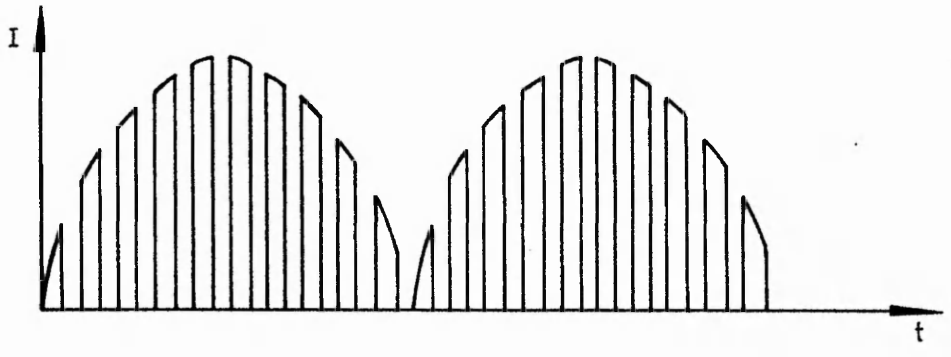


Fig. 2.6 Typical waveform for the IGC ballast load current

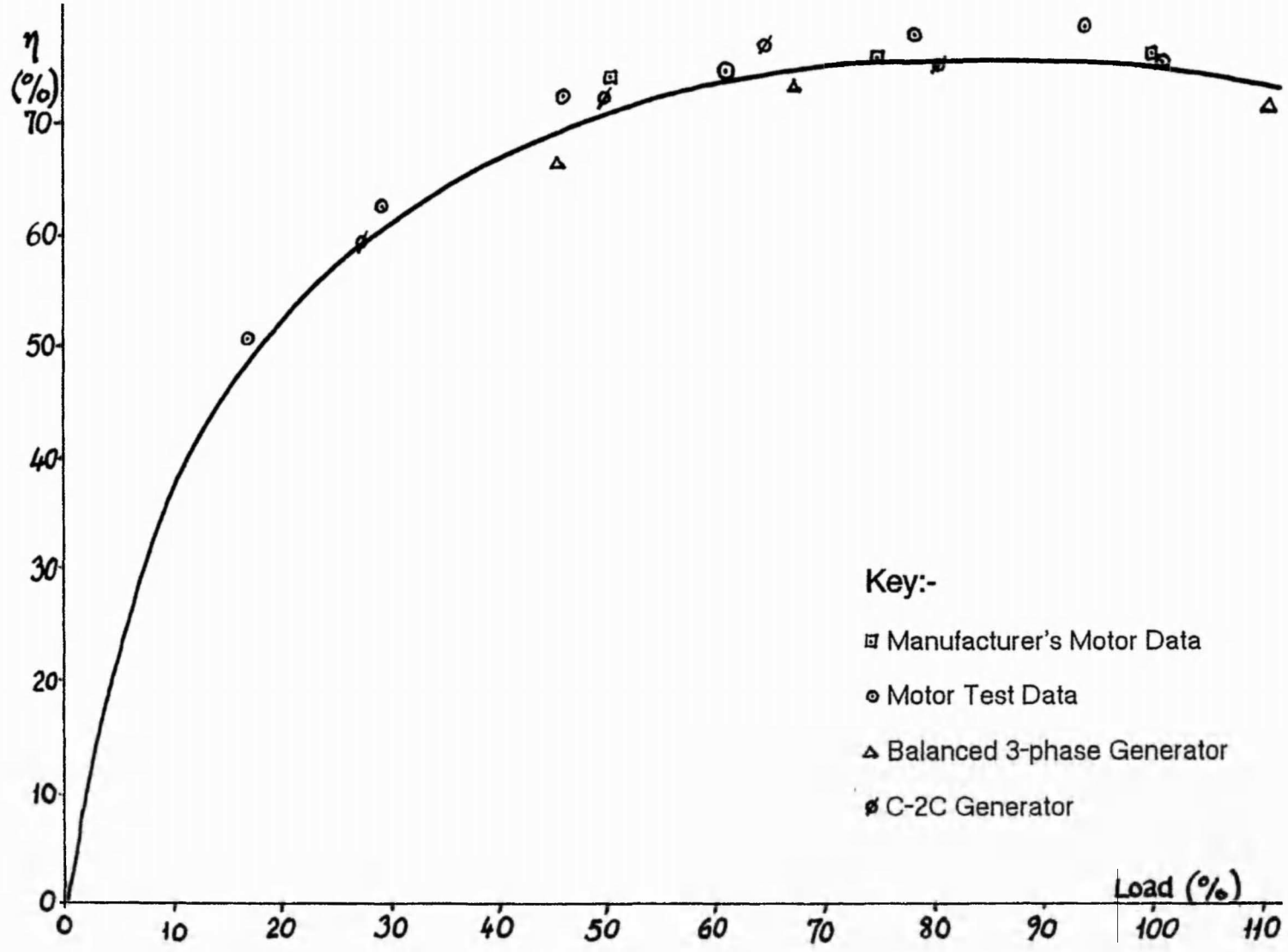


Fig. 2.7. Performance of a 1.1kW 2-pole 3-phase Induction Machine

### 2.2.2 Operation of the Induction Generator Controller (IGC)

The Induction Generator Controller (IGC) fixes the supply voltage by varying the amount of power being fed into a ballast load. When a load is disconnected from the generator output, the controller detects the rise in voltage and increases the power being fed into the ballast load in order to bring the voltage back down to the desired level. The ballast load current is rectified a.c. which is chopped at a frequency of around 1 kHz and fed to a single resistive element, usually an air or water heater. The amount of power fed to this load is controlled using a variable mark-space ratio, ie. the ratio of the on-time relative to the off-time in each cycle is altered in order to achieve a constant voltage. Typical waveforms of the ballast load current are shown in Fig. 2.6 and a block diagram of the controller is shown in Fig. 2.8.

If an inductive load, such as a small motor or flourescent lamp, is connected to the supply, the IGC keeps the voltage at the predetermined level. However, the additional reactance in the circuit changes the frequency at which the generator will run. In the case of an inductive load, which effectively cancels part of the excitation capacitance, the total reactance of the external circuit will decrease, and the frequency will increase. This increase in frequency has no ill-effects on any electrical equipment which is likely to be supplied from a micro-hydro scheme. Capacitive loads, which would cause a drop in the generated frequency, are very unlikely to occur.

In the case of starting a larger motor, the controller may not be able to keep the voltage constant initially, due to the high starting current. However, once the motor has started, the inductive current will fall, and the voltage can return to the predetermined value.

The alternating current supplied to the main loads on the system, otherwise known as the user loads, is smoothed by the generator excitation capacitance. It is therefore almost free from ripple, despite the high-frequency chopping of the ballast load. Hence, use of this type of controller does not require further derating of the generator.

The IGC also contains circuitry to protect the generator and the equipment being supplied. In case of faults on the ballast load circuit, an overcurrent trip operates in the event of a short-circuit and an overvoltage trip operates in the event of the ballast load becoming disconnected. Both of these trips disconnect the load from the generator entirely, and therefore result in the generator reaching runaway conditions.

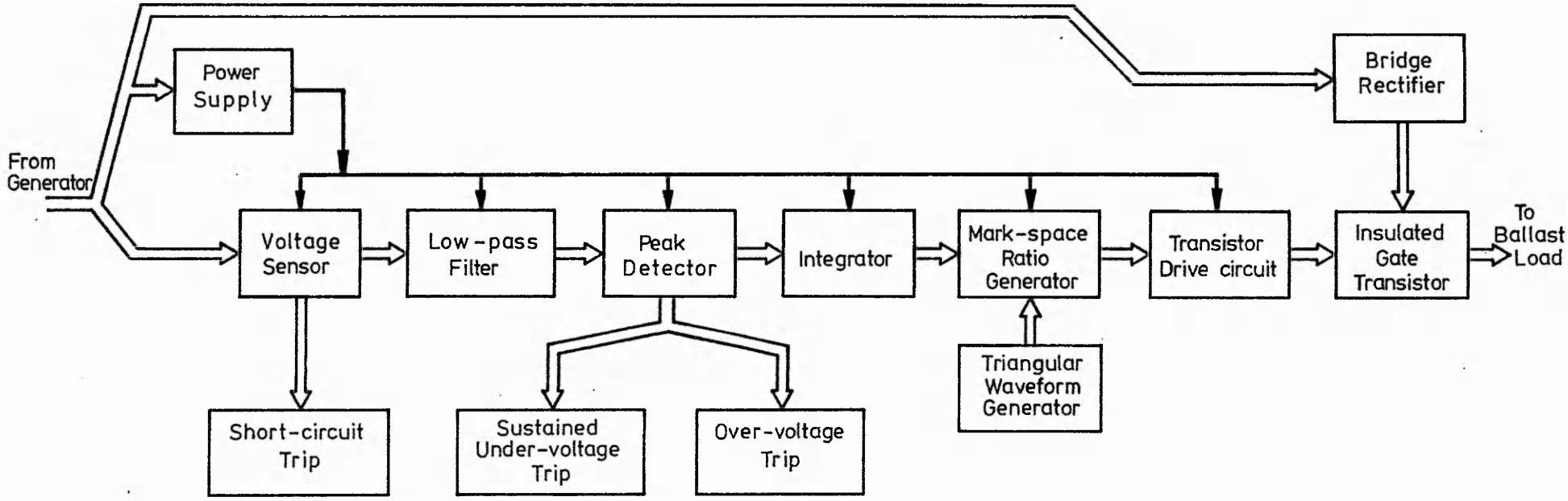


Fig. 2.8 Block diagram of the Induction Generator Controller

If the fault is on the main circuit only, then the generator continues to run at rated output with the ballast load connected, and can be reconnected to the main load circuit by pressing a 'reset' switch. A severe undervoltage trip is used to protect the generator in case of a short-circuit on the main load circuit. In case of normal overloading on the main circuit, a sustained undervoltage trip is used. This trip has a time delay so that an instantaneous overload, such as the starting current for a large motor, can be supplied by the generator. The controller in fact removes the entire ballast load when a low voltage is detected, which enables as much power as possible to be available for starting a motor. However, if a motor fails to start, the sustained undervoltage trip operates to disconnect the user load and thus protect the generator. This trip also comes into operation when the turbine is closed down, and therefore the remanent magnetism of the generator is retained on shutting down the system.

## 2.3 Compatibility of Pump-as-Turbine with Induction Generator and Induction Generator Controller

### 2.3.1 Performance characteristics of typical Pumps-as-Turbines

Before investigating the interaction between a pump-as-turbine and an induction generator controlled by an IGC, the likely performance characteristics of the PAT must be known. When a PAT is installed at a particular site, the operating point is determined by the intersection of the site head-flow characteristic with the PAT head-flow characteristic. The site head-flow characteristic depends on the vertical height between intake and turbine, and the head loss characteristic of the penstock.

Since the PAT is a fixed geometry machine, the PAT characteristic can be described by a series of curves for constant speed operation. The general shape of these curves depends on the specific speed of the pump. A purely radial-flow PAT has a characteristic such as that shown in Fig. 2.9, whereas an axial-flow PAT has a characteristic of the type illustrated in Fig. 2.10.

It is important to note one of the main differences between the two sets of curves. In the case of the radial-flow machine, the runaway curve lies to the left of the locked rotor curve. Under no-load conditions, eg. in the case of generator load rejection, the turbine speed will increase, but the flow-rate will decrease. In the case of the axial-flow machine, the flow-rate tends to increase with increasing speed. In between these extremes, the change in flow at overspeed may be very small, as is the case for the pump of specific speed 150 shown in Fig. 2.11. This diagram is based on results presented by Strub[5].

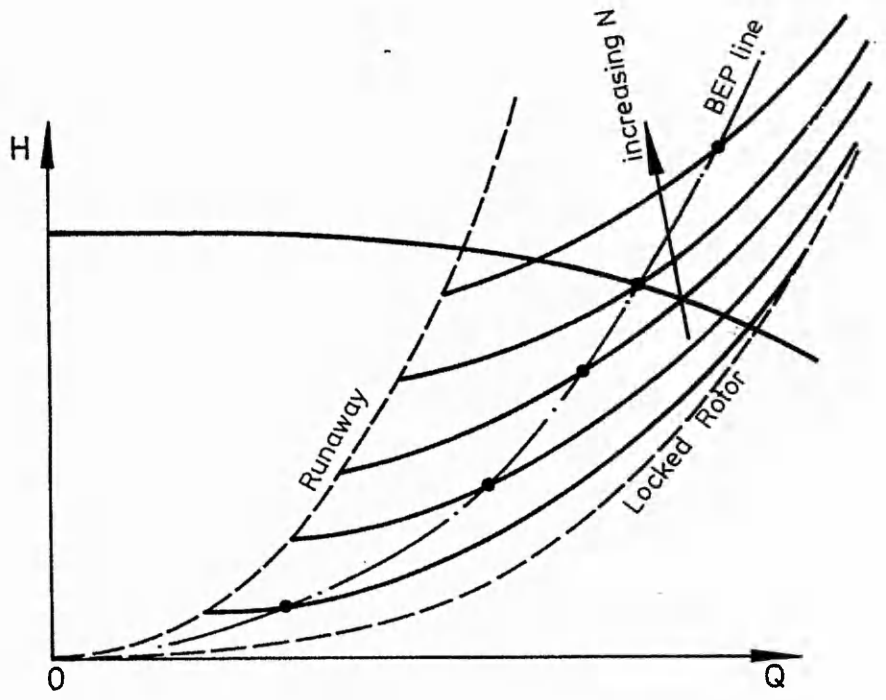


Fig. 2.9 Typical performance curve for a radial flow PAT

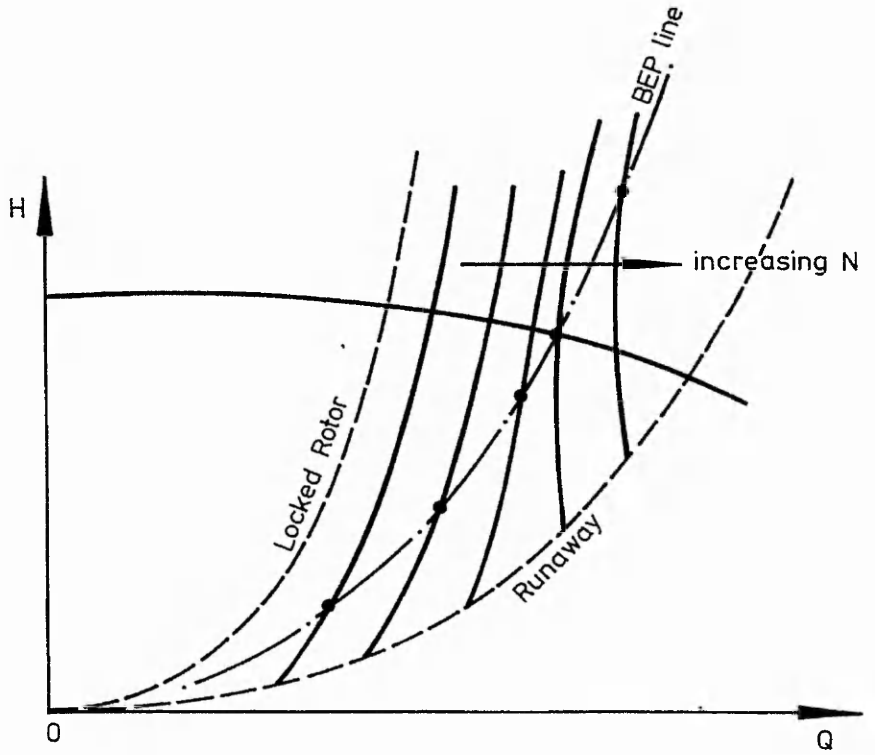


Fig. 2.10 Typical performance curve for an axial flow PAT

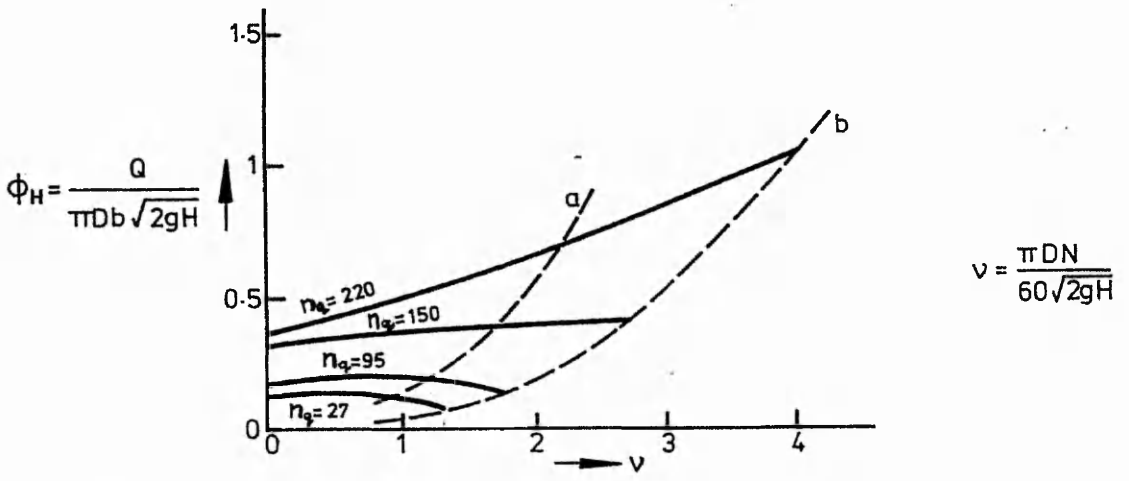


Fig. 2·11 PAT Flow–speed characteristics for constant head

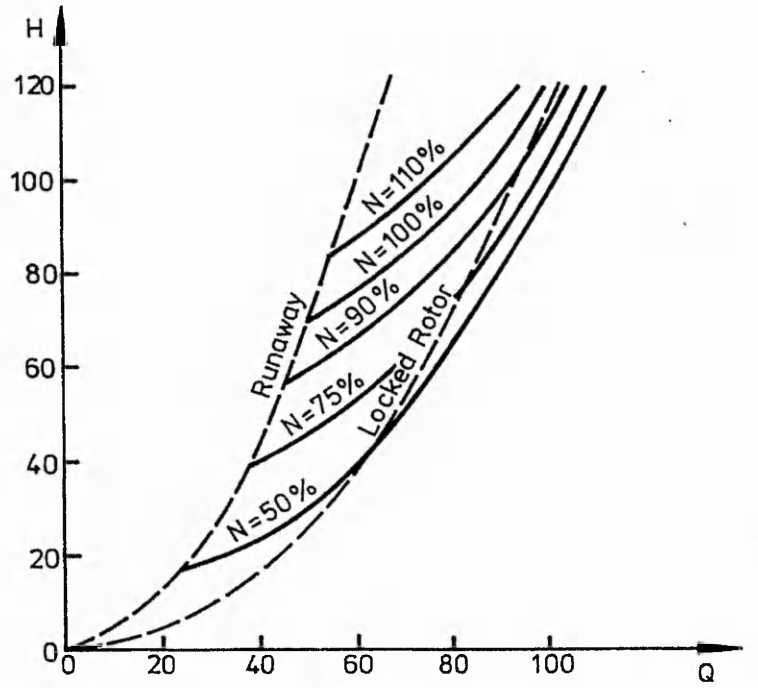


Fig. 2·12 Performance curve for a single volute pump, $n_q$=41

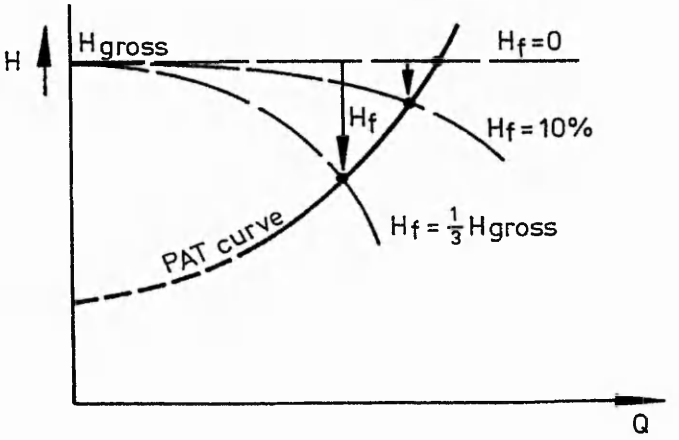


Fig. 2·13 Typical system curves for a micro–hydro scheme

It is interesting to note that for some mixed-flow pumps, the flow for constant head conditions first increases and then decreases as the speed is increased. The head-flow characteristics are therefore not constrained between the locked rotor curve and the runaway curve, as suggested by some authors[57]. A curve for a single volute pump of specific speed, $n_q$ = 41*, which has been derived from the data presented by Knapp[58], is shown in Fig. 2.12 to illustrate this point more clearly. A similar set of curves is given by Kobori[59] for a large two-stage double suction pump used in a pumped storage scheme. This machine has an equivalent specific speed of 30*.

### 2.3.2. System characteristic for a typical micro-hydro scheme.

The system characteristic for a micro-hydro scheme will lie between the limits shown in Fig. 2.13. The lower limit is determined by the maximum hydraulic power which can be obtained from a particular diameter of penstock, which occurs when the head loss in the pipe is one third of the gross head. The justification for this is given in Appendix Q. Since in micro-hydro schemes, the capital cost of equipment is usually a more important design criterion than the overall efficiency of the plant, a head loss in the penstock of between 10% and 30% is typical.

### 2.3.3 Turbine operating characteristics resulting from the use of an Induction Generator and Induction Generator Controller.

One effect of using an induction machine is that the speed of the generator is greater than the speed of the motor when used for driving the same unit as a pump. For a PAT of 3 kW output, the generator slip will be approximately 3%, and the speed will therefore be 6% greater than the pump speed if a direct drive is used. This must be taken into account when selecting a pump unit, since the effect of a 6% increase in speed will be a 12.5% increase in head, and a 19% increase in power.

Under normal operation, the IGC keeps the speed of the generator, and hence of the turbine, constant to within 2%. The power output of the turbine will therefore remain almost constant. However, in case of a fault on the ballast load circuit, the IGC will cause the load to be disconnected entirely, and the turbine will overspeed. This phenomenon is important to analyse for its effect on the generator, the turbine and the penstock. The speed of the generator also undergoes sudden changes when a relatively large motor is started, and this case can also be analysed for its effect on the various components of the system.

---

* Note: The definition of specific speed used throughout this thesis is:-

$$n_q = \frac{N\sqrt{Q}}{H^{0.75}}$$ (where N is in rpm, Q in $m^3/s$ and H in m).

In the first case, where the load on the generator is disconnected entirely, the PAT will speed up to its runaway speed. For axial-flow units, the runaway speed may be as much as twice the normal running speed. For radial-flow and mixed-flow PATs, the runaway speed is unlikely to be more than 50% above the normal operating speed. For an induction generator, overspeed causes more damage to the bearings than to the machine itself because of the rigid construction of the rotor. If a synchronous machine were to be used, an overspeed could cause the rotor windings to be forced outwards, resulting in major damage to the machine.

The limitation on the overspeed for squirrel-cage induction machines is the friction and wear of the bearings, not the physical construction of the rotor, as is the case with wound rotor machines. An overspeed of 50% for several hours may cause accelerated wear of the bearings, but it is unlikely to result in a complete failure of the generator. With synchronous generator installations, an emergency brake or valve shut-off is often required to prevent overspeed in case of a fault which causes complete load rejection. This type of equipment is not needed for an induction generator. However, when designing the penstock, it is important to take account of possible pressure surges which a rapid change of turbine speed will cause. A more detailed analysis of these hydraulic transients is presented in a later section.

CHAPTER 3

# REVIEW OF PREDICTION METHODS FOR PUMP-AS-TURBINE PERFORMANCE

## 3.1 The Importance of Accurate Prediction

A purpose-built water turbine is fitted with guide vanes or a spear valve which are adjustable, to accommodate changes in the flow through the machine. If a standard centrifugal pump is used as a turbine then no such adjustment is possible. A pump-as-turbine is therefore a fixed-flow unit, with head-flow curves as described in section 2.3.

With a direct-drive electric pump unit, the turbine and generator are directly coupled and the speed of the turbine is the same as that of the generator, which is constrained by the need to generate at a more or less constant frequency. The generated frequency, which in a stand-alone system may be allowed to increase up to 10% from the desired value, is directly proportional to the rotational speed. The power output of the turbine must also be limited to prevent overloading of the generator, either mechanically or electrically.

### 3.1.1 Flow Duration Curves

At the design stage, it is necessary to select the pump unit for a particular site. The system parameters for an installation at a particular site are fixed, once the positions of the intake and generator have been decided and the size of penstock selected. The flow available for driving the turbine will normally vary with time. For a micro-hydro scheme with a small catchment area, the variation of flow could be very large. This variation is usually described by a flow duration curve, in which flow is plotted against the probability of the flow being above the given value. Fig. 3.1 shows a typical flow duration curve for small catchments (4 to 10 $km^2$) given by Nèmec[60] for moderately forested low elevation mountains within the catchment of the River Elbe (Central Europe).

This type of catchment is typical for micro-hydro schemes in temperate regions of the world. Flow duration curves derived for catchments with various soil types for application in the UK are given in reference[61]. In sub-tropical countries, the flow duration curve may be affected by monsoon type climate, or by the presence of glacial run-off from high mountains. However the same criterion applies, which is that mean flow is usually available for less than 30% of the year for small catchment

areas. Unless an existing reservoir can be used, storage of water for more than a few hours is not economically viable for a micro-hydro scheme.

The effect of a poor turbine performance prediction, which results in the flow being different from the design flow, can be found using Fig. 3.1. This is based on the assumption that the pump has been selected for operation on average 330 days per year (13% of mean flow). If an error in the turbine performance prediction results in the actual flow being 30% above the design flow, then the turbine will run for an average of only 305 days per year.

### 3.1.2 Results of errors in Pump-as-Turbine prediction

Most of the methods for predicting the turbine performance of a pump concentrate on the prediction of the turbine best efficiency point. However, a simple comparison between the predicted values of head and flow at best efficiency with test results does not give an accurate picture of the effects of poor prediction. This is because the operating point is determined by the intersection of the system curve with the turbine characteristic, which in the case of a PAT is defined by a single curve. A more useful comparison is made by calculating the change in output power, flow and efficiency due to an error in the turbine performance prediction, taking into account typical PAT characteristics and site conditions. For this comparison, the results of tests by Knapp[62] for a radial-flow pump and Swanson[63] for a mixed-flow pump, published by Stepanoff[64], have been used, since they show the turbine performance over a wide range of heads, flows and speeds.

The results of the comparison are shown in Tables 3.1 and 3.2. Although the two types of pump have very different performance characteristics, the effects of errors in the turbine performance prediction follow a similar pattern.

It is interesting to note that where a site has been designed with a high friction loss in the penstock, the effects of poor turbine prediction on the power output, flow required and turbine efficiency are less than in the case of no head loss in the penstock. A design with large losses in the penstock may often be incorporated when a PAT is employed because both are consistent with the need to cut initial capital costs. If additional finance is available to provide a larger diameter penstock, in order to reduce the friction losses, then the additional investment required for a conventional turbine may also be justified. Figure 3.2 illustrates how a poor prediction under these conditions does not result in a large difference from the expected output power. The area QH represents the input power to the turbine, so that, as long as the efficiency is not far from the maximum, the output of the turbine remains almost constant for different operating points.

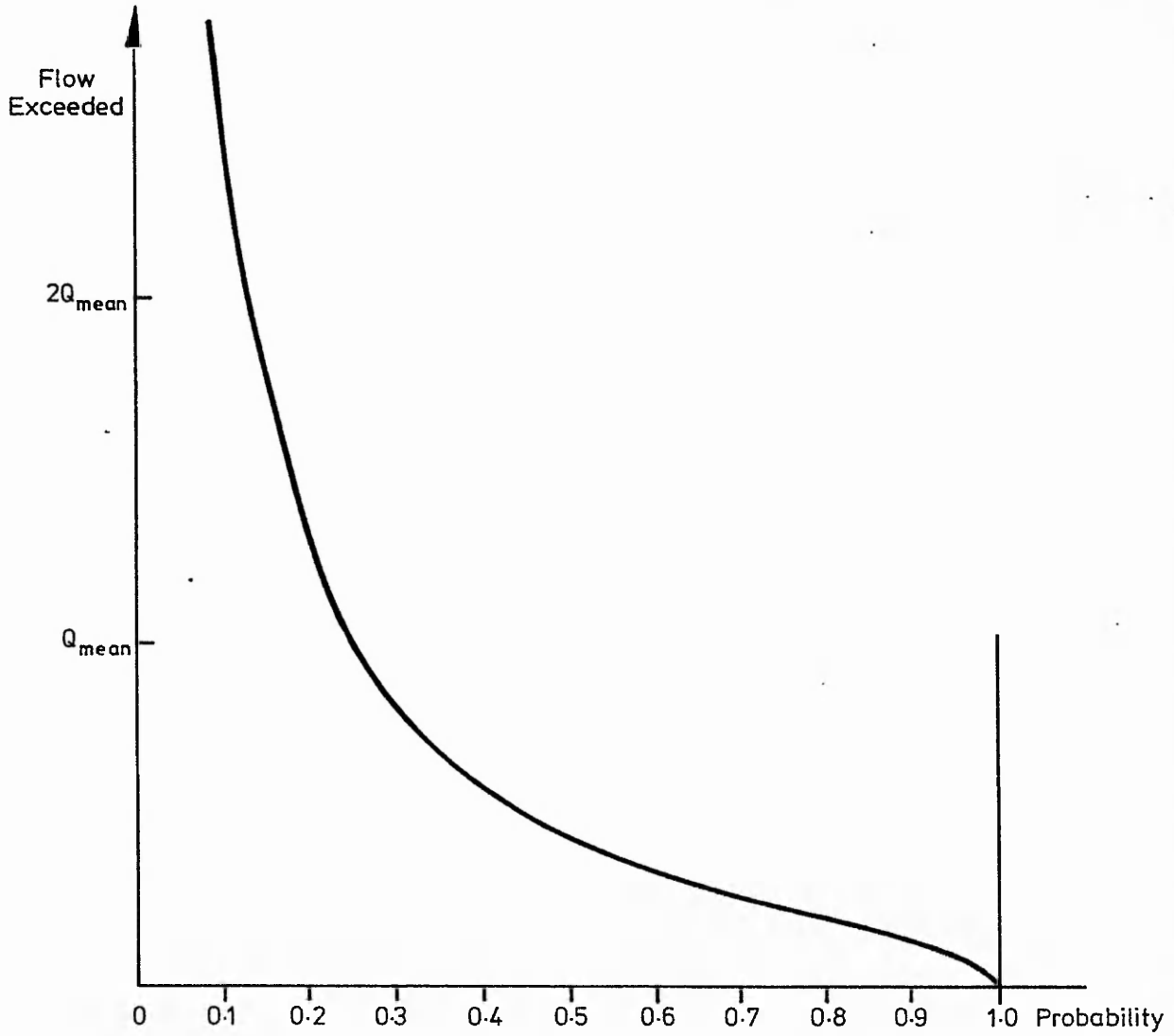


Fig. 3·1 Flow Duration Curve for typical small catchment

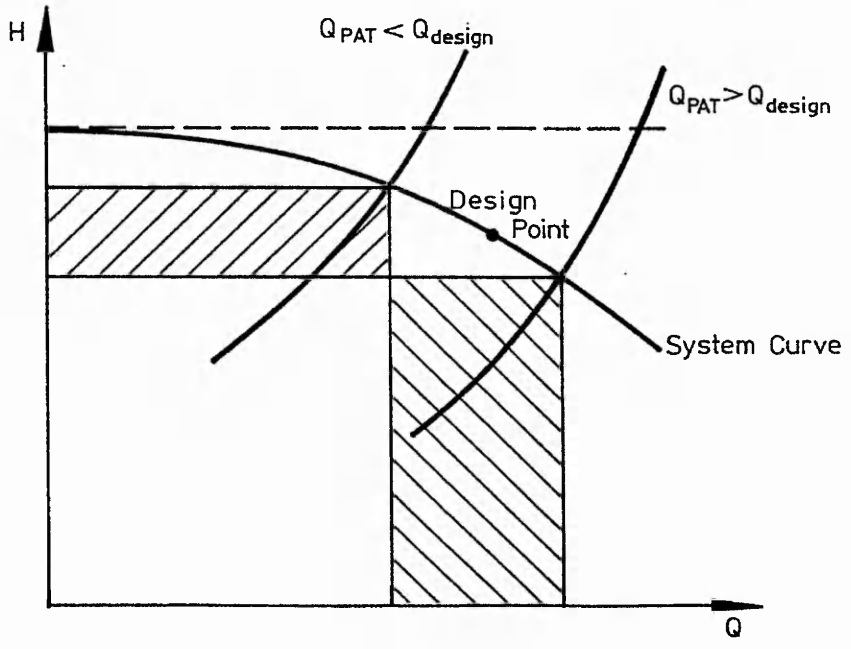


Fig. 3·2 Effects of poor PAT prediction with large friction loss in Penstock

**Table 3.1 Effects of poor PAT prediction: Radial flow pump**

Actual performance of the pump-as-turbine is shown as a percentage of the predicted performance.

| | Zero pipe Head loss | | | 20% pipe Head loss | | |
|---|---|---|---|---|---|---|
| | P | Q | η | P | Q | η |
| $H_{bep}$ = 80%<br>$Q_{bep}$ = 80% | 89 | 92 | 97 | 94 | 94 | 97 |
| $H_{bep}$ = 120%<br>$Q_{bep}$ = 80% | 66 | 67 | 96 | 82 | 75 | 98 |
| $H_{bep}$ = 80%<br>$Q_{bep}$ = 120% | 134 | 138 | 97 | 105 | 125 | 99 |
| $H_{bep}$ = 120%<br>$Q_{bep}$ = 120% | 99 | 103 | 96 | 98 | 102 | 96 |

**Table 3.2 Effects of poor PAT prediction: Axial flow pump**

Actual performance of the pump-as-turbine is shown as a percentage of the predicted performance.

| | Zero pipe Head loss | | | 20% pipe Head loss | | |
|---|---|---|---|---|---|---|
| | P | Q | η | P | Q | η |
| $H_{bep}$ = 80%<br>$Q_{bep}$ = 80% | 88 | 87 | 100 | 92 | 88 | 99 |
| $H_{bep}$ = 120%<br>$Q_{bep}$ = 80% | 72 | 76 | 94 | 86 | 78 | 100 |
| $H_{bep}$ = 80%<br>$Q_{bep}$ = 120% | 131 | 131 | 100 | 108 | 124 | 100 |
| $H_{bep}$ = 120%<br>$Q_{bep}$ = 120% | 108 | 114 | 94 | 96 | 111 | 92 |

Another conclusion, which can be drawn from Tables 3.1 and 3.2, is that the effects of an inaccurate prediction of the turbine best efficiency point are more significant if the error in predicted head is opposite in sign to the error in predicted flow. The pump-as-turbine has a head-flow characteristic for which the head increases with increasing flow. Therefore, if the error in the prediction of head has the same sign as the error in the predicted flow (ie. they are both too high or both too low), then the actual operating point of the turbine will be close to the predicted H-Q curve, and, since the system H-Q curve is fixed, the actual operating point will be close to the required head and flow.

In the case of a PAT for which the predicted head is 20% lower than the actual head at best efficiency, and the predicted flow is 20% higher than the actual value of Q at best efficiency, the actual H-Q curve of the PAT will be to the left of the predicted curve. Therefore, the turbine output power will be lower than the design power, but the turbine will run at a lower flow rate. In the case of a prediction 20% too high in H and 20% too low in Q, the output power will be greater than expected, but the flow will be greater, which is likely to result in the turbine not running at times when the available flow rate is low.

### 3.1.3 Accuracy of Pump Performance Data

Since many of the methods for predicting PAT performance are based on calculations involving the pump performance data, it is important to consider the accuracy of this data. In the UK, pump manufacturers' data is often given according to the British Standard Specification for Acceptance Tests for Pumps, BS 5316[65]. In this standard, the criteria for acceptance of a pump are given in terms of the overall error of head and flow for the pump best efficiency compared with the manufacturers' guaranteed figures.

The British Standard defines an ellipse on the H-Q chart centred on the guaranteed best efficiency point, through which the test curve must pass. For tests on large pumps, where the performance characteristics can by closely specified, the limits of Class B tests are used (BS 5316 Part 2). For the size of pump used for micro-hydro installations, the limits are normally those of Class C tests (BS 5316 Part 1), in which the maximum error of H is ± 4%, and the maximum error of Q is ± 7%, as illustrated in Fig. 3.3. For pumps manufactured in developing countries, no such standards exist for the accuracy of manufacturers' data. Using this data as the sole basis for predicting the turbine performance of a pump restricts the accuracy of the final result, even if the prediction method itself is highly accurate.

### 3.1.4 Acceptable limits for Pump-as-Turbine performance prediction

In order to check whether the limits of accuracy of a particular turbine performance prediction are acceptable, it is necessary to consider the turbine performance characteristic and the site conditions. The effects of a similar inaccuracy in two different pump units designed for two different sites could vary significantly, in one case leading to satisfactory operation, and in the other requiring expensive modifications to the scheme.

Considering economic factors, as shown in Appendix G, the assumption can be made that the system curve for the penstock is designed to allow for a 15% head loss at the flow-rate required by the pump-as-turbine. As shown in sub-section 3.1.2, the effects of an error in the turbine performance prediction will be less if the head loss is greater than this. For turbine maximum efficiency, the limits for acceptable prediction are assumed to be ± 5%. The turbine best efficiency point (bep) must give a corresponding point on the H-Q characteristic which lies within the ellipse which has as its major axis the line:

$$H = \left(\frac{H_{bep}}{Q_{bep}}\right) Q$$

with limits of ±30% for both H and Q. The minor axis of the ellipse allows for limits of ±10% in H and ±10% in Q. Figure 3.4 illustrates the limits of these errors.

The data which is given by Yedidiah[66] for a 4 kW end-suction radial flow pump has been used together with the flow duration curve of Nèmec (Fig. 3.1) to calculate the effects of errors in the turbine performance prediction. The figures in Table 3.3 represent the worst case conditions, using the assumptions stated above.

The difference between the predicted bep and the actual bep for the PAT may be defined by $\Delta a$, the proportional difference parallel to the major axis of the ellipse and $\Delta b$, parallel to the minor axis of the ellipse. The criterion for an acceptable prediction is that $Cr \leq 1$, where

$$Cr^2 = \left(\frac{\Delta a}{0.3}\right)^2 + \left(\frac{\Delta b}{0.1}\right)^2. \qquad (3.1)$$

The equations relating $\Delta a$ and $\Delta b$ to H and Q are derived in Appendix H.

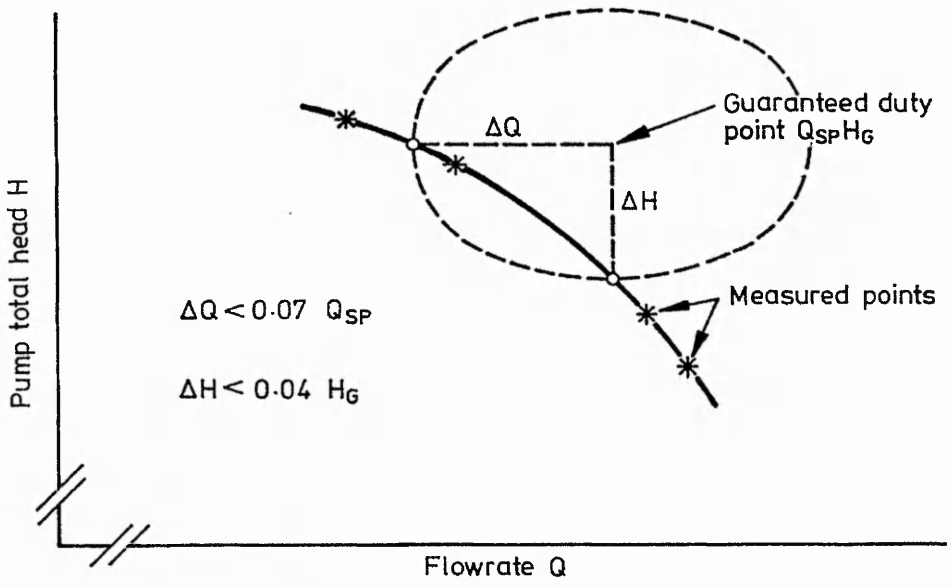


Fig. 3.3 Pump guarantee test limits

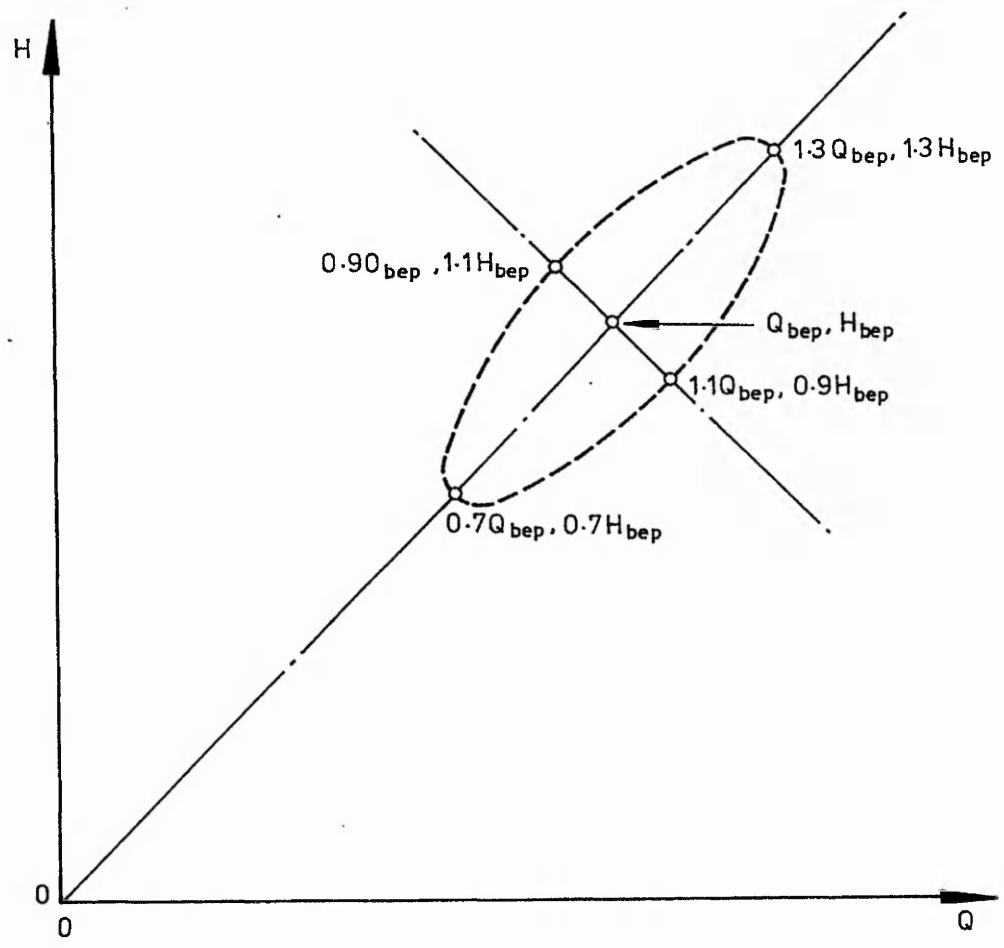


Fig. 3.4. Acceptable limits for PAT prediction

**Table 3.3 Typical effects of poor PAT prediction**

Actual performance of a radial flow pump-as-turbine is shown as a percentage of the predicted performance, assuming a penstock head loss of 15%. The number of days of operation has been calculated using the typical flow duration curve shown in Fig. 3.1. The values below show the worst case conditions for Cr = 1.

| | $\eta_t$ | $P_{out}$ | $Q_t$ | Mean days/yr operation |
|---|---|---|---|---|
| $H_{bep}$ = 100%<br>$Q_{bep}$ = 100%<br>$\eta_{bep}$ = 100% | 64 | 100 | 100 | 330 |
| $H_{bep}$ = 110%<br>$Q_{bep}$ = 90%<br>$\eta_{bep}$ = 95% | 60 | 85 | 87 | 338 |
| $H_{bep}$ = 90%<br>$Q_{bep}$ = 110%<br>$\eta_{bep}$ = 105% | 67 | 114 | 114 | 318 |
| $H_{bep}$ = 130%<br>$Q_{bep}$ = 130%<br>$\eta_{bep}$ = 95% | 58 | 93 | 104 | 328 |
| $H_{bep}$ = 70%<br>$Q_{bep}$ = 70%<br>$\eta_{bep}$ = 95% | 59 | 85 | 89 | 337 |

## 3.2 Turbine Performance Prediction using Best Efficiency Value

Several authors have published papers on the use of pumps as turbines, in which the turbine performance is predicted using the values of head and flow at pump best efficiency, and scaling them up to produce turbine head and flow values, using a factor which are a function of the efficiency. Several different formulae, which have been proposed by the various authors, are considered in the following sections.

### 3.2.1 Direct use of pump efficiency

The earliest available paper which presented such a method was published in 1962, written by Childs[67]. He stated that the turbine best efficiency and pump best efficiency for the same machine are approximately equal. He further assumed that the turbine output power for best efficiency operation was equal to the pump input power.

Hence:

$$P_t = \rho g Q_t H_t \eta_t = \frac{\rho g Q_p H_p}{\eta_p} = P_p . \qquad (3.2)$$

It is also assumed that $Q_t/Q_p = H_t/H_p$ and hence

$$\frac{Q_t}{Q_p} = \frac{1}{\eta_p} \text{ and } \frac{H_t}{H_p} = \frac{1}{\eta_p}. \qquad (3.3,4)$$

No further theoretical analysis is given in Child's paper.

The same method was also presented by McClaskey & Lundquist[13], and by Lueneburg & Nelson[68], who added the proviso that it should only be used as a preliminary method, and that further analysis or testing should be carried out to obtain a performance characteristic for design calculations. Hancock[69] outlined a similar method, but used $1/\eta_t$ for the ratios instead of $1/\eta_p$. He also stated that for most pumps, the turbine best efficiency lies within ± 2% of the pump best efficiency.

### 3.2.2 Stepanoff's Method

Stepanoff[20] also proposes a method which depends on the pump efficiency, which is based on the theoretical work of Engel[18]. This relates the ratios of turbine and pump head and flow to the hydraulic efficiency of the pump, by the following equations:

$$\frac{Q_t}{Q_p} = \frac{1}{\eta_{hp}} \text{ and } \frac{H_t}{H_p} = \frac{1}{\eta_{hp}^2}. \qquad (3.5,6)$$

Since the hydraulic efficiency is not normally known, the following simplification has been incorporated:

$$\eta_{hp} = \sqrt{\eta_p} \qquad (3.7)$$

which results in:

$$\frac{Q_t}{Q_p} = \frac{1}{\eta_p} \text{ and } \frac{H_t}{H_p} = \frac{1}{\eta_p}. \qquad (3.8,9)$$

### 3.2.3 Sharma's Method

Sharma[70] has developed a prediction method which also uses ratios dependent on the pump efficiency. He uses the initial assumptions, as in the method presented by Child, that $P_p = P_t$ and $\eta_p = \eta_t$, which results in:

$$\frac{Q_t H_t}{Q_p H_p} = \frac{1}{\eta_p^{\,2}}. \tag{3.10}$$

Using another of the equations developed by Engel[18], which relates the two specific speeds for pump and turbine operation, and incorporating the simplification of equation (3.7), gives:

$$n_{qt} = \sqrt{\eta_p}.\, n_{qp} \tag{3.11}$$

i.e.
$$\frac{\sqrt{Q_t}}{H_t^{0.75}} = \sqrt{\eta_p}.\frac{\sqrt{Q_p}}{H_p^{0.75}}. \tag{3.12}$$

(Note, that in these equations, $n_{qt}$ is the specific speed as normally defined for a pump, ie. $n_{qt} = \frac{N_t\sqrt{Q_t}}{H_t^{0.75}}$ ).

Combining equations (3.10) and (3.12) gives the following ratios:

$$\frac{Q_t}{Q_p} = \frac{1}{\eta_p^{\,0.8}} \text{ and } \frac{H_t}{H_p} = \frac{1}{\eta_p^{\,1.2}}. \tag{3.13,14}$$

These are the equations which are derived from the assumptions given, although they are not as given in the original paper.

### 3.2.4 Alatorre-Frenk's Method

The method presented by Alatorre-Frenk[71] is based on fitting equations to a limited number of PAT data. The equations are again based on the pump efficiency, and can be expressed in the form:

$$\frac{H_t}{H_p} = \frac{1}{0.85\eta_p^{\,5} + 0.385} \tag{3.15}$$

$$\frac{Q_t}{Q_p} = \frac{0.85\eta_p^{\,5} + 0.385}{2\eta_p^{\,9.5} + 0.205}. \qquad (3.16)$$

All of the above methods can be used to estimate the best efficiency point in turbine operation from the manufacturer's pump performance data.

### 3.2.5 Schmiedl's Method

The turbine prediction method presented by Schmiedl[72] uses an estimated value of hydraulic efficiency. In this case the hydraulic efficiency is given by the following equation:

$$\eta_{hp} = \sqrt{\eta_p^{\,0.5}\,\eta_t^{\,0.5}} \qquad (3.17)$$

and the equations for the turbine best efficiency point are:

$$\frac{Q_t}{Q_p} = -1.4 + \frac{2.5}{\eta_{hp}} \qquad (3.18)$$

$$\frac{H_t}{H_p} = -1.5 + \frac{2.4}{\eta_{hp}^{\,2}}. \qquad (3.19)$$

The graphs published by Schmiedl show a large scatter around the lines given by these equations. Section 3.4 will cover the results of a comparison of all the simple PAT prediction methods available.

## 3.3 Turbine Performance Prediction using Specific Speed

Several authors have proposed other equations, which relate the head and flow ratios for pump and turbine operation to the pump or turbine specific speed. Buse[73] proposed the use of factors for estimating turbine performance for pumps with specific speeds in the range $n_{qp}$ = 10 to 54. He does not give a formula for these factors, but only gives their ranges as 2.2 to 1.1 for $Q_t/Q_p$ and $H_t/H_p$, and 0.92 to 0.99 for $\eta_t/\eta_p$. Two other methods which are based on the specific speed are documented in a paper by Lewinsky-Kesslitz[74]. Both of these methods use the specific speed for turbine operation, $n_{qt}$, which is defined in the same way as the pump specific speed, but using the values of $N_t$, $Q_t$ and $H_t$ for the turbine best efficiency. The two methods are presented below.

### 3.3.1 Grover's Method

The method of Grover[75] is presented in metric units in reference[74] as:

$$\frac{H_t}{H_p} = 2.693 - 0.0229\, n_{qt} \tag{3.20}$$

$$\frac{Q_t}{Q_p} = 2.379 - 0.0264\, n_{qt}\,. \tag{3.21}$$

These equations are restricted in their application to specific speeds in the range $10 < n_{qt} < 50$.

### 3.3.2 Hergt's Method

This method is presented in graphical form in reference[74], which shows a band of head and flow ratios, each given as a function of turbine specific speed. Simple equations have been found which match the centre of the bands. These equations are:

$$\frac{H_t}{H_p} = 1.3 - \frac{6}{n_{qt} - 3} \tag{3.22}$$

$$\frac{Q_t}{Q_p} = 1.3 - \frac{1.6}{n_{qt} - 5}\,. \tag{3.23}$$

## 3.4 Comparison of simple Pump-as-Turbine prediction methods

All of the methods for turbine performance prediction described in sections 3.2 and 3.3 have been compared with test results for a range of pumps, which have been drawn from various published papers. The value of the prediction criterion, as defined in section 3.1.4, has been calculated for each of the methods, and a mean value calculated for the 34 pumps. For the Grover prediction method, some pumps have been excluded because they are outside the specified range of specific speeds. In this case, the mean value of the prediction criterion has been calculated for the remaining 27 pumps. A summary of the results is given in Table 3.3. Details of the results, including reference numbers for each of the pump test results, are given in Appendix I.

**Table 3.4 Comparison of prediction criteria for simple methods.**

| Author of method | Mean value of prediction criterion | % of PATs for which criterion < 1 |
|---|---|---|
| Child | 0.921 | 59 |
| Stepanoff | 0.846 | 65 |
| Hancock | 0.906 | 71 |
| Sharma | 0.733 | 79 |
| Alatorre-Frenk | 0.852 | 71 |
| Schmiedl | 1.173 | 62 |
| Hergt et al | 0.865 | 68 |
| Grover | 1.333 | 19 |

It can be seen from Table 3.4 that the most accurate method, defined either by the lowest mean value of criterion, or by the highest percentage falling within the limit Cr < 1, is the method of Sharma. The particular assumption on which Sharma's method has been based, equation (3.11), has been checked for the same 34 pumps. The mean value of $\sqrt{\eta_p}.\frac{n_{qp}}{n_{qt}}$ is 1.052 and a standard deviation of 0.128. This shows that the assumption is valid, within reasonable limits.

## 3.5 Kittredge's Pump-as-Turbine Prediction Method

### 3.5.1 Use of Normalized Performance Characteristics

The method proposed by Kittredge[76] entails using a series of 'model' pumps for which the turbine characteristics are known. The pump and turbine characteristics are first converted to a dimensionless form, divided by the values at pump best efficiency (denoted by subscript n). Thus, the dimensionless, or normalized quantities become:

$$q = \frac{Q}{Q_n} \text{ for flow rate}$$

$$h = \frac{H}{H_n} \text{ for head}$$

$$p = \frac{P}{P_n} \text{ for shaft power}$$

$$\nu = \frac{N}{N_n} \text{ for rotational speed}$$

$$m = \frac{T}{T_n} \text{ for torque .}$$

Kittredge suggests that the turbine characteristics can be predicted using the model pump which has characteristics closest to the pump under investigation. The assumption is made that two pumps with similar normalized pump characteristics will have similar normalized turbine characteristics. A description of the method is given in reference[77], together with an example of how it could be applied to selecting the correct size of pump for a particular application.

### 3.5.2 Limitation of Kittredge's method

A limitation in the application of Kittredge's method was originally outlined by Williams et al[78], with a suggestion for improving the accuracy of the prediction. The prediction of turbine performance by the Kittredge method depends on the maximum efficiencies of the model pump and the pump under investigation being equal. As the following example shows, the prediction with unequal pump efficiencies leads to inaccuracy in the entire turbine performance prediction.

Consider the characteristics of a Worthington-Simpson end-suction centrifugal pump. As can be seen in Fig. 3.5, the normalized pump characteristics are similar to the Voith single suction pump characteristics given by Kittredge. In turbine mode the normalized values at best efficiency are as follows:-

$$\frac{\nu}{q} = 0.85; \quad \frac{h}{q^2} = 0.94; \quad \frac{p}{\nu q^2} = \frac{m}{q^3} = 0.80$$

De-normalizing to obtain the predicted turbine characteristics at rated speed ($\nu = 1$) gives:-

$$Q_{nt} = \frac{Q_n}{\left(\frac{q_t}{\nu_t}\right)} = \frac{2.0}{0.85} = 2.35 \text{ l/s} \qquad (3.24)$$

(Value from test: 3.68 l/s)

$$H_{nt} = H_n \times q_t^2 \times \frac{h_t}{q_t^2} = 21.7 \times 1.3 \qquad = 28.2 \text{ m.} \qquad (3.25)$$

(Value from test: 51.9 m)

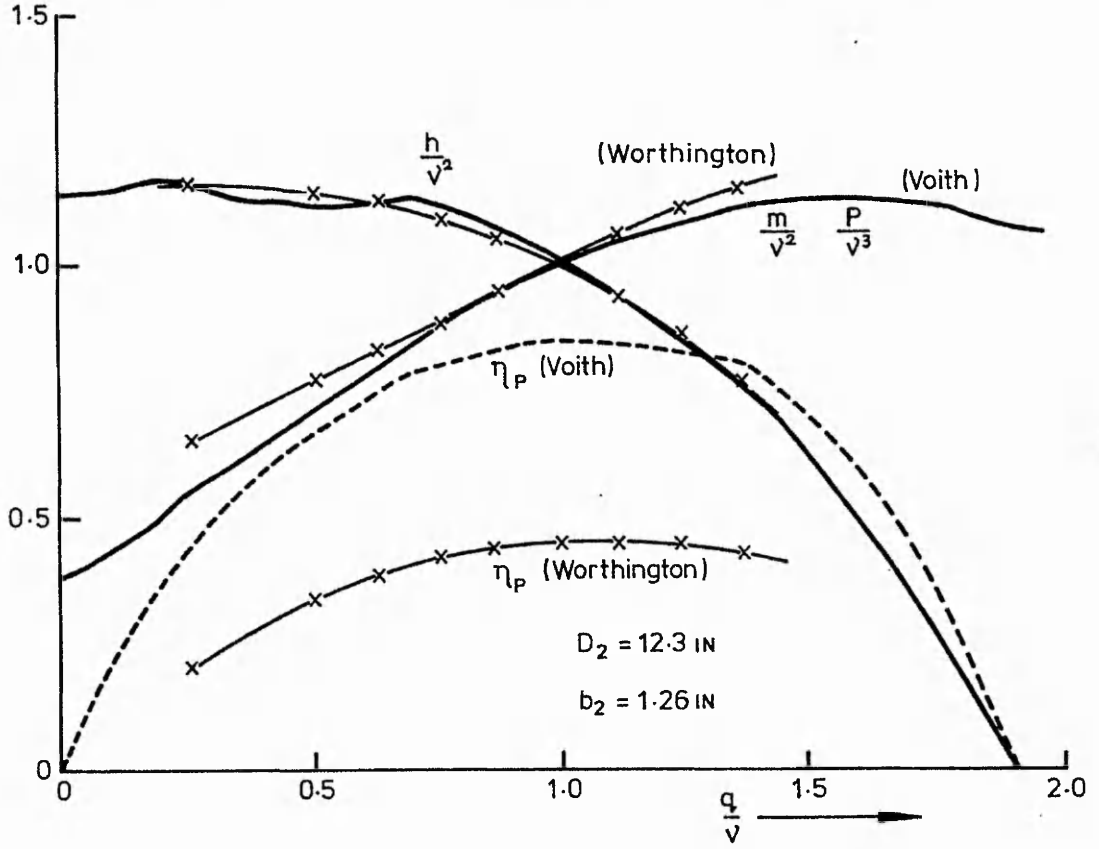


Fig. 3·5a Dimensionless characteristic curves of normal pump operation for Voith single suction pump, and Worthington-Simpson pump

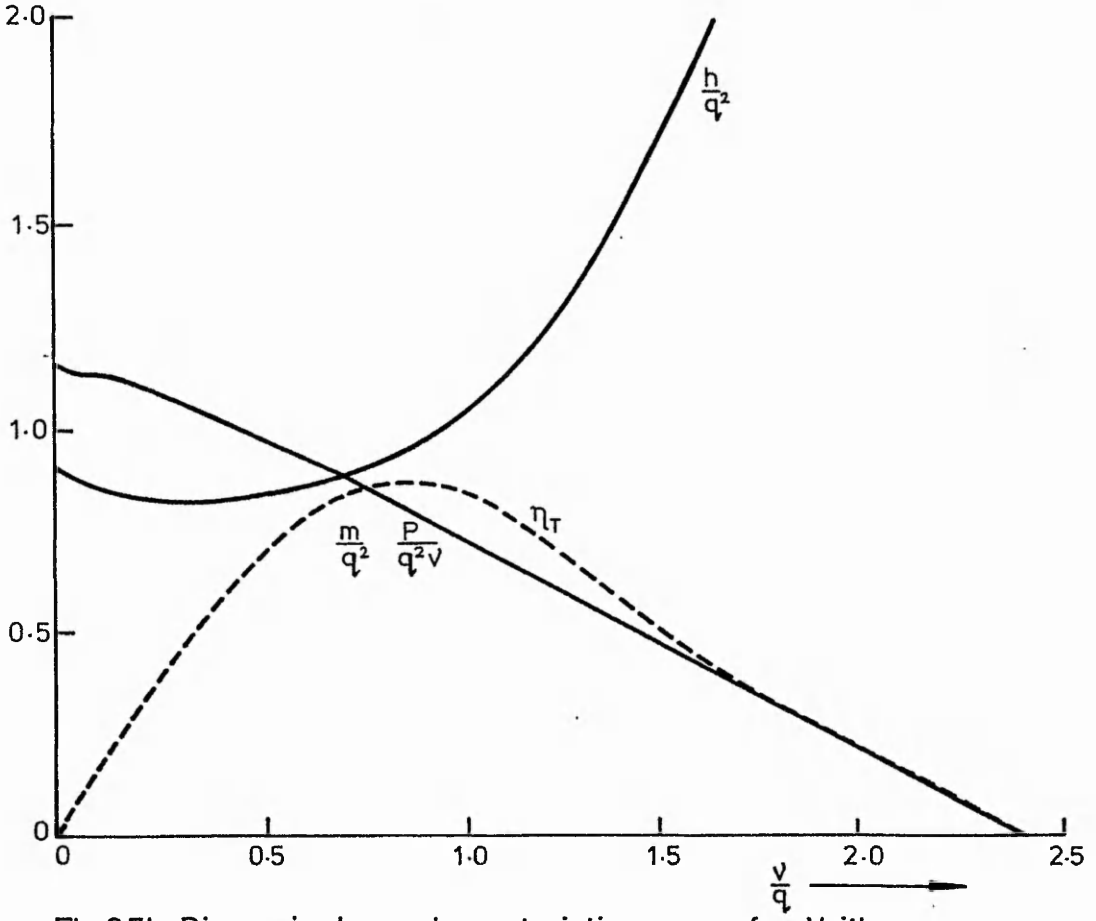


Fig.3·5b Dimensionless characteristic curves for Voith pump - normal turbine operation

$$P_{nt} = P_n \times q_t^2 \times \frac{p_t}{\nu_t q_t^2} = 0.925 \times 1.11 \quad = 1.024 \text{ kW.} \qquad (3.26)$$

(Value from test: 0.867 kW)

The turbine efficiency is given by:-

$$\frac{P_{out}}{P_{in}} = \frac{P_{nt}}{H_{nt} Q_{nt} \rho g} = \frac{1024}{28.2 \times 2.35 \times 10^{-3} \times 9.81 \times 10^3} \qquad (3.27)$$

= 1.58 or 158% !

The reason for this surprising result is that the efficiency of the test pump is much less than that of the model. The analysis outlined below highlights the problem. Using $\eta_n$, $Q_n$, $H_n$, $P_n$ for the test pump and $\eta_n^*$, $Q_n^*$, $H_n^*$, $P_n^*$ for the model pump, at the turbine best efficiency point:-

$$\frac{p_t^*}{q_t^* h_t^*} = \frac{\frac{P_{nt}^*}{P_n^*}}{\frac{Q_{nt}^*}{Q_n^*} \cdot \frac{H_{nt}^*}{H_n^*}} = \frac{P_{nt}^*}{Q_{nt}^* H_{nt}^*} \cdot \frac{Q_n^* H_n^*}{P_n^*} . \qquad (3.28)$$

But $$\frac{Q_n^* H_n^*}{P_n^*} = \frac{\eta_n^*}{\rho g} \qquad (3.29)$$

and $$\frac{P_{nt}^*}{Q_{nt}^* H_{nt}^*} = \eta_{nt}^* \cdot \rho g . \qquad (3.30)$$

Using Kittredge's method, the best efficiency in turbine mode is

$$\eta_{nt} = \frac{P_{nt}}{\rho g Q_{nt} H_{nt}} = \frac{P_n . p^*}{\rho g Q_n . q^* H_n h^*} = \frac{1}{\eta_n} \frac{p^*}{q^* h^*} = \frac{1}{\eta_n} \cdot \eta_n^* \eta_{nt} . \qquad (3.31)$$

Therefore, if $\eta_n < \eta_n^*$ then $\eta_{nt} > \eta_{nt}^*$.

In practice it is more likely that a pump which runs less efficiently than the model when in pump mode will run less efficiently than the model in turbine mode. Since pump and turbine efficiencies for the same machine are often nearly equal,

it is better to assume that

$$\frac{\eta_{nt}}{\eta_{nt}^*} = \frac{\eta_n}{\eta_n^*}. \qquad (3.32)$$

In order for the turbine efficiency to match this assumption, a factor must be incorporated into the equation for the de-normalized efficiency:

$$\eta_{nt} = \frac{P_n p^*}{\rho g\, Q_n q^*\, H_n h^*} \left(\frac{\eta_n}{\eta_n^*}\right)^2. \qquad (3.33)$$

Note that the value of $P_t$ calculated in equation (3.26) is closer to the test value than the values of $Q_t$ or $H_t$. It is therefore necessary to apply correction factors to the calculations of $Q_t$ and $H_t$. Using the analysis given in section 3.2.3, the predicted turbine best efficiency is given by:

$$Q_{nt} = Q_n q^* \left(\frac{\eta_n}{\eta_n^*}\right)^{0.8} = 2.35 \times 1.62 = 3.80 \text{ l/s} \qquad (3.34)$$

$$H_{nt} = H_n h^* \left(\frac{\eta_n}{\eta_n^*}\right)^{1.2} = 28.2 \times 2.06 = 58.1 \text{ m} \qquad (3.35)$$

$$\eta_{nt} = \frac{P_{nt}}{\rho g\, Q_{nt} H_{nt}} = \frac{1024}{9.81 \times 3.8 \times 58.1} = 0.47. \qquad (3.36)$$

These values are much closer to the test results than the original prediction. The best efficiency from the test was found to be 0.46, the same as the pump efficiency.

## 3.6 Acres American Computer Programme

### 3.6.1 Differences between computer programme and Kittredge method

A report produced by Acres American Inc. on behalf of the U.S. Department of Energy in 1980[7] includes details of a computer programme which is based on the method for turbine performance prediction published by Kittredge. The programme, which is written in Fortran, was installed on the Polytechnic VAX computer and tested in order to find out its accuracy in predicting PAT performance. In the Acres American computer programme, some changes have been made to the published procedure.

Firstly, an error in the turbine performance graphs published by Kittredge has been corrected. Kittredge shows the lines of $m/q^2$ and $p/q^3$ as being the same. However, $p = \nu m$, and therefore $m/q^2 = p/\nu q^2$. In the computer programme, this is corrected by storing values of $p/q^3 x\ q/\nu$.

Secondly, the programme includes the use of scale factors for efficiency, based on the work of Moody[79] and Hutton[80]. However, the way in which the scale factors have been included in the programme, they produce inconsistent results, since the power calculation has not been changed. Thus the predicted efficiency is not the same as the value calculated from the de-normalized head, flow and power.

### 3.6.2 Alterations to the Acres American programme

Once the programme had been tested, it was edited in order to produce better results. The main alterations to the programme are listed below:-

i) Efficiency scale factors were removed from the programme.

ii) A mistake in the calculation of the pump normalized speed, $\nu_p$, was found and corrected.

iii) In the original programme, the value of the pump bep head was being truncated to the nearest foot. Until this was corrected, significant errors occurred in the prediction of low-head PAT performance.

iv) It was found that the data stored for representing the model pumps contained discontinuities and other errors. These were corrected by comparing the stored values with graphs published in the original papers.

v) In its final form, the programme was converted to S.I. units.

Once corrections had been made to the programme, it was used to test the validity of Kittredge's prediction method.

### 3.6.3 Accuracy of Acres American programme.

In the Acres American report only one pump is used for making a comparison between the programme output and turbine test results. Although the curves for the Byron-Jackson pump, shown in Fig. 3.6, appear to be similar, the predicted best efficiency performance in turbine mode is significantly different from the test results. The values of turbine best efficiency performance found by using the first simulation (which is the logical thing to do, not knowing the test results) are compared with the test results in Table 3.5.

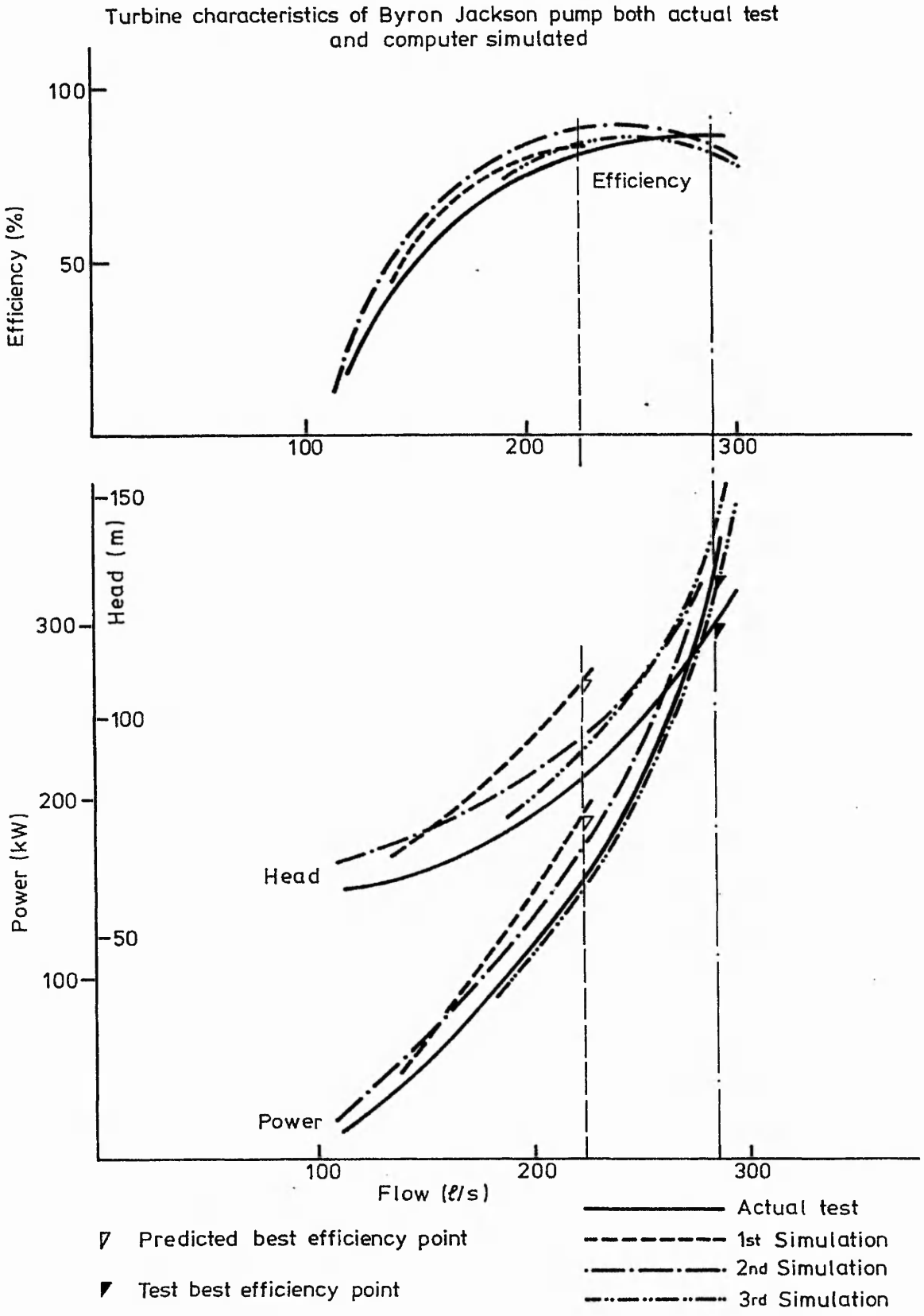


Fig. 3.6 Comparison of Acres American prediction with test

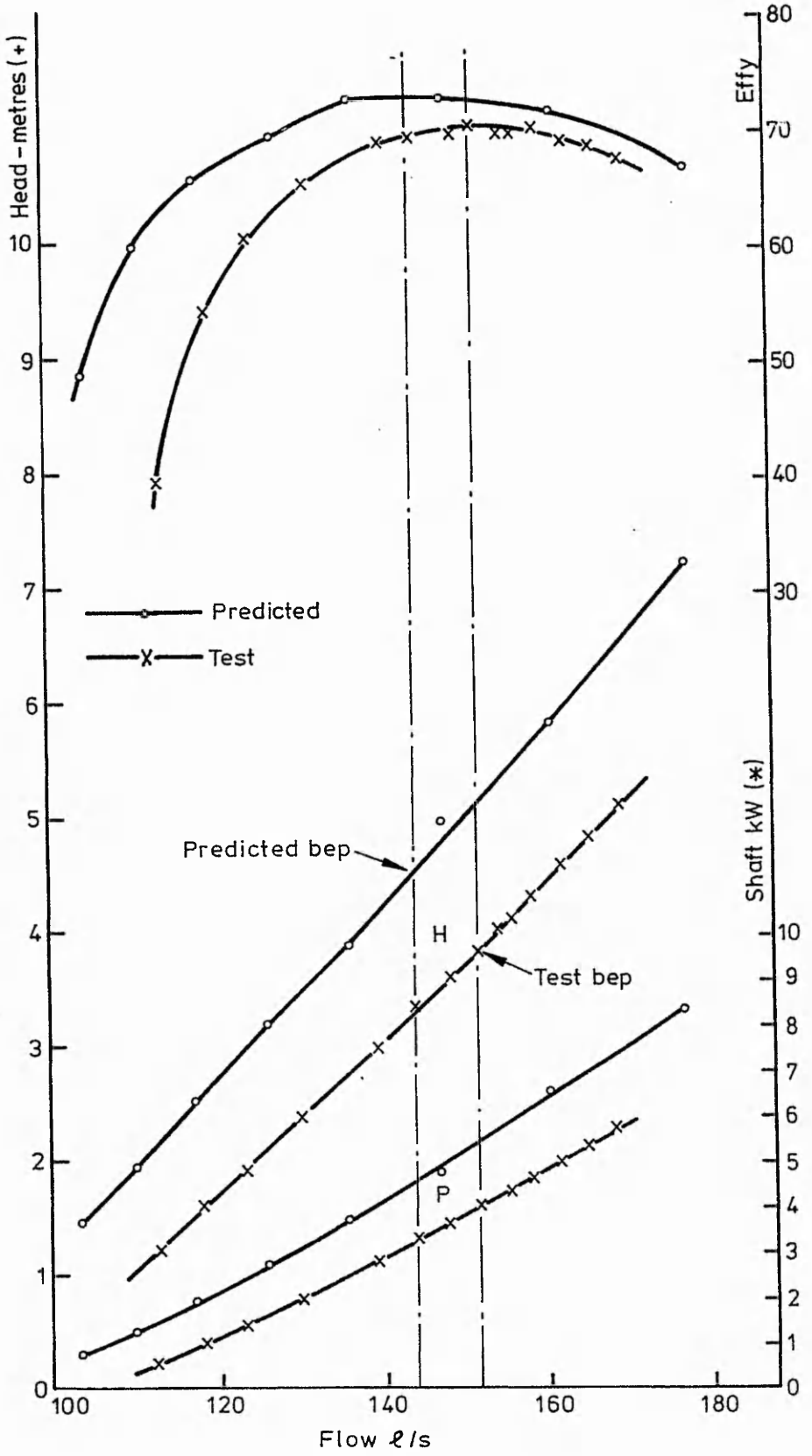


Fig. 3.7 Peerless 10PL PAT: Comparison of Kittredge prediction with test

**Table 3.5 Comparison of Acres American prediction with turbine test results for Byron-Jackson pump**

| | Q(USgpm) | H(ft) | P(hp) |
|---|---|---|---|
| Test | 4,555 | 495 | 430 |
| Predicted | 3,565 | 355 | 255 |

The value of the prediction criterion, Cr, is:

$$Cr = \sqrt{\left(\frac{0.219}{0.3}\right)^2 + \left(\frac{0.219}{0.1}\right)^2} = 2.30.$$

This value is not acceptable according to the analysis of section 3.1.4, since it is much greater than 1.

Another comparison was made using results supplied by Stirling Fluids of tests on a Peerless 10PL axial-flow pump . In this case, the pump tested was the same type as one of the pumps which Kittredge used for his model data, except that the impeller blade angle was different. The turbine performance characteristics are shown in Fig. 3.7. The correction to the Kittredge method specified by equations (3.34) - (3.36) has been applied, as the model pump has a maximum efficiency of 0.79 compared with 0.768 for the test pump. The best efficiency values are compared in Table 3.6 below.

**Table 3.6 Comparison of turbine test results with prediction by modified Kittredge and Sharma methods, for Peerless 10PL pump**

| | $Q(m^3/hr)$ | H(m) | P(kW) | $\eta(\%)$ |
|---|---|---|---|---|
| Test | 545 | 3.85 | 4.0 | 70.2 |
| Predicted(mod. Kitt.) | 515 | 4.55 | 4.5 | 72.8 |
| Predicted(Sharma) | 383 | 3.30 | 2.65 | 76.8 |

The value of the prediction criterion, Cr, for the Kittredge prediction is:

$$Cr = \sqrt{\left(\frac{0.118}{0.3}\right)^2 + \left(\frac{0.111}{0.1}\right)^2} = 1.18,$$

and for the Sharma prediction:

$$Cr = \sqrt{\left(\frac{-0.12}{0.3}\right)^2 + \left(\frac{0.113}{0.1}\right)^2} = 1.31.$$

The two pumps are the same type and the same size, therefore, using the data from one should result in an accurate prediction for the turbine performance of the other. However, the results are still outside the acceptable limits laid down earlier. Despite the complexity of this prediction method, the results are hardly more accurate than many of those obtained by the more simple methods described in section 3.2.

CHAPTER 4

# PERFORMANCE PREDICTION USING THE AREA RATIO METHOD

## 4.1 Background to the Area Ratio method.

### 4.1.1 Analysis of performance from pump geometry

The performance of centrifugal pumps was originally analysed by applying Euler's equation to the rotating impeller. The discrepancy between the actual performance characteristic and the theoretical line (the Euler head) was explained in part by the 'head slip' which was evaluated by Busemann[81]. Anderson[82,83] later demonstrated that the performance of a centrifugal pump is determined by the interaction of the impeller and the volute. He showed that the major features of the hydraulic performance may be related to a single geometrical parameter known as the Area Ratio. The Area Ratio, Y, is defined as the ratio of the exit area between the impeller blades and the throat area of the volute. Anderson demonstrated excellent correlation between Y and the design head and flow for a large number of centrifugal pumps. In 1963, Worster[84] published an analytical basis for explaining these correlations. More recently Thorne[85] has refined the area ratio method for both centrifugal pump design and for performance prediction.

A paper by Ventrone and Navarro[86] suggests the use of the velocity triangle at the outer edge of the impeller to predict the turbine performance, although it does not mention the area ratio method. These authors proposed that the turbine best efficiency occurs when there is a match between the volute flow and the impeller blade angle. However, the method which they describe incorporates factors that produce an accurate prediction for the particular pumps which they investigated, without any proof that they can be applied to a wider range of pumps. The turbine performance prediction method described in this chapter is easier to apply, and is not dependent on an accurate knowledge of the pump performance. Before presenting this method, the essential parts of the area ratio theory, as applied to pumps, are outlined below.

### 4.1.2 Area ratio relationships for pump operation

Figure 4.1 shows the ideal and slip-adjusted velocity diagrams for flow leaving the tips of a centrifugal pump impeller. For a given absolute meridional velocity component $V_{m2}$, the ideal absolute tangential velocity component $V_{u2}$ is reduced by the slip $(1 - h_0)U_2$, where $h_0$ is the slip factor and $U_2$ the impeller tip velocity.

The main cause of slip, besides general lack of blade guidance at exit, is a strong relative eddy between the blades of the impeller. Since the flow enters the impeller as substantially irrotational, the main body of the flow will remain irrotational as it passes between the blades of the impeller. This implies that the flow will have a counter rotation $-\Omega$ relative to the impeller and of equal magnitude to the impeller angular velocity $\Omega$. There are several ways of calculating the slip factor, but the most consistently accurate method has been found to be that of Bothmann & Reffstrupp[87]. This gives the following value:-

$$h_0 = \frac{1}{2}\left\{1 + e^{-\left(\frac{2\pi}{Z}\right)\sin\beta}\right\} \qquad (4.1)$$

where Z is the number of impeller blades, and $\beta$ is the impeller blade angle. Bothmann stipulates a limit for the formula, because the recirculating flow which causes the impeller slip is distorted when the ratio of the impeller eye diameter to outside diameter is large. Thus the limit is:

$$\frac{D_1}{D_2} < e^{-\left(\frac{2\pi}{Z}\right)\cos\beta} . \qquad (4.2)$$

The energy per unit mass added to the flow by the impeller $U_2V_{u2}$ slightly exceeds the energy $gH_p$ delivered at the discharge branch, owing to irreversibilities in the volute represented by an efficiency $\eta_{vp}$. Thus:-

$$\frac{gH_p}{\eta_{vp}} = U_2V_{u2} . \qquad (4.3)$$

From the velocity diagram

$$\frac{gH_p}{\eta_{vp}U_2^2} = h_0 - \left(\frac{V_{m2}}{U_2}\right)\cot\beta_2 . \qquad (4.4)$$

The circumferential exit area across which $V_{m2}$ is passing is $b_2(\pi D_2 - Zt)$, where $b_2$ is the width of the impeller passage in the axial direction and t is the circumferential thickness of the blades. Thus the velocity normal to the impeller is given by:

$$V_{m2} = \frac{Q}{b_2(\pi D_2 - Zt)} = \frac{Q}{a_2} . \qquad (4.5)$$

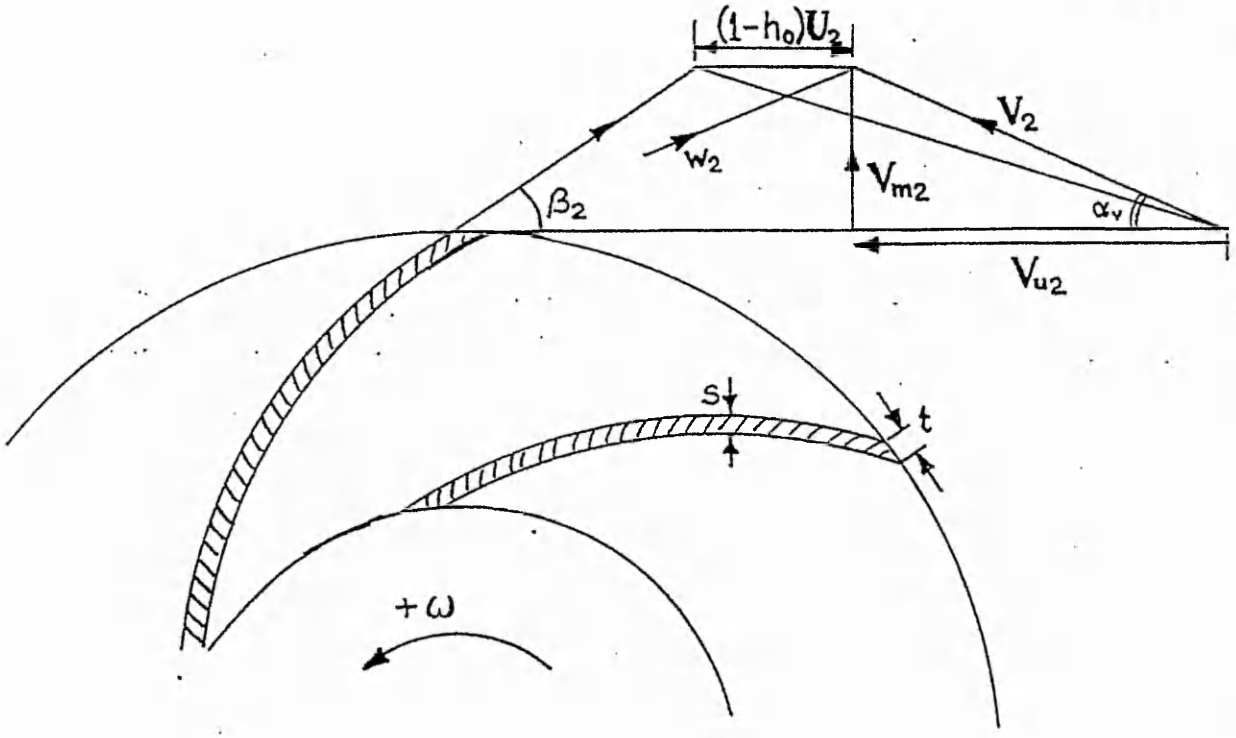


Fig. 4.1. Velocity diagram for Pump Operation

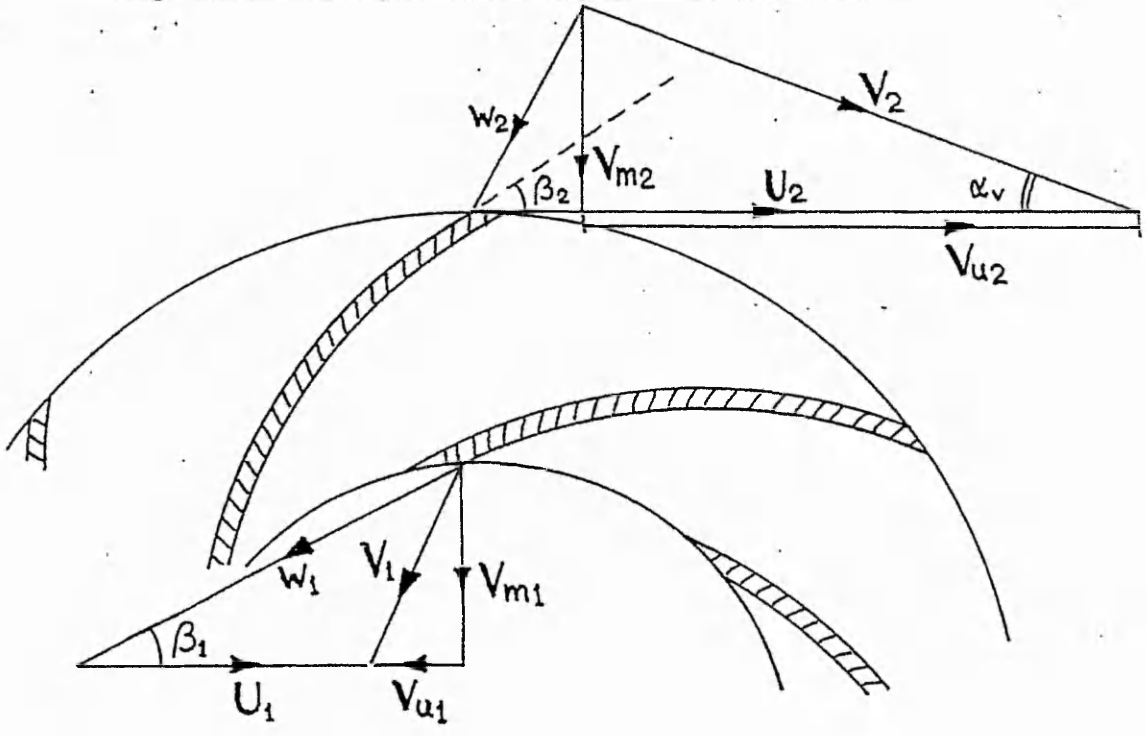


Fig. 4.2. Velocity diagram for Turbine Operation

Substituting (4.5) into (4.4) gives:

$$\frac{gH_p}{\eta_{vp} U_2^2} = h_0 - \frac{Q}{U_2 B^2}\left(\frac{B^2}{a_2 \tan \beta_2}\right). \qquad (4.6)$$

The expression $\frac{(a_2 \tan \beta_2)}{B^2}$ is the 'Area Ratio' as defined by Worster, which is given the symbol Y.

The equation now simplifies to:

$$\frac{gH_p}{\eta_{vp} U_2^2} = h_0 - \frac{1}{Y}\left(\frac{Q}{U_2 B^2}\right) \qquad (4.7)$$

This is the rotor characteristic, and is only valid when the operation is close to the pump best efficiency point.

The volute characteristic, is evaluated using the assumption that in order to obtain the best performance, there is a free vortex flow pattern within the scroll. The velocity distribution in the volute throat is given by taking V proportional to 1/r and the resulting shape of the volute is a logarithmic spiral of constant angle $\alpha_v$ where:-

$$\tan \alpha_v = \frac{V_{m2}}{V_{u2}}. \qquad (4.8)$$

The resulting volute characteristic is given by Worster[84] as:-

$$\frac{gH_p}{\eta_{vp} U_2^2} = \frac{\frac{2B}{D_2}}{\log_e\left(1 + \frac{2B}{D_2}\right)} \cdot \frac{Q_p}{U_2 B^2}. \qquad (4.9)$$

Simultaneous solution of (4.7) and (4.9) for a given pump geometry, and judicious choice of $\eta_{vp}$ and $h_0$, will yield the dimensionless head $(gH_p/U_2^2)$ and flow $(Q_p/U_2B^2)$ for best efficiency pump operation.

It is now possible to rewrite the volute angle in terms of geometrical parameters.

Substituting back from equation (4.9) into (4.3) gives:-

$$V_{u2} = \frac{gH_p}{\eta_{vp} U_2^2} \cdot U_2 = \frac{\frac{2B}{D_2}}{\log_e\left(1 + \frac{2B}{D_2}\right)} \cdot \frac{Q}{B^2} \qquad (4.10)$$

and substituting from equation (4.5) into (4.8) gives:

$$\tan \alpha_v = \frac{V_{m2}}{V_{u2}} = \frac{B^2}{a_2} \cdot \frac{\log_e\left(1 + \frac{2B}{D_2}\right)}{\frac{2B}{D_2}} . \qquad (4.11)$$

This angle is important since it also determines the angle with which the flow will approach the impeller when running in turbine mode.

## 4.2 Use of the Area Ratio for Turbine Performance Prediction

### 4.2.1 Area ratio relationships for turbine operation

It will be convenient to retain subscript 2 for all parameters relating to the outer periphery of the impeller, although this becomes the point of flow entry under turbine operation. The energy per unit mass available at entry to the volute, $gH_t$, will be reduced by irreversibilities in the volute. Consequently the energy per unit mass at the rotor tip will be given by $\eta_{vt} gH_t$, where $\eta_{vt}$ is the volute efficiency in turbine mode. The energy transferred from the fluid to the impeller, neglecting for the moment losses in the impeller, is equal to the change in angular momentum, as given by the Euler equation:-

$$gH_{t(imp)} = U_2 V_{u2} - U_1 V_{u1} \qquad (4.12)$$

The turbine is not able to make use of the exit kinetic energy lost because of the whirl velocity at exit from the impeller. This is taken into account incorporating a factor of utilisation $\varepsilon$, where:-

$$\varepsilon = \frac{\text{Energy per unit mass utilised by the turbine}}{\text{Energy per unit mass available to the turbine}}$$

$$\varepsilon = \frac{\psi_t \frac{U_2^2}{g}}{\psi_t \frac{U_2^2}{g} + \frac{V_{u1}^2}{2g}} . \qquad (4.13)$$

Incorporating $\varepsilon$ into equation (4.12) then yields:-

$$\varepsilon \eta_{vt} g H_t = U_2 V_{u2} - U_1 V_{u1} \qquad (4.14)$$

During turbine operation the water approaches the rotor at an angle $\alpha_v$, which is determined by the volute shape. As in the pump mode, the ratio of radial to tangential flow at the outer diameter of the impeller is given by equation (4.8):-

$$\frac{V_{m2}}{V_{u2}} = \tan \alpha_v .$$

Using this and the other relationships determined by the inlet and exit velocity diagrams (Figure 4.2) in equation (4.14) yields:-

$$\frac{\varepsilon \eta_{vt} g H_t}{U_2^2} = \frac{V_{m2}}{U_2} \cot \alpha_v + \frac{V_{m1}}{U_2} \frac{U_1}{U_2} \cot \beta_1 - \frac{U_1^2}{U_2^2} . \qquad (4.15)$$

Letting $\frac{D_1}{D_2} = \nu$ and using:-

$$V_{m1} = \frac{Q_t}{\pi D_1 b_1 - \frac{Zsb_1}{\sin \beta_1}} \text{ and } V_{m2} = \frac{Q_t}{\pi D_2 b_2 - \frac{Zsb_2}{\sin \beta_2}}$$

gives: $$\left(\frac{V_{m1}}{V_{m2}}\right)_t = \frac{a_1}{a_2} . \qquad (4.16)$$

This is the ratio of the areas normal to the flow direction at the periphery and at the eye of the impeller.

Substituting for cot $\alpha_v$ from (4.11), and using the notation $c_v$ for the volute constant $\dfrac{\frac{2B}{D_2}}{\log_e\left(1+\frac{2B}{D_2}\right)}$ reduces (4.15) to:

$$\frac{\varepsilon\eta_{vt}\, gH_t}{U_2^2} = \frac{Q_t}{U_2 B^2}\left(c_v + \nu\frac{B^2}{a_1 \tan\beta_1}\right) - \nu^2 \ . \qquad (4.17)$$

This, the turbine mode rotor characteristic, is certainly more complex than the equivalent pump expression (4.7). However, the picture becomes much clearer by recourse to the combined characteristic diagram.

### 4.2.2 Graphical Representation of Pump and Turbine Characteristics

In order to plot the theoretical pump and turbine characteristics on the same graph, the head and flow are plotted in dimensionless form. The flow coefficient, for both pump and turbine modes, is defined by $\phi = Q/U_2B^2$ and the head coefficient is defined by:- $\psi_p = \dfrac{gH_p}{\eta_{vp} U_2^2}$ and $\psi_t = \dfrac{\varepsilon\eta_{vt}\, gH_t}{U_2^2}$ (4.18,19)

Figure 4.3 shows the three straight-line relationships for the pump rotor characteristic (4.7), the no-whirl volute characteristic (4.9) and the turbine rotor characteristic (4.17). It can clearly be seen that the gradients of the three lines in the diagram depend entirely upon rotor and volute geometry, particularly the area ratio, Y; viz:-

slope of pump rotor characteristic $= -\dfrac{1}{Y} = m_p$ (4.20)

slope of the volute characteristic $= c_v = m_v$ (4.21)

slope of the turbine rotor characteristic $= c_v + \dfrac{\nu B^2}{a_1 \tan\beta_1} = m_t$ . (4.22)

As shown by Worster [84], the intersection of the pump rotor characteristic (of slope $m_p$) with the volute characteristic (of slope $m_v$) will approximate to the point of peak efficiency running as a pump. This is indicated as point I in Fig.4.3. It is the point at which the flow leaving the rotor just "fits" the volute shape.

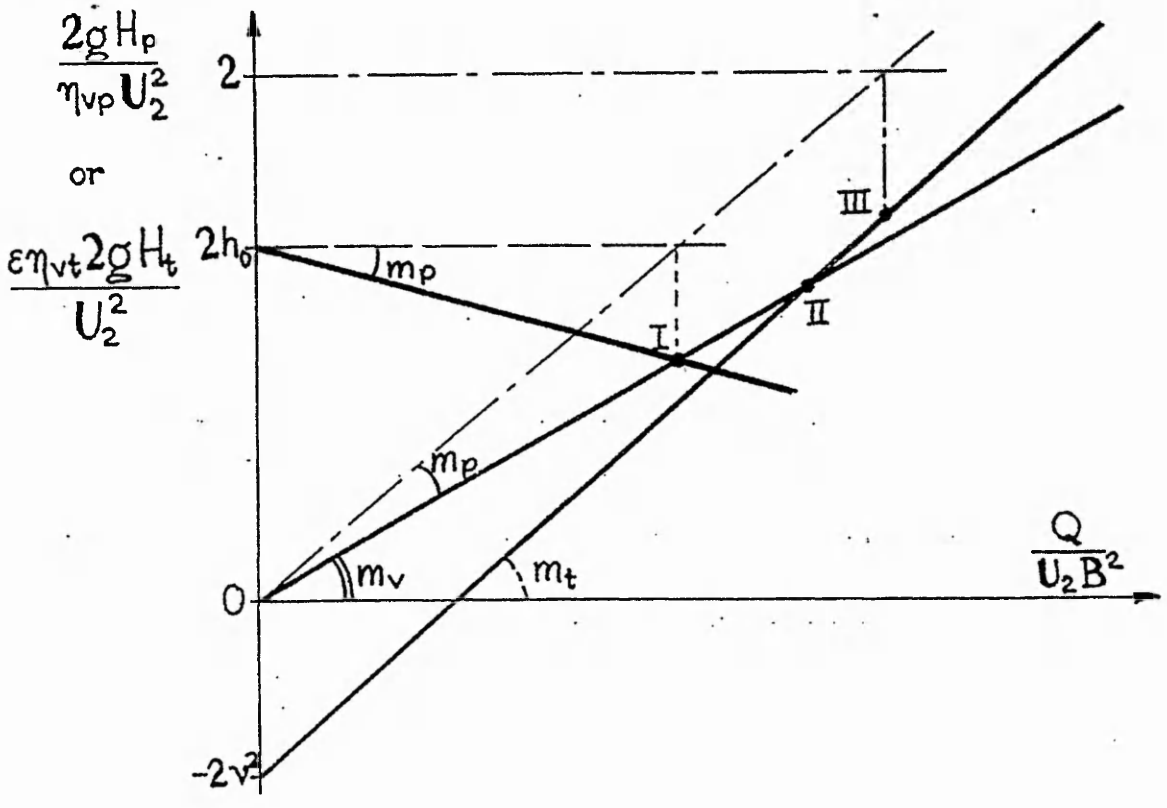


Fig. 4.3. Diagram for estimating Pump and Turbine Performance

Point I Pump best efficiency

Point II Turbine operation; no whirl at exit

Point III Turbine operation; shock-free entry,
ie. $V_{rel}$ at entry matches angle $\beta_2$

Under turbine operation two particular points are of interest. The first is point II, where the volute characteristic (of slope $m_v$) cuts the turbine rotor characteristic (of slope $m_t$). The equation of the point of intersection is:-

$$\psi = c_v\phi = \left( c_v + \frac{\nu B^2}{a_1 \tan \beta_1} \right)\phi - \nu^2 , \qquad (4.23)$$

or, rearranging

$$\phi = \frac{a_1}{a_2} \cdot \frac{\nu a_2 \tan \beta_1}{B^2} . \qquad (4.24)$$

Hence,

$$\phi = \frac{V_{m2}}{V_{m1}} \cdot \frac{\nu a_2 \tan \beta_1}{B^2} . \qquad (4.25)$$

Substituting the value of $V_{m2}$ from (4.5) gives:

$$\frac{Q}{U_2 B^2} = \frac{Q}{B^2} \cdot \frac{\nu \tan \beta_1}{V_{m1}} \qquad (4.26)$$

which simplifies to:

$$\frac{U_1}{V_{m1}} = \tan \beta_1 . \qquad (4.27)$$

This demonstrates that point II represents turbine operation in which the flow leaves the centre of the impeller with zero whirl velocity. At this point the factor of utilisation has its maximum value.

Point III in Figure 4.3 is the point at which the absolute velocity of flow leaving the volute at angle $\alpha_v$ with respect to the impeller periphery is just large enough for the relative flow velocity to match the angle of the blade tip $\beta_2$. Point III is most easily located in the diagram by adding a further line through the origin of gradient $m_v + \frac{1}{Y}$. From where it intersects the line $\psi_t = 1$, a vertical line is drawn to intersect with the turbine impeller line at point III.

The point at which the flow is parallel to the the blades at entry to the impeller can be determined from Fig. 4.2 and is found from the equation:-

$$U_2 = V_{m2} \cot \beta_2 + V_{m2} \cot \alpha_v . \qquad (4.28)$$

Substituting for $V_{m2}$ from equation (4.5) gives:-

$$U_2 = \frac{Q}{B^2} \cdot \frac{B^2}{a_2}\left(\frac{1}{\tan \beta_2} + \frac{1}{\tan \alpha_v}\right). \qquad (4.29)$$

Putting $\frac{Q}{U_2 B^2} = \phi_t$, and substituting for $\tan \alpha_v$ from equation (4.11) gives:-

$$1 = \phi_t\left(\frac{1}{Y} + c_v\right). \qquad (4.32)$$

Since, from equation (4.21), $m_v = c_v$, the value of $\phi_t$ for which there is shock-free flow at the entry to the impeller is given by the intersection of the line $\psi_t = 1$ with the line $\psi_t = m_v + \frac{1}{Y}$.

### 4.2.3 Determination of the Turbine operating point

The exact point of peak turbine efficiency is determined by a compromise between running at II with no whirl at outlet, so as to maximise the factor of utilisation, and running at III with minimum shock loss at entry to the impeller blade. Curves of utilization factor calculated by Hergt et al[88], show that the value of $\varepsilon$ falls very gradually after the maximum value. The actual best efficiency point in turbine mode is usually close to the point III, because then the loss of efficiency due to a non-zero exit whirl velocity is negligible. In contrast, the loss of efficiency due to shock loss at the impeller inlet when operating at point II may be considerable. Calculations of the utilization factor at points II and III for two pumps of different designs are given in Appendix L. Since the turbine efficiency curves tend to be flat at over capacity (see Fig. 1.1) it is usually desirable to design for a rated capacity slightly greater than the best efficiency point. Point III is therefore taken as the design point for turbine operation.

In calculating the actual values of head and flow for the best efficiency points, it is important to take into account the leakage through the internal running clearances. During turbine operation, a small part ($q_t$) of the flow entering the volute leaks through the wear rings rather than passing through the impeller. This means that turbine flows indicated by points (II) or (III) in Figure 4.3 need to be multiplied by a leakage factor ($1 + q_t/Q_t$). In contrast, during pump operation, the discharge flow indicated by point I in Fig. 4.3 is corrected for leakage by multiplying by a factor ($1 - q_p/Q_p$) so as to determine the real pump discharge. The turbine leakage flow, $q_t$, is larger than the pump leakage flow, $q_p$, because of the increased head for turbine operation.

### 4.2.4 Example of applying the Area Ratio method to a Pump-as-Turbine

The data for a Worthington-Simpson end-suction pump given below in Table 4.1 have been used as an example of applying the area ratio method to predict the turbine performance. The pump was tested in the laboratory in both pump and turbine modes, and these results are compared with the area ratio predictions.

**Table 4.1. Data for Worthington-Simpson 25WB125 pump**

| | | | | | | | |
|---|---|---|---|---|---|---|---|
| $D_2$: | 134 mm | $b_2$: | 6.54 mm | $\beta_2$: | 34.5 | N: | 2900 rpm |
| $D_1$: | 30 mm | $b_1$: | 12.5 mm | $\beta_1$: | 26.5 | Z: | 5 |
| $B^2$: | 194 $mm^2$ | | | $a_2$: | 2522 $mm^2$ | $a_1$: | 758 $mm^2$ |

For the calculation of the pump impeller line (equation (4.7)), it is necessary to evaluate the head slip factor, $h_0$. Using the Bothmann's equation (4.1) gives the following value:-

$$h_0 = \frac{1}{2}\left\{1 + e^{-\left(\frac{2\pi}{5}\right)\sin 34.5^\circ}\right\}$$

$$= \frac{1}{2}\left(1 + e^{-0.712}\right)$$

$$= 0.745 \ .$$

The peripheral velocity of the impeller is given by:-

$$U_2 = \frac{\pi D_2 N}{60} \qquad (4.32)$$

$$= 20.35 \text{ m/s} \ .$$

The volute constant is given by:-

$$c_v = \frac{\frac{2B}{D_2}}{\log_e\left(1 + \frac{2B}{D_2}\right)} = 1.101 \ .$$

Based on these values, the lines are:

Pump impeller: $\psi_p = 0.745 - 0.112\phi$

Pump volute: $\psi_p = 1.101\phi$

Turbine impeller for zero exit whirl velocity: $\psi_t = 1.184\phi - 0.050$ .

The points of interest are as follows:-

Point I, intersection of pump impeller and volute lines:-

$$0.745 - 0.112\phi = 1.101\phi, \text{ hence } \phi = 0.614, \psi_p = 0.676$$

Point II, intersection of turbine impeller and volute lines:-

$$1.184\phi - 0.050 = 1.101\phi, \text{ hence } \phi = 0.687, \psi_t = 0.756.$$

Point III, determined by $1.213\phi = 1$; hence:-

$$\phi = 0.824, \psi_t = 1.184\phi - 0.050 = 0.926 .$$

From these values of dimensionless head and flow, the predicted values may be derived by calculating, as near as possible, the values of $\eta_{vp}$, $\eta_{vt}$, $\varepsilon$, $q_p$ and $q_t$. In order to do this it is first necessary to make an estimate of $Q_p$ and $H_p$.

Assuming that the value of volute efficiency is 0.9, and the leakage flow is 5% of the total flow:-

$$Q_p = \phi U_2 B^2 \left(1 - \frac{q_p}{Q_p}\right) \approx 0.614 \times 20.35 \times 194 \times 10^{-6} \times 0.95$$

$$\approx 2.30 \times 10^{-3} \text{ m}^3/\text{s}$$

$$H_p = \frac{\psi_p U_2^{\,2} \eta_{vp}}{g} \approx \frac{0.676 \times 20.35^2 \times 0.9}{9.81}$$

$$\approx 25.7 \text{ m.}$$

The values of $H_t$ and $Q_t$ for point III can be calculated in a similar manner. In order to produce 50 Hz supply, the turbine speed must be 3100 rpm. $U_2$ is therefore 21.75 m/s. $H_t$ is found by rearranging equation (4.18) to give:

$$H_t = \frac{\psi_t U_2^{\,2}}{g\varepsilon\eta_{vt}}; \quad Q_t = \phi_t U_2 B^2 \left(1 + \frac{q_t}{Q_t}\right).$$

Taking an initial guess by using $\eta_{vt} = 0.9$ and $\varepsilon = 0.9$ gives:

$$H_t \approx \frac{0.926 \times 21.75^2}{9.81 \times 0.81} = 55.1 \text{ m.}$$

and $$Q_t \approx 0.824 \times 21.75 \times 194 \times 10^{-6} + q_t = 3.48\ \text{l/s} + q_t.$$

The value of the leakage flow is proportional to $\sqrt{H}$, thus:

$$q_t \approx 0.05 \times 2.3 \times \sqrt{\frac{55.1}{25.7}} = 0.168\ \text{l/s},$$

giving the total flow rate to be 3.65 l/s. More accurate values for the pump and turbine best efficiency points may be obtained by taking into account the individual losses in pump and turbine modes, as shown in section 4.3.2.

## 4.3 Pump selection using the Area Ratio Method

### 4.3.1 Variation of turbine performance with design parameters

The values of head and flow at predicted points I and III can be determined using the equations (4.7,4.9,4.17,4.30). These give the following co-ordinates on the ($\phi$,$\psi$) diagram:-

$$\phi_p = \frac{h_0}{\frac{1}{Y} + c_v}, \quad \psi_p = \frac{c_v h_0}{\frac{1}{Y} + c_v} \tag{4.33}$$

$$\phi_p = \frac{1}{\frac{1}{Y} + c_v}, \quad \psi_p = \frac{\frac{\nu B^2}{a_1 \tan\beta_1} + c_v}{\frac{1}{Y} + c_v} - \nu^2 . \tag{4.34}$$

The ratios of these dimensionless parameters at pump and turbine best efficiency conditions is therefore given by:-

$$\frac{\phi_t}{\phi_p} = \frac{1}{h_0}; \quad \frac{\psi_t}{\psi_p} = \frac{1}{h_0}\left\{1 + \frac{\nu}{c_v Y}\left(\frac{a_2 \tan\beta_2}{a_1 \tan\beta_1} - 1\right) - \nu^2\right\}. \tag{4.35,36}$$

From these equations can be drawn the conclusion that $\phi_t/\phi_p$ is always greater than 1, and will increase for a pump with fewer impeller blades or a smaller outlet angle, $\beta_2$. $\psi_t/\psi_p$ will usually be greater than $\phi_t/\phi_p$, since for most pumps $a_2 > a_1$, $\tan\beta_2 > \tan\beta_1$ and $\nu < 0.6$. $\psi_t/\psi_p$ will depend on Z and $\beta_2$ in a similar way to $\phi_t/\phi_p$, but will also be affected by the values of $\nu$, Y, $a_2/a_1$ and the ratio of the angles at each end of the impeller blades.

The ratios of the actual head and flow in pump and turbine mode are given by:-

$$\frac{Q_t}{Q_p} = \frac{\left(1 + q_t/Q_t\right)\phi_t}{\left(1 - q_p/Q_p\right)\phi_p} \tag{4.37}$$

and

$$\frac{H_t}{H_p} = \frac{1}{\varepsilon\eta_{vp}\eta_{vt}}\frac{\psi_t}{\psi_p} . \tag{4.38}$$

### 4.3.2 Consideration of Pump and Turbine Losses

The losses in a pump or turbine are made up of a combination of mechanical loss, leakage loss, disc friction loss and other hydraulic losses in the impeller and volute. In order to calculate the efficiency in turbine mode, each of these losses must be calculated separately. In the analysis below, the same Worthington-Simpson pump is used as an example for evaluating the losses in pump and turbine mode.

The disc friction loss may be calculated using the method given by Stepanoff[89] and outlined in Appendix J. As with the disc friction loss, bearing and seal losses are approximately proportional to the square of the rotational speed. According to Anderson[90], the bearing loss is typically half of the disc friction loss, and the loss in a gland packing about the same. For pumps with mechanical seals, there is virtually no friction loss caused by the seal. Therefore, for a pump with a mechanical seal, the bearing and seal friction losses are estimated to be 50% of the disc friction loss, whereas for a pump with gland packing the bearing and seal losses are estimated to be 100% of the disc friction loss.

Using Stepanoff's calculation for the Worthington-Simpson pump under consideration, gives 97 W for the disc friction loss. The bearing and seal losses are estimated to be 50% of this, giving a total mechanical loss of 145 W in pump mode. The leakage loss can be calculated using the equation given by Thorne[85], which is included in Appendix K. The value of pump leakage flow is calculated to be 0.34 l/s, ie. the leakage loss is 86 W.

At the best efficiency point in pump mode, there should be no shock losses at the impeller inlet or exit. The remaining losses are due to viscous shear and diffusion in the impeller and volute. Accurate calculation of these losses is difficult, because it depends on an accurate knowledge of the internal flows in the pump, and the shape of the flow channels.

Using the manufacturer's data for the pump, the maximum efficiency is given as 46%. The pump output power is given by $\rho g Q_p H_p$ = 640 W, and the input power is therefore 1391 W. In the absence of a more accurate method of calculation, the

remaining loss has been split equally between the impeller and the volute. The energy balance for pump best efficiency operation is shown in Table 4.2, and the volute efficiency is:

$$\eta_{vp} \approx \frac{1160 - 260}{1160} = 0.776 .$$

The final estimates for pump best efficiency point are therefore:-

$$H_p = 22.1 \text{ m}; \quad Q_p = 2.08 \text{ l/s}.$$

Tests give the pump best efficiency point at 20.6 m, 2.40 l/s.

**Table 4.2 Energy balance for pump best efficiency.**

| | |
|---|---|
| Input power : 640/0.46 = | 1 391 |
| Mechanical losses | 145 |
| Leakage losses | 86 |
| | 1 160 |
| Impeller losses | 260 |
| Volute losses | 260 |
| Hydraulic output power | 640 W |

In turbine mode, the losses can be estimated from the pump losses, taking into account the higher speed, head and flow in turbine mode. The mechanical loss, which is assumed to be proportional to the square of the rotational speed is therefore:

$$P_{mech} \approx 145 \times \frac{3100^2}{2900^2} = 166 \text{ W}.$$

The leakage flow is proportional to the square root of the head, and the loss is therefore:

$$q_t \approx 0.34 \times \sqrt{\frac{54.8}{22.1}} = 0.54 \text{ l/s}.$$

A better estimate of $\varepsilon$ may now be obtained using a revised value for $Q_t$ of 4.02 l/s.

At point III,

$$\varepsilon = \frac{\psi_t U_2^2}{\psi_t U_2^2 + \frac{V_{u1}^2}{2}} = \frac{0.926 \times 21.75^2}{0.926 \times 21.75 + \frac{5.77^2}{2}} = 0.963 .$$

In turbine mode, the losses in the volute are relatively smaller than those in pump mode, because in turbine mode the volute represents a converging, rather than a diverging passage, in which the diffusion losses are lower. As an estimate of the volute losses, the turbine volute loss is taken to be 80% of the pump volute loss, ie.

$$1 - \eta_{vt} = 0.8\left(1 - \eta_{vp}\right) = 0.8 \times 0.224 . \qquad (4.39)$$

In this case, $\eta_{vt}$ is therefore 0.821. Hence, a more accurate value for the predicted head for turbine operation with no shock loss at the impeller inlet is:

$$H_t = \frac{0.926 \times 21.75^2}{9.81 \times 0.963 \times 0.821} = 56.5 \text{ m.}$$

From this, the total input power is 2200 W and the volute loss is:

$$P_{vol} = (1 - 0.821) \times 2217 = 397 \text{ W},$$

and the leakage loss is:

$$P_{leak} = 0.53 \times 56.5 \times 0.821 \times 9.81 = 242 \text{ W}.$$

The impeller loss has been calculated in a similar way to the volute loss:

$$1 - \eta_{t(imp)} = 0.8\left(1 - \eta_{p(imp)}\right). \qquad (4.40)$$

The impeller efficiency in pump mode is given by:

$$\eta_{p(imp)} = \frac{640}{640 + 260} = 0.711 .$$

The turbine impeller loss is therefore:

$$P_{imp} = 0.8(1 - 0.711) \times 1520 = 351 \text{ W}.$$

The complete energy balance, from these estimated loss figures, is shown in Table 4.3. The resulting predictions of turbine head and flow at best efficiency are 56.5 m and 4.00 l/s, and the turbine efficiency is 45%. Tests on this pump give 59.3 m and 3.93 l/s, at a maximum efficiency of 48%. A comparison of these predicted operating points with test results is shown on a plot of $\psi$ against $\phi$ in Fig. 4.4.

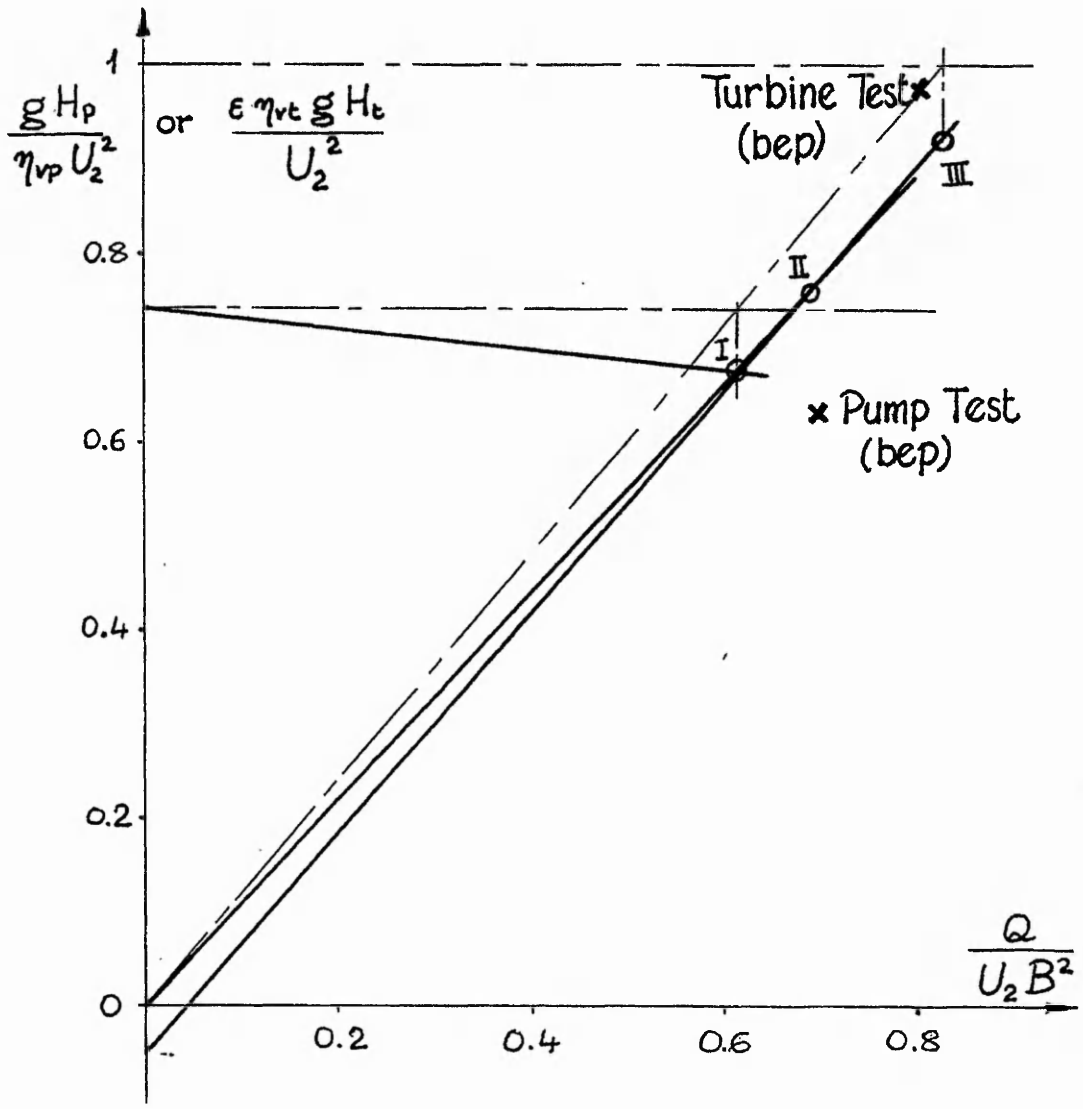


Fig. 4.4. Comparison of predicted and Test results for Worthington-Simpson WB pump in Pump and Turbine operation

**Table 4.3 Breakdown of losses for turbine best efficiency.**

| | | |
|---|---|---|
| Turbine input power | 2 217 | |
| Volute losses | 397 | |
| Leakage loss | 242 | |
| Available power input | 1 578 | |
| Exit losses | 58 | |
| Impeller input power | 1 520 | |
| Impeller losses | 351 | |
| Mechanical loss | 166 | |
| Mechanical output power | 1 003 | W |

### 4.3.3 Modifications to Pumps-as-Turbines according to the Area Ratio analysis

The area ratio analysis shows that there are various options for changing the turbine operating point of a particular pump. It has been stated by several authors, including Meier[6] and Naber[91], that the turbine speed may be changed in order to alter the turbine operating point. However, for a direct-coupled pump unit, the amount by which the speed can be varied is limited by the acceptable range of generated frequency, usually no more than ± 5%. The effect of changing the turbine speed is that the best efficiency point moves along a curve on which $H_t$ is proportional to $Q_t^2$, and $Q_t$ is proportional to the rotational speed, N.

Changing the impeller diameter may be expected to have an effect similar to that of changing the turbine speed, since it also changes the value of $U_2$. This has been suggested by Mikus [16]. However, Yedidiah[66] warns that the effect of changing the impeller diameter is not as great as would be expected from looking at the pump curves. This has been investigated further, and some results of tests are included in Chapter 5.

Changing either the turbine speed or the impeller diameter tends to produce a limited change in the actual operating point, since the turbine head-flow curve is also approximately parabolic, and the curves for different speeds or different diameters are often very close together near the best efficiency points. This is illustrated in Fig. 4.5.

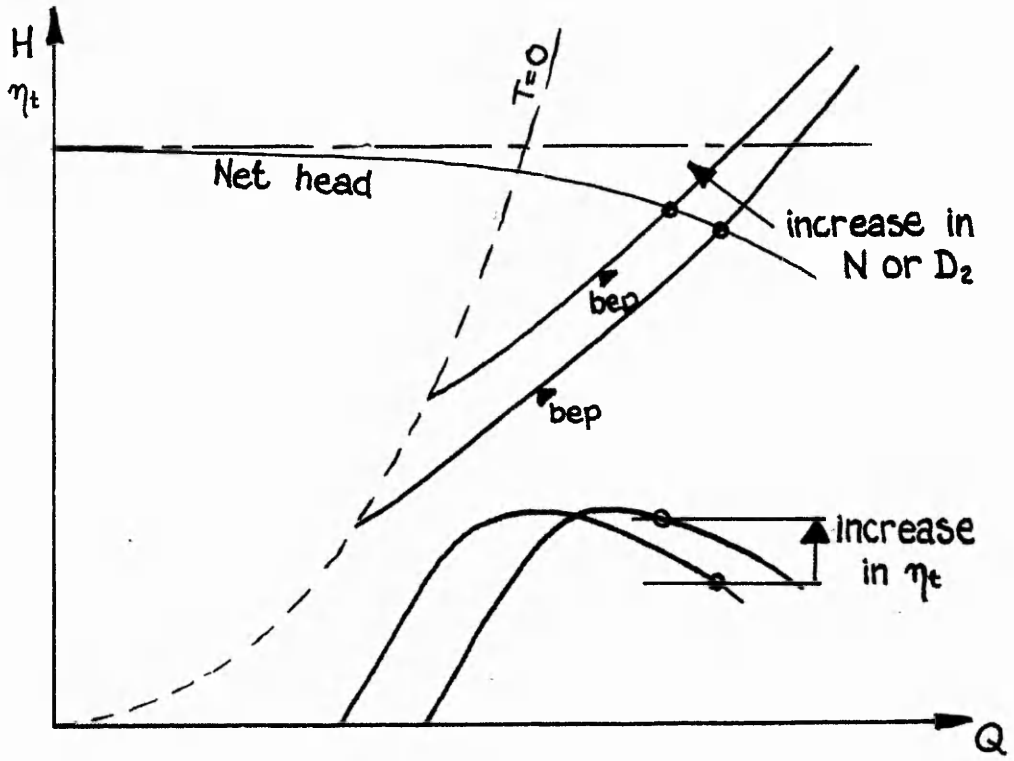


Fig. 4.5. Effect on PAT performance of changing speed or diameter

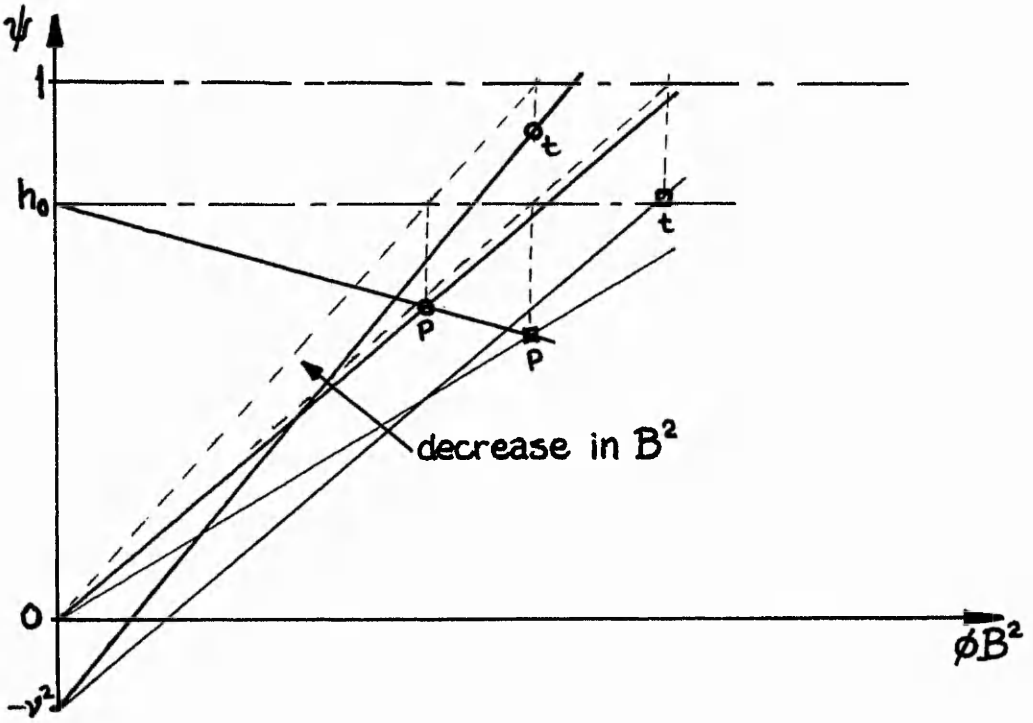


Fig 4.6. Effect on PAT performance of changing Volute cross-sectional area

From the area ratio analysis, changing the value of the volute cross-section, $B^2$, provides a more direct method of changing the operating flow without moving the best efficiency point relative to the system curve, as shown in Fig. 4.6. In most pumps it is possible to reduce the value of $B^2$ by inserting a conical sleeve into the volute discharge branch. This modification was carried out on a pump installed as a turbine at a demonstration site. The effect was to reduce the flow rate required from 17 l/s to 15 l/s, while the electrical output increased from 2.6 kW to 2.8 kW.

Options for changing the turbine operating point are given in Table 4.4.

**Table 4.4**
**Options for adjusting the operating point of a pump-as-turbine**

| PAT bep compared with design | Solution |
|---|---|
| Head too high, flow too low : | Decrease $D_2$ or N and run at $Q > Q_{bep}$ |
| Head too high, flow too high: | Decrease $D_2$ or N and $B^2$ |
| Head too low, flow too high : | Decrease $B^2$ |
| Head too low, flow too low : | Run at $Q > Q_{bep}$ or change pump! |

# CHAPTER 5

# LABORATORY TESTING OF PUMPS-AS-TURBINES

## 5.1 Introduction to the testing of Pumps-as-Turbines

### 5.1.1 Requirements and options for testing pumps-as-turbines

The performance characteristics of a centrifugal pump are usually presented as a constant speed plot, showing head varying against volume flow rate. The efficiency at various points on the curve is frequently given. The British Standard 5316 [65] lays out procedures and limits for the testing of pumps. This is equivalent to internationally recognized standards ISO 2458 and 3555. A separate British Standard (BS 5860) is used for the testing of hydraulic turbines, but this is not applicable to the small size of turbine which is being considered here.

In carrying out tests on pumps in turbine mode, the procedures of BS 5316 Part 2 have been followed wherever possible. However, additional constraints are encountered when testing pumps-as-turbines, which result in a more complicated test procedure. In order to test a PAT it is necessary to provide a flow of water at high pressure in order to drive the turbine and overcome losses in the pipe system feeding the turbine. The pressure may be provided by a header tank, which is refilled by a pump, or provided directly from the output of a service pump. In all the tests described in this chapter, the head required by the PAT could not easily be provided by a header tank, so a service pump (or pumps) was used to produce the hydraulic input power.

Turbine test results may be presented either as constant speed curves, or as constant head curves. For a particular site, the head may be considered to be constant, and therefore the constant head curves give the performance characteristics which can be expected at an actual installation. The constant speed characteristics, on the other hand, can be used to check the range of sites at which the PAT can be employed, given that it is coupled to a generator running at constant speed.

Whether the turbine test is carried out at constant head, or constant speed, there must be a flow control valve in the system and a variable load connected to the turbine shaft. Often it is difficult to adjust the head or speed to the exact value required, because of the sensitivity of the system to changes in the valve setting or the turbine load. In these cases, the affinity laws may be used to correct the values to the constant head or speed required.

### 5.1.2 Description of test equipment and procedures

In all of the tests carried out during this project, except for measurements taken at the demonstration installations, an open-circuit test rig was used, with two service pumps supplying the necessary hydraulic power. In the Fluid Dynamics laboratory at Nottingham Polytechnic, a test rig was set up and used, with certain modifications, for testing the pump and turbine operating charcteristics of several different centrifugal pumps. The two service pumps are identical units, which can be connected in series or in parallel, enabling an output from approximately 10 l/s at 50 m head to 60 l/s at 15 m head. The water is circulated through a large (45 $m^3$) tank, which enables tests to be carried out over a long duration without any significant change in water temperature. This is important because of the effect that changes in temperature have on water viscosity, and hence on hydraulic efficiency.

The test rig is equipped with an orifice flow meter having a differential pressure transducer. Pressure transducers may also be used to measure the static pressures at the pump inlet and outlet. Signals from the transducers are fed to an Apple microcomputer, which can also be used for controlling the actuator circuit of a motorized valve. Various equipment was employed for the measurement of mechanical power, including a torque drum, a differential strain gauge torque transducer, and a dynamometer. In some tests the electrical output from a generator was measured and the mechanical power calculated by taking the generator efficiency into account. If reliable data on generator efficiency was not available, seperate testing of the generator was carried out. A diagram of the basic elements of the test apparatus is shown in Fig. 5.1. Each of the transducers was calibrated using a dead weight tester, and the flow measurements were calibrated against timed volume flow measurements using an intermediate tank of known dimensions.

The results of tests on a small Gilkes Centuri pump were obtained using a purpose-built laboratory test rig with a Venturi flow meter. Power output is measured using a spring balance on a d.c. dynamometer coupled directly to the pump. The rig incorporates a tank with a V-notch for calibrating the flow meter.

Tests were also carried out using the test facility at ITT Flygt Ltd. This facility is designed for the testing of pumps to obtain their head - discharge performance characteristics. It is not possible to use the flow meters installed to measure the flow into a pump running in turbine mode. The flow may be calculated from the head across the service pump, having first obtained an accurate head-flow characteristic for this pump. The efficiency of the pump in turbine operation was again found from the electrical output of the generator. A detailed description of these tests is given in Appendix M.

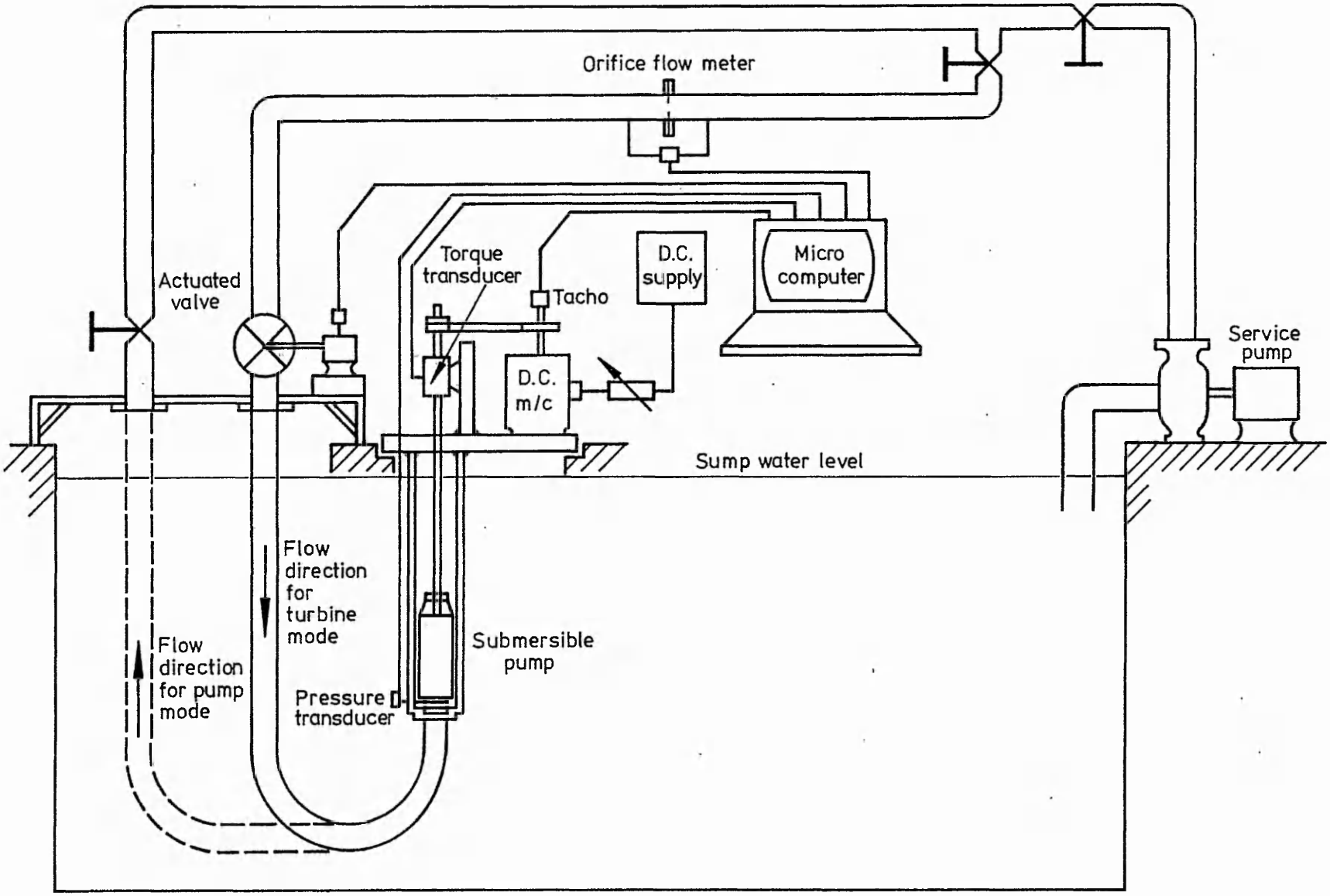


Fig. 5.1 Pump as Turbine Test Rig.

### 5.1.3 Pumps found to be unsuitable for turbine operation

Three of the pumps tested were found to be unsuitable for turbine operation, for different reasons. In the case of two of these pumps, their mechanical design is unsuitable for reverse operation. Both pumps, though of different designs, are submersible pumps designed for use in narrow boreholes.

The first, a Hayward-Tyler two-stage pump has a 'wet-type' electric motor, which is situated below the pump stages, as shown in Fig. 5.2. At the bottom of the motor unit is the main thrust bearing, which is a tilting-pad hydrodynamic type, designed to operate in one drection of rotation only. It would therefore be impossible to run this pump as a turbine in a practical installation without changing the thrust bearing. During tests carried out in the laboratory, the pump was separated from the motor, and an external arrangement of bearings was used. The test results for this pump, although published previously [78], have not been included in this chapter because of the doubtful accuracy of the torque measurements.

Another two-stage submersible pump was tested at the ITT Flygt test facility. In this case the unit has a 'dry motor', which is placed above the pump stages. Each stage has a semi-open impeller, which runs against hard a rubber coating on the diffuser in order to cut the leakage losses. The edges of the impeller blades which run against the diffuser are machined at an angle, which results in a sharp trailing edge (when in pump mode). However, when running in reverse as a turbine, these sharp edges of the impeller blades became locked into the rubber, preventing the pump from turning.

In the case of the third pump that was found to be unsuitable, the hydraulic design is such that the pump runs inefficiently as a turbine. In this case, the pump is an end-suction design with impeller and volute made from fabricated stainless steel. The volute is a simple circular channel with an outlet pipe, as shown in Fig. 5.3. In pump mode, the high surface finish of the stainless steel components results in a high efficiency relative to a cast iron pump of similar dimensions. However, because of the lack of guidance in the volute, the maximum turbine efficiency was only 70% of the maximum pump efficiency. Modifying the volute to produce a spiral channel has improved the turbine performance, although the turbine efficiency is still lower than the pump efficiency. Details of the tests on the modified pump are given in a report by Butterworth[92].

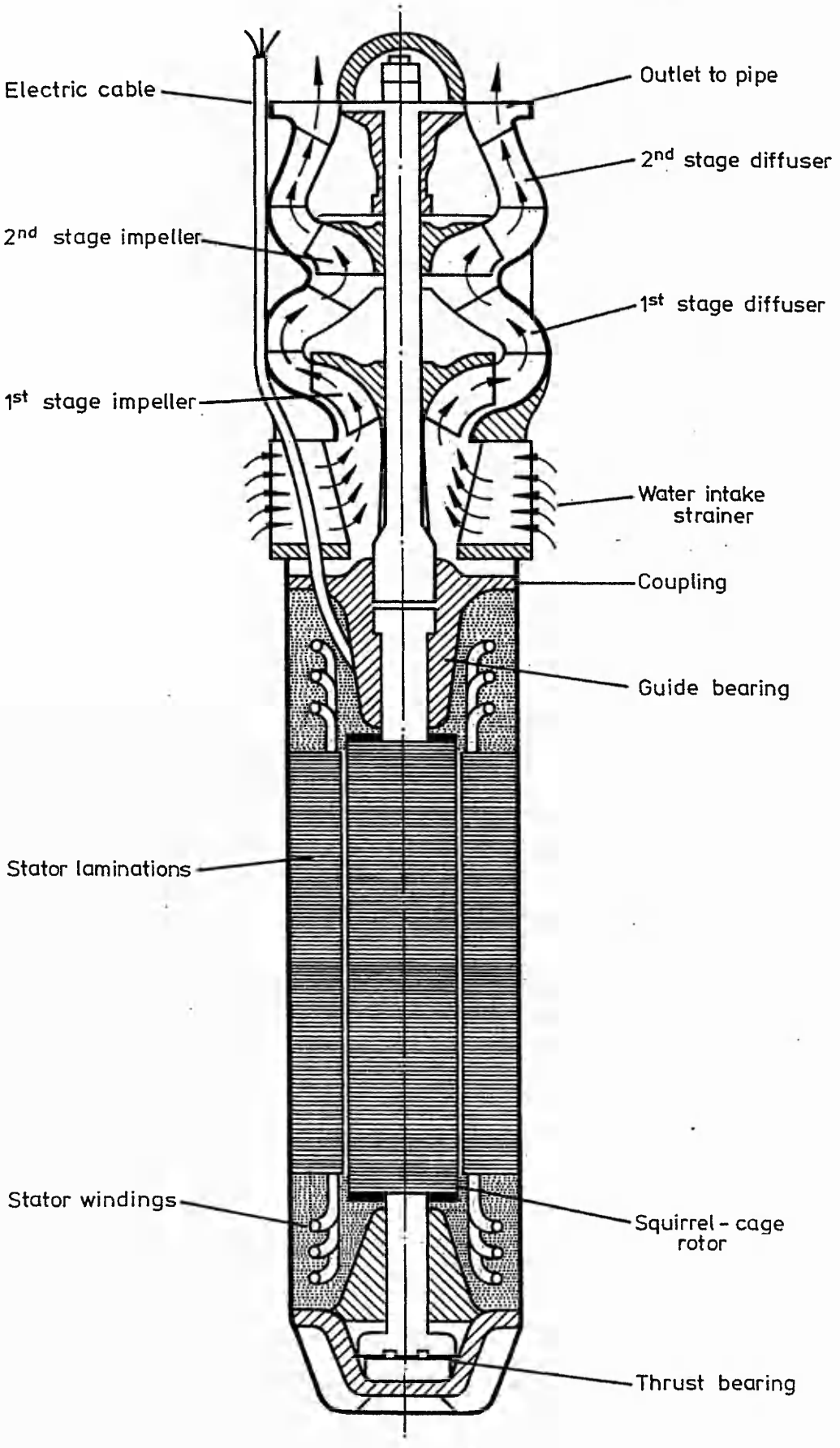


Fig. 5.2 Wet-motor submersible pump

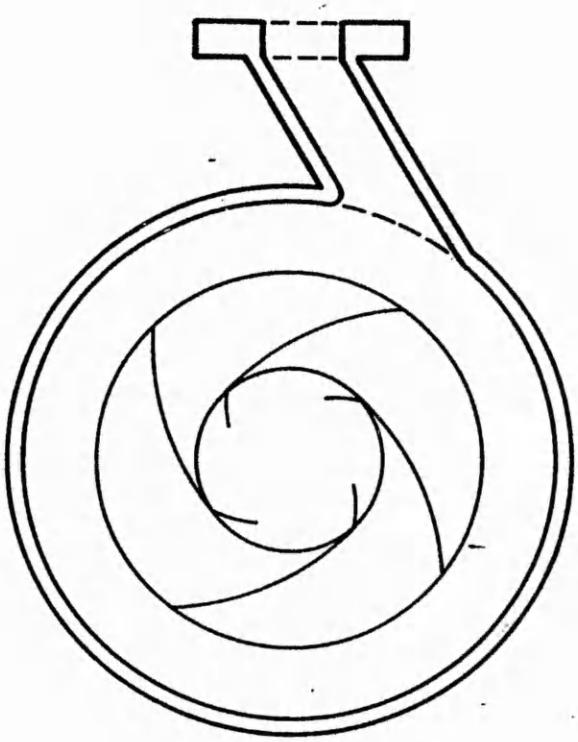

Fig. 5.3 Volute pump with no spiral

## 5.2 Presentation of test results

### 5.2.1 Double-suction radial-flow pump

A Worthington-Simpson double-suction pump was the first pump to be tested as a turbine at Nottingham Polytechnic. The pump was originally tested as a pump and then as a turbine by Hadid[93], but the results presented have been found to contain errors. The same pump was later tested in turbine mode only by Cheng[94], who used the impeller as originally supplied, and then with the impeller diameter turned down by 10%. The pump with cut-down impeller was also tested as a turbine by Smith[95], who extended the head and flow range over which the tests were carried out, in order to assess the runaway performance. The data from the tests by Smith are illustrated in Fig. 5.4. The curve of pump performance was supplied by the manufacturer for various impeller diameters and interpolated to give the head-flow characteristic for the 10% cut-down impeller. For this pump the maximum efficiency in turbine mode is considerably lower than in pump mode. This drop in efficiency (58% as a turbine, compared with 73% as a pump), may be caused by vanes in the pump inlet disturbing the outlet flow in turbine mode.

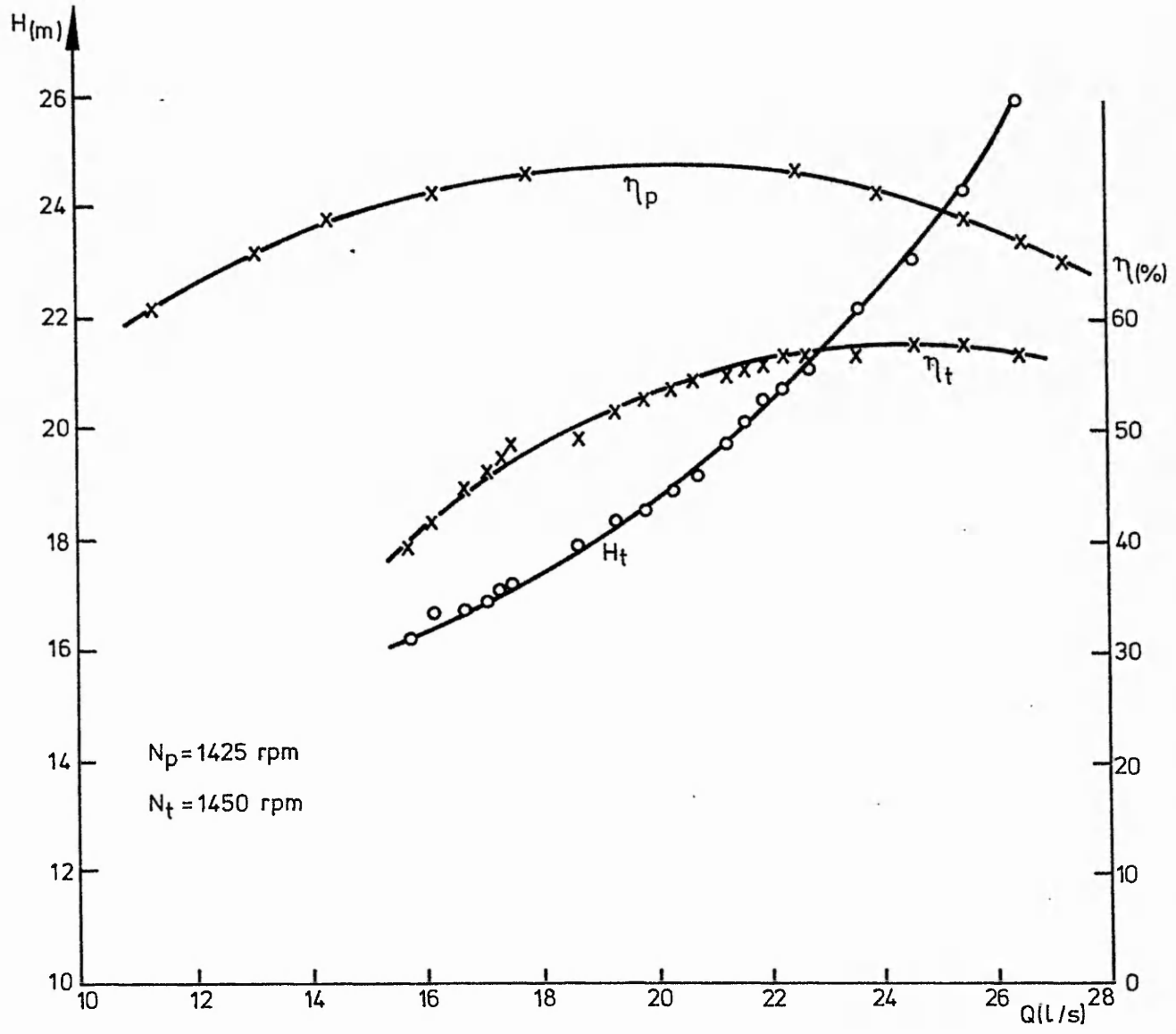


Fig. 5.4 Performance of double-suction pump

### 5.2.2 End-suction radial-flow pump

A low specific speed, 1.1 kW pump unit, designed to meet international standards, was donated by Worthington-Simpson for laboratory testing. This pump, which has been used for the worked example in chapter 4, was tested initially with its original impeller, later with the impeller blade tips rounded, and then with smaller diameter impellers. Results of some of these tests are given by Thomsett[96], in his project report. Pump and turbine performance curves, normalized to the pump speed of 2900 rpm, are shown for the unmodified impeller of diameter 134 mm, in Fig. 5.6. To calculate the pump and turbine efficiencies, the mechanical power was deduced by carrying out tests on the induction machine which was supplied with the pump, running it in both motor and generator modes. Details of these tests have been described in chapter 2, section 1.5. For this pump, the maximum turbine efficiency is significantly greater than the maximum pump efficiency.

### 5.2.3 Effect of impeller modifications

Test results were obtained for the same Worthington-Simpson end-suction pump with some modifications to the impeller, firstly with the impeller blade tips filed to produce rounded ends, as shown in Fig. 5.5. This was to investigate whether grinding down the sharp tips of the impeller blades improves the turbine efficiency, as proposed by Lueneburg and Nelson[68]. Operating the pump-as-turbine with the modified impeller, as shown in Fig. 5.7, requires a greater flow-rate for the same head, as compared with the original impeller.

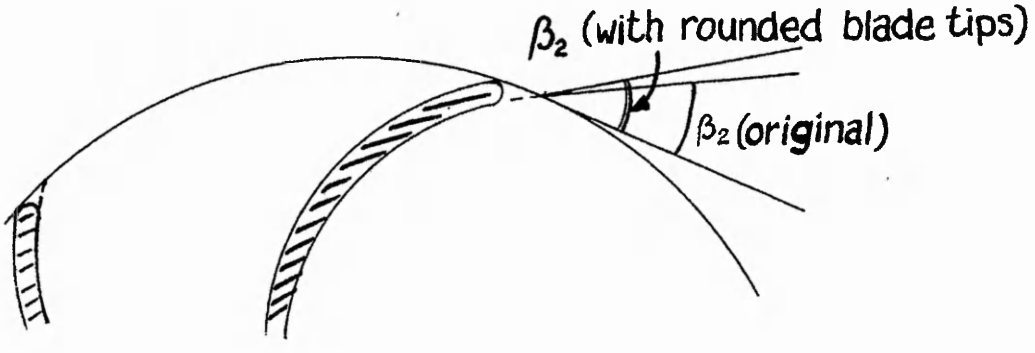


Fig. 5.5 Effect of rounding impeller blade tips

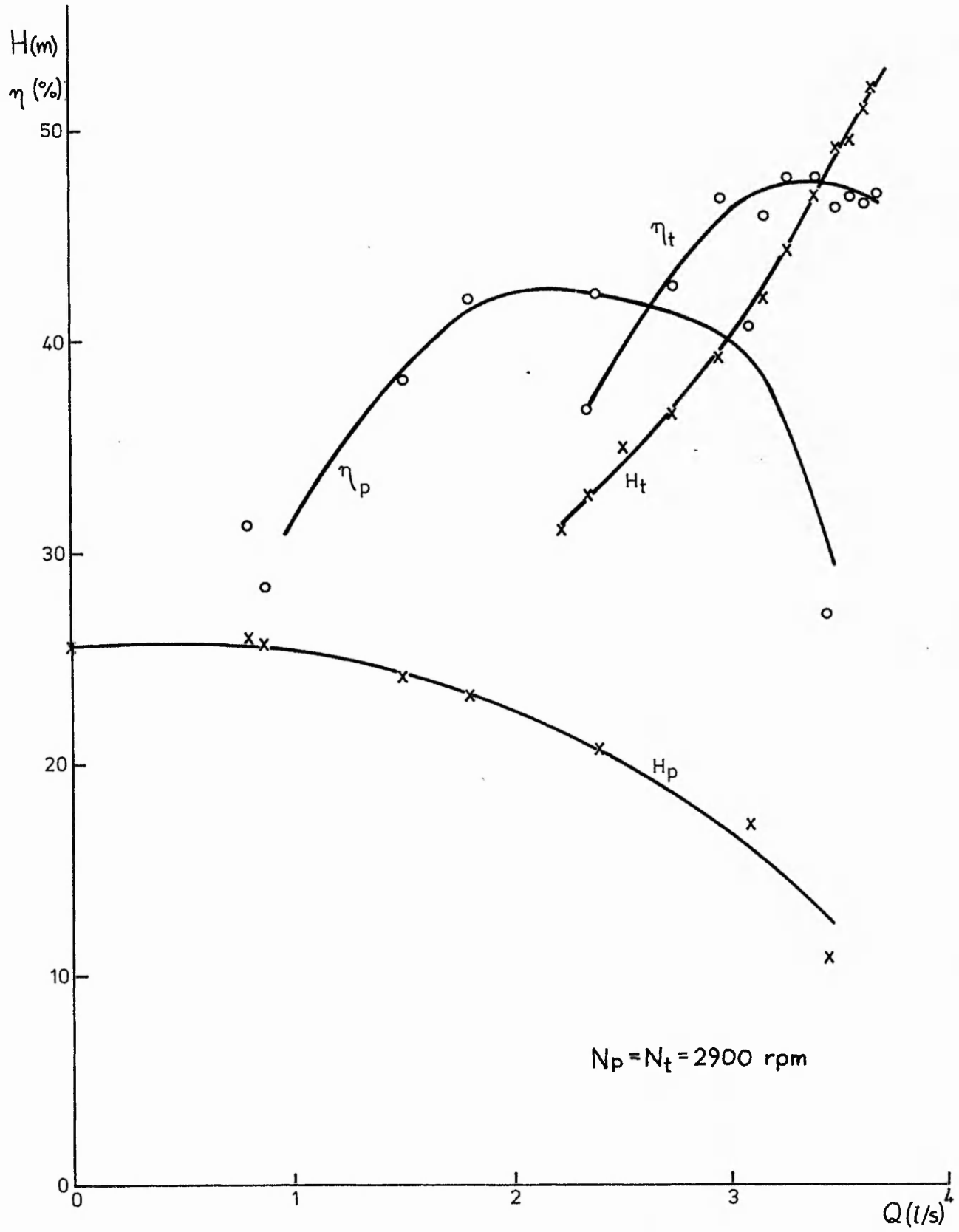


Fig. 5.6 Pump and Turbine performance of 25 WB 125 pump

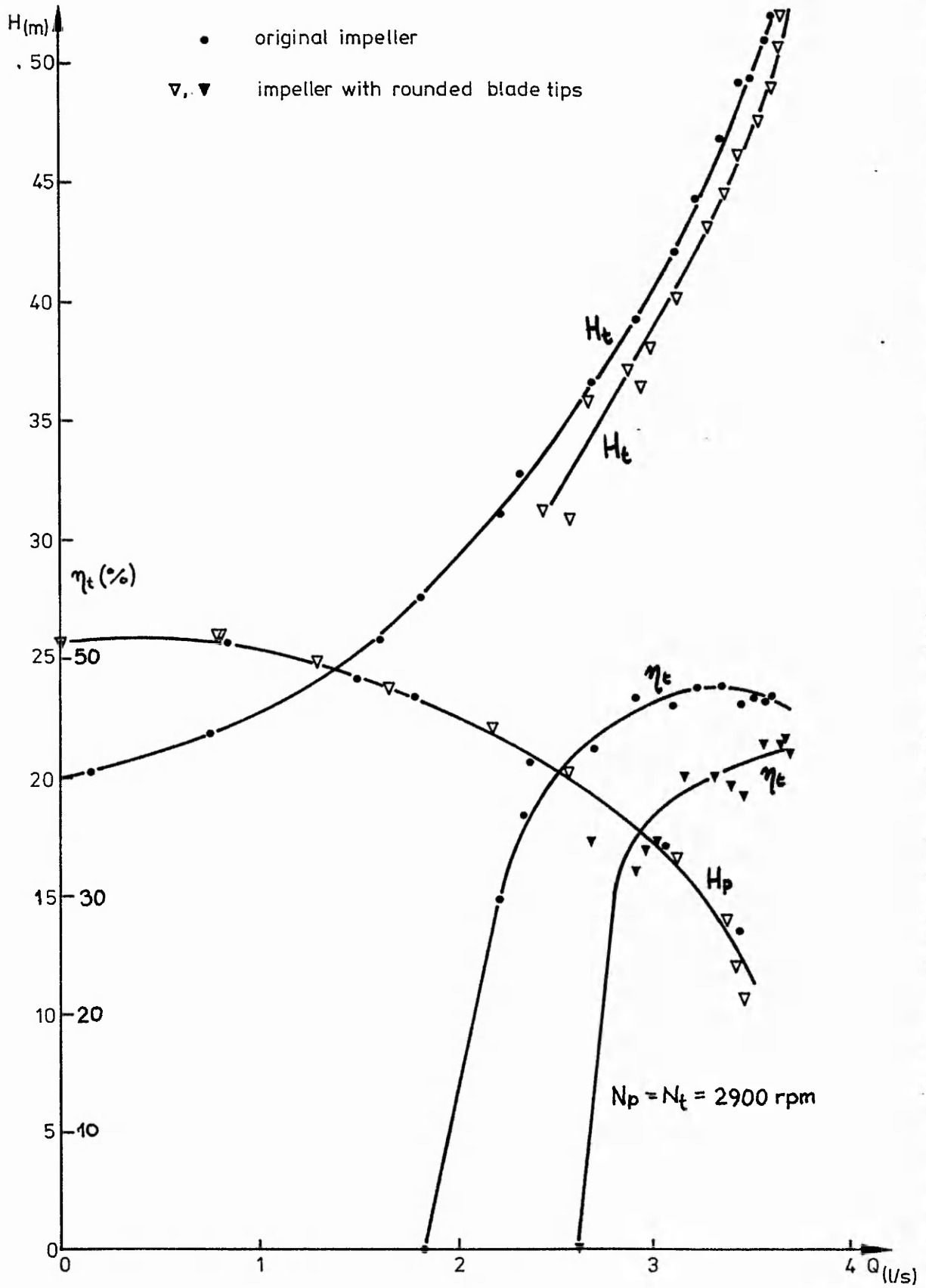


Fig.5.7 Turbine performance of impeller with rounded blades

With regard to efficiency, the results are not entirely conclusive because of the large scatter in the test points, and because the best efficiency point for the impeller with rounded blades appears to be at a greater head and flow than the test equipment permitted. However, it is likely that the maximum turbine efficiency of the modified impeller is at least 2% lower than the original impeller. Such a modification is therefore of doubtful benefit to turbine performance.

In another test, the outside diameter of the impeller was turned down by 4 mm. An impeller of very similar design, with the same eye diameter, impeller angles and widths, with outer diameter 108 mm, was also tested in the same volute casing. This impeller is normally fitted in a pump with smaller diameter volute. The results of tests of pump and turbine performance are shown in Fig. 5.8. Again there is a certain amount of scatter in the efficiency values, making it difficult to pinpoint the best efficiency conditions, particularly for the 130 mm diameter impeller. The results of similar tests carried out by Cheng on the double-suction pump with two impeller diameters are shown in Fig. 5.9.

Simple theory suggests that these changes to the impeller diameter should alter the head at best efficiency in proportion to the diameter squared, and the flow-rate in proportion to the impeller diameter. This rule has been compared with the test results in Fig. 5.10, where the results have been 'normalized' to the full impeller diameter and the performance normalized for each pump to 2900 rpm. The curves only overlap each other just below the point of zero power output. Below this point, the curves for the reduced impeller diameters lie above the curve for the full diameter impeller, and above this value, the reduced diameter impellers require a proportionately greater head. The estimated points of maximum efficiency for the three impellers have similar values of $Q/D_2$, and therefore the relationship $Q \propto D$ holds.

However, the values of $H/D^2$ at maximum efficiency are not constant. In fact, H is nearly proportional to $D^{1.5}$ at best efficiency. A suggested explanation for this is that there is a head loss which increases with the space between volute casing and impeller. This would also explain the decrease in maximum turbine efficiency with decreasing diameter, which incidentally, is much greater than the corresponding decrease in maximum pump efficiency. for the full diameter impeller, the maximum turbine efficiency is 5% greater than the maximum pump efficiency, but for the 108 mm impeller, the maximum efficiency is 41% in both modes of operation. In the case of the double-suction pump, the change in the efficiency curve is so great that the head required for best efficiency operation of the smaller diameter impeller is greater than that required for the full-size impeller.

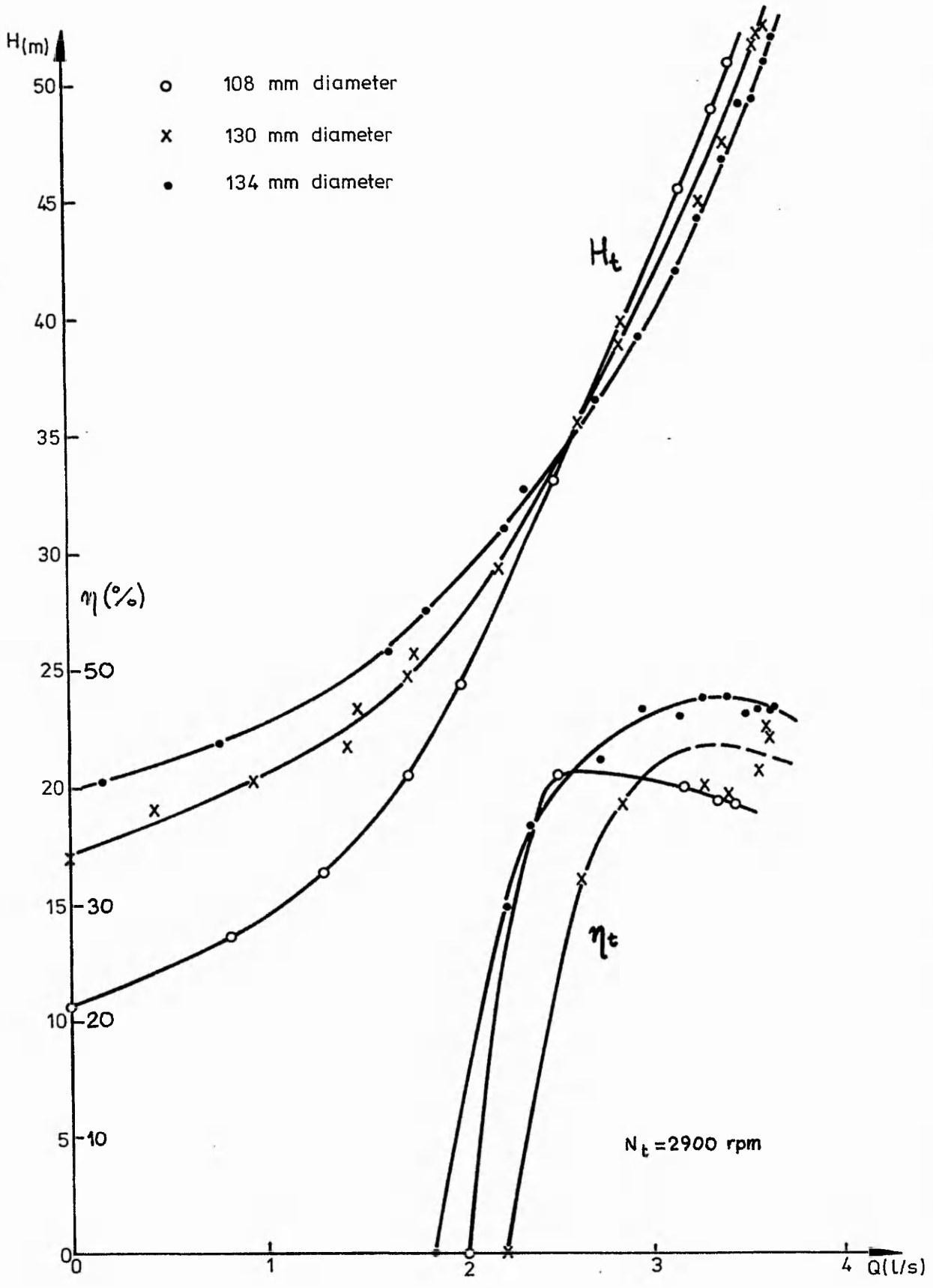


Fig. 5.8 Turbine performance for 3 impeller diameters

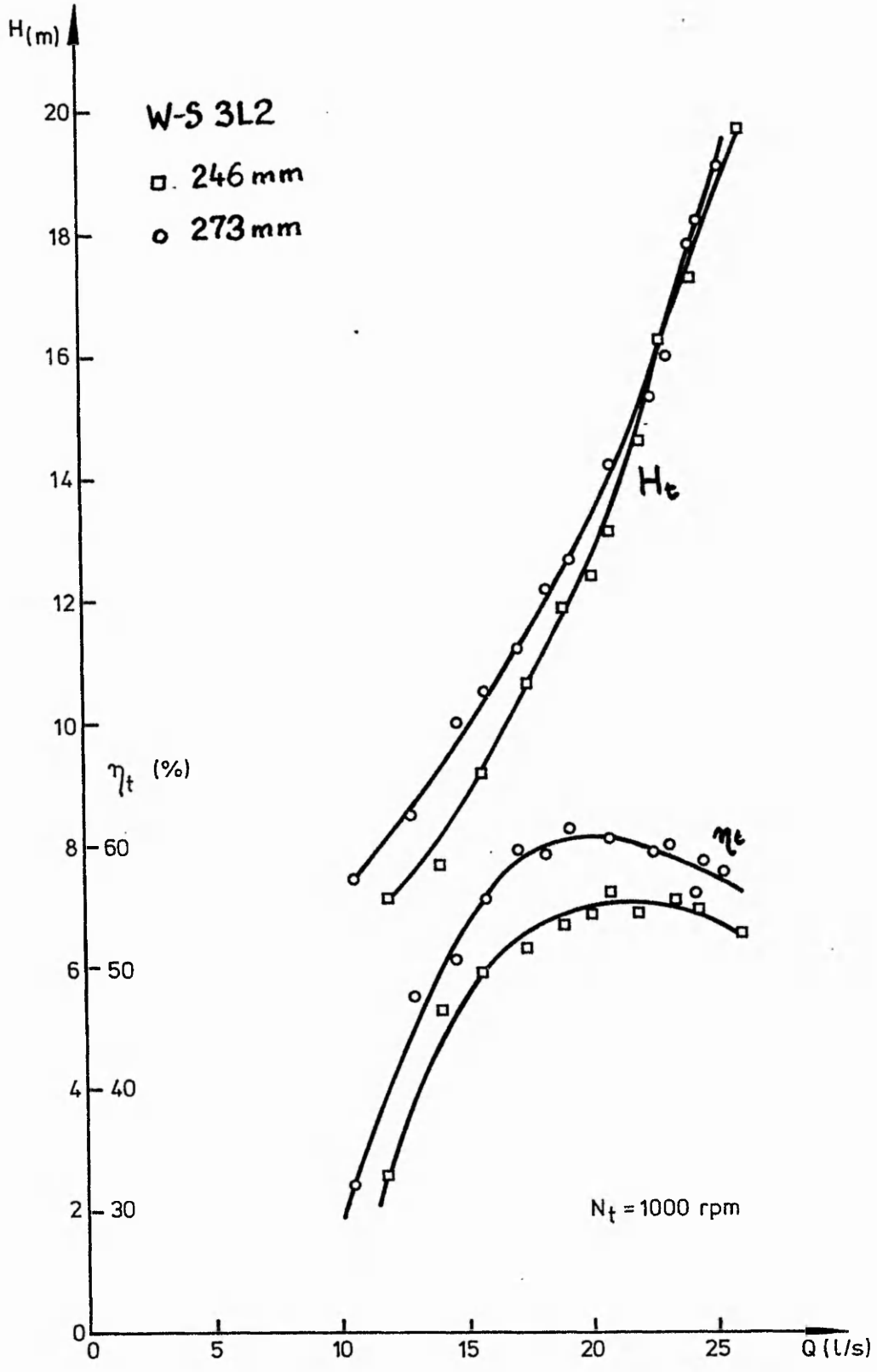


Fig. 5-9. Turbine performance for 2 impeller diameters

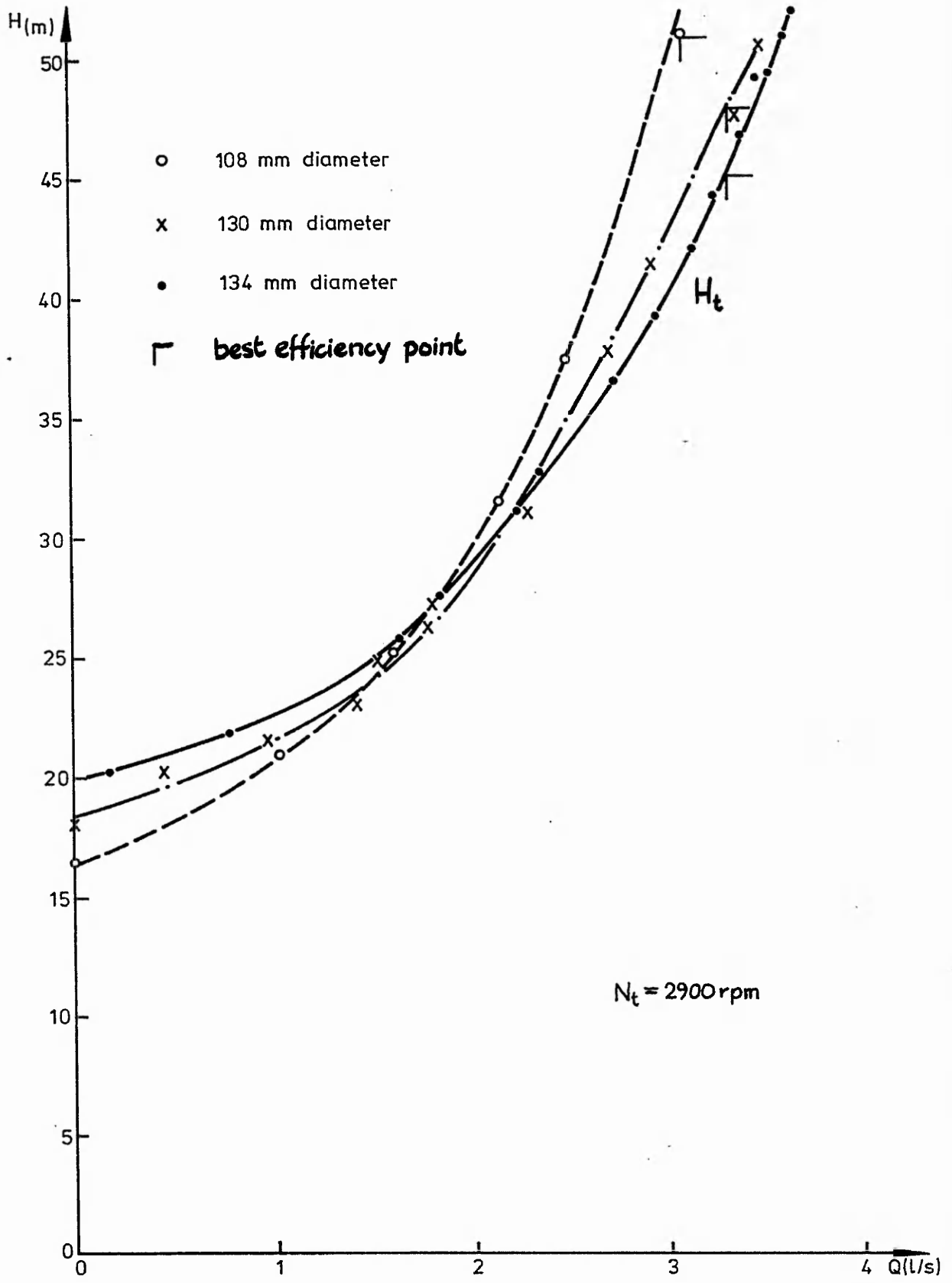


Fig. 5·10 Turbine results for cut-down impellers "normalised" to full dia.

### 5.2.4 Radial-flow pump with semi-open impeller

A Gilkes Centuri pump was used to obtain turbine performance data for a radial-flow pump with semi-open impeller. The impeller of this pump has blades which have no shroud on the suction side but are machined flat, and run, with a small clearance, next to the casing. Detailed test results can be found in the report by Senu[97]. These results were confirmed by the author's tests and found to be accurate.

Results of the tests, for a speed of 2500 rpm, are shown in Fig. 5.11. The pump maximum efficiency of 52% was found to occur at 7.73 m, 1.5 l/s. Turbine tests on this pump give an operating head of 25.3 m and flow-rate of 2.6 l/s, at a maximum efficiency of 56%.

### 5.2.5 Submersible dewatering pump with semi-open impeller

Tests were carried out on both a medium head and high head version of a Flygt 'B-type' submersible dewatering pump. The set up of the test facility, and the tests on the medium head version, are described more fully in Appendix M. The pump is fitted with a semi-open impeller, and a diffuser, as shown in Fig. 5.12. A strainer, which is fitted to the bottom of the pump, was removed for the turbine tests, increasing the output by more than 5%. For comparison purposes, the strainer was also removed for the pump performance test. Later, a draft-tube was designed for attachment to the pump when operating as a turbine. Results of tests carried out by Crossland[98], show an improvement of less than 1% in efficiency with the draft-tube fitted. However, when a similar pump unit was installed at Malham (see Appendix D), a draft-tube was fitted because of the practical advantages of a well-designed outlet, to direct the water into the outlet channel.

The pump and turbine curves for the medium head version, normalized to 3000 rpm, are shown in Fig. 5.13. The maximum turbine efficiency of 67% is the same as the maximum pump efficiency. Normalizing the pump test results gives a head of 14.2 m and flow of 26.3 l/s. The turbine best efficiency point is at 23.8 m and 42.3 l/s. The turbine head and flow for this pump is outside the range for standard centrifugal pumps, such as those shown in Fig. 1.4, running at 2-pole speed. Hence, although this pump is more expensive than a standard end-suction type, it can run under site conditions for which only a much larger standard pump, running at a slower speed, would be suitable.

The test performance curves for the high head version are shown in Fig. 5.14. For the high head version, the turbine efficiency is less than the pump efficiency (51% compared with 56%). The pump best efficiency point is at approximately 25 m, 10 l/s and the turbine best efficiency point is at 38 m, 18 l/s.

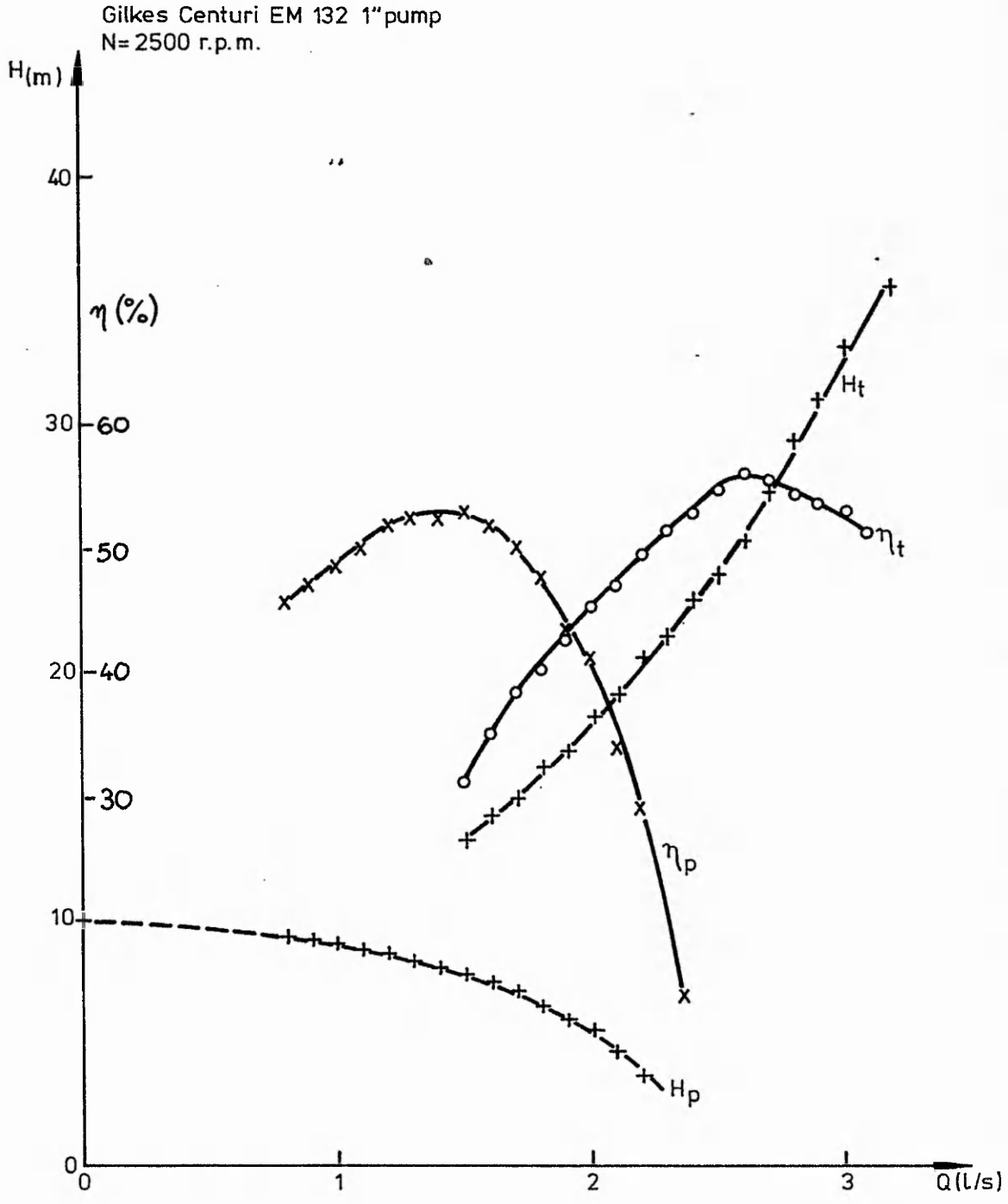


Fig. 5.11 Pump and turbine performance for Gilkes EM132 pumps

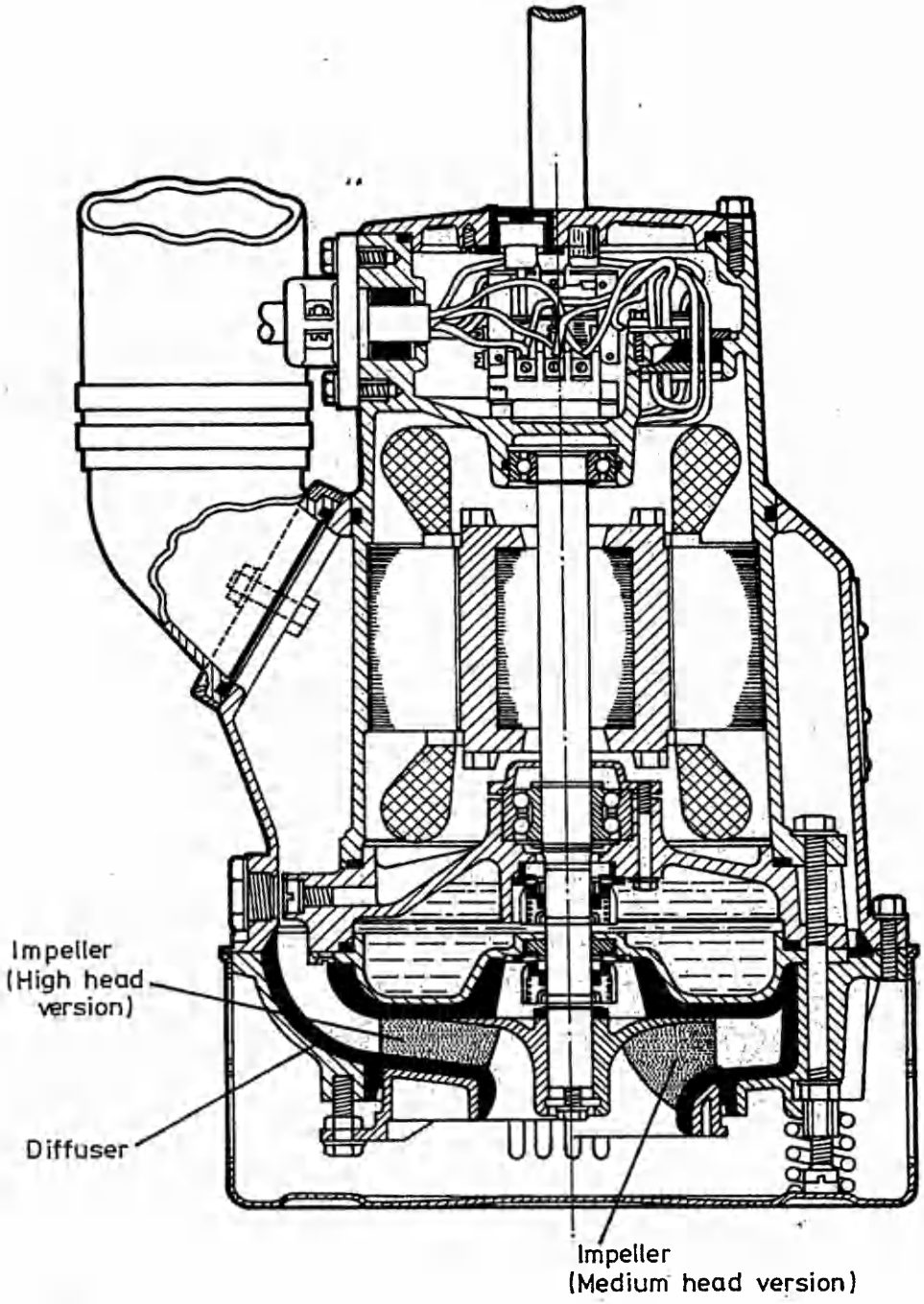


Fig. 5·12. Cross-section of submersible de-watering pump

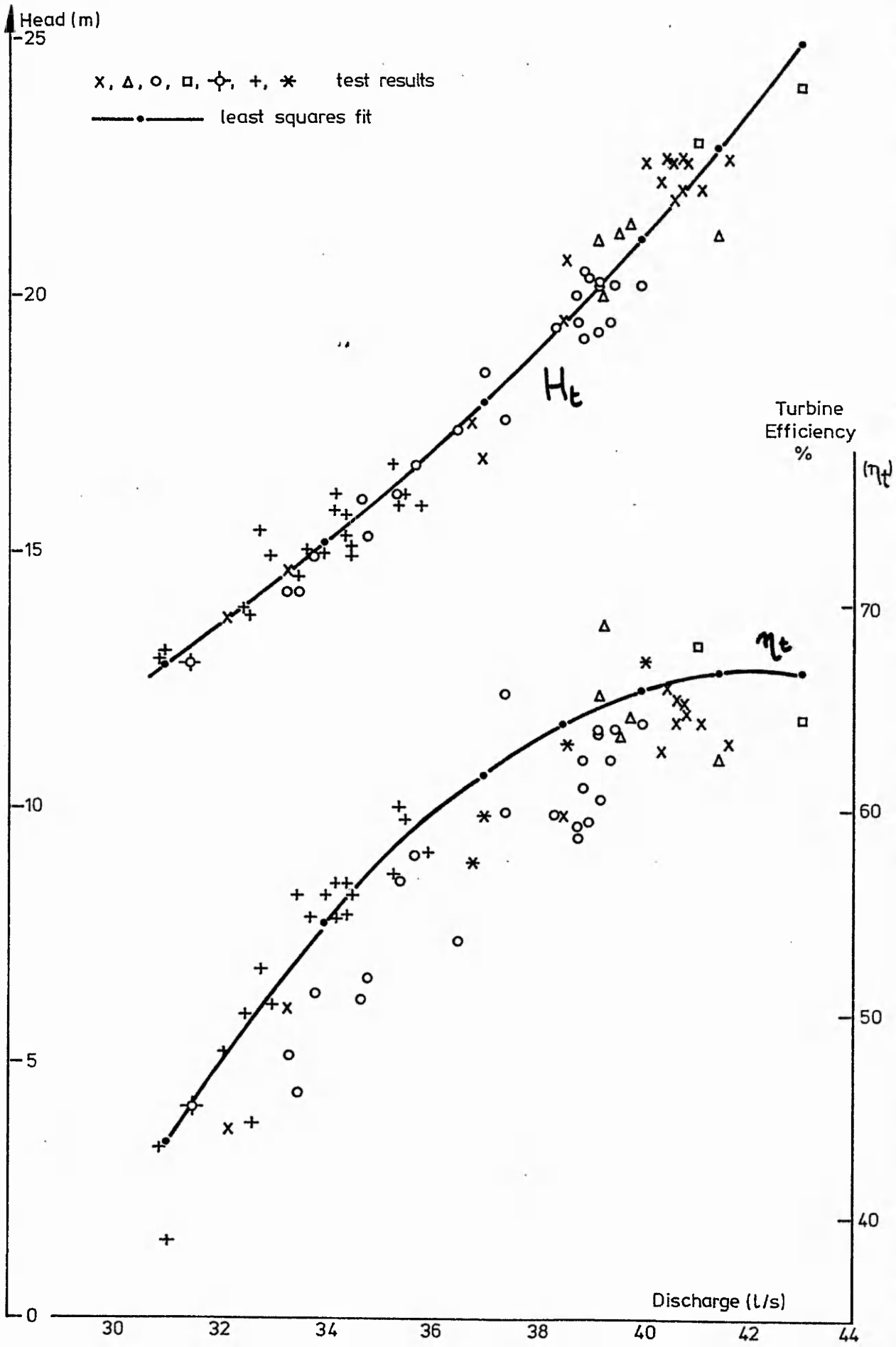


Fig. 5·13. FLYGT BS2102MT Pump as Turbine. Results normalised to 3000 r.p.m.

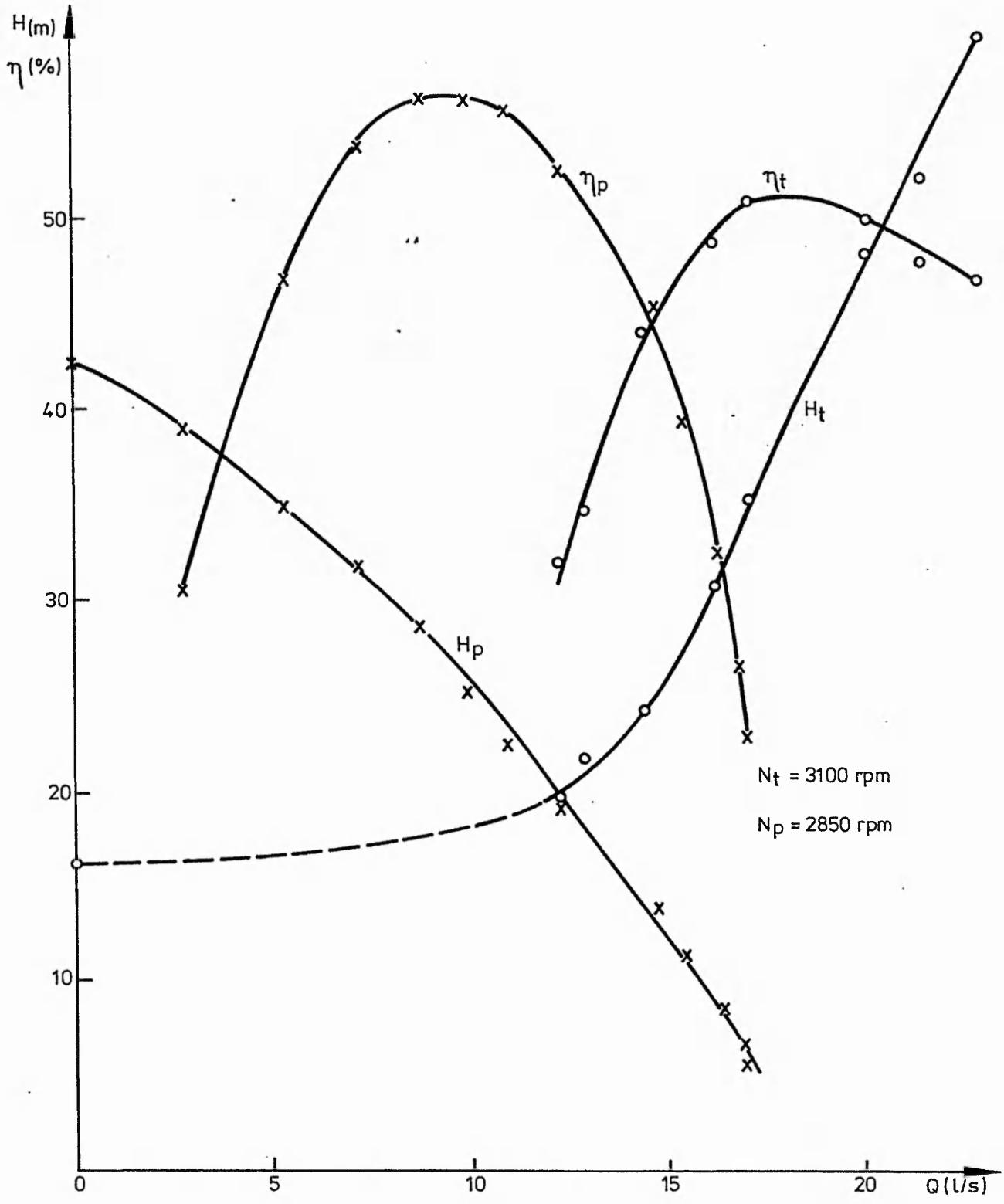


Fig. 5.14 Pump and turbine performance of Flygt BS2102HT

## 5.3 Comparison of tests with area ratio prediction

### 5.3.1 Double-suction radial-flow pump

The geometry of the double-suction pump that was tested is illustrated in Fig. 5.15, which shows how the dimensions have been defined. The data for this pump with reduced impeller diameter are given in Table 5.1 alongside the data for the other pumps tested. The pump has two inlets and therefore the velocity triangles have been calculated on the basis of half of the total flow. The inlet area, $a_1$ has been taken to include both sides of the impeller eye. The inlet diameter is taken as the effective mean of the diameter at the impeller inlet, ie:-

$$D_1 = \frac{1}{\pi}\left(\frac{a_1}{2b_1} + \frac{Zt}{\sin\beta_1}\right) \qquad (5.1)$$

With these definitions, equations (4.1) to (4.32) are all valid.

By using the same procedure for calculating the predicted values as in the previous chapter, sections 4.2.4 and 4.3.2, the results shown in Tables 5.2 and 5.3 are obtained. The theoretical lines for pump and turbine head and flow coefficients are shown in Fig. 5.16, together with the points of pump and turbine best efficiency given from tests.

The same method as in chapter 4 is used for evaluating the losses in pump and turbine mode except that the bearing and seal friction losses, are estimated to be 100% of the disc friction loss because there is a greater loss through friction with a packing gland than there is with a mechanical seal. For operation as a pump, the performance prediction is close to the test results, but the predicted flow at turbine best efficiency is too large, and the efficiency drop observed in turbine mode is not predicted by the area ratio method.

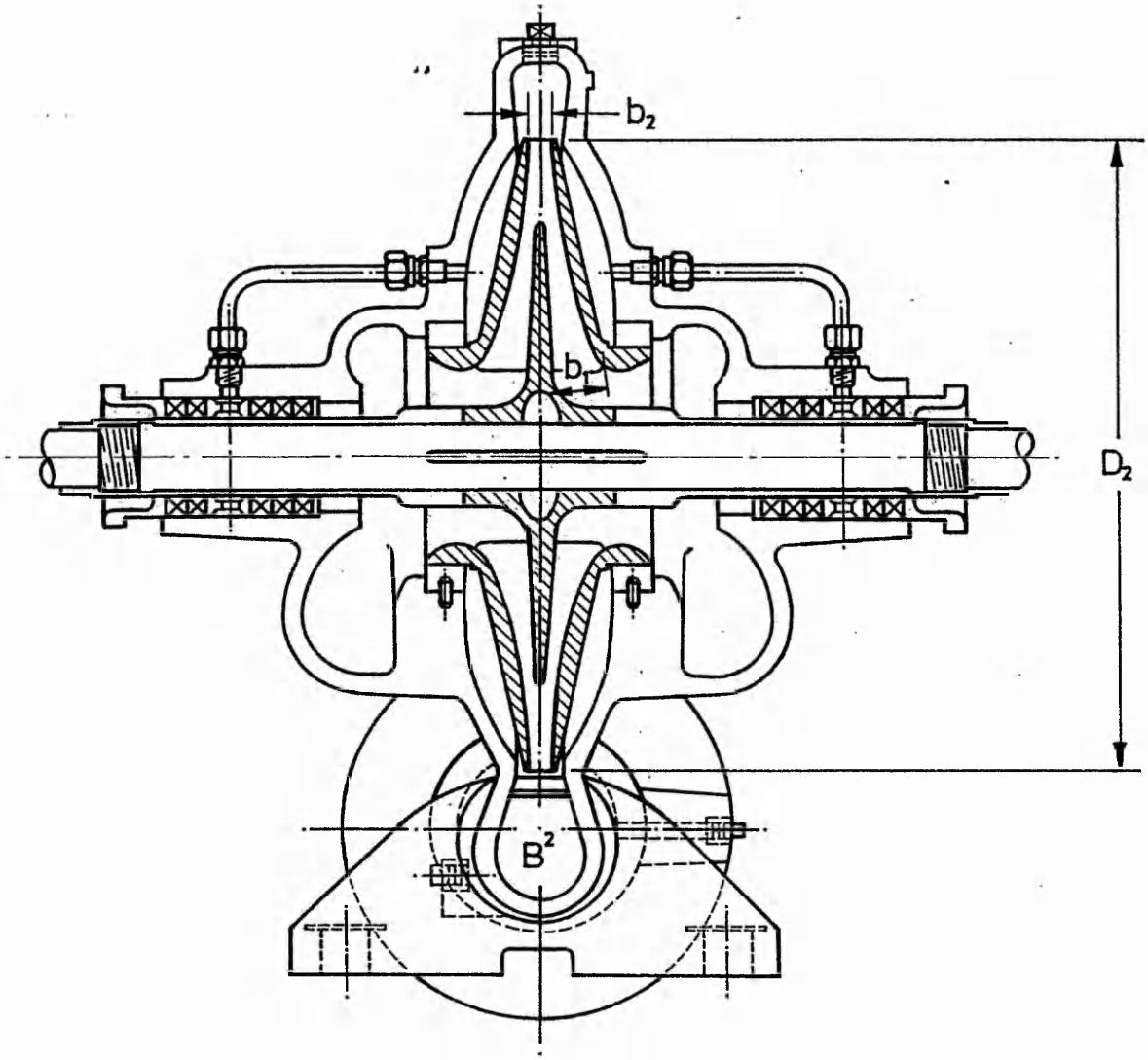


Fig. 5.15 Cross-section of double-suction pump

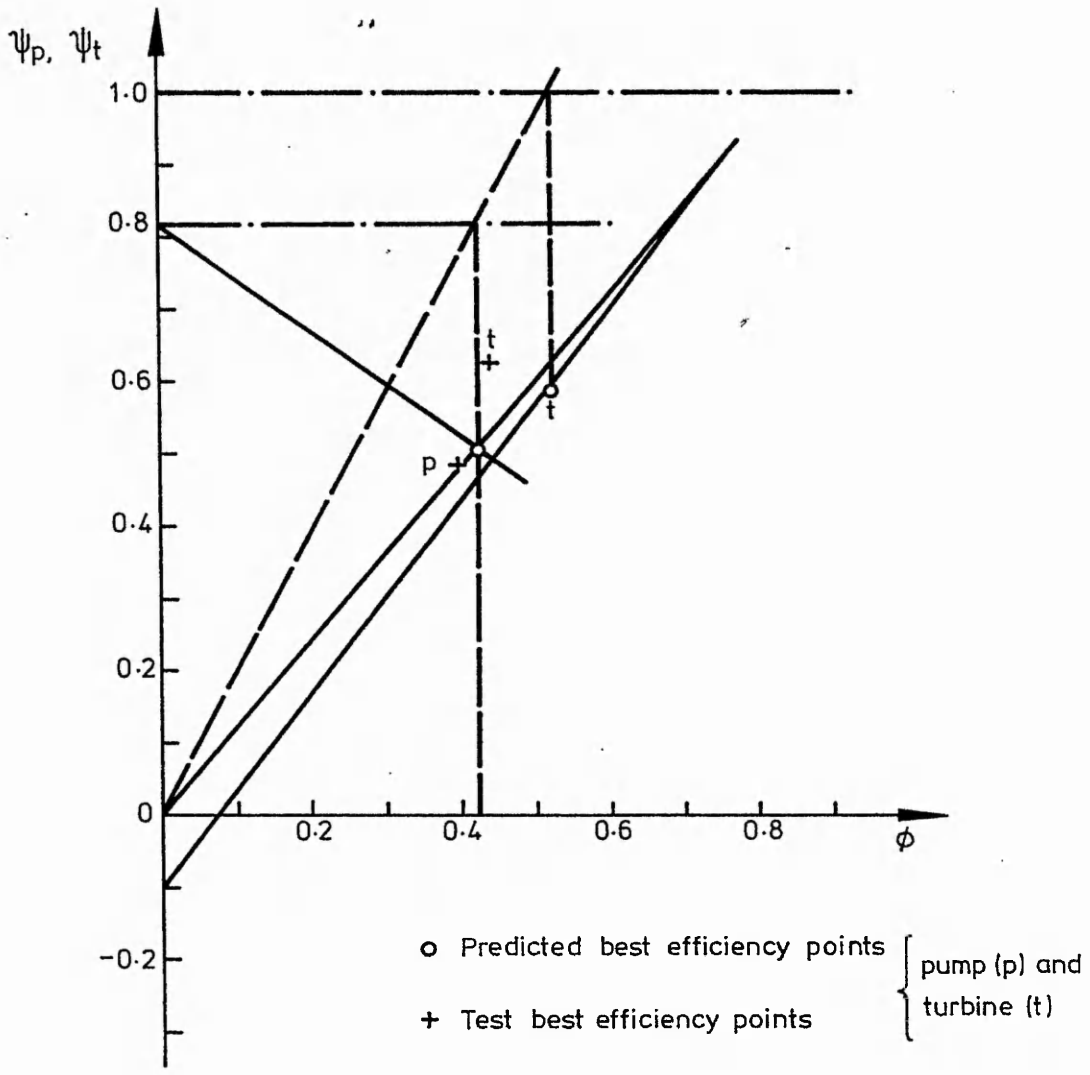


Fig. 5·16 Turbine prediction for double-suction pump

**Table 5.1. Data for pumps tested as turbines.**

| | | | | |
|---|---|---|---|---|
| | | **Geometrical data** | | |
| **Pump:** | Worth. 3L2 | Worth. 25WB125 | Gilkes EM132 | Flygt BS2102HT |
| $D_2$(mm) | 246.0 | 108.0 | 101.4 | 184.0 |
| $D_1$(mm) | 81.0 | 30.0 | 40.5 | 50.0 |
| $b_2$(mm) | 15.0 | 6.54 | 4.7 | 15.0 |
| $b_1$(mm) | 22.0 | 12.5 | 7.7 | 17.0 |
| $\beta_2$ | 21.7° | 20.0° | 25.0° | 18.6° |
| $\beta_1$ | 32.0° | 17.5° | 26.5° | 15.0° |
| $a_2$(mm$^2$) | 10014 | 1741 | 1338 | 7896 |
| $a_1$(mm$^2$) | 9960 | 555 | 733 | 1867 |
| $B^2$(mm$^2$) | 2903 | 194 | 194.6 | 1682 |
| Z | 5 | 5 | 6 | 3 |
| $N_p$(rpm) | 1425 | 2900 | 2500 | 2850 |
| $N_t$(rpm) | 1450 | 3100 | 2500 | 3100 |
| | | **Calculated Data** | | |
| $\nu$ | 0.329 | 0.277 | 0.400 | 0.270 |
| $U_{2p}$(m/s) | 18.35 | 16.40 | 13.27 | 27.46 |
| $U_{2t}$(m/s) | 18.68 | 17.53 | 13.27 | 29.34 |
| $h_0$ | 0.814 | 0.825 | 0.821 | 0.756 |
| $c_v$ | 1.206 | 1.124 | 1.132 | 1.209 |
| $\varphi_p$ | 0.421 | 0.577 | 0.569 | 0.411 |
| $\psi_p$ | 0.508 | 0.648 | 0.644 | 0.496 |
| $q_p$(l/s) | 1.23 | 0.27 | 0.01 | 0.03 |
| $\eta_{vp}$ | 0.920 | 0.755 | 0.730 | 0.800 |
| $\phi_t$ | 0.517 | 0.699 | 0.693 | 0.543 |
| $\psi_t$ | 0.594 | 0.896 | 0.772 | 1.079 |
| $q_t$(l/s) | 1.35 | 0.43 | 0.01 | 0.05 |
| $\eta_{vt}$ | 0.936 | 0.805 | 0.784 | 0.840 |
| $\varepsilon$ | 0.996 | 0.815 | 0.9995 | 0.454 |
| $Q_p$(l/s) | 21.2 | 1.71 | 1.46 | 18.9 |
| $H_p$(m) | 15.7 | 13.4 | 8.2 | 30.5 |
| $Q_t$(l/s) | 29.4 | 2.81 | 1.80 | 24.9 |
| $H_t$(m) | 22.7 | 42.8 | 17.7 | 215.5 |
| $\eta_t$ | 0.77 | 0.34 | 0.53 | 0.32 |
| | | **Test data** | | |
| $Q_p$(l/s) | 20.0 | 1.54 | 1.50 | 10.0 |
| $H_p$(m) | 15.4 | 13.1 | 7.73 | 25.0 |
| $\eta_p$ | 0.73 | 0.41 | 0.48 | 0.59 |
| $Q_t$(l/s) | 25.0 | 2.69 | 2.60 | 17.4 |
| $H_t$(m) | 23.7 | 37.8 | 25.3 | 35.9 |
| $\eta_t$ | 0.58 | 0.41 | 0.56 | 0.51 |

**Table 5.2 Energy balance for pump best efficiency.**

| | | |
|---|---|---|
| Input power : 3335/0.73 = | 4 574 | |
| Mechanical losses | 424 | |
| Leakage losses | 210 | |
| | 3 940 | |
| Impeller losses | 315 | |
| Volute losses | 290 | |
| Hydraulic output power | 3 335 | W |

**Table 5.3 Breakdown of losses for turbine best efficiency.**

| | | |
|---|---|---|
| Turbine input power | 6 532 | |
| Volute losses | 418 | |
| Leakage loss | 280 | |
| Available power input | 5 834 | |
| Exit losses | 24 | |
| Impeller input power | 5 810 | |
| Impeller losses | 372 | |
| Mechanical loss | 439 | |
| Mechanical output power | 4 999 | W |

### 5.3.2 Effect of impeller modifications to end-suction pump

In the case of the impeller with rounded blade ends, the analysis required for turbine performance prediction is almost the same as that for the original impeller. Assuming that the effect of rounding the blade ends is to increase the impeller outlet angle, $\beta_2$ ,by, say 3°, and increase the value of $a_2$ and $A_{II}$ by 4%, but to make negligible changes to the other parameters, the performance can be recalculated. The pump impeller line becomes $\psi_P = 0.733 - 0.096\phi$ instead of $0.745 - 0.112\phi$, and the criterion for turbine best efficiency (point III) gives a new value of $\phi_t = 0.835$ instead of 0.824. This predicted increase in flow is borne out by the test results, but the increase at best efficiency according to the test results is much more than the 1% predicted.

Considering the performance at a particular flow rate, for example 3.35 l/s at 2900 rpm, the modified impeller operates as a turbine at a reduced head of 43.2 m compared with 45.2 m. The lower value of $H_t$ suggests a higher value of $\eta_{vt}$ for the modified impeller, but the lower value of power output (568 compared with 707 W) suggests that the impeller losses are much greater for the modified impeller. The area ratio method fails to predict this drop in turbine efficiency which was observed

under test. Note however that in pump mode the modification has very little effect on the performance.

In the case of the reductions in impeller diameter, the performance prediction has to be completely recalculated because the values of $U_2$ change. The performance of the pump fitted with the smallest diameter impeller has been predicted by the area ratio method, taking into account also the different impeller blade angles. The data for this impeller are shown in Table 5.1.

**Table 5.4 Breakdown of losses for pump best efficiency.**

| | | |
|---|---|---|
| Input power : 273/0.41 = | 549 | |
| Mechanical losses | 88 | |
| Leakage losses | 35 | |
| | 426 | |
| Impeller losses | 104 | |
| Volute losses | 97 | |
| Hydraulic output power | 225 | W |

**Table 5.5 Breakdown of losses for turbine best efficiency.**

| | | |
|---|---|---|
| Turbine input power | 1 180 | |
| Volute losses | 230 | |
| Leakage loss | 145 | |
| Available power | 805 | |
| Exit losses | 149 | |
| Impeller input power | 656 | |
| Impeller losses | 158 | |
| Mechanical loss | 101 | |
| Mechanical output power | 397 | W |

The theoretical impeller and volute characteristics are shown in Fig. 5.17 and the breakdown of predicted losses for pump and turbine operation are given in Tables 5.4 and 5.5 respectively. The predicted values, as shown in Table 5.1, are close to those obtained from tests.

### 5.3.3 Radial-flow pump with semi-open impeller

The data for a Gilkes end-suction pump with semi-open impeller are also given in Table 5.1. The manufacturer could not supply a value for the pump maximum efficiency, but the value of 48% from pump tests was used to give the energy balance for pump best efficiency operation as shown in Table 5.6. The complete breakdown of losses for turbine mode is shown in Table 5.7.

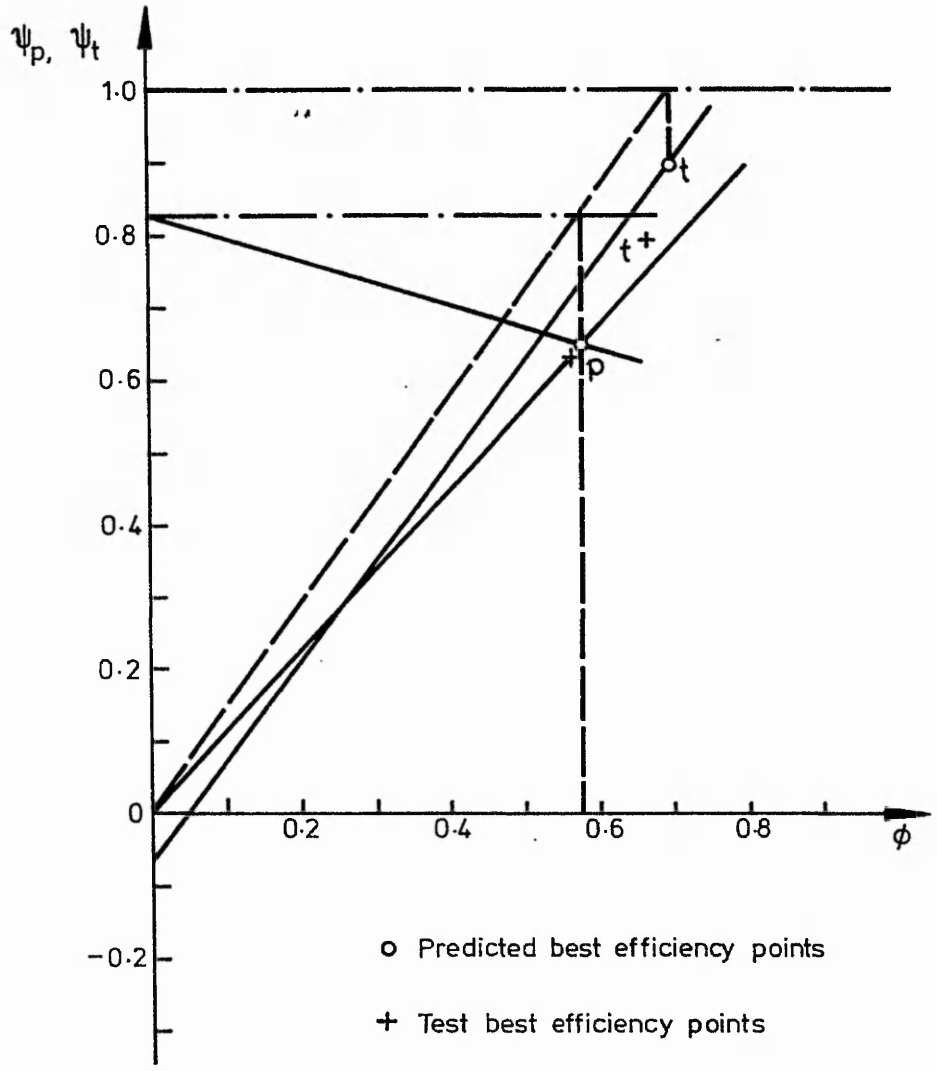


Fig. 5·17 Turbine prediction for radial flow pump with reduced diameter impeller

**Table 5.6 Breakdown of losses for pump best efficiency.**

| | | |
|---|---|---|
| Input power : 121/0.48 = | 254 | |
| Mechanical losses | 26 | |
| Leakage losses | 1 | |
| | 227 | |
| Impeller losses | 61 | |
| Volute losses | 45 | |
| Hydraulic output power | 121 | W |

**Table 5.7 Breakdown of losses for turbine best efficiency.**

| | | |
|---|---|---|
| Turbine input power | 312 | |
| Volute losses | 67 | |
| Leakage loss | 2 | |
| Available power | 243 | |
| Exit losses | 0 | |
| Impeller input power | 243 | |
| Impeller losses | 53 | |
| Mechanical loss | 26 | |
| Mechanical output power | 164 | W |

### 5.3.4 Submersible dewatering pump with semi-open impeller

The internal geometry of this pump is more complicated than that of the other pumps tested. The diffuser consists of four channels to take the water away from the impeller and up into the space which surrounds the pump motor. The value of 'throat area', $B^2$, was taken as the total area of these channels at the point at which they begin to diverge. The full geometrical data (given in Table 5.1) were obtained for the HT (high head) version.

Using this data in the area ratio method gives the pump best efficiency point at 29.9 m, 18.9 l/s. This is markedly different from the results of 25.0 m and 10.0 l/s obtained from tests. The graph of theoretical head coefficient against flow coefficient is shown in Fig.5.18, together with the best efficiency point from pump tests. The turbine performance predicition at 3100 rpm gives $H_t = 82.18/\eta_{vie}$, and $Q_t = 24.92$ l/s. When the value of utilization factor, $\varepsilon$, is calculated for point III, it is found that the value is 0.454, because there is a very large exit whirl from the eye of the impeller in turbine mode. In the case of this pump, the position of the best efficiency point is therefore not close to the point of zero shock at the impeller inlet.

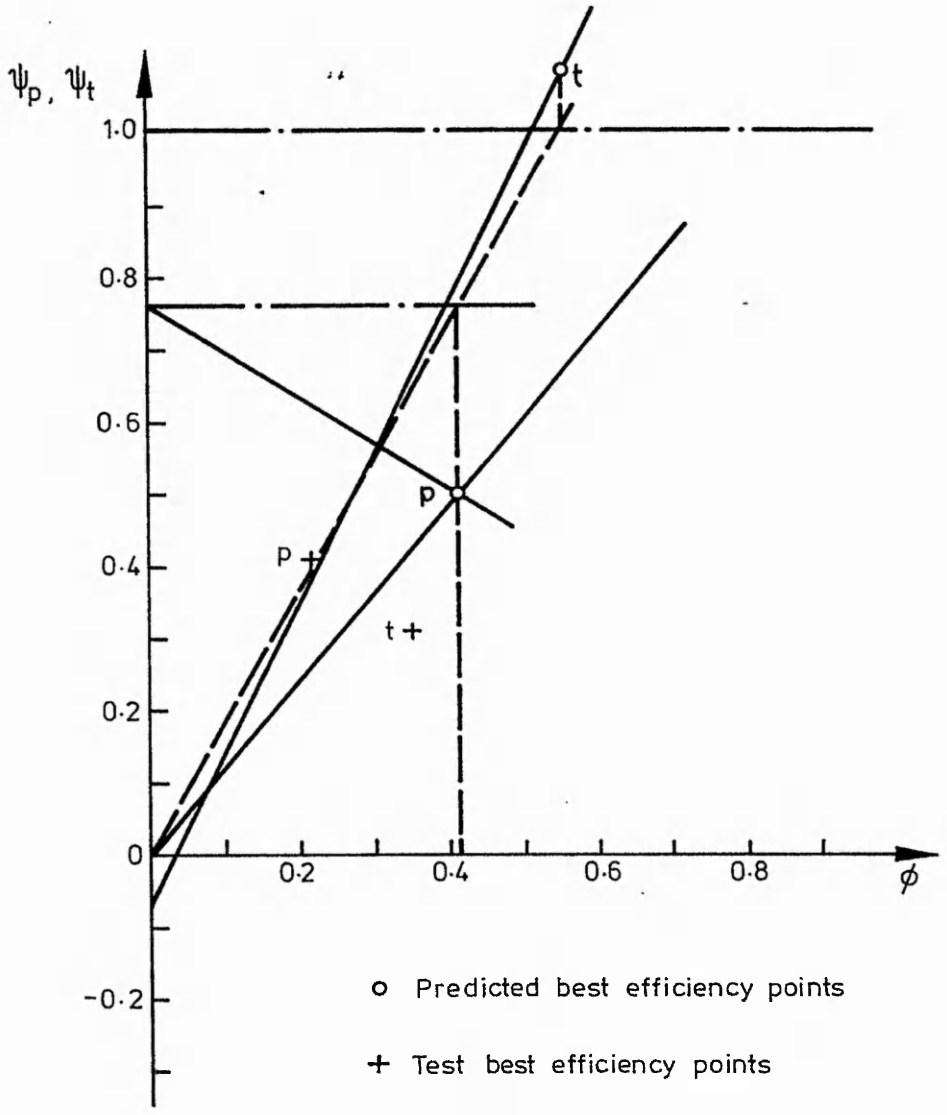


Fig. 5·18 Turbine prediction for submersible pump

As can be seen from the position of the points on the $\psi$ against $\phi$ diagram (Fig. 5.18), there is a large difference in performance between the operation at point III compared with point II. The actual best efficiency point in turbine mode is certain to lie between these two points, but it can be defined only if the inefficiency due to shock loss at the impeller inlet is known. Tests in turbine operation show that the best efficiency point is 35.9 m and 17.4 l/s at 3100 rpm.

For this pump, the area ratio method, as developed so far, is not able to predict the turbine performance at best efficiency. Even the pump performance prediction is not accurate. Further consideration of the pump design, in which the shroud of the impeller is cut away at the impeller channels, leads to the conclusion that the effective diameter of the impeller is less than the outside diameter of the impeller blade tips, as given in Table 5.1. The investigations carried out by Varley[99] demonstrate that, where an impeller is relatively narrow, and the shroud has a high relative roughness, which is the case for the pump being considered, the shroud makes a considerable contribution to the development of the pump outlet head. To take this into account, the predicted pump performance was recalculated using an impeller diameter of 158 m, which is the average of the shroud diameter and the blade tip diameter. This gives the predicted power balance shown in Table 5.8, and the pump performance of 15.65 l/s and 22.0 m, using the pump efficiency of 58.5% from the manufacturer's data. These values are closer to the measured values, which are 10.0 l/s and 25.0 m head.

**Table 5.8 Breakdown of losses for pump best efficiency.**

| | | |
|---|---|---|
| Input power : 3378/0.585 = | 5 774 | |
| Mechanical losses | 180 | |
| Leakage losses | 7 | |
| | 5 587 | |
| Impeller losses | 1 243 | |
| Volute losses | 966 | |
| Hydraulic output power | 3 378 | W |

## 5.4 Comparison of area ratio prediction with some published test results

Two published papers, which give results of turbine tests of centrifugal pumps, also give enough geometrical data to carry out predictions by the area ratio method. The test results and comparison with predicted performance are given in this section.

**Table 5.9. Data for published pumps run as turbines.**

| | Geometrical data | |
|---|---|---|
| **Pump** | Peck 'B' | Grand Coulee |
| $D_2$(mm) | 273.0 | 374.7 |
| $D_1$(mm) | 152.4 | 196.9 |
| $b_2$(mm) | 25.4 | 47.6 |
| $b_1$(mm) | 34.8 | 71.0 |
| $\beta_2$ | 20.0° | 30.0° |
| $\beta_1$ | 20.0° | 27.0° |
| $a_2$($mm^2$) | 18960 | 53260 |
| $a_1$($mm^2$) | 14705 | 30085 |
| $B^2$($mm^2$) | 13965 | 14518 |
| Z | 6 | 8 |
| $N_p$(rpm) | 1200 | 2000 |
| $N_t$(rpm) | 1200 | 2000 |
| | **Calculated Data** | |
| $\nu$ | 0.558 | 0.525 |
| $U_{2p}$(m/s) | 17.15 | 39.24 |
| $U_{2t}$(m/s) | 17.15 | 39.24 |
| $h_0$ | 0.850 | 0.838 |
| $c_v$ | 1.388 | 1.295 |
| $\varphi_p$ | 0.249 | 0.474 |
| $\psi_p$ | 0.346 | 0.614 |
| $q_p$(l/s) | 0.63 | 2.93 |
| $\eta_{vp}$ | 0.900 | 0.952 |
| $\phi_t$ | 0.293 | 0.566 |
| $\psi_t$ | 0.522 | 0.800 |
| $q_t$(l/s) | 0.78 | 3.68 |
| $\eta_{vt}$ | 0.920 | 0.962 |
| $\varepsilon$ | 0.961 | 0.994 |
| $Q_p$(l/s) | 59.0 | 267.0 |
| $H_p$(m) | 9.3 | 92.5 |
| $Q_t$(l/s) | 71.0 | 326.0 |
| $H_t$(m) | 17.7 | 129.0 |
| $\eta_t$ | 0.77 | 0.90 |
| | **Test data** | |
| $Q_p$(l/s) | 51.3 | 246.0 |
| $H_p$(m) | 9.5 | 86.9 |
| $\eta_p$ | 0.75 | 0.88 |
| $Q_t$(l/s) | 71.5 | 291.0 |
| $H_t$(m) | 16.7 | 110.6 |
| $\eta_t$ | 0.75 | 0.88 |

### 5.4.1 Radial flow pump with semi-open impeller

The data for this pump are from a paper by Peck[100], in which a pump was made specially for tests to investigate the change in flow patterns due to changing flow rates through the pump. In this pump, the blades were of true logarithmic spiral form, with the same angle at inlet and outlet. Various configurations were tested, but test results in turbine mode are given only for the case where there are no guide vanes, and the impeller is fitted with longer blade tips.

The geometrical data, predicted performance and test results are given in Table 5.9. The theoretical lines for pump and turbine head and flow coefficients are shown in Fig. 5.19, together with the points of pump and turbine best efficiency given from tests. This pump has a packing gland seal, and therefore the bearing friction losses have been taken as 100% of the disc friction loss. The breakdown of losses is shown in Tables 5.10 and 5.11.

**Table 5.10 Breakdown of losses for pump best efficiency.**

| | | |
|---|---|---|
| Input power : 5405 W/0.75 = | 7 206 | |
| Mechanical losses | 426 | |
| Leakage losses | 64 | |
| | 6 716 | |
| Impeller losses 711 | | |
| Volute losses | 600 | |
| Hydraulic output power | 5 405 | W |

**Table 5.11 Breakdown of losses for turbine best efficiency.**

| | | |
|---|---|---|
| Turbine input power | 12 340 | |
| Volute losses | 980 | |
| Leakage loss | 120 | |
| Available power | 11 230 | |
| Impeller exit losses | 450 | |
| Impeller input power | 10 780 | |
| Impeller losses | 860 | |
| Mechanical loss 430 | | |
| Mechanical output power | 9 490 | W |

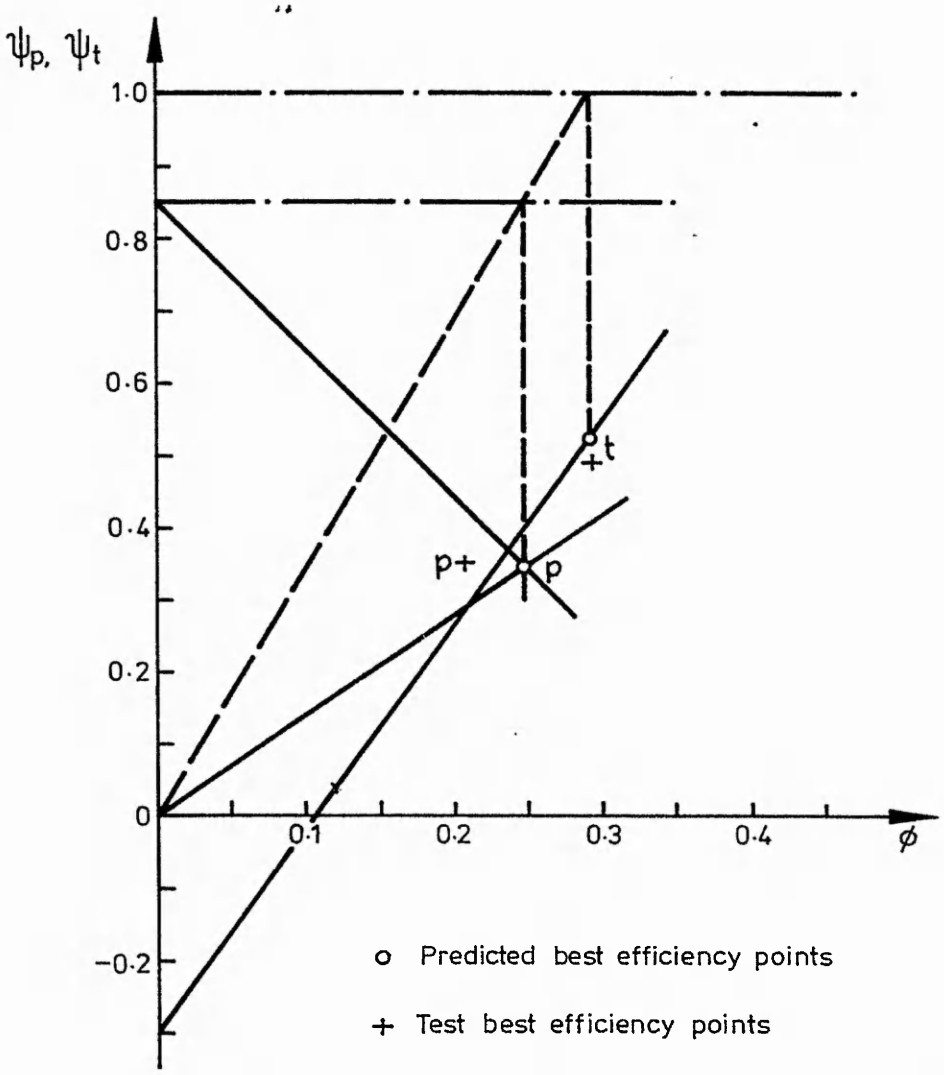


Fig. 5·19 Turbine prediction for pump data from Peck

### 5.4.2 Reversible Pump-Turbine with guide-vanes

The data for this pump are from a paper by Terry & Jaski[101], which also gives enough data on the geometry of the pump to enable the area ratio prediction method to be applied, and a comparison to be made with the test results. The pump tested was a model for a reversible pump-turbine for a large pumped-storage scheme built at Grand Coulee, USA. The data and test results used, have been taken for one particular setting of the guide vanes, which gives a high efficiency in both pump and turbine modes. The data for the pump are shown in Table 5.9.

Some of the data are not given explicitly in the original reference but have been deduced, either from the cross-sectional drawing, or from approximations. For example, the allowance for the blade thickness at the impeller outlet has been calculated using the equation used by Anderson[102], which gives:

$$a_2 \approx 0.95\ \pi\ D_2\ b_2 = 53\ 260\ \text{mm}$$

The value used for the throat area has not been taken as the area at the smallest part of the conical outlet diffuser, but has been taken as the area between the guide vanes. This gives:

$$B^2 = b_3\ d_3\ Z_v = 47.63 \times 19.05 \times 16 = 14\ 518\ \text{mm}^2 \qquad (5.2)$$

where $Z_v$ is the number of guide vanes, $b_3$ is the width of the vanes and $d_3$ is the perpendicular distance between adjacent vanes.

Since the angle of the guide vanes is known, it is possible to check the validity of the equation used for volute angle (4.12), which gives the following value:-

$$\alpha_v = \tan^{-1}(B^2/a_2 c_v) = 11.9^o$$

which is close to the value of 13.0° given in the original reference.

The theoretical lines for pump and turbine head and flow coefficients are shown in Fig. 5.20, together with the points of pump and turbine best efficiency given from tests at the California Institute of Technology. The same method as in chapter 4 is used for evaluating the losses in pump and turbine mode, with the bearing friction losses taken as 50% of the disc friction loss. The final estimates for pump best efficiency point are again shown in Table 5.9, and the beakdown of losses in Table 5.13.

The predictions of turbine head and flow at best efficiency are 129 m and 326 l/s, at an efficiency of 90%. Tests on this pump in turbine mode give 110.6 m and 291 l/s, at a maximum efficiency of 88%. Turbine losses are shown in Table 5.13.

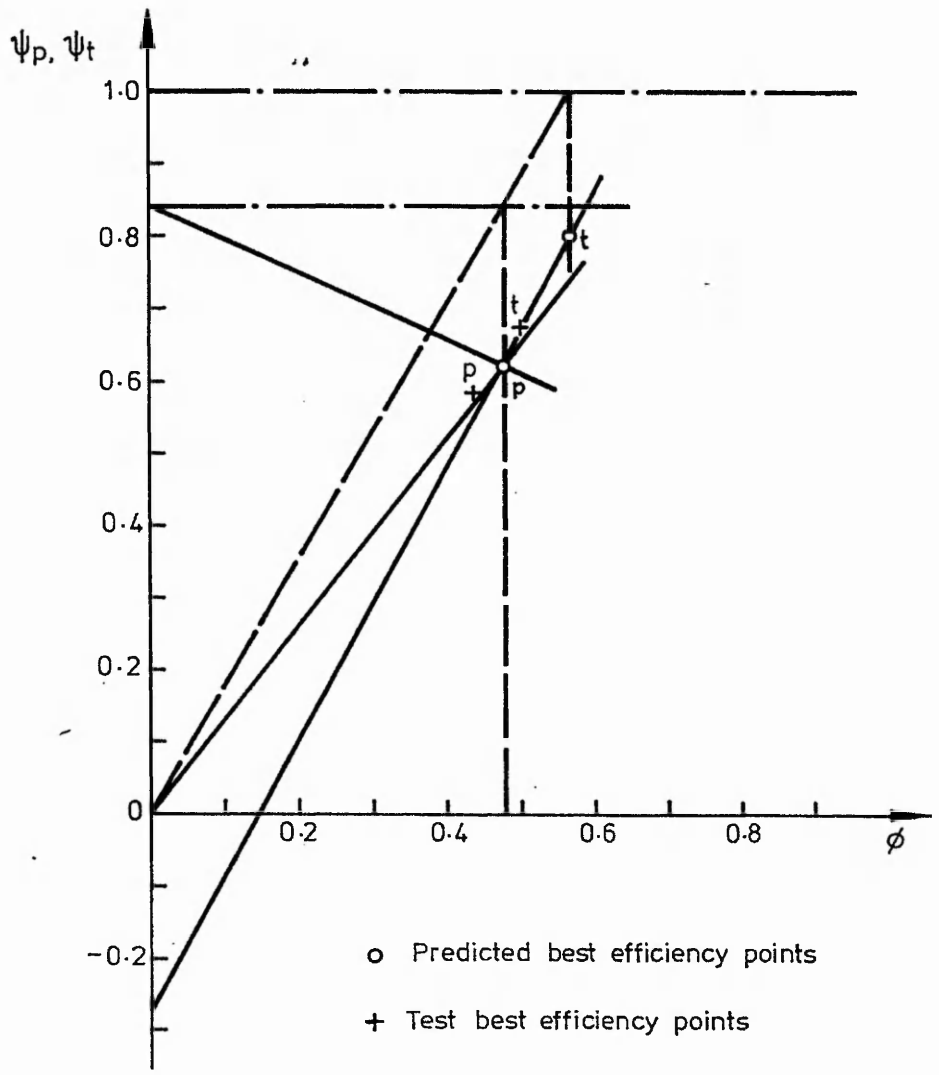


Fig. 5·20 Turbine prediction for Grand Coulee model pump

**Table 5.12 Breakdown of losses for pump best efficiency.**

| | | |
|---|---|---|
| Input power : 240 kW/0.88 = | 273 240 | |
| Mechanical losses | 5 400 | |
| Leakage losses | 2 660 | |
| | 265 180 | |
| Impeller losses | 12 640 | |
| Volute losses | 12 090 | |
| Hydraulic output power | 240 450 | W |

**Table 5.13 Breakdown of losses for turbine best efficiency.**

| | | |
|---|---|---|
| Turbine input power | 411 880 | |
| Volute losses | 15 820 | |
| Leakage loss | 4 200 | |
| Available power | 391 860 | |
| Impeller exit losses | 2 380 | |
| Impeller input power | 389 480 | |
| Impeller losses | 14 960 | |
| Mechanical loss 5 400 | | |
| Mechanical output power | 369 120 | W |

## 5.5 Summary of test results

The test results and their respective predicted values, according to the area ratio method, are set out in Table 5.14. The values predicted by the relatively simple method of Sharma are included in the table, and also the values of the prediction criterion, as defined in chapter 3.

Turbine performance predictions by the area-ratio method were possible for a total of six pumps. Of these, only the result for the Worthington-Simpson double-suction pump was significantly worse than by the Sharma method. The prediction for the Gilkes pump is also just outside the limit of acceptability stated in chapter 3 ($Cr < 1$), but the prediction is significantly better than by any of the other methods. On average, the prediction criterion for the area ratio method is 0.06 lower than for the method of Sharma, and therefore the area ratio prediction is slightly better than the best of the prediction methods available previously.

## Table 5.14 Comparison of Turbine Tested and Predicted Results

| | Test | | | Area Ratio | | | | Sharma | | |
|---|---|---|---|---|---|---|---|---|---|---|
| | Head | Flow | Eff'cy | Head | Flow | Eff'cy | Criterion | Head | Flow | Criterion |
| [Flygt BS2102 | 35.9 | 17.4 | 51% | - | - | - | - | 56.3 | 16.7 | 3.16] |
| W-S 134 mm | 59.3 | 3.93 | 48% | 56.5 | 4.00 | 53% | 0.33 | 62.4 | 4.42 | 0.46 |
| W-S 108 mm | 37.8 | 2.69 | 41% | 42.8 | 2.81 | 34% | 0.53 | 43.6 | 3.36 | 0.82 |
| W-S 3L2 | 23.7 | 25.0 | 58% | 22.7 | 29.4 | 77% | 1.14 | 23.1 | 26.0 | 0.34 |
| Gilkes EM132 | 25.3 | 2.60 | 56% | 17.7 | 1.80 | 53% | 1.01 | 16.9 | 2.53 | 1.63 |
| Gr. Coulee | 111 | 291 | 88% | 129 | 326 | 90% | 0.53 | 101 | 272 | 0.27 |
| Peck 'B' | 16.7 | 71.5 | 75% | 17.7 | 71.0 | 77% | 0.35 | 13.4 | 64.5 | 0.69 |
| **Average value of Prediction Criterion (Cr)** | | | | | | **0.64** | | | **0.70** | |

# CHAPTER 6

# CONCLUSIONS

During the research project, a variety of different pump designs and a range of sizes have been investigated with the aim of broadening knowledge of the use of pumps as turbines. From these investigations it has been found that many centrifugal pumps, though by no means all, may be used as turbines. Those pumps which are unsuitable tend to be specialized types. Standard end-suction centrifugal pumps with spiral volute casings, which are usually relatively low-cost, have always been found to be suitable for use as turbines. For medium head sites (10 - 40 metre), the main advantage of using a conventional turbine is its capability of running efficiently over a wide range of flow rates. Therefore, for any application where a constant flow is available, or a fixed load is required, the advantages of using a PAT rather than a conventional turbine usually outweigh the disadvantages. In particular, a centrifugal pump is likely to be much less expensive than a crossflow turbine for power outputs lower than 10 kW.

In many isolated electricity generation schemes, the use of a combined induction motor-pump unit, as a turbine and generator, results in further benefits. These units are very widely available, and with the addition of certain electrical equipment, can often be installed without any modifications.

The main reason why pumps have not been more widely employed as turbines is that an accurate turbine performance is difficult to obtain. A pump manufacturer is likely to charge a high price for measuring the performance by testing, because the test procedure is relatively complicated and the market for small turbines is insignificant compared with that for small pumps. The alternative, which is to predict the turbine performance by calculation, has until now been difficult because of the unreliable accuracy of the prediction methods. There are many of these methods, all of which calculate the turbine performance from the pump performance data at maximum efficiency.

In order to assess the accuracy of these turbine performance prediction methods, a prediction criterion has been defined which takes into account the likely effects of an inaccurate prediction of the turbine best efficiency, given the running conditions and hydrology for a typical micro-hydro site. Of the methods already published, the method of Sharma has been found to give the most reliable results.

A more complex method has been formulated for prediction of pump-as-turbine performance which is based on physical geometry, rather than pump performance data. This new turbine performance prediction method is an extension of the area ratio method, which has been developed by several authors for use in design and performance prediction of centrifugal pumps (Anderson[102], Worster[84], Thorne[103]). For the six pumps for which full turbine performance prediction was carried out, the average value of the prediction criterion for the area ratio method is more than 10% lower than for the method of Sharma. For three out of five pumps which were tested under laboratory conditions, and for one of the two pumps where sufficient published data were available, the area ratio method gives a more accurate prediction of turbine performance than the method of Sharma. For the small radial-flow semi-open impeller pump tested in the laboratory, the area ratio method is the only one to give a prediction which is within acceptable limits of accuracy (ie. $Cr < 1$).

In the case of one of the other pumps tested, the area ratio method in its present form is not able to predict the best efficiency performance because of the unusual operating conditions in turbine mode. However, the turbine mode performance of this pump could not be predicted accurately by any of the previously published methods. Further investigation is required to produce a method for calculating the shock loss at impeller inlet in turbine mode. It would then be possible to extend the area ratio method to predict the turbine best efficiency performance in such cases, and also to predict the turbine performance on either side of the best efficiency point.

The area ratio method has some advantages and disadvantages compared with other prediction methods. Its greatest advantage is that it does not rely on manufacturers' pump performance data, which may be inaccurate or difficult to obtain from some suppliers, particularly in developing countries. A method such as that of Samani[104] could be used to predict the pump performance in these circumstances, but this may not be very accurate. If the pump performance data is inaccurate, using any of the existing methods introduces another source of error into the turbine performance prediction. The major disadvantage of using the area ratio method is that it requires a thorough knowledge of the pump geometry, which may be difficult to measure, even if the pump is easily disassembled. It also requires considerably more complicated calculations than any of the methods which rely on pump performance data.

The area ratio method has a secondary advantage in that it provides some insights into the operation of pumps as turbines. For example, where the exit whirl velocity is large for shock-free impeller conditions (as with the Flygt BS2102HT), the turbine

best efficiency will be a compromise between zero entry shock loss and zero exit losses, and the turbine efficiency will be noticably lower than the pump best efficiency - in this case 51% compared with 58.5%.

The area ratio method can be used to predict the performance change due to a reduction in either the diameter of the impeller, or the area of the volute throat. It shows the possibility of correcting for a mismatch between PAT performance and site conditions by inserting a sleeve into the volute to reduce the throat area and thus reduce the flow rate for best efficiency operation. This modification was carried out on one of the pumps installed at the demonstration scheme at Malham (see Appendix E).

On the other hand, the area ratio method was not able to predict the magnitude of the change in performance due to rounding off of the impeller blades; nor was it able to predict the drop in turbine efficiency in that case. The test results from the modified impeller showed that a relatively small change in the geometry of a pump may have significant, and sometimes unpredictable, effects on the turbine performance. This fact has long been recognized in pump design, as shown by Turton[105], Kováts[106] and others. The accurate performance prediction of pumps in the normal mode of operation is also difficult, and there are many different approaches to the problem, all of which have their limitations. It is therefore no surprise that the simple methods for predicting turbine performance of pumps are not always accurate, and even the area ratio method, which has been developed from pump design theory, has limitations when applied to the full range of pump designs.

In conclusion, the area ratio method provides an additional tool to evaluate pump-as-turbine performance. For more than half of the pumps under investigation, the area ratio method gave a more accurate turbine performance prediction than any of the previously published methods. Unlike any of the other methods, it may be used for predicting the turbine performance of a pump for which accurate pump performance data is not available. It may also be used for evaluating the effects of simple modifications to the pump impeller and volute in order to adjust the turbine performance to match particular site conditions.

# REFERENCES


[1] United States Academy of Science, 'Direct and indirect uses of solar energy', Paper 4 of "Energy in the Developing World" ed. by V Smil and W E Knowland, Oxford University Press, 1980, pp 53-55.

[2] Bingli, D, 'Small hydro in China: progress and prospects', Water Power & Dam Construction, Feb 1985, pp 15-17.

[3] Thoma, D, 'Vorgänge beim Ausfallen des Antriebes von Kreiselpumpen', Hydr. Inst. Tech. Hochschule München, 1931.

[4] Spetzler, O, 'Die Turbinenpumpe im Stauwerk Baldeney', Zeitschrift Vereines deutsche Ing., Vol 78, No 41, 13 Oct 1934, pp1183-1188.

[5] Strub, R A, 'Investigations and Experiments on Pump-Turbines', Sulzer Tech. Review, 1959, No 2, pp 87-94.

[6] Meier, W, 'Pompes-Turbines', Bulletin Escher-Wyss, 1962, Pt 2, pp 6-12.

[7] Acres American Inc, 'Small Hydro Plant Development Program', U.S. Dept of Energy, Idaho National Engineering Lab., Oct 1980, Report No. DOE/ID/01570-T21.

[8] Cooper, P & Worthen, R, 'Feasibility of using large vertical pumps as turbines for small-scale hydropower', U.S. Dept of Energy, Idaho Nat. Eng. Lab., 1981, Report No. DOE/ID/12160-T1.

[9] McKinney, J D, Warnick, C C et al, 'Microhydropower Handbook', U.S. Dept of Energy, Jan 1983, Report No. IDO/10107.

[10] Marquis, J A, 'Design and Evaluation of Small Water Turbines', U.S. Dept of Energy, Feb 1983, Report No. DOE/R4-10243-T1.

[11] Chappell, J, Hickman, W & Seegmiller, D, 'Pumps as Turbines Experience Profile', U.S. Dept of Energy, 1982, Report No. IDO/10109.

[12] Laux, C H, 'Reversible Multistage Pumps as Energy Recovery Turbines in Oil Supply Systems', Sulzer Tech. Review, 1980, No 2, pp 61-65.

[13] McClaskey, B M, & Lundquist, J A, 'Hydraulic Power Recovery Turbines', ASME Conference, 19 Sept 1976, Paper 76-Pet-65.

[14] Apfelbacher, R, & Etzold, F, 'Energy-saving, Shock-free throttling with the aid of a Reverse Running Centrifugal Pump', KSB Tech Berichte, 1988, Vol 24e, pp 33-41.

[15] Steel, D A, 'Hydraulic energy recovery by means of submersible generators', Int. Power Generation, Feb 1986, pp 27-30.

[16] Mikus, K, 'Erfahrungen mit Kreiselpumpenanlagen zur Energierück-gewinnung aus dem Trinkwassersystem', Das Gas und Wasserfach, 1983, Vol 124, Pt H.4, pp159-163.

[17] Taylor, I, 'Some installed power-recovery turbines found unstable, due to misconceptions of process and performance', ASME Conf on Fluid Machinery, FED-6, 13 Nov 1983, pp 107-110.

[18] Engel, L, 'Die Rücklaufdrehzahlen der Kreiselpumpen', doctoral dissertation, Tech. Hochschule Braunschweig.

[19] de Kováts, A, & Desmuir, G, 'Pumps, Fans and Compressors', Blackie & Sons, Paris, 1958, pp 79-82.

[20] Stepanoff, A J, 'Centrifugal and Axial Flow Pumps', J Wiley & Sons, 1957, p 276.

[21] Kittredge, C P, 'Centrifugal Pumps Used as Hydraulic Turbines', Trans. A.S.M.E., J. Eng. Power, Ser. A, Jan 1961, pp 74-78.

[22] Nicholas, W G, 'Pumps as Turbines: Selection and Application', Hydro '88 Conference, 24 April 1988, pp 309-315.

[23] Smith, N P A, Williams, A A, Brown, A, 'Stand-alone induction generators for low-cost micro-hydro installations', World Renewable Energy Congress, Reading, Sept. 1990, pp 2904-08.

[24] Yang, C S, 'Performance of the Vertical Turbine Pumps as hydraulic turbines', ASME Conf. FED-6, 13 Nov 1983, pp97-102.

[25] Waltham, M, correspondence from ITDG Nepal, April, 1992.

[26] Holland, R, 'Machinery and equipment for micro hydro plants', Water Power & Dam Construction, Nov 1986, pp17-19.

[27] Noyce, S A, 'Syphon Intake for Intermittent Operation of a Micro-hydro Turbine', BEng (Mechanical) project report, Nottingham Polytechnic, 1992.

[28] Hettiaratchi, P, Brown, A, 'Battery Charging in Sri Lanka', Hydronet, 1991, No.2, pp6-7.

[29] Ndeuwo, G, 'Milling power for Tanzanian villages', Hydronet, 1989, No. 3, p5.

[30] Schumacher, E F, 'Small is beautiful', Abacus, London, 1974.

[31] Intermediate Technology Development Group, 'Putting Partnership into Practice', Nov 1989.

[32] Monosowski, E, 'Dams and sustainable development in Brazilian Amazonia', Water Power & Dam Construction, May 1991, pp53-54.

[33] Raphals, P, 'The hidden cost of Canada's cheap power', New Scientist, 15 Feb 1992, pp50-54.

[34] Jobin, W R, 'Designing hydro reservoirs to prevent tropical diseases', Water Power & Dam Construction, Nov 1986, pp19-22.

[35] Borsos, B, 'Socio-political aspects of the Bös-Nagymaros barrage system', Water Power & Dam Construction, May 1991, pp57-59.

[36] Jackson, R, 'The Varied Career of Rural Electrification', Appropriate Technology, Vol. 13,No. 2, Sept 1986, pp5-7.

[37] Hislop, D, 'Micro-hydro programme in Nepal - a case study', IIED Conf. on Sustainable Development, 1987.

[38] Munasinghe, M, 'Power for Development', IEE Review, March 1989, pp101-105.

[39] Water Energy Commission Secretariat, 'Five Workshops' report, Kathmandu, Nepal, 1985.

[40] Brown, N E, Howe, J W, 'Solar energy for Tanzania', Science, Vol 199, 10 Feb 1978, pp 651-7.

[41] Williams, A A, Smith, N P A, Mathema, S, 'Application of Appropriate Technology to Small-Scale Hydroelectric Power', Science, Tech & Development, Vol 7, No. 2, Aug 1989, pp98-112.

[42] Hislop, D,'Microhydro brings change to Nepal', World Water, Oct 1987, pp39-41.

[43] Shrestha, G R, Singh, K M, 'Improved ghattas in Nepal', Appropriate Technology, Vol 16, No. 3, Dec 1989, p9.

[44] Wishart, G, 'Long-term Agreement Reached with Nepalese Bank', I T News, June 1989, within Appropriate Technology, Vol 16, No. 1.

[45] Waltham, M, 'Micro-hydro for rural energy in Nepal', Appropriate Technology, Vol 18, No. 3, Dec 1991, pp6-8.

[46] Pandey, B, Cromwell, G, 'Monitoring micro hydro in Nepal', Appropriate Technology, Vol 16, No. 4, Mar 1990, pp8-10.

[47] Smith, N P A, Williams, A A, Harvey, A B, Waltham, M, Nakarmi, A-M, 'Directly Coupled Turbine-Induction Generator systems for low-cost Micro-hydro Power.', World Renewable Energy Congress, Reading, UK, 14-18 Sept, 1992, pp 2509-2516.

[48] Appropriate Technology Development Organization, 'Micro Hydel Plant', Govt. of Pakistan, 1983.

[49] Junejo, A A, 'Detailed Survey Report on Micro-Hydro Power Plants in Northern Areas and N.W.F.P.', Pakistan Council for Appropriate Technology, 1988.

[50] Meier, U, 'Report on Mission to PCAT, Pakistan', GTZ/GATE, Eschborn, Germany, 15 June, 1989.

[51] Conroy, C, 'Rural development in the mountains of northern Pakistan', Appropriate Technology, Vol 17, No. 4, Mar 1991, pp5-7.

[52] Brown, A P, 'Falling water and raising standards', Physical World, Apr 1992, pp28-29.

[53] Hindmarsh, J, 'Electrical Machines and their Applications', 3rd Ed, Pergamon, 1977.

[54] Elder, J M, Boys, J T, Woodward, J L, 'The process of self excitation in induction generators', Proc IEE, Vol 130, Pt B, No 2, 1983.

[55] Bhattacharya, J L, Woodward, J L, 'Excitation balancing of a self-excited induction generator for maximum power output'

[56] Smith, N P A, 'Self-excited Micro-hydro Generator with Voltage and Frequency Control', PhD Thesis, Nottingham Polytechnic, 1992.

[57] Engeda, A, Rautemberg, M, 'Auswahl von Kreiselpumpen als Turbinen', Pumpentagung VDMA, Karlsruhe, 1988, Section A6.

[58] Knapp, R T, 'Centrifugal Pump Performance as Affected by Design Features', Trans. ASME Vol. 63, 1941, pp 251-260.

[59] Kobori, T, 'Experimental Research on Water Hammer in the Pumping Plant of the Numazawanuma Pumped Storage Power Station', Hitachi Review, February 1954, pp 65-74.

[60] Nèmec, J, 'Engineering Hydrology', McGraw-Hill, 1972, p233.

[61] Salford Civil Engineering Limited, 'Small Scale Hydroelectric Gereration in the UK', Dept. of Energy report no. ETSU-SSH-4063-P1, 1989, Vol. 1.

[62] Knapp, R T, 'Complete Characteristics of Centrifugal Pumps and their use in the Prediction of Transient Behavior', Trans. ASME, November 1937, pp 638-689.

[63] Swanson, W M, 'Complete Characteristics Circle Diagram for Turbo-Machinery', Trans. ASME, 1953, Vol. 75, pp 819-826.

[64] Stepanoff, A J, 'Centrifugal and Axial Flow Pumps', J Wiley & Sons, 1957, Figs. 13.1-3, pp270-1.

[65] BS 5316: Parts 1 & 2: 'Acceptance Tests for centrifugal, mixed flow and axial pumps', British Standards Institution, 1977.

[66] Yedidiah, S, 'Application of centrifugal pumps for power recovery purposes', ASME Conference FED-6, November 1983, pp 111-119.

[67] Childs, S M, 'Convert Pumps to Turbines and Recover HP', Hydrocarbon Processing and Petroleum Refiner', October, 1962, Vol. 41, No. 10, pp 173-174.

[68] Lueneburg, R, and Nelson, R M, 'Hydraulic Power Recovery Turbines', Chapter 14 of 'Centrifugal Pumps: Design and Application', Ed. Val S Lobanoff, 1985, Gulf Publishing Co.

[69] Hancock, J W, 'Centrifugal Pump or Water Turbine', Pipe Line News, June 1963, pp 25-27.

[70] Sharma, K R, 'Small Hydroelectric Projects - Use of centrifugal pumps as turbines', Kirloskar Electric Co., Bangalore, India, 1985.

[71] Alatorre-Frenk, C and Thomas, T H, 'The Pumps-as-turbines approach to Small Hydropower', World Renewable Energy Congress, Reading, U K, Sept, 1990.

[72] Schmiedl, E, 'Serien-Kreiselpumpen im Turbinenbetrieb', Pumpentagung Karlsruhe, Oct 1988, Section A6.

[73] Buse, F, 'Using centrifugal pumps as hydraulic turbines', Chemical Engineering, Jan, 1981, pp 113-117.

[74] Lewinsky-Kesslitz, H-P, 'Pumpen als Turbinen fur Klein-kraftwerke', Wasserwirtschaft, Vol. 77, No. 10, 1987, pp 531-537.

[75] Grover, K M, 'Conversion of Pumps to Turbines', GSA Inter Corp, Katonah, New York, 1980.

[76] Kittredge, C P, 'Centrifugal Pumps Used as Hydraulic Turbines', Trans. A.S.M.E., J. Eng. Power, Ser. A, pp 74-48.

[77] Karassik, I J, et al (Editors), 'Pump Handbook', McGraw Hill Book Co., 1976, Section 3.2 (by C P Kittredge), pp 2-177 to 2-190.

[78] Williams, A A, Keysell, M, Pratt, J M K, Smith, N P A, 'Characteristics of a submersible pump unit for use as a micro-hydropower generator.', 23rd Universities Power Engineering Conference, Trent Polytechnic Nottingham, Sept. 1988, Section 5a.

[79] Moody, L F and Zowski, T, Hydraulic Machinery, sect. 26 of 'Handbook of Applied Hydraulics', Edited by Davis and Sorenson, 3rd Ed., McGraw Hill Book Co., 1970.

[80] Hutton, S P, 'Component losses in Kaplan Turbines and the prediction of efficiency from model tests', Proc. I Mech E, 1954, Vol. 168, pp743-762.

[81] Busemann, A, 'The delivery head of radial centrifugal pumps with logarithmic spiral blades', Z. Angew. Math. Mech. 1928, Vol. 8, No.5, p 372.

[82] Anderson, H H, 'Mine pumps', Journal of Mining Society, England, July 1938.

[83] Anderson, H H, 'Modern developments in the use of large single entry centrifugal pumps', Proc. I.Mech.E. Vol.169, No.6, 1955.

[84] Worster, R C, 'The flow in volutes and its effect on centrifugal pump performance', Proc. I.Mech.Eng. Vol.177, No.31, 1963.

[85] Thorne, E W, 'Design by the area ratio method', 6th Technical Conference of the BPMA, 1979.

[86] Ventrone, G, Navarro, G, 'Utilizzazione dell'energia idrica su piccola scala: pompa come turbina', L'Energia Elettrica, 1982, Vol. 59, No. 3, pp 101-106.

[87] Bothmann, V, Reffstrupp, J, 'An improved slipfactor formula', 7th Fluid Machinery Conf., Hungarian Academy of Sc., Budapest, Sept. 1983, pp59-68.

[88] Hergt, P, Krieger, P, Thommes, S, 'Die strömungstechnischen Eigenschaften von Kreiselpumpen im Turbinenbetrieb', Pumpentagung Karlsruhe, October 1984, VDMA, Frankfurt.

[89] Stepanoff, A J, 'Centrifugal and Axial Flow Pumps', J Wiley & Sons, 1957, pp 190-192.

[90] Anderson, H H, 'Centrifugal Pumps', Trade & Technical Press, 3rd Edition, 1980, pp95-96.

[91] Naber, G & Hausch, K, 'Reversible Pumpturbinen in Trinkwasserfernleitungen', Wasserwirtschaft, Vol 77 No 10, 1987, pp 538-545.

[92] Butterworth, S, 'Design of a volute for a pump running as a turbine', Nottingham Polytechnic, B Eng Mechanical Engineering Project Thesis, May 1992.

[93] Hadid, A, 'Turbine Operation of a Centrifugal Pump', Trent Polytechnic, B Eng Mechanical Engineering Project Thesis, May 1980.

[94] Cheng, W, 'Reverse Running of a Centrifugal Pump', Trent Polytechnic, B Eng Mechanical Engineering Project Thesis, May 1983.

[95] Smith, N P A, PhD laboratory book no. 4 (unpublished), Nottingham Polytechnic, 1986.

[96] Thomsett, A J, 'Turbine Operation of Centrifugal Pumps', Nottingham Polytechnic, B Eng Mechanical Engineering Project Thesis, May 1990.

[97] Senu, Z, 'A Centrifugal Pump as an Inward Flow Turbine', Nottingham Polytechnic, B Eng Mechanical Engineering Project Thesis, May 1990.

[98] Crossland, P J, 'Design and Testing of a Draft Tube for a Pump run as a Turbine', Nottingham Polytechnic, B Eng Mechanical Engineering Project Thesis, May 1990.

[99] Varley, F A, 'Effects of impeller design and surface roughness on the performance of centrifugal pumps', Proc I Mech E, Vol 175, No 21, 1961, pp955-969.

[100] Peck, J F, 'Investigations concerning flow conditions in a centrifugal pump, and the effect of blade loading on head slip', Proc. I.Mech.E, Vol 164, 1951, pp 1-30.

[101] Terry, R V, Jaski, F E, 'Test Characteristics of a Combined Pump-Turbine Model with Wicket Gates', Trans ASME, Nov. 1942, Vol 64, pp731-744.

[102] Anderson, H H, 'Hydraulic design of centrifugal pumps and water turbines', ASME, Vol 61, 1961, Paper 61-WA-320.

[103] Thorne, E W, 'Analysis of an end suction pump by the area ratio method', I Mech E Conf 1982-11, 'Centrifugal Pumps - Hydraulic Design', pp 25-28.

[104] Samani, Z, 'Performance estimation of close-coupled centrifugal pumps', Applied Eng. in Agriculture, Vol 7, Part 5, 1991, pp 563-565.

[105] Turton, R K, 'The effect of discharge diffuser arrangement on the performance of a centrifugal pump', IAHR/VDI Symposium on Pumps in Power Stations, Germany, 1966, pp G17-24.

[106] Kováts, A, 'Modification of the performance curve of centrifugal pumps', IAHR/VDI Symposium on Pumps in Power Stations, Germany, 1966, pp D1-8.

[107] Hydraulics Research Station, 'Tables for the hydraulic design of pipes', Metric edition, HMSO, 1977.

[108] Thorne, E W, information supplied regarding tests carried out at Worthington-Simpson Pumps, Newark, UK.

[109] Engeda, A, 'Untersuchungen an Kreiselpumpen mit offenen und geschlossenen Laufrädern im Pumpen- und Turbinenbetrieb', University of Hannover, PhD Thesis, 1987.

[110] Laux, C H, 'Reverse-running standard pumps as energy recovery turbines', Sulzer Tech. Review, 1982, No.2, pp23-27.

[111] Rodriguez, J A, 'Operacion de Bombas Centrifugas como Turbinas Hidraulicas, Investigacion Preliminar', Universidad Los Andes, Bogotá, Colombia, Thesis, Aug. 1989, pp68-71.

[112] Jyoti Company Newsletter, Jyoti Ltd., India.

[113] Giddens, E P, Spitall, W, Watson, D B, 'Small hydro from a submersible pump', Water Power & Dam Constr., Dec. 1982, pp33-35.

[114] Schultz-Grunow, F, 'Der Reibungswiderstand rotierender Scheiben in Gehäusen', Zeitung Angew. Math., Mech. Bull. No. 4, Verein Deutscher Ingenieure, July 1935, pp 194-204.

[115] Pfleiderer, C, 'Die Kreiselpumpen', Julius Springer, Berlin, 1932, p64.

[116] Burton, J D, Williams, A A, 'Performance prediction of pumps as turbines using the area ratio method, 9th Fluid Machinery Conf., Hungarian Academy of Sciences, Budapest, Sept. 1991, pp76-83.

[117] Shepherd, D G, 'Principles of Turbomachinery', Macmillan, New York, 1965, pp76-77.

APPENDIX A

# OPERATION OF A PUMP-AS-TURBINE AT REDUCED FLOW

Once a PAT has been selected and installed at a particular site, it will run at a fixed value of head and flow, at the point where the site net head curve intersects with the PAT head curve. If the flow rate at the site falls below this value, then the intake will draw air, as shown in Fig. A.1, and the pump will run at a lower head until the penstock refills itself. It has been found that on a site with a gross head of 63 m, the PATs will operate down to a head of around 35 m before flow surges in the penstock cause the system to become unstable. At this head the flow may be reduced to 75% of the normal flow, but the power output will have fallen to around 25% of normal, because of the drop in efficiency.

In conclusion, a pump-as-turbine may be run with a reduced flow provided that air does not become trapped in the penstock, thus causing flow surges or even a complete break in the flow of water.

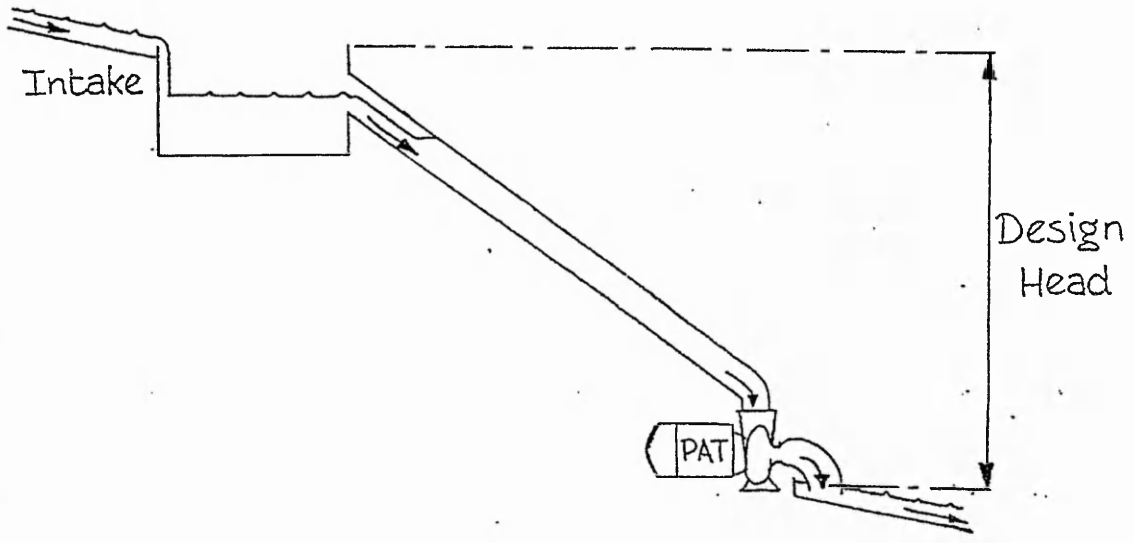


Fig. A.1. Air drawn into penstock due to decrease in flow

APPENDIX B

# VISIT TO ALTERNATE HYDRO ENERGY CENTRE, ROORKEE, INDIA. April 1988

At the University of Roorkee, near Saharanpur, in the state of Uttar Pradesh, considerable experience has been gained in the use of centrifugal pumps as turbines. Within the university, which is one of India's foremost technological institutions, an Alternative Hydro Energy Centre was set up in 1982, to carry out research and development. A turbine similar to the Nepalese MPPU has been developed from the traditional *gharat* water wheel of northern India. Various systems for productive end-uses of electricity in rural areas have also been developed, including a nitrogen fertilizer unit, an electrolysis unit for producing hydrogen and oxygen, and a process for making fuel briquettes from rice husk.

At the Centre is a test rig which has been used for testing 8 different pumps-as-turbines. Several of these have subsequently been installed at sites in Uttar Pradesh. Various types of pump, including an axial-flow type and a submersible unit have been installed. However, induction generators have not been used, but the pumps have been coupled via a belt-drive to a synchronous generator.

As a general rule, for turbine installations, a head and flow-rate 15-20% above the rated pump output have been used. This has been found to give a reasonable efficiency without putting mechanical parts under excessive stress. For sites above 50 kW output, the additional capital cost of a conventional turbine has been found to be justified by the gain in efficiency compared with a pump installation. Also, with one unit of 100 kW output, the pump bearings disintegrated after only six months of service.

At the time of visiting, research was being carried out at Roorkee into the production of a binary weighted electronic load controller for use with synchronous generators. Although part of an academic institution, much of the research work being carried out is aimed at practical rural development.

APPENDIX C

# VISIT TO BAGHICHA, NORTHERN PAKISTAN.

15 May, 1991

The site at Baghicha, situated on the road between Gilgit and Skardu, has a 8 inch pump installed as a turbine, and running at 1,400 rpm. It is connected via a double belt drive (1:1 ratio) to a 10kVA 4-pole Chinese synchronous generator. The cost of such a pump (excluding motor) is Rs 8,000 (£200). A flywheel has been mounted on the pump shaft. The penstock is 82 m long, 8 inch (200 mm) diameter steel pipe, and the gross head is 24 m. A gate valve is fitted before the inlet to the turbine. The installation has been operating since 1988 and is used only in the evenings for electric lighting. The bearings have been replaced about 4 times and the shaft straightened once.

If the discharge is 6 cusecs (170 l/s) as quoted, then the head loss in the pipe is approximately 12 metres, leaving a net head of 12 m. The maximum output was reckoned to be 6 kW, although when measured by Nigel Smith in October 1990, it was found to be only 2.7 kW. The overall efficiency of the turbine and generator, is therefore:

$$\eta_o = \frac{2700}{9.81 \times 12 \times 170} = 13.5\%$$

The power output was probably higher when the pump was first installed. The poor efficiency may be due to a bent shaft or partially blocked runner. The flow-rate may be too small for the turbine, so that it is running well below best efficiency. In this case, a smaller pump could be installed, reducing the flow-rate and therefore the penstock losses and increasing the turbine efficiency.

Apart from the low efficiency of the system, the main difficulty, as with many sites, is the need for regular maintenance. At the time of the visit, the stuffing box was tightened as far as possible but was still leaking because the jute packing material *(dori)* needed replacing, as it does every 3 to 4 months. It seems that as long as there is electricity, any problems are left to get worse, rather than reventative action being taken. Thus, the seal had been allowed to continue leaking, which was resulting in corrosion of the bolts on the bearing housing and may lead to water getting into the bearing itself.

APPENDIX D

# DEMONSTRATION SCHEME AT TENNANT GILL FARM, MALHAM, N. YORKS.

## Installed: 1990-91

### D.1. Background.

The micro-hydroelectric scheme at Tennant Gill Farm, Malham Tarn Estate is one of three demonstration schemes in the UK, assisted by funds from the government's Overseas Development Administration (ODA) through Intermediate Technology Development Group (ITDG). The aim of the demonstration sites is to be able to test the systems which have been developed at Nottingham Polytechnic, before carrying out installations in developing countries. The other two demonstration schemes are at Caudwell's Mill near Matlock in Derbyshire, and Batworthy Farm near Chagford in Devon.

The project is a joint venture between Intermediate Technology and the National Trust. Ms Dorothy Fairburn, the National Trust's Land Agent for the Malham Tarn Estate, put forward Tennant Gill Farm as a possible site at a meeting at Gibson Mill, Hardcastle Craggs. An initial suggestion from the National Trust of building a demonstration scheme at Gibson Mill was found to be impractical in the timescale available.

At each of the demonstration sites a standard industrial motor is used for generating electricity using a novel type of electronic controller, known as the Induction Generator Controller, or IGC. At Tennant Gill another innovative feature is employed - using standard centrifugal pumps running in reverse as water turbines. Industrial pumps of this type are supplied with an integral motor, which in this case is used as an induction generator. Two of the motor-pump units at Tennant Gill were supplied without charge by the companies which manufactured them - one from Dresser UK (Worthington-Simpson Pumps) and one from ITT Flygt Ltd.

Overall responsibility for design and implementation of the scheme has been with Arthur Williams, who has been carrying out research at Nottingham Polytechnic on the use of pumps as turbines since 1987. The scheme would not have been possible without the support of Alister Clunas, Estate Warden at Malham Tarn, and the enthusiasm and hard work put in by Bill Cowperthwaite, who farms at Tennant Gill.

## D.2. Design of the scheme.

A first visit to the Malham Tarn Estate was made in January 1990, in order to make an initial assessment of the site. A report was compiled giving details of the findings and setting out some of the options for developing a scheme. Overall, the site appeared to have good potential, and the next stage was to carry out a more detailed feasibility study, and to clarify the areas of co-operation between the research group at Nottingham Polytechnic and the National Trust.

Information on rainfall was obtained from the Malham Tarn Field Studies Centre and from the National Rivers Authority. Some information on soil types was obtained from the British Geological Survey. Further readings of streamflow were taken using a temporary V-notch weir. Adam Harvey, with advice from colleagues at Intermediate Technology, designed the intake tank, which is situated at a suitable point on Tennant Gill, below the farm's water supply intake, and close to a sink hole which takes the overflow.

## D.3. Construction and Civil Works

The intake tank was built at the end of August, 1990. It is a concrete tank, approximately 20 feet (6 m) long in total and 4 feet (1.2 m) wide. The first part has a gently sloping base to collect silt from the stream water. The water then flows through a V-notch weir, which acts as a flow measuring device. The second tank, in which the entrance to the main pipe is situated, is about 3 feet (1 m) deep. The top of the pipe has a wire mesh filter over it to prevent floating debris, such as dried grass or leaves, from reaching the turbines. It also has an overflow weir which takes away excess water.

Most of the work in constructing the tank and laying the pipe was done by the Employment Taining Team employed by the National Trust on the Malham Tarn Estate. The pipe (known technically as the penstock) leading from the intake tank to the generator building, is made from uPVC, and follows the line of the original stream bed. The first 150 metres of pipe are 6" (150 mm) diameter, after which it is reduced to 4" (100 mm). This enabled some cost savings on the lower part of the penstock, which takes greatest pressure, without reducing too much the available pressure at the turbine inlet.

The siting for the building which houses the pump units (turbine and generators) is below the sheep pens beside the farmyard, where the water can discharge through a drainage grill into a culvert. The total length of the penstock is 500 m, and the fall to the turbine site from the intake is 63 m. The penstock was laid during September and October 1990. The generator building was then constructed from concrete

blocks, and completed with local stone outer walls, and stone slate roof. The pipe will be buried, once the installation is complete, partly to increase the life of the pipe, and also for environmental reasons.

### D.4. Selection of Pump Units.

Pumps used as turbines run efficiently over a small range of flows. It was therefore decided to install three pumps as turbines, each designed to run at a different flow rate. The smallest of these units was donated by Worthington-Simpson and was originally used for a student project at the Polytechnic. This is a standard 'close-coupled' pump with a 1.1 kW motor. The power available from the stream is determined by the flow rate and the head of water at the turbine. The head is calculated by subtracting the head loss in the pipe from the difference in height between intake and turbine.

$$P_{out(elec)} = Q \times 9.8 \times (63\,m - H_f) \times \eta_t \times \eta_{gen}$$

If Q is in l/s, then $P_{out(elec)}$ is given in W.

As a turbine, the smallest unit requires a flow of 4 l/s, and generates 800 W, with an overall efficiency (water-to-wire) of 33%. At this flow, the head loss in the pipe is around 1 metre. The unit was installed in February, 1991, and has been generating for more than 2,000 hours.

The largest pump is a Flygt BS2102 HT submersible dewatering pump, fitted with a 5.2 kW motor. ITT Flygt Ltd market a range of large low-head pumps for use as turbines. They have donated the pump unit as part of their collaboration with the project. Tests were carried out on this pump at Flygt's factory near Nottingham during August 1990, and the unit was installed in the following March. This unit runs at around 45 m head, because of the pressure loss in the penstock, and takes 19 l/s flow. The electrical output is 4 kW, giving an overall efficiency of 48%. This unit will only run when the flow in the stream is well above average.

Originally, a 3 kW Lowara pump unit was installed as the medium sized turbine-generator, but this did not work efficiently as a turbine, perhaps because of the unusual design of the pump casing. A MECO pump unit, donated by the Pakistan Council for Appropriate Technology, has now been installed in order to test out a pump typical of those available in developing countries. This pump produces around 2.8 kW from a flow of 15 l/s. With some minor modifications to the pump volute, it has been running successfully for more than 300 hours. The cost of such a unit in Pakistan is 4,500 rupees ( a little over £ 100 ).

### D.5. Electrical Installation.

The generators produce alternating current electricity, held by a load controller at 240 volts, and between 48 and 53 Hz. Although the pump motors are three-phase, they are connected with excitation capacitors in such a way as to produce a single-phase output. The small variation in frequency will have no adverse effects on any of the electrical equipment in common use on the farm or in the house.

The Induction Generator Controller keeps the voltage constant by diverting any power not required by the main circuit, into 'ballast loads', which are two 2 kW convector heaters placed at convenient positions in the farm house. The hydro system has been connected so that the existing diesel generator can easily be switched in when necessary. The smallest of the generators can provide enough power to charge the batteries which supply household lights, run the TV, vacuum cleaner and other household electrical equipment. It is not powerful enough to run the washing machine or immersion heater, and a special starting module has been added to ensure that it will start the freezer. The largest pump unit can provide enough power for all these appliances, except that the washing machine cannot run simultaneously with the water heater.

### D.6. Running Experience.

As can be expected with any experimental plant, there have been several minor problems since it began running. On the electrical side, a safety trip installed was found to be over-sensitive, and had to be modified. Also it has been found that when the ballast loads are running, interference occurs when listening to long wave or medium wave radio in the farmhouse. No simple solution has been found for this difficulty, apart from tuning in the radio on VHF.

A modification had to be made to the penstock intake in order to filter out debris without becoming blocked. The present filter, which was installed in June 1991, has operated well through dry and wet conditions. The whole system is being monitored closely, particularly over the first 12 months of operation. This has already provided useful information on the use of pumps as turbines for such small-scale schemes. A second demonstration scheme using a pump-as-turbine installed at a village in the Northern Areas of Pakistan, has been operating successfully since May 1991.

APPENDIX E

# DEMONSTRATION SCHEME AT HAMÀRAN, NORTH PAKISTAN

Installed: May, 1991

## E.1. Summary

The village of Hamàran in Bagroth Valley, Gilgit district, was chosen by the Aga Khan Rural Support Programme (AKRSP) as a suitable site for a pump-as-turbine (PAT) and induction generator demonstration project. The village, although small, has an active Village Organisation (VO), which participated in the initial work in putting in the scheme, and made an agreement with AKRSP to maintain the equipment provided.

A site survey was carried out to determine the best position for the power house. A pump was first tested as a turbine at AKRSP's test site before being installed at Hamàran. The penstock was constructed using 150 mm diameter steel pipe. Initially, a 3 hp single-phase induction generator, already tested in the workshop was installed. This was run on site and generated up to 2 kW. The transmission line and connections to the houses will be completed by the VO.

The combination of PAT and induction generator has not before been installed in a developing country, as far as is known. Although the use of a separate pump unit and belt-driven generator has some disadvantages, for this site it is the most appropriate system, since any mismatching of the turbine to site conditions can be corrected by changing the pulley ratio. Also, it is proposed that the 3 hp generator be replaced by a 10 hp three-phase induction generator, connected to give a single-phase output. This would then enable 6 kW to be generated, while using the existing single-phase transmission line. With this output the cost of the equipment is less than £ 300/kW (US $ 500/kW).

## E.2. Background to the Project

### E.2.1 Aga Khan Rural Support Programme (AKRSP)

The AKRSP is the main organisation supporting integrated rural development in the Northern Areas of Pakistan. It began working in the area around Gilgit in 1983, and has been involved in the installation of 18 micro-hydroelectric schemes. AKRSP has provided technical assistance and grants towards the cost of these schemes, and

the village organisations have carried out construction and installation work, and in some cases have paid for part of the cost out of their own savings.

Among the schemes installed, four have used standard pumps as turbines (PATs), two axial flow and two radial flow units. Until now all PAT schemes have used a belt-driven synchronous generator, from 2 to 10 kW.

### E.2.2 ITDG Induction Generator Project

Intermediate Technology Development Group (ITDG), a charity based in the UK, has been involved in micro-hydro technology for developing countries for more than 10 years. In 1989, a three-year project was set up to develop the innovative work on induction generators which had begun at Nottingham Polytechnic.

This project, which is funded by the UK Overseas Development Administration (ODA), includes installation and monitoring of six demonstration schemes in the UK and overseas. Part of the induction generator project is to investigate the combination of pump-as-turbine and induction generator. One PAT demonstration scheme has already been installed in the UK during 1990-91.

It was decided to install a demonstration project in Pakistan, as pump units are manufactured in the country and are readily available at low cost. Furthermore, AKRSP have already considerable experience with the installation of pumps for micro-hydro.

### E.2.3 The village of Hamàran.

Hamàran is a small village of 25 households situated at 1,750 m above sea level, on a narrow ridge between the two Bagroth valleys, 40 km from the town of Gilgit. There is an active Village Organisation, which with the assistance of AKRSP carried out the widening of an irrigation channel in 1985-6, and is now constructing a 100 m suspension bridge. At present, access to the village is by a steep path into and out of the gorge, which connects to a narrow jeep road which runs for 8 km before joining the metalled road.

The micro-hydroelectric scheme could provide about 6 kW of power (average 240 W per house) which will initially be used for lighting, but could also power a small sawmill. The power will enable the villagers to save kerosene fuel, normally used for lighting, and dry-cell batteries used for radios, tape recorders etc.

## E.3. Site Survey

A survey of the site was carried out on 23 May, 1991 using an altimeter and measuring tape. The flow in the irrigation channel was estimated, from velocity and cross-sectional area measurements, to be at least 85 l/s (3 cusecs). The irrigation channel reaches the top of the village at an altitude of 5990 ft, from where the main stream falls steeply. The site chosen for the power house is at an altitude of 5910 ft, at a distance of 250 ft (76 m) from the top channel. The site for the turbine is just below the uppermost watermill *(pan-chakki)*, giving a gross head of 24 m (80 ft). A possible site for a second turbine was also identified at an altitude of 5810 ft, 30 m below the first turbine. The layout of the village and of the distribution system is shown in Fig. E.1.

The distance between the poles for the transmission cable was chosen to be 57 m (188 ft). The number of poles required is 14, and the total length of the line is 750 m (2,444 ft). The amount of cable required for single-phase distribution is therefore 1,500 m.

## E.4. Proposal for Equipment

### E.4.1 Penstock

The penstock (the main pipe leading from the intake tank to the turbine) is made from 6" diameter (150 mm) steel pipe, which is manufactured in Lahore and brought by road to Gilgit. The wall thickness of the pipe is 3.85 mm. It is available in 10 ft (3 m) lengths with bolted flange connections. For a flow of 56 l/s (2 cusecs), the head loss in the penstock is 4.8 m, leaving a net head of 19.6 m. (see Appendix E.i for full calculation).

### E.4.2 Turbine

Initially the site has been set up with a 6" x 6" pump, connected by a V-belt drive to a single-phase induction machine. The pump was tested at AKRSP's test site at Pari where it was found to run at between 1,100 and 1,200 rpm producing an output approximately 10 kW from a 30 hp induction generator. The flow was measured to be 63 l/s (2.2 cusecs). An estimate of the turbine performance of the pump is shown in Fig. E.2. This is based on a prediction using published pump performance data for a similar pump, and the test data from Pari. At Hamàran, the pump ran at around 1,600 rpm with the valve fully open and no load. This shows that the estimated performance curve matches the actual characteristic.

## LAYOUT OF MICRO-HYDRO SCHEME AT HAMĀRAN VILLAGE

Fig. E.1.

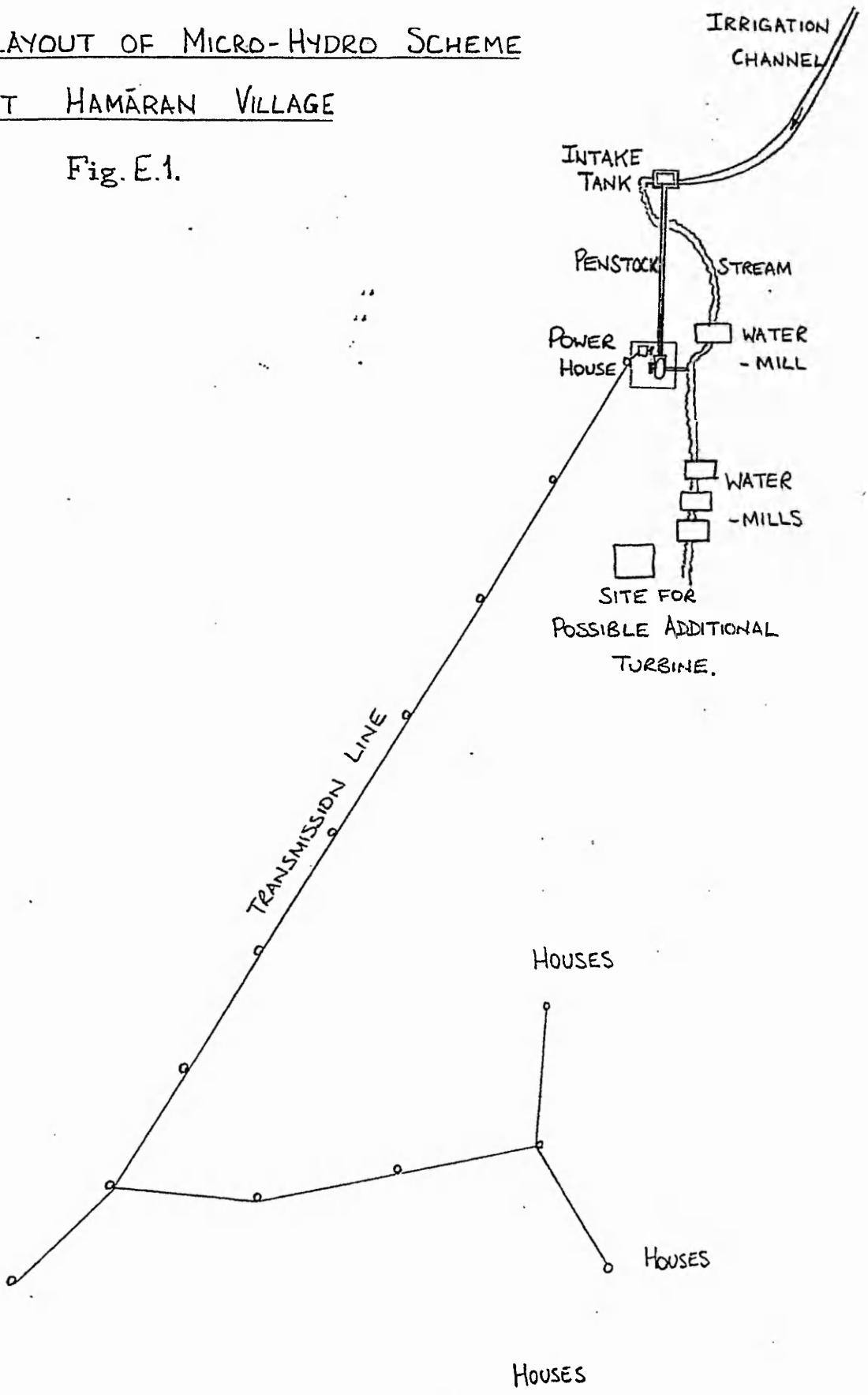

# Estimate of PECO 6" (125 M 259)

## Pump as Turbine Performance

Fig.E.2

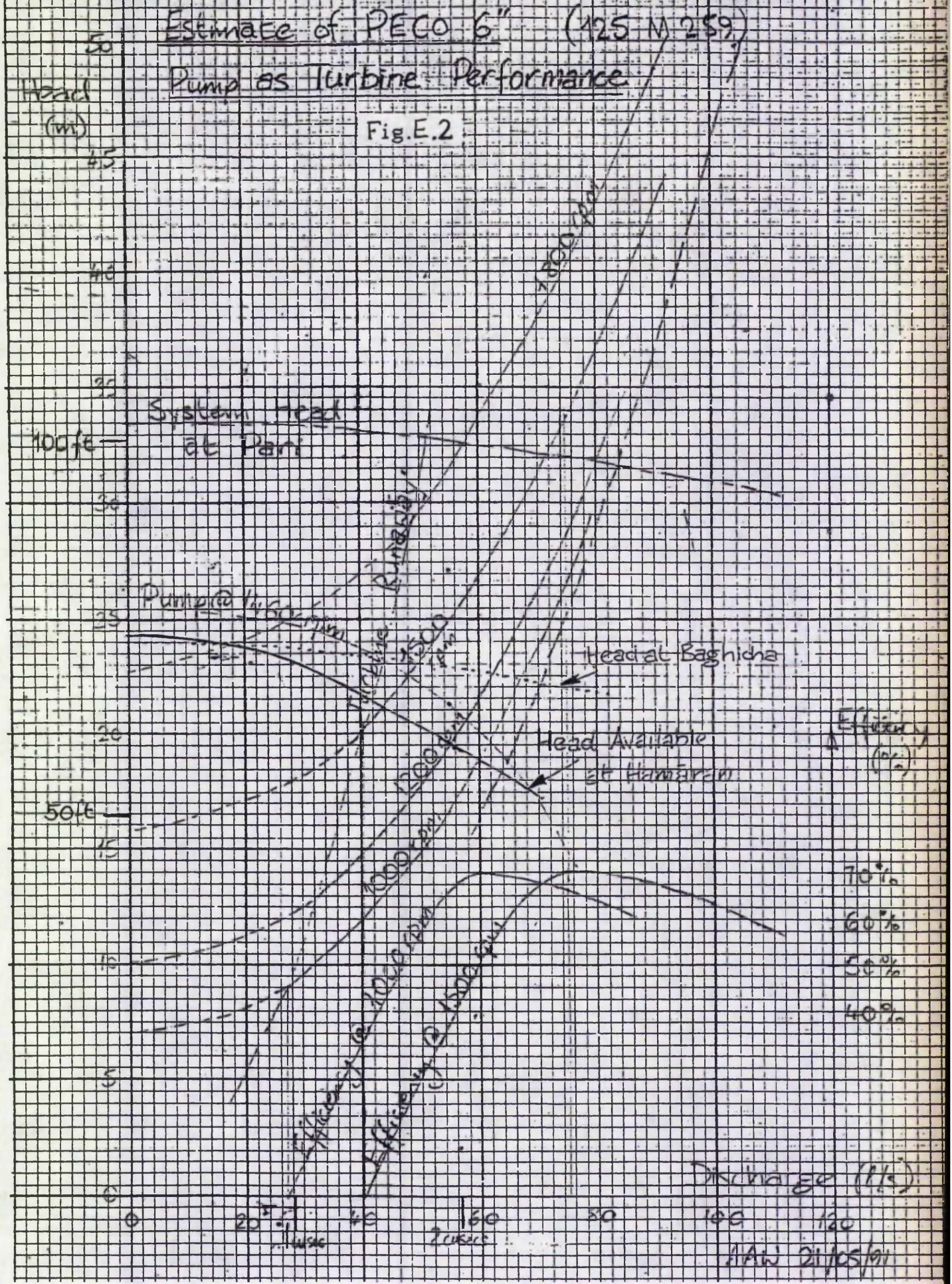

### E.4.3 Generator

A 3 hp single-phase induction motor was first tested as a generator in the workshop in Gilgit, to determine the amount of excitation capacitance required. At Hamàran, the same generator was installed with a pulley ratio of 5" to 3" and a capacitance of 100 μF. With an electrical load of 2 kW, the voltage was 240 V at a frequency of 52 Hz, and approximate generator speed, 1,600 rpm. It is recommended that the capacitors are protected by a fuse, or better still a miniature circuit breaker (MCB), which should be rated at 10 A. This will also protest the generator if the load is lost. The layout of the turbine and generator is shown in Fig. E.3.

Since the turbine output is estimated to be more than 7 kW for the site at Hamàran (see Appendix E.ii), the electrical output could be much more than 2 kW if a larger generator is installed. However, single-phase induction motors are not available for greater than 3 hp output. A three-phase generator could be used, but would require four cables for the transmission line. In Gilgit, copper cables of a suitable diameter are relatively expensive, and not easily available. Three-phase distribution would therefore require twice as much cable as single-phase, resulting in an additional cost of Rs 27,000/- (£ 675). Three-phase distribution also has the disadvantage for such a small scheme, that it is difficult to ensure load balance between the phases. It is therefore recommended that the 10 hp motor, at present at Hamàran, be brought back to Gilgit and rewound for 240 V/phase (as for a three-phase star-connected machine). It can then be connected for single-phase output using the "C-2C" configuration (see Fig. E.4). This type of connection has been used successfully at two of the demonstration schemes in the UK.

The generator should be tested, either using the 12 hp diesel engine at the workshop in Gilgit, or, preferably, using the crossflow turbine at Pari. This would enable the correct connection for balanced voltages and the appropriate values of capacitance to be found. As an initial estimate, the values of 120 μF and 240 μF should be used, as calculated in Appendix E.iii.

### E.4.4 Load controller

Initially, the electricity will be supplied on the basis of a fixed load, ie. all the lights in the village will be switched on and off at the same time from the power house. Mr Ain-ul Hayat, an electrical engineer at AKRSP attended a course at Nottingham Polytechnic during the summer of 1991 on the design and production of Induction Generator Controllers. Using this relatively inexpensive controller, the generator load can be varied while the voltage and turbine speed remain almost constant. An IGC could be installed at Hamàran at a later date to give more flexibility to the system, and enable more productive loads to be used.

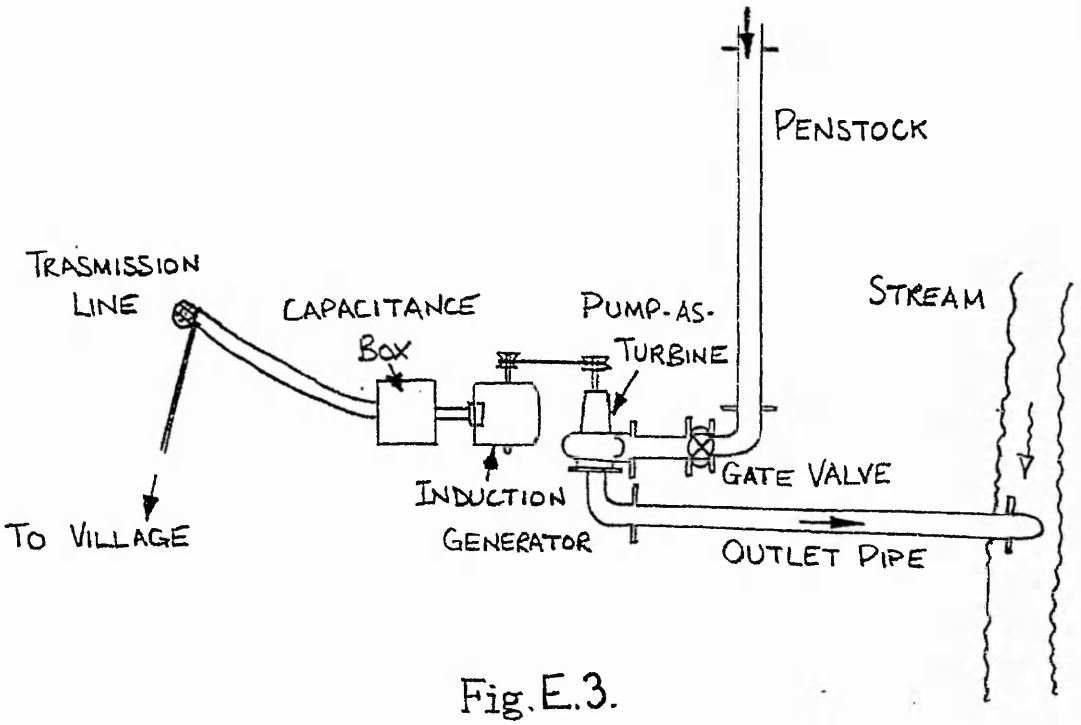


Fig. E.3.

LAYOUT OF TURBINE AND GENERATOR

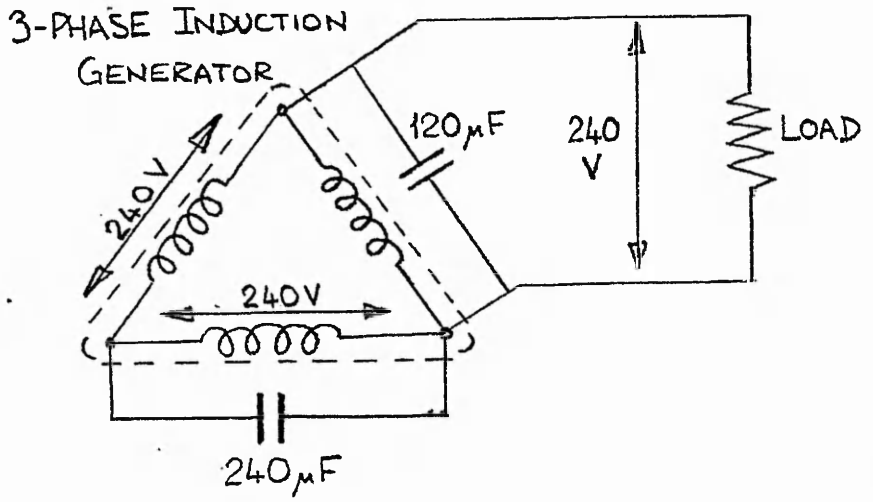


Fig. E.4.

"C-2C" GENERATOR CONNECTION

## E.5. Costings

(i) Turbine & 10 hp generator 10,000

| | |
|---|---|
| Penstock pipe: 260 x Rs 85/ft | 22,100 |
| 6" Gate valve | 5,000 |
| Transmission cable (aluminium) 750m x 2 x Rs 18/m | 27,000 |
| Poles: 14 x Rs 500 | 7,000 |
| Total (in Pakistani Rupees) | 71,100 |

(ii) The above total, converted to Sterling at current exchange rates ( 1: Rs 40/-), is £ 1,778, which represents a cost per kilowatt installed of less than £ 300. However this does not take into account the cost of engineering time donated by AKRSP and ITDG. In US $ the cost is $ 2,960.

(iii) Of the total amount, ITDG will cover the cost of the turbine and generator and penstock:

| | |
|---|---|
| Turbine & generator | 10,000 |
| Penstock | 22,100 |
| | 32,100 |

This represents £ 800 at current exchange rates, which is less than the cost in the UK of a 6" pump unit and 7.5 kW (10 hp) induction machine.

(iv) The Village Organisation has already contributed considerable labour in transporting the equipment to site, building the intake tank and installing the penstock. The VO will also take responsibility for providing and erecting 14 transmission poles (made from locally grown poplars), and the connection of the aluminium transmission cable, and subsequent feeder cables to individual houses.

## E.6. Maintenance

An agreement has been drawn up between the Hamàran VO and AKRSP regarding the microhydro scheme. The equipment is provided by AKRSP on the basis that it is used and maintained by the VO. Further training will be available for members of the VO, if this is found to be necessary, although at present there are residents of the village with enough technical training to carry out the basic maintenance of the system.

The maintenance costs of the system will be covered by a charge levied by the VO on each household. The likely charge will be Rs 25 or 30 per household per month. This compares with a cost of Rs 41 per month for running three kerosene lamps, which provide inferior illumination (see Appendix E.iv).

## E.7. Conclusions

The site at Hamàran is suitable as a demonstration site to show the viability of using a standard pump as a turbine, in conjuction with a standard induction motor as a generator. The innovational aspects of the scheme have been tested, and the major part of the installation completed by the end of May 1991. It is recommended that the present 3 hp generator be substituted for a 10 hp unit as soon as possible.

Initially, it was suggested to use this site for demonstration of a monoblock PAT installation. However, the difficulty of selecting a suitable pump, and the small improvement in efficiency which may be possible, would suggest that it would be better to find another site for such a demonstration, unless problems arise with the present arrangement.

If, in the future, the demand for electricity at Hamàran exceeds 6 kW, then it would not be difficult to install an additional turbine below the present one. If it is found that the flow available in the irrigation channel is always much greater than that used by the present turbine, it would be worthwhile to install an 8" diameter (200 mm) penstock for the second installation. The potential additional output would then be 14 kW (see Appendix E.v), which would provide nearly 1 kW per household. The present transmission cable, however, would not be adequate for the additional current.

---

## Appendix E.i. **Calculation of head loss in penstock.**

The diameter of the penstock is 150 mm (6"), and the roughness factor is likely to be around 0.06 mm. For a discharge of 56 l/s (2 cusecs), the loss given by the tables of the British Hydraulic Research Station[107] is 0.06 x pipe length.

The net head at Hamàran is therefore:

24.4 - (0.06 x 80m) = 19.6 m. (64 ft)

## Appendix E.ii. **Estimated output of turbine.**

The mechanical output of the turbine is calculated from:

Net Head x Discharge x g x turbine efficiency

The estimated PAT efficiency is 70%, hence the mechanical output is:

19.6 x 56 x 9.81 x 0.70 = 7,540 W (10.1 hp)

If the generator efficiency is 85%, the electrical output will be:

7.54 x 0.85 = 6.4 kW.

---

## Appendix E.iii. **Calculation of Capacitance for 10 hp generator.**

Assuming that the power factor of the machine is 0.8, the total current is given by:

Output watts = V x I x 0.8

Therefore, for each phase of the three-phase generator:

I = 2500/(0.8 x 220) = 14.2 A

The reactive current, which must be supplied by the capacitors, is given by:

$$I_X = \sqrt{1 - 0.8^2} \times I = \sqrt{0.36} \times I$$

$$= 0.6 \times I = 8.5 \text{ A}$$

The capacitance required is:

$$C = \frac{I_X}{2\pi f \times V} = \frac{8.5}{314 \times 220} = 123\mu F$$

The values of capacitance required for the "C-2C" connection are therefore approximately 120 and 240 μF.

## Appendix E.iv. **Calculation of the cost of kerosene lighting.**

The amount of kerosene required for one lamp is 0.05 litre/hr. Assuming that the lights are required for 4 hours each evening, the amount of kerosene used for 3 lamps during one month is:

$$0.05 \times 4 \times 3 \times 30 = 18 \text{ litre/month}$$

The cost of kerosene in Gilgit is Rs 21 for 2 gallons, ie. Rs 2.30 per litre. The total cost of the kerosene for three lamps is therefore:

$$18 \times 2.30 = \text{Rs } 41/\text{- per month.}$$

---

## Appendix E.v. **Power output available from additional scheme.**

Assuming that the second scheme uses 200 mm (8") diameter steel penstock pipe, and the flow is available, it can be designed to run from 85 l/s (3 cusecs). The net head will be: $30.5 - (100 \times 0.03) = 27.5$ m (90 ft)

The power output, assuming the same efficiencies, will be:

$$27.5 \times 85 \times 9.81 \times 0.70 \times 0.85 = 13{,}640 \text{ W.}$$

Assuming 240 V output from the generators, the total current from the original generator and the additional generator will be:

$$I = (13{,}640 + 6{,}400)/240 = 84 \text{ A}$$

The cable used is 7 x 0.122 sq.inch, aluminium, which has a total cross-section of 52.8 $mm^2$.

The resistivity of aluminium is 27 $n\Omega m$; the total length of the cable is 1,500 m, hence the total resistance is:

$$R = (27 \times 10^{-4} \times 1.5 \times 103)/\ 551 \times 10^3 = 0.767 \text{ ohms}$$

The voltage drop will therefore be:

$$V = I \times R = 64 \text{ volts.}$$

An additional transmission cable would therefore be required if an additional turbine and generator are attached to the system in the future. It would be possible for the second generator to be an induction type. The only change to the operation of the system would be that the two generators must be excited simultaneously in order to ensure synchronisation of their alternating voltages.

APPENDIX F

# VISIT TO GHARA, DHAULAGIRI, NEPAL.

## 24 March, 1988

From the information available through local turbine manufacturers, there is only one micro-hydro installation in Nepal which uses a pump-as-turbine. The site of this scheme is at Ghara, a village on a popular trekking route between Pokhara and Tatopani. The pump used is an Ebara end-suction centrifugal type, made in Japan. As a pump it is designed to produce 6 m head at 133 l/s with a rated input power of 10 kW. It is coupled to a 3 kVA synchronous generator which supplies two lodges and six houses with electricity for lighting via a single-phase transmission line about 500 m long.

The pump is installed to run from 6.2 m head, which, being almost the same as the rated pumping head, is too low for best efficiency. However, the output demand is such that the generator had been overloaded, and was out of use at the time of the visit. Alongside the pump-as-turbine installation is a traditional *ghatta* driving a corn mill and rice huller. The same civil works have been used for the pump-as-turbine, with a simple sluice arrangement in the water channel. The generator is run for five hours each evening, with a fixed lighting load.

This scheme illustrates the problems which may occur when a pump-as-turbine is installed by someone who has limited technical knowledge. The matching of the pump to the site, and the generator to the pump are both unsatisfactory. A much smaller pump could have been used, which would have reduced the cost of the scheme and also limited the output of the generator, thus preventing the overload. Installation of an induction generator would also have prevented permanent damage, since when overloaded, an induction machine ceases to excite.

APPENDIX G

# ECONOMIC ANALYSIS FOR THE DESIGN OF A PENSTOCK

This analysis is made on the basis of costs which are typical for a micro-hydro scheme in the UK. Costs in a developing country will be less, but similar in relation to each other.

Let the cost of a penstock of diameter $D = D_o$, with an assumed head loss of 1%, be £5,000 per kW installed.

The cost of the penstock is proportional to $D^2$, ie.

$$C_P = 5000\left(\frac{D}{D_o}\right)^2 \qquad (£/kW). \qquad (G.1)$$

The fractional head loss, $h_f = \frac{H_f}{H_{gross}}$, is inversely proportional to the penstock cross-sectional area, ie.

$$h_f = 0.01\left(\frac{D_o}{D}\right)^2. \qquad (G.2)$$

The value of the electricity produced is taken to be £0.05 per kW-hour.

Since the output is proportional to the net head,

$$V_E = 0.05(1 - h_f) \quad £/kW\text{-hr}$$

$$= 438(1 - h_f) \quad £/kW\text{-year}. \qquad (G.3)$$

Combining equations (G.1) and (G.2) gives the relationship

$$C_P = \frac{50}{h_f} \qquad (£/kW). \qquad (G.4)$$

The marginal, ie. incremental, cost, $\Delta C_P$, of a change in head loss of $\Delta h_f$, can be found from differentiating equation (G.4) with respect to $h_f$, which gives

$$\frac{\Delta C_P}{\Delta h_f} = -\frac{50}{h_f^2}$$

or $$\Delta C_P = -\frac{50}{h_f^2}\Delta h_f. \qquad \text{(G.5)}$$

Similarly, by differentiating equation (G.4), the marginal value of the change in output due to a change in head loss in the penstock is given by

$$\Delta V_E = -438\Delta h_f \quad (£/kW\text{-year}).$$

Assuming a payback period of 7 years on the capital cost, and a discount rate of 10%, ie. assuming that £110 of income after one year is equivalent to £100 now,

$$\Delta V_E = -438\sum_{n=1}^{7}(1.1)^{-n}\Delta h_f = -2132\,\Delta h_f. \qquad \text{(G.6)}$$

Solving (G.5) and (G.6) for $\Delta C_P$ $=(1.1)^{-n}\Delta h_f = -2132\,\Delta h_f$.

$$\frac{50}{h_f^2} = 2132\,h_f^2 \quad \text{or} \quad h_f = 0.153. \qquad \text{(G.7)}$$

The value of $h_f$ used in the calculation of acceptable turbine performance prediction errors, is 15% or 0.15. This value gives the most economic size of penstock given the assumptions used in the above calculation.

APPENDIX H

# ANALYSIS OF THE PREDICTION CRITERION FOR TURBINE PERFORMANCE

In order to calculate the value of the prediction criterion, Cr, it is necessary to be able to express the equation (3.1) in terms of h and q rather than a and b. Refering to Fig. H.1, let us consider the point with co-ordinates $(1+\Delta q, 1+\Delta h)$. If $\Delta w$ and $\Delta z$ are the distances from (1,1) at $45^\circ$ to the q,h axes, then from Pythagoras' theorum,

$$\Delta w^2 + \Delta z^2 = \Delta q^2 + \Delta h^2 \qquad \text{(H.1)}$$

and

$$(\sqrt{2} + \Delta w)^2 + \Delta z^2 = (1 + \Delta q)^2 + (1 + \Delta h)^2 . \qquad \text{(H.2)}$$

Subtracting equation (H.1) from (H.2) gives

$$2\sqrt{2}\Delta w + 2 = 1 + 2\Delta q + 1 + 2\Delta h$$

ie.
$$\Delta w = \frac{(\Delta q + \Delta h)}{\sqrt{2}} . \qquad \text{(H.3)}$$

Substituting back into (H.1) gives

$$\Delta z^2 = \Delta q^2 + \Delta h^2 - \tfrac{1}{2}(\Delta q + \Delta h)^2$$

$$= \tfrac{1}{2}\Delta q^2 + \tfrac{1}{2}\Delta h^2 - \Delta q \Delta h . \qquad \text{(H.4)}$$

The value of Cr is given in terms of $\Delta a$ and $\Delta b$, which are related to $\Delta w$ and $\Delta z$ by the equations

$$\Delta a = \frac{\Delta w}{\sqrt{2}}; \quad \Delta b = \frac{\Delta z}{\sqrt{2}}. \qquad \text{(H.5)}$$

Substituting these values into (H.4) and (H.5) gives

$$\Delta a = \tfrac{1}{2}(\Delta q + \Delta h) \qquad \text{(H.6)}$$

and
$$\Delta b = \frac{1}{2}\sqrt{\Delta q^2 + \Delta h^2 - 2\Delta q \Delta h} . \qquad \text{(H.7)}$$

These equations are used in evaluating the prediction criterion, Cr.

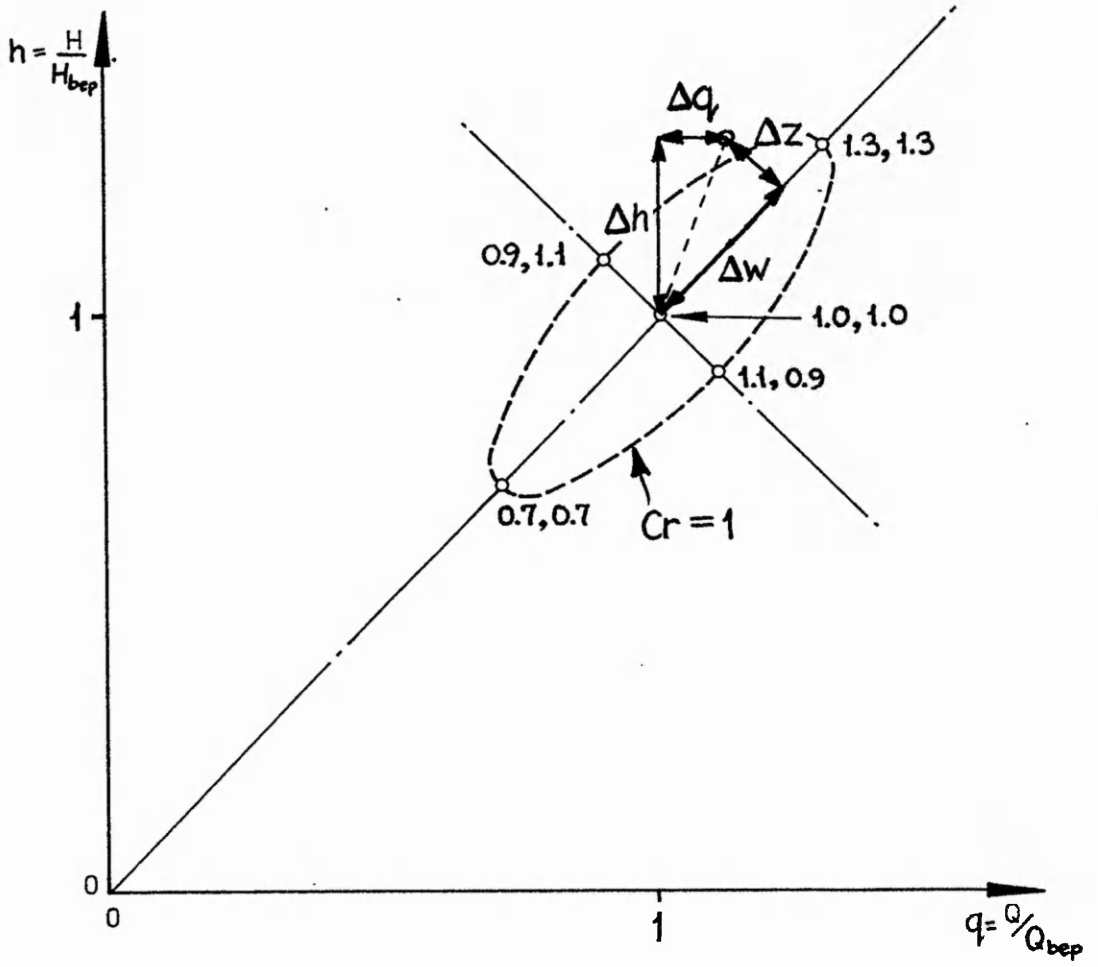


Fig. H.1. Relationships between Δw, Δz and Δq, Δh.

APPENDIX I

# DETAILS OF THE COMPARISON OF TURBINE PREDICTION METHODS

A computer programme was written to carry out the calculation of turbine prediction for 34 pumps from various published data, for eight of the simple turbine prediction methods. The value of the turbine prediction criterion, Cr, was calculated for each one, as shown in Table I.2, overleaf. The table also shows the pump specific speed, and the ratio of actual turbine specific speed to predicted turbine specific speed given by equation (3.11). The mean value of this ratio is 1.052. In Table I.1, below, is listed the mean values of Cr for each of the eight prediction methods, and also the number of pumps for which the value of Cr is greater than 1, ie. for which the error is outside the acceptable limits. The method which has the lowest number of pump predictions out of range and the lowest value of Cr, is Sharma's method. The methods of Alatorre, Stepanoff, Hergt and Hancock are also resonably accurate. Table I.3 gives a list of the pumps used in the comparison of these turbine prediction methods, including the references from which the data was obtained.

**Table I.1 Comparison of turbine prediction methods**

| Prediction Method | Mean value of Cr | No. of Pumps out of range |
|---|---|---|
| Childs | 0.921 | 14 |
| Stepanoff | 0.847 | 12 |
| Hancock | 0.906 | 10 |
| Sharma | 0.733 | 7 |
| Alatorre-Frenk | 0.852 | 10 |
| Schmiedl | 1.173 | 13 |
| Hergt | 0.865 | 11 |
| Grover | 1.333 | 22 |

## Table 1.2

Values of pump specific speed and criteria for turbine performance prediction criteria for various methods

| Pump Type | nqp | Chilcs | Step. | Hancock | Sharma | Alat. | Schmiedl | Hergt | Grover | nqt ratio |
|---|---|---|---|---|---|---|---|---|---|---|
| HTyl_2*DP2 | 32.6 | 0.592 | 0.333 | 0.612 | 0.309 | 1.155 | 1.285 | 0.288 | 0.952 | 0.965 |
| Flygt2102M | 65.8 | 0.158 | 0.228 | 1.005 | 0.840 | 0.985 | 2.380 | 0.477 | 0.000 | 0.906 |
| Flygt2102H | 25.5 | 1.079 | 2.001 | 2.197 | 2.240 | 2.347 | 3.798 | 1.673 | 2.126 | 0.761 |
| W-S_WB134i | 13.7 | 1.643 | 1.823 | 0.562 | 0.176 | 0.420 | 1.545 | 0.285 | 1.689 | 0.986 |
| W-S_WB108i | 16.7 | 2.254 | 2.254 | 1.379 | 1.248 | 1.444 | 0.485 | 1.643 | 2.195 | 1.258 |
| W-Simp_3L2 | 18.3 | 1.091 | 0.170 | 0.751 | 0.653 | 1.552 | 0.505 | 0.114 | 2.023 | 1.110 |
| GlkesEM132 | 20.9 | 2.658 | 2.877 | 1.473 | 1.631 | 2.108 | 1.264 | 1.827 | 2.830 | 1.333 |
| W-Simp_6L1 | 46.3 | 1.367 | 1.053 | 1.323 | 1.281 | 1.180 | 1.103 | 0.893 | 0.622 | 1.241 |
| W-Simp_6L2 | 22.6 | 0.437 | 0.234 | 0.473 | 0.329 | 0.026 | 0.306 | 0.870 | 2.256 | 1.021 |
| Peck_Imp_3 | 50.2 | 1.092 | 1.092 | 0.769 | 0.693 | 1.473 | 0.411 | 0.777 | 0.000 | 1.119 |
| Byron4inDS | 23.9 | 0.563 | 0.886 | 0.557 | 0.441 | 0.192 | 0.449 | 0.629 | 2.056 | 1.045 |
| Byron_DSuc | 33.8 | 0.478 | 0.584 | 0.211 | 0.335 | 0.499 | 0.876 | 1.343 | 3.047 | 0.981 |
| Byron_SSuc | 48.4 | 1.089 | 1.209 | 0.845 | 0.875 | 0.563 | 1.141 | 0.911 | 1.369 | 1.150 |
| KnappBSVol | 41.5 | 0.525 | 0.625 | 0.409 | 0.348 | 0.327 | 0.510 | 0.440 | 1.561 | 1.051 |
| KnappBDVol | 41.5 | 0.481 | 0.481 | 0.323 | 0.317 | 0.644 | 0.760 | 0.756 | 1.971 | 1.049 |
| Engeda__30 | 29.9 | 0.746 | 0.800 | 0.523 | 0.429 | 0.791 | 0.435 | 0.221 | 1.767 | 1.066 |
| Engeda__44 | 42.7 | 0.452 | 0.459 | 0.787 | 0.651 | 0.374 | 0.577 | 0.633 | 1.310 | 0.964 |
| Engeda__65 | 63.5 | 0.597 | 0.178 | 0.443 | 0.303 | 0.669 | 0.709 | 0.287 | 0.000 | 1.039 |
| Sulzer__21 | 23.6 | 0.410 | 0.669 | 0.418 | 0.238 | 0.425 | 0.212 | 0.764 | 2.204 | 1.011 |
| H-Ncwa_130 | 19.8 | 1.394 | 0.911 | 1.229 | 0.930 | 0.813 | 0.343 | 1.182 | 1.188 | 1.127 |
| Jyoti_RadF | 28.6 | 0.329 | 0.615 | 0.650 | 0.411 | 0.983 | 0.739 | 0.410 | 1.407 | 0.969 |
| Jyoti_MixF | 96.8 | 2.154 | 1.546 | 1.721 | 1.809 | 2.563 | 1.641 | 2.063 | 0.000 | 1.407 |
| NZ_Submers | 73.0 | 0.919 | 1.348 | 0.900 | 0.600 | 0.466 | 3.368 | 1.099 | 0.000 | 0.923 |
| I-Rand30B1 | 157.4 | 1.074 | 0.949 | 0.820 | 0.849 | 0.554 | 3.515 | 1.081 | 0.000 | 1.145 |
| I-Rand30B2 | 183.3 | 1.553 | 1.482 | 1.196 | 1.266 | 1.277 | 5.352 | 1.591 | 0.000 | 1.225 |
| Buse___665 | 12.7 | 0.775 | 0.596 | 1.160 | 0.826 | 0.042 | 0.937 | 1.031 | 0.584 | 0.986 |
| Worth1.5*5 | 20.1 | 0.471 | 0.471 | 0.921 | 0.620 | 0.625 | 1.000 | 0.677 | 0.989 | 0.960 |
| Worth2.5RW | 17.1 | 0.804 | 0.804 | 0.911 | 0.686 | 0.762 | 0.305 | 0.629 | 1.219 | 1.044 |
| Worth__2CN | 23.0 | 1.109 | 1.109 | 0.318 | 0.240 | 1.778 | 0.770 | 0.237 | 1.957 | 1.028 |
| Worth2.5CN | 24.8 | 1.151 | 1.151 | 1.467 | 1.319 | 0.561 | 1.141 | 1.283 | 0.969 | 0.960 |
| Worth__3CN | 34.0 | 0.438 | 0.438 | 0.797 | 0.663 | 0.402 | 0.482 | 0.831 | 1.689 | 0.957 |
| Worth__3HN | 23.8 | 0.499 | 0.499 | 0.950 | 0.764 | 0.353 | 0.690 | 0.940 | 1.470 | 0.954 |
| Worth_6HND | 23.2 | 0.479 | 0.479 | 0.570 | 0.391 | 0.364 | 0.083 | 0.659 | 1.903 | 1.016 |
| TracyModel | 44.6 | 0.453 | 0.453 | 0.123 | 0.199 | 0.261 | 0.769 | 0.878 | 1.972 | 1.018 |

**Table I.3**

**References for Pumps listed in Table I.2.**

| Pump Type | Description | Reference |
|---|---|---|
| HTyl_2*DP2 | Hayward-Tyler 2-stage submersible | Williams[78] |
| Flygt2102M | Flygt BS2102 medium-head submersible | see Appendix M |
| Flygt 2102H | Flygt BS2102 high-head submersible | see chapter 5.3.4 |
| W-S_WB134i | Worthington-Simpson monoblock pump | [96] & chapter 4 |
| W-S_WB108i | As above, with reduced dia. impeller | see chapter 5.3.2 |
| W-Simp_3L2 | Worthington-Simpson double-suction | [94] and Smith [95] |
| GilkesEM132 | Small radial-flow pump with open imp. | Senu[97] |
| W-Simp_6L1 | Large double-suction pump | Thorne[108] |
| W-Simp_6L2 | Large doube-suction pump | Thorne[108] |
| Peck_Imp_B | Radial-flow pump with semi-open imp. | Peck[100] |
| Byron4inDS | Byron-Jackson 4" Double-suction pump | Knapp[61] |
| Byron_DSuc | Byron-Jackson 10" Double-suction pump | Swanson[62] |
| Byron_SSuc | Byron-Jackson 10" Single-suction pump | Knapp[61] |
| KnappBSVol | 'Type B' Single-volute pump | Knapp[57] |
| KnappBDVol | 'Type B' Double-volute pump | Knapp[57] |
| Engeda_30 | Radial-flow pump with semi-open imp | Engeda[110] |
| Engeda_44 | Radial-flow pump with semi-open imp | Engeda[110] |
| Engeda_65 | Mixed-flow pump with semi-open imp | Engeda[110] |
| Sulzer__21 | Large radial-flow pump | Laux[111] |
| H-Nowa_130 | Halbert-Nowa, small radial-flow pump | Rodriguez[112] |
| Jyoti_RadF | Jyoti, small radial-flow pump | Jyoti[113] |
| Jyoti_MixF | Jyoti, small mixed-flow pump | Jyoti[113] |
| NZ_Submers | Brown, small submersible borehole pump | Giddens et al[114] |
| I-Rand30B1 | Ingersoll-Rand, large vertical axis pump | Cooper & W.[8] |
| I-Rand30B2 | Ingersoll-Rand, large vertical axis pump | Cooper & W.[8] |
| Buse___665 | Radial-flow pump | Buse[73] |
| Worth1.5*5 etc | Worthington radial-flow pumps (inch sizes) | Yedidiah[65] |
| TraceyModel | Model for large radial-flow pump | Yedidiah[65] |

APPENDIX J

# CALCULATION OF DISC FRICTION LOSS

This calculation is based on the method of Stepanoff, which itself relies on the work of Schultz-Grunow[114] and Pfleiderer[115]. The equation given by Stepanoff uses imperial units, but has been converted to S.I. units. The chart showing values of numerical friction coefficient, K, (Fig. J.1) has been taken directly from Stepanoff, and a conversion factor included in the equation, which is required for the change in units, and also includes the density of water, assumed to be 1000 kg/m$^3$. The equation, giving the disc friction loss in watt, is:

$$P_d = 0.17K\, D_2^{\,2} U_2^{\,3} \qquad \text{(J.1)}$$

where $D_2$ is in metre and $U_2$ is in m/s. K is found from Fig. J.1, and depends on the ratio of disc diameter to wall clearance, and Reynolds number, Re = ur/v.

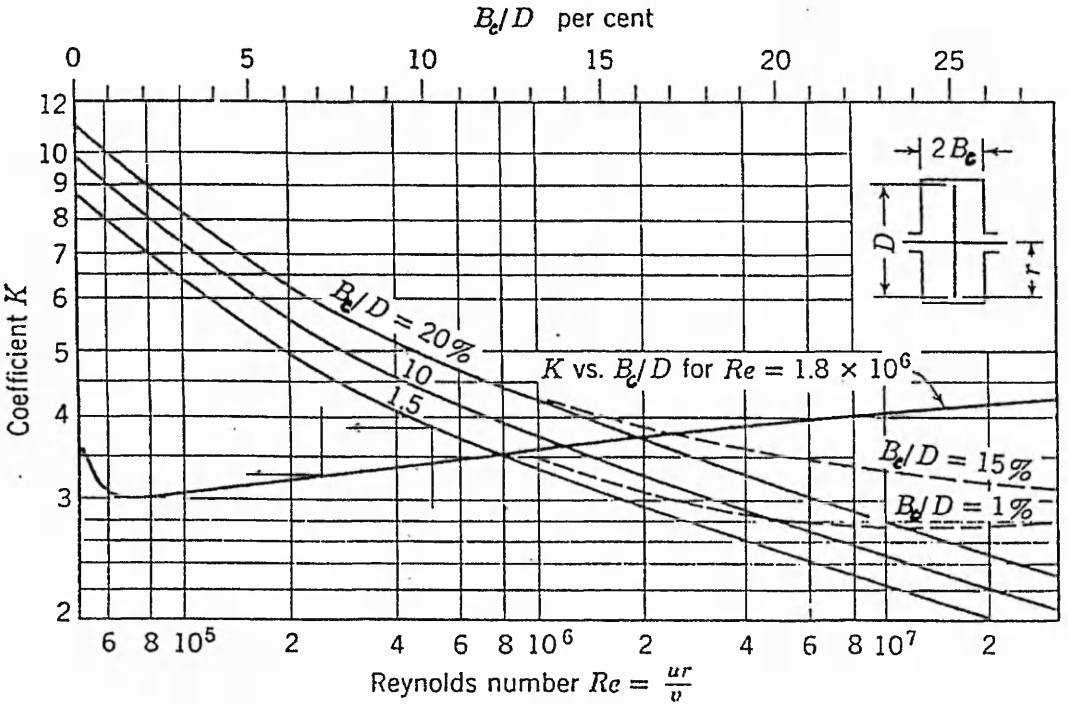


Fig. J.1. Disc friction coefficient versus Reynolds number from Stepanoff[89]. Full lines represent smooth disc; dashed lines, rough disc.

## APPENDIX K

# CALCULATION OF LEAKAGE LOSS.

Thorne's equation (see ref[85]):-

$$H_f = 0.76H_p - \frac{U_2^2 - U_r^2}{8g} = \frac{1}{2g}\left(\frac{2q_p}{\pi D_r \delta}\right)^2 \left(\frac{fl}{\delta} + 1.5\right)$$

where $\delta$ is the total clearance on the diameter between the impeller and the casing at the impeller eye, l is the length of the clearance, $D_r$ is the external diameter of the impeller eye and f is a dimensionless friction coefficient (found from the Moody diagram).

As an example, take the Worthington-Simpson pump described in chapter 4.2.4. The additional data required to calculate the leakage flow is given below:

$D_r$: 39.5 mm; l: 12.2 mm; $\delta$: 0.5 mm.

The initial estimates of head and flow for the pump best efficiency condition are given in section 4.2.4 as: $Q_p$ = 2.54 l/s, $H_p$ = 25.7 m. These values can be substituted to calculate a more exact value of the leakage flow, using equation (K.1). First, it is necessary to calculate the value of f, the friction coefficient, which requires the value of Reynold's number in the clearance annulus.

The leakage path area is given by:

$$A_L = \frac{\pi D_r \delta}{2} = \frac{\pi \times 39.5 \times 0.5}{2} = 31.02 \text{ mm}^2 \qquad \text{(K.2)}$$

The value of Reynold's number is given by:

$$Re = \frac{V_L \delta \rho}{\mu} = \frac{q_L \delta \rho}{A_L \mu}. \qquad \text{(K.3)}$$

Assuming that the leakage flow is 5% of the total flow, as a first estimate, ie. $q_L \approx 0.115$ l/s,

$$Re \approx \frac{115 \times 0.0005 \times 1000}{31.02 \times 1.00 \times 10^{-3}} \approx 1860$$

Using the Moody diagram, f ≈ 0.036, which, when substituted into equation (K.1) gives:

$$H_f = 19.53 - 4.82 = \frac{1}{19.6}\frac{q_L^2}{0.0322^2}(0.88 + 1.5)$$

ie. $q_L = 0.355$ l/s.

This value is much greater than the initial estimate, and it is therefore advisable to recalculate the friction factor based on this value of leakage flow. The new value of Re is 5740, giving f = 0.037, and $q_L$ = 0.34 l/s.

In turbine mode, the initial estimates of head and flow are 55.5 m and (3.47 + $q_t$) l/s. As an initial estimate, the leakage flow is calculated by taking $q_L$ proportional to $\sqrt{H}$, which gives $q_t$ = 0.52 l/s. This, together with the more accurate value of $H_t$ from sction 4.2.4 can be used to calculate a more accurate value of leakage flow using equation (K.1). $V_L$ = 16.76 m/s, which gives Re = 8380, and f = 0.034.

$$H_f = 41.65 - 5.51 = \frac{1}{19.6}\frac{q_L^2}{0.0322^2}(0.8 + 1.5)$$

ie. $q_L = 0.48$ l/s.

This value is within 10% of the original estimate, which changes the value of the total flow by only - 1%. It is therefore sufficient in most cirumstances to calculate only the pump leakage flow, $q_p$, from equation (K.1), and to calculate the turbine leakage flow from:

$$q_t = \sqrt{\frac{H_t}{H_p}} \cdot q_p \qquad \text{(K.4)}$$

# APPENDIX L

# CALCULATION OF UTILIZATION FACTOR

In the original explation of the area ratio method, as applied to pumps-as-turbines, Burton and Williams[116] used the utilization factor defined by Shepherd[117]. This gives the theoretical energy transferred from the fluid to the impeller. In this equation the exit velocity head ($V_{m1}^2/2g$), due to the meridional velocity from the eye of the impeller is included in the head available to the impeller. In a practical situation, this velocity head is not included in the turbine head $H_t$ because there is an equal, or sometimes greater velocity head at the turbine inlet (the area of a pump outlet tends to be larger than the suction area). Therefore in order to obtain the turbine head $H_t$ from the head coefficient of the turbine impeller it is necessary to take into account only the lost energy due to the whirl velocity at exit ($V_{u1}^2/2g$) in the calculation of the utilization factor. The equation used is the same as that given by Hergt, Krieger and Thommes[88]:

$$\varepsilon = \frac{\psi_t U_2^2}{\psi_t U_2^2 + \frac{V_{u1}^2}{2}} \qquad \text{(L.1)}$$

For the Worthington-Simpson end-suction pump analysed in chapter 4, the utilization factor at point III has already been calculated to be 0.963 (see section 4.3.2). At point II, there is no exit whirl velocity and the equation for the utilization factor simplifies to:

$$\varepsilon = \frac{\psi_t U_2^2}{\psi_t U_2^2} = 1$$

Hence, the loss of output power due to the exit whirl velocity at point III is only 3.7%. The loss of output power due to the shock loss at inlet to the impeller at point II is likely to be much greater than this, and therefore the turbine best efficiency point, in this case, is closer to point III.

APPENDIX M

# REPORT ON THE RUNNING OF A FLYGT BS2102 SUBMERSIBLE PUMP AS A STAND-ALONE TURBINE AND INDUCTION GENERATOR

## M.1. INTRODUCTION

This report gives the background to and results from tests carried out at Flygt Pumps, Colwick, Nottingham by A Williams, Research Assistant in the Faculty of Engineering at Nottingham Polytechnic. The tests form part of a research project to investigate the performance of standard induction motor-pump units as stand-alone micro-hydrogenerators. This research is closely related to the work of Nigel Smith, Research Fellow at the Polytechnic, who has designed an Induction Generator Controller suitable for controlling stand-alone induction generators powered by small water turbines.

Mr M R Sinclair, Technical Sales Manager of Flygt Pumps (UK), showed interest in this controller for use with Flygt PL Hydro Turbine Generators. He also showed interest in the possibility of using smaller pumps as turbine generator units, and invited collaboration between Flygt Pumps and the research group at Nottingham Polytechnic.

Tests were carried out using the pump test rig at Colwick, running a BS2102 MT 5.2 kW pump unit in reverse. The induction machine was run as a self-excited generator by connecting capacitors in parallel with a resistive load bank. These excitation capacitors provide the reactive current which would otherwise be supplied from a mains connection.

The Flygt range of B pumps appeared to be suitable for use as turbines because of its capability of handling dirty water, and because its construction would enable easy installation as a turbine-generator at a remote site. This particular pump was chosen for the tests because the output matches the electrical equipment available and because it requires a relatively low head. Sites with heads greater than 40 m are relatively rare, especially in the U.K., and would require a long length of pipe, making them economically less attractive.

## M.2. TEST PROCEDURES

The test tank and associated equipment at Flygt Pumps' Colwick works were used for the tests, with the addition of electrical equipment brought from the Polytechnic. The test rig is designed primarily for testing pumps to obtain their head-discharge performance characteristics.

The layout of the equipment made it impossible to measure the discharge directly, while running one pump as a turbine. Hence, before carrying out the turbine test, a head-discharge curve was obtained by measuring $Q_1$ and $H_1$ for the driving pump (see Fig.1). The turbine test was then performed and the discharge calculated from the values of $H_1$. The turbine head was calculated from the measured head at a pressure tapping on the inlet hose ($H_2$ in Fig.2). Friction head loss between the pressure tapping and the turbine inlet, and velocity head difference between turbine inlet and outlet were taken into account.

Initially the tests used a CP3152 HT pump for driving the BS2102 pump as a turbine. However, because of the head losses, this was not able to produce 24 m head at 44 *l*/s required by the BS2102 when running as a turbine. A CP3201 HT (impeller 456) was therefore used as the driving pump. Fig.3 shows a comparison between the test data for the actual pump used, and the standard manufacturer's performance curve. All points were within the tolerance for an acceptance test.

It was found that by removing the strainer of the B pump, which serves no useful purpose in turbine mode, the output power was increased by more than 5%. A curve was obtained for comparison purposes of the BS2102 running as a pump with the strainer removed. The results of this test are shown in Fig.4, along with results for the pump running as a turbine.

Turbine and generator tests were carried out at various values of output voltage and excitation capacitance. A power analyser was used to measure electrical output power, voltage and frequency to a claimed accuracy of 0.8%, 0.3% and 0.2% respectively. The loads on the three phases were adjusted to give balanced currents.

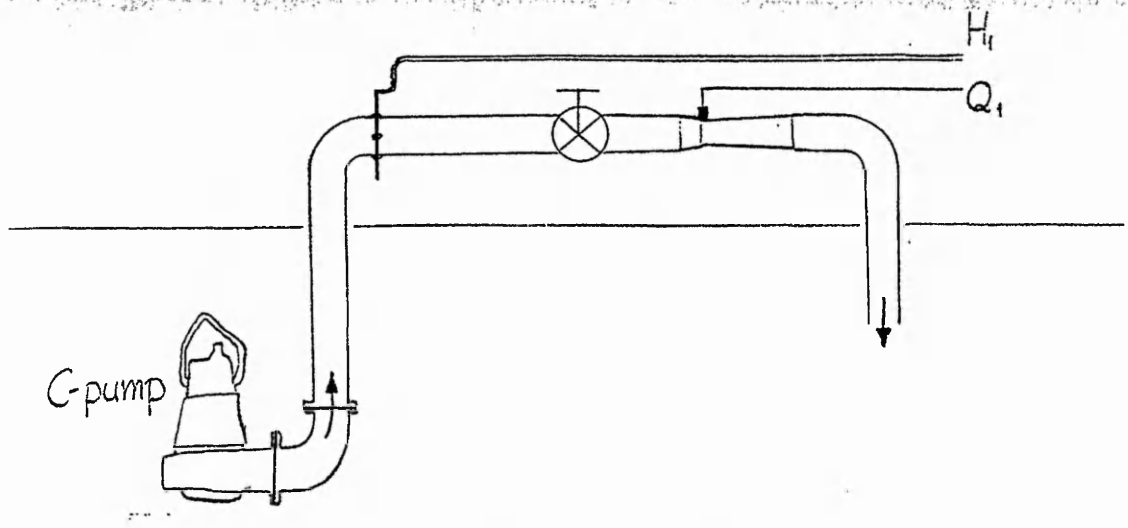


Fig.M.1. Drive pump test arrangement.

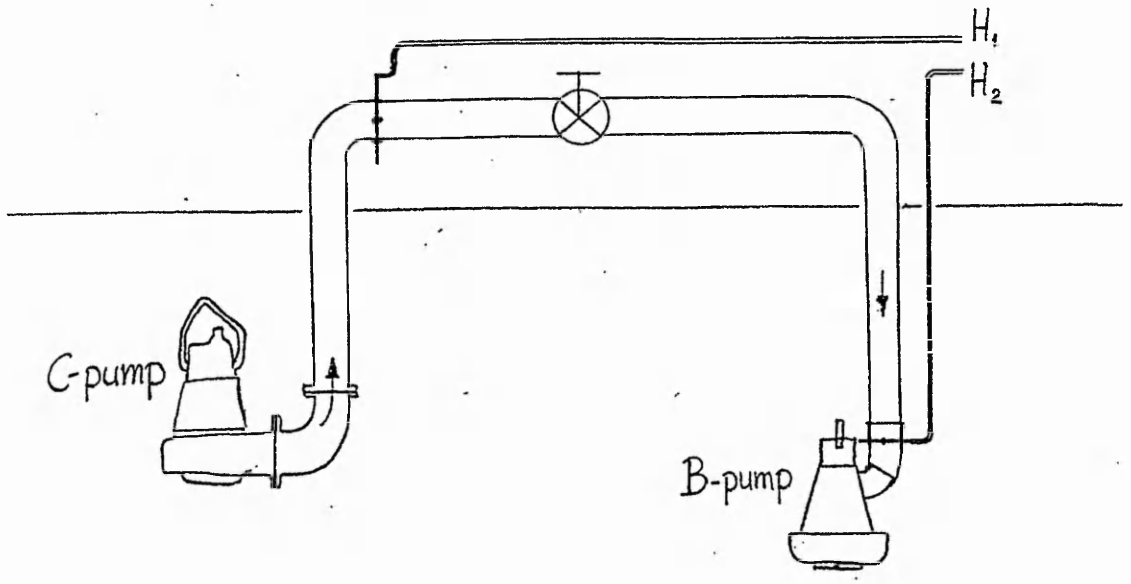


Fig.M.2. Turbine-mode test arrangement.

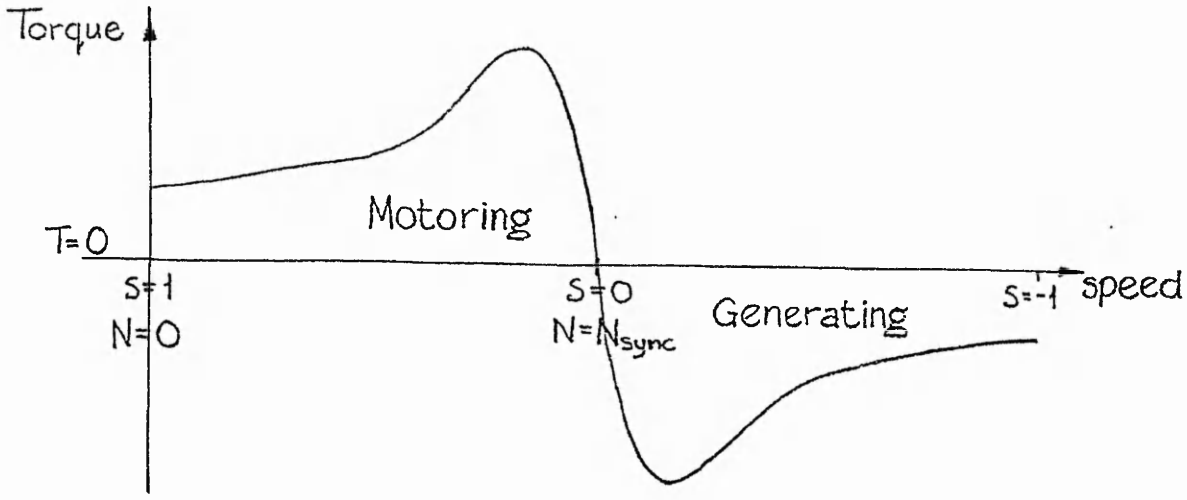


Fig.M.5. Torque-speed curve of an induction machine.

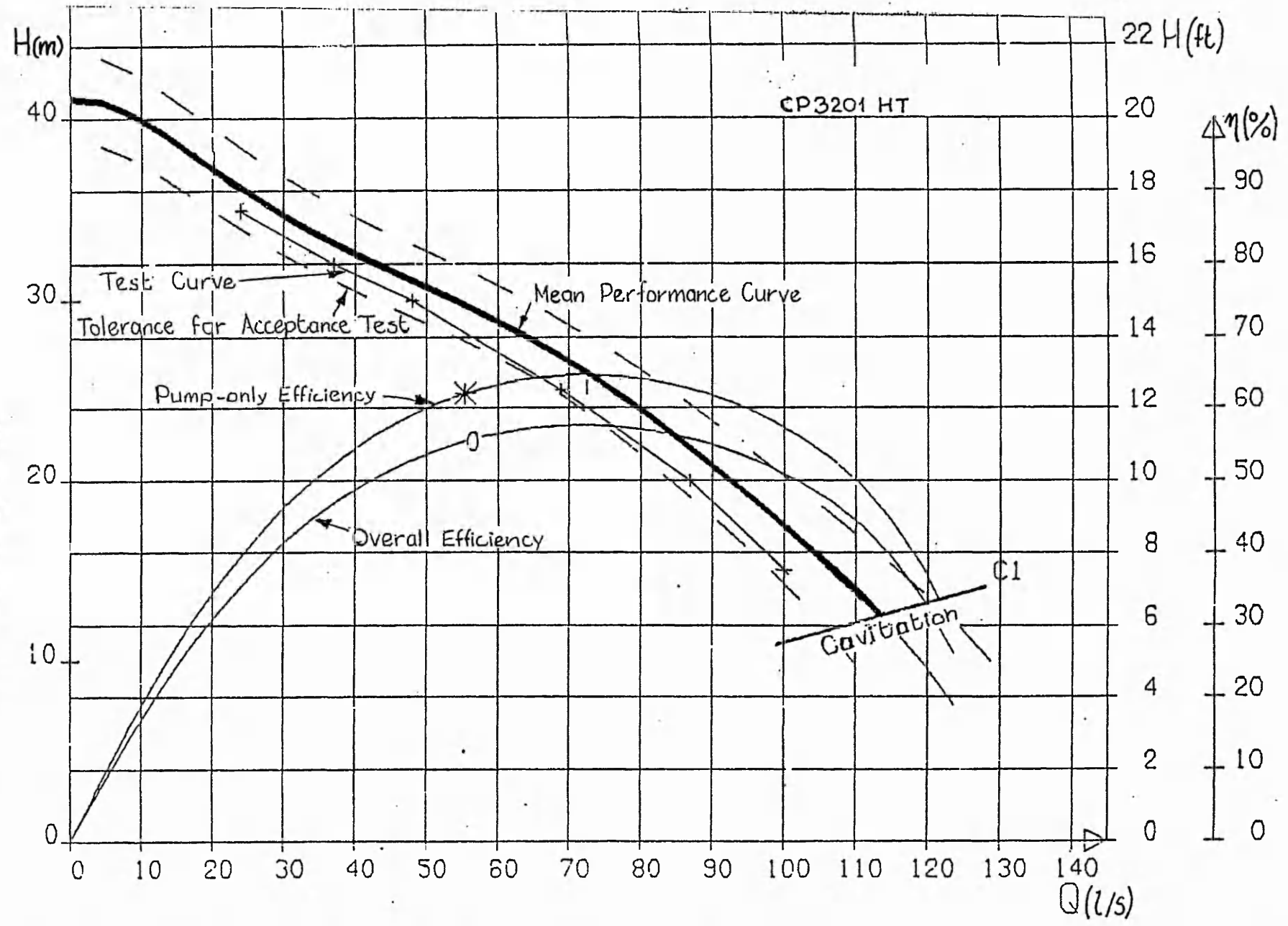


Fig.M.3. Driving Pump Performance

## M.3. TEST RESULTS

The turbine-mode performance curves for the BS2102 pump, with strainer removed, are shown in Fig.4. The test was carried out with the generator output line-line voltage held constant at 400V. The speed therefore varied with the load. The excitation capacitance for this test was 67 microfarad, which results in the generator requiring a relatively low input power to produce 400 V output at 50 Hz. The best efficiency point for turbine operation is compared with the best efficiency for pump operation in the table below.

| | Pump | Turbine |
|---|---|---|
| Flow (*l*/s) | 25 | 40 |
| Head (m) | 12.8 | 19.2 |
| Efficiency (overall) | 53 % | 58 % |
| Output Power(kW) | 4.7 | 4.4 |

As can be seen the generator output power at best efficiency is well within the rated power of the induction machine (5.2kW), and is therefore not overloaded under these conditions.

### M.3.1 Normalised performance characteristics

In order to compare these test results with those from other pumps run as turbines, the values of head and flow can be "normalised", ie. related to a fixed speed, by using the affinity laws which hold for centrifugal pumps and turbines. Under dynamically similar conditions, discharge, Q, is proportional to rotational speed, N, and head, H, is proportional to $N^2$.

However, the speed of the pump could not be measured directly, and was calculated from the generator frequency. For an induction generator, the speed is greater than the synchronous speed by the amount of the magnetic slip. The synchronous speed is given by

$$N_{sync} = 60 \times f$$

and the running speed by

$$N = 60 \times f(1-s)$$

where s is negative for a generator and positive for a motor.

A typical induction machine torque-slip curve is shown in Fig.5. Since power is equal to the product of torque and speed, slip, s, must be related to the generator or motor power. Around s=0, the torque curve is linear, and hence for small values of s, the power-slip curves are also practically linear. Unfortunately, no generator performance data were available for the Flygt 19-09-2 motor which powers the BS2102 pump under investigation.

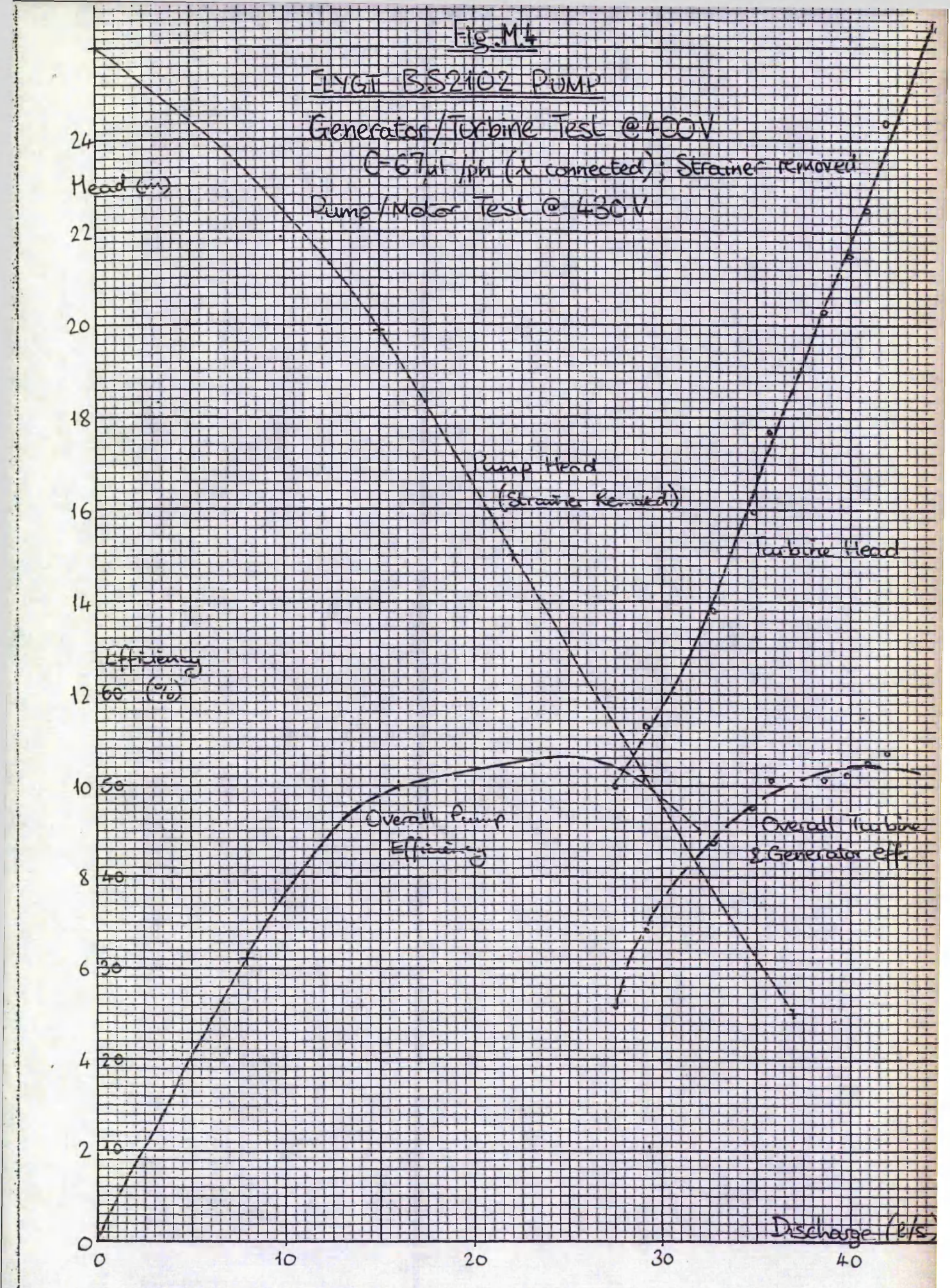
Fig. M4
FLYGT BS2402 PUMP
Generator/Turbine Test @ 400V
C=67μF Δ/ph (Δ connected); Strainer Removed
Pump/Motor Test @ 430V
Head (m)
Efficiency (%)
Discharge (l/s)
Pump Head (Strainer Removed)
Turbine Head
Overall Pump Efficiency
Overall Turbine & Generator eff.
0
2
4
6
8
10
12
14
16
18
20
22
24
10
20
30
40
50
60

M.3.2 GEC Induction motor/generator tests

In order to estimate the generator performance of the Flygt induction machine, tests were carried out on a 2.2 kW, 4-pole GEC machine in the laboratory at Nottingham Polytechnic. Slip was measured accurately for both motoring and generating conditions by using a stroboscope triggered at the machine frequency and directed onto the rotating shaft. Mechanical power was measured using a strain-guage type torque transducer and an accurate rotational speed counter.

The relation between generator slip and electrical output power was found to be linear, with an offset at zero power resulting from the no-load losses. As a motor, the slip-power relation is also linear if the electrical input power is used. The results are shown in Fig.6, which also shows that the gradients of the slip-power lines are equal. Taking motoring slip as positive

$$s(\text{motoring}) = 2.5 \frac{P_{in}}{P_{rated}} - 0.25 \ (\%)$$

$$s(\text{generating}) = -2.5 \frac{P_{in}}{P_{rated}} - 0.25 \ (\%)$$

or if P is in kW, then:

$$s(\text{motoring}) = 1.136\ P_{in} - 0.25 \ (\%)$$

and $$s(\text{generating}) = -1.136\ P_{in} - 0.25 \ (\%)$$

The manufacturer's data for the Flygt motor are plotted in Fig.7, showing that

$$s(\text{motoring}) = 0.923\ P_{in} - 0.38 \ (\%)$$

and from the previous results we can assume that if the motoring slip is $(mP_{in} - s_o)$, then the generating slip is $(-mP_{in} - s_o)$.

Therefore the equation: $s(\text{generating}) = -0.923\ P_{in} - 0.38 \ (\%)$

has been used to calculate the generator (and hence the turbine) speed. The normalised head-flow characteristic for the BS2102 pump as turbine is shown in Fig.8. The line drawn through the points is a quadratic fit calculated using least-squares regression, which has a 98 % correlation with the test results.

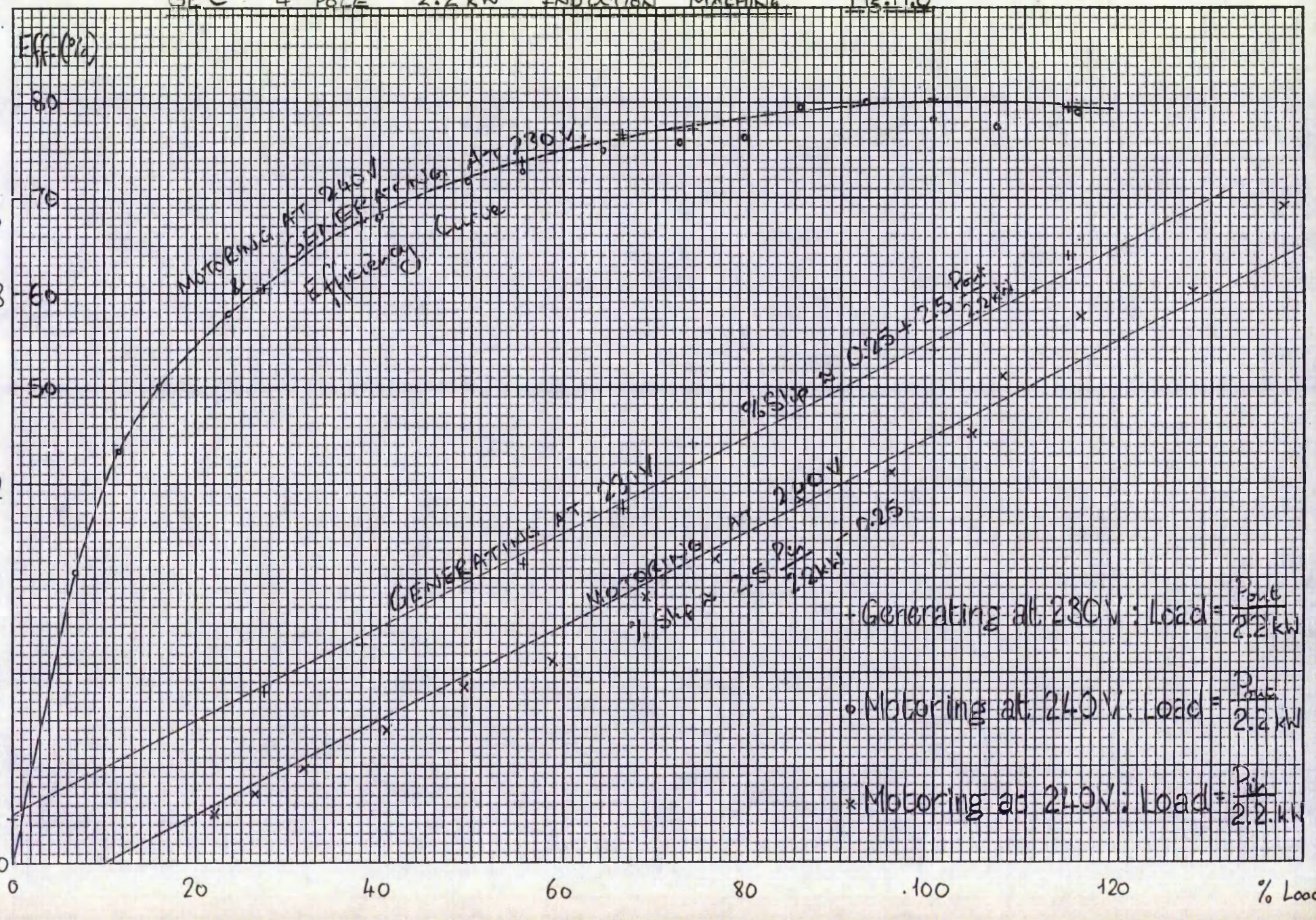
GEC 4-POLE 2.2kW INDUCTION MACHINE Fig.M.6
Eff. (%)
Slip %
MOTORING AT 240V
GENERATING AT 240V
EFFICIENCY CURVE
GENERATING AT 230V
MOTORING AT 230V
% Slip = 0.25 + 2.5 P_out / 2.2kW
% Slip = 0.25 + 2.5 P_in / 2.2kW
+ Generating at 230V: Load = P_out / 2.2 kW
• Motoring at 240V: Load = P_out / 2.2 kW
* Motoring at 240V: Load = P_in / 2.2 kW
0
20
40
60
80
100
120
% Load

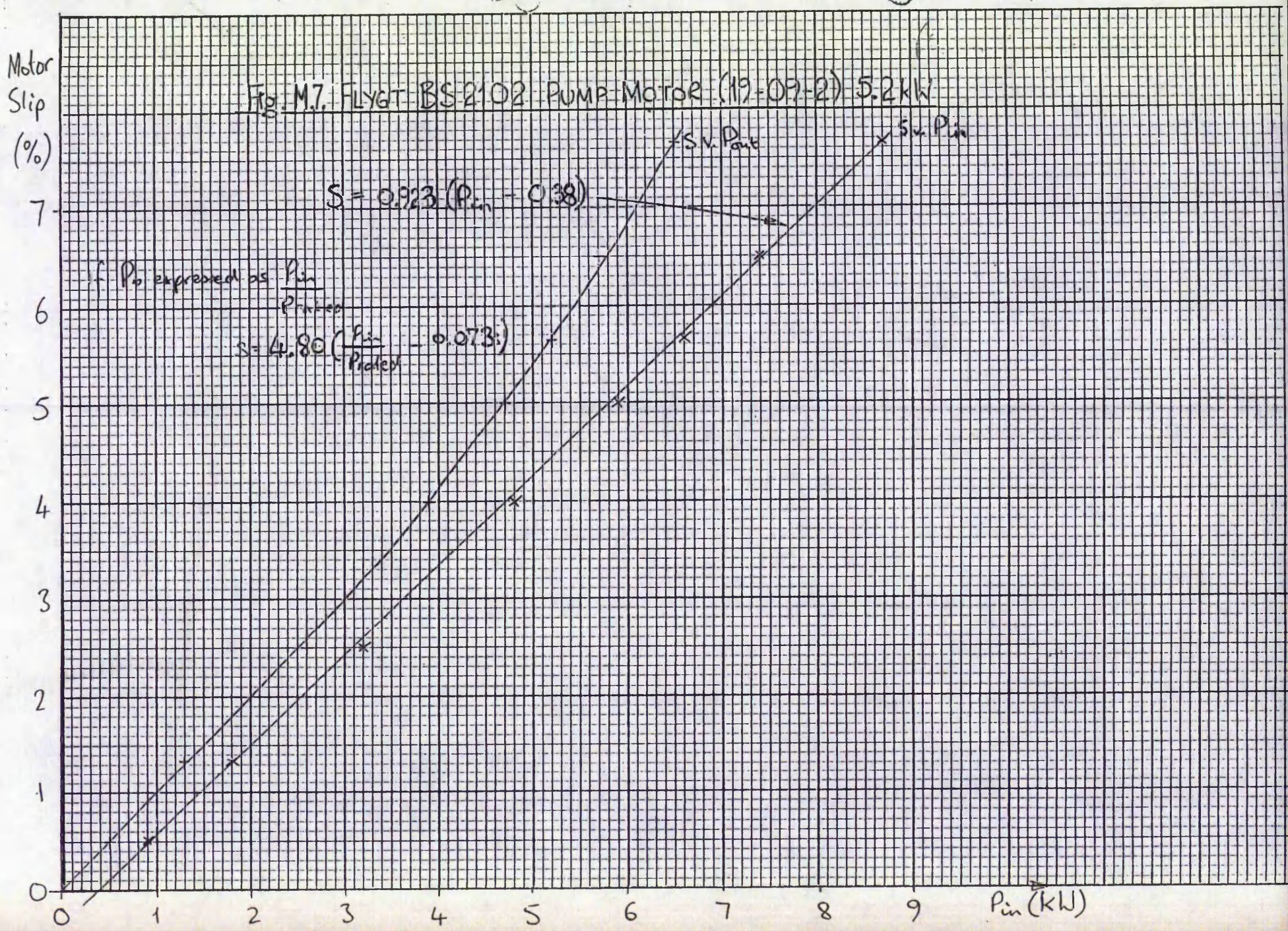
Fig. M.7. FLYGT BS 2102 PUMP MOTOR (19-07-2) 5.2kW
Motor Slip (%)
S v. P_out
S v. P_in
S = 0.923 (P_in - 0.38)
If P_in expressed as P_in / P_rated
S = 4.80 (P_in / P_rated - 0.073)
0
1
2
3
4
5
6
7
8
9
P_in (kW)

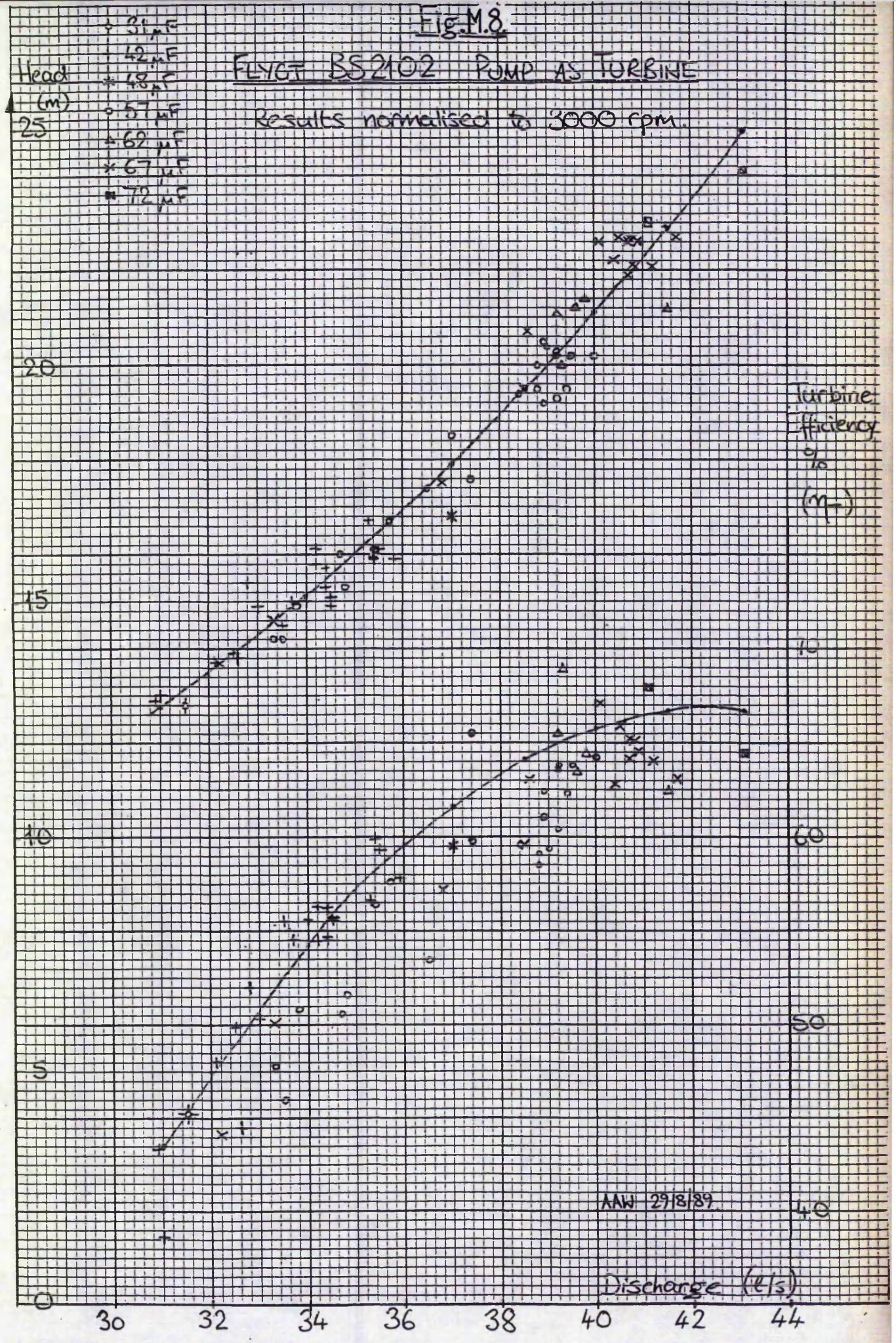
Fig. M.8.
FLYGT BS2102 PUMP AS TURBINE
Results normalised to 3000 rpm.
31 μF
42 μF
48 μF
57 μF
62 μF
67 μF
72 μF
Head (m)
25
20
15
10
5
0
Turbine Efficiency % (η_T)
10
60
50
40
AAW 29/8/89
30
32
34
36
38
40
42
44
Discharge (l/s)

### M.3.3 Efficiency Calculation

From the series of tests on the GEC machine it was found that the efficiency curve for motoring at 240 V (plotted against output power) is closely correlated with the generator efficiency curve at 230 V (again, plotted against output power). Hence the Flygt motor data were used to find the generator efficiency for the turbine tests. The overall efficiency is given by:

$$\frac{P_{out(electrical)}}{\rho Q g H} = \eta_{gen} \times \eta_{turbine}$$

The turbine efficiency has been plotted against discharge in Fig.8. A quadratic line of best fit is also shown, and gives the maximum efficiency of the turbine at Q = 42.3 *l*/s. The line of best fit has been calculated using least squares regression and has a correlation coefficient of 93 %.

Thus at 3000 rpm, 230 V output, the best efficiency conditions are:-

| | |
|---|---|
| Discharge, Q | = 42.3 *l*/s |
| Head, H | = 23.8 m |
| Efficiency, $\eta_T$ | = 66.8 % |
| Input power, $P_T$ | = 6.87 kW |
| Generator efficiency, $\eta_{gen}$ | = 78 % |
| Generator output | = 5.36 kW |
| Generator slip | = 5.33 % |
| Frequency | = 47.5 Hz. |

## M.4. CONCLUSIONS

The results of these tests confirm that the BS2102 pump can be run as a turbine-generator unit. By selecting an appropriate value of excitation capacitance, the induction machine will run as a self-excited generator, producing approximately rated power at rated voltage. Hence, the machine will not be electrically overloaded when running in reverse as a pump and motor. If the strainer is removed, the overall efficiency is greater than when running as a pump.

## M.5. RECOMMENDATIONS

### M.5.1 Testing with an IGC

A self-excited induction generator requires some form of control, unless it is supplying a fixed load. A suitable electronic controller, which diverts unused power into a ballast load, has been designed at Nottingham Polytechnic. Nigel Smith has tested a 2.2 kW, single-phase version of the induction generator controller (IGC), and is presently investigating suitable components for higher power versions. Once a 5.5 kW version has been constructed, it would be useful to test this in conjunction

with the BS2102 pump. A combination of capacitors, connected as shown in Fig.9, can be used to produce a single-phase supply from a three-phase induction generator.

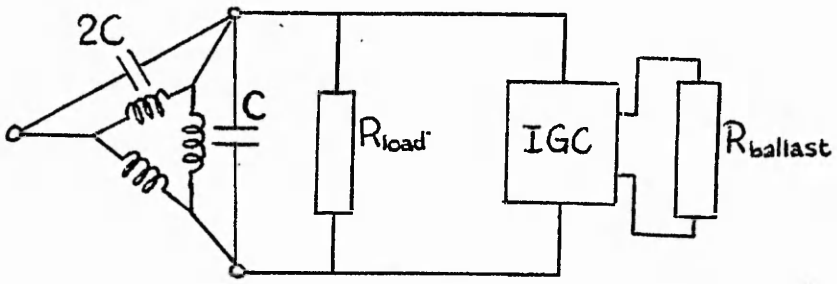


Fig. .9. C-2C connection for single-phase output.

M.5.2 Testing with a draft-tube

The importance of the turbine outlet design was demonstrated by the improved efficiency when removing the strainer. The addition of a simple conical draft-tube may recover a significant proportion of the velocity head, which for turbine-mode operation is approximately 1.5 m. It may be possible to design and construct such a draft-tube at the Polytechnic, and to test this at the same time as the IGC, ie. within the next three months.

M.5.3 Other investigations

There are three other aspects of the pump design which would be valuable to investigate for turbine-mode operation. Firstly, wear on the pump thrust bearing may be increased when running as a turbine. In order to assess this it would be useful to carry out measurements of the axial thrust produced be the impeller. Secondly, rounding off the impeller blade ends may result in an improvement in efficiency at very little additional cost. This would require a pump impeller to be made available specifically for these tests. Finally, the effect of varying the submergence of the pump needs to be investigated, since cavitation may occur more readily in turbine-mode operation.